Determinants of cell cycle progression in human mammary epithelial MCF12 cells

Alexandra Ouertani

Thesis submitted for the degree of

Doctor of Philosophy

UCL School of Pharmacy

University of London

2012

This thesis describes research conducted in the UCL School of Pharmacy between October 2008 and September 2011 under the supervision of Prof Andreas Kortenkamp and Dr Elisabete Silva. I certify that the research described is original and that any parts of the work that have been conducted by collaboration are clearly indicated. I also certify that I have written all the text herein and have clearly indicated by suitable citation any part of this dissertation that has already appeared in publication.

Signature: _____   Date: _____

ABSTRACT

Cancer of the mammary gland is the most common type of cancer in women worldwide, and the vast majority of breast cancers originate from a cluster of malignant cells in the epithelial tissue of the breast, which initially confines the ductal carcinoma *in situ*. Research has shown that the signalling pathways that increase differentiation and maintain proliferation in normal epithelial cells are of utmost importance for sustaining this barrier against malignant cells. As a model for normal mammary epithelial cells, the MCF-12A cell line was used to determine factors that are required for cell cycle progression of these cells. A discontinuous treatment assay was developed in which the MCF-12A cells were treated with epidermal growth factor (EGF) and insulin at two distinct times to induce cell cycle re-entry. The use of these chemically defined growth factors enabled us to determine that continuous stimulation with mitogenic factors is not required for these cells to re-enter the cell cycle. An initial activation of the MAP kinase pathway and an up-regulation of the transcription factor c-Myc, followed by activation of the PI3K pathway, resulted in full competence to progress into S phase. The order in which the growth factors were applied, and thus the sequence in which the subsequent proteins were triggered, was of great importance for successful S phase entry.

We found that estradiol (E2) was unable to induce the factors necessary for cell cycle progression. Furthermore, we report for the first time that E2 did not affect estrogen-regulated genes which normally are under the control of a ligand-bound estrogen receptor (ER). We suggest that the mechanism by which the ligand-activated ER usually interferes with the estrogen responsive element in the promoter region of the target genes is defective in the MCF-12A cell line.

The results presented here may contribute to new approaches in chemotherapy, taking advantage of the diverse molecular mechanism in place for cell cycle progression and proliferation in malignant cells compared to normal mammary epithelial cells.

TABLE OF CONTENTS

LIST OF FIGURES

LIST OF TABLES

Akt	protein kinase B
AP-1	activator protein 1
ATF	activating transcription factor
BCL-2	B-cell lymphoma 2
BRCA1/BRCA2	breast cancer type 1/2 susceptibility protein
BSA	bovine serum albumin
CCND1	cyclin D1
CD-HS	charcoal-dextrane treated horse serum
CDK	cyclin dependent kinase
cDNA	complementary DNA
Cip1	CDK inhibitor protein 1
DAG	diacylglycerol
DCIS	ductal carcinoma in situ
DMEM	Dulbecco's Modified Eagle Medium
DMSO	dimethyl sulfoxide
DNA	deoxyribonucleic acid
E2	estradiol
ECL	enhanced chemiluminescence
EDTA	ethylenediaminetetraacetic acid
EGF	epidermal growth factor
EGFR	epidermal growth factor receptor
ErbB1/2/3/4	epidermal growth factor receptor 1/2/3/4
ERE	estrogen responsive element
Erk	extracellular regulated kinase
ERα/β	estrogen receptor alpha/beta
ESR1/2	estrogen receptor alpha/beta (gene)
EtOH	ethanol
Gab-1/2	Grb associated binder
GPER	G-protein coupled estrogen receptor
Grb2	growth factor receptor bound protein 2
GSK3	glycogen synthase kinase 3
HBSS	Hank's balanced salt solution

HER	human epidermal growth factor receptor
HRP	horseradish peroxidase
IDC	invasive ductal carcinoma
IGF-1	insulin-like growth factor 1
IP3	inositoltriphosphate
IRS1/2	insulin receptor substrate 1/2
JNK	Jun amino-terminal kinase
kDa	kilo Dalton
MAPK	mitogen-activated protein kinase
MEK	MAPK kinase
mRNA	messenger ribonucleic acid
NFκB	nuclear factor kappa B
PBS	phosphate buffered saline
PCR	polymerase chain reaction
PDGF	platelet derived growth factor
PGR	progesterone receptor (gene)
PH	pleckstrin homology
PI	propidium iodide
PI3K	phosphatidyl-inositol-3-kinase
PKB	protein kinase B
PKC	protein kinase C
PLC	phospholipase C
PR	progesterone receptor
pRb	retinoblastoma protein
PTEN	Phosphatase and tensin homolog
Ras	rat sarcoma protein
RNA	ribonucleic acid
RT	room temperature
RTK	receptor tyrosine kinase
rt-PCR	real time PCR
SDS	sodium dodecyl sulfate
SEM	standard error of the mean
Ser	serine
SH domain	Src homology domain

Shc	Src homology domain containing protein
Sos	son of sevenless
Sp-1	specificity protein 1
Src	sarcoma proto-oncogene tyrosine kinase
STAT	signal transducer and activator of transcription
TBS (-T)	Tris base solution (with Tween®)
TEMED	Tetramethylethylenediamine
Thr	threonine
Tyr	tyrosine

Chapter 1: Introduction

1 GENERAL INTRODUCTION

Breast cancer is the most frequently diagnosed cancer and now the leading cause of cancer deaths among women. It accounts for almost a quarter of all cancer cases worldwide, and for 14% of all cancer deaths. This corresponds to almost half a million women who have died from breast cancer in 2008, and incidence rates are still rising in most countries (Jemal et al. 2011). It is of utmost importance to investigate the reasons why some women will be diagnosed with breast cancer, whereas some women will not. Although some of the risk factors for developing mammary carcinoma are known, the molecular mechanisms for the development and progression of the disease are not yet fully understood. Independent of the known risk factors, almost all cancers originate in the milk ducts. Most of these neoplasms remain within the duct, confined by a protective barrier of healthy epithelial cells, however, some neoplasms will be able to break down this barrier and become invasive tumours.

Much emphasis has been placed on the characterisation of the malignant cells. However, the signals that maintain proliferation in normal epithelial cells are the key element for sustaining the barrier against invasion and the research presented here focuses on the signalling pathways activated for cell cycle progression in normal epithelial cells. A better knowledge of the signalling network in normal cells can also provide the basis for understanding how the "wrong" signals can lead to increased proliferation, ultimately resulting in malignant transformation, and giving rise to the very first cancer cells.

2 CANCER OF THE MAMMARY GLAND

Cancer of the mammary gland is the most common type of cancer in women worldwide (Jemal et al. 2011). The risk for developing a mammary tumour increases with age, and 75% percent of women diagnosed with breast cancer are over the age of 50 (DeSantis et al. 2011). However, the disease also occurs in younger women (around 5% of all patients are under the age of 40), thus other risk factors must exist.

2.1 Risk factors for breast cancer

Screening of tumour tissue has revealed that in around one quarter of all samples, one of the human epidermal growth factor receptors (HER), HER2, was overexpressed (Slamon et al. 1987). This amplification is acquired over time, as a result of genetic damage, and increases the risk for the development of a tumour, since aberrant signalling through this receptor is believed to play a direct role in malignant transformation and progression (Wilson et al. 2005; Pietras et al. 1995; Pierce et al. 1991). The overexpression of HER2 in human breast cancer cells can also enhance their metastatic potential (Tan et al. 1997). As a result of these findings, the drugs trastuzumab as well as lapatinib were developed, which interfere with the HER2 receptor and provide a more targeted therapy for the disease.

Also a strong indicator for the risk of developing breast cancer is a woman's genetic predisposition. For example, women with germline mutations on the breast cancer genes (BRCA1 or BRCA2) have a much higher risk of developing mammary carcinomas (Miki et al. 1994; Ford et al. 1994). A consequence of this finding was to develop a screening programme that monitors women affected by this genotype at close intervals from a young age, since they are prone to early-onset breast cancers.

There are also external and life-style factors that increase the risk for developing a mammary carcinoma. Many of these are well known and include the late onset of menopause, use of menopausal hormone replacement therapy (HRT), (late) age at first pregnancy and nulliparity, as well as alcohol consumption and being overweight. Long term (> 10 years) use of HRT increases the risk for breast cancer by 30%, and a delay of 5 years in the onset of menopause results in an additional 17% risk (Colditz 1998; King and Schottenfeld 1996). Nulliparous women increase their risk for developing a mammary carcinoma by around one third (Schonfeld et al. 2011), whereas each full term pregnancy provides a protective effect (Hulka and Moorman 2001; Kelsey et al. 1993). The rise in cancer cases caused by alcohol consumption is modest (regular alcohol intake results in a 30% augmented risk), but obesity, especially post-menopausal, increases the risk for developing breast cancer considerable (three times higher than for women with a normal body mass index (BMI)) (Hulka and Moorman 2001; King and Schottenfeld 1996; Longnecker et al. 1995). Not to be dismissed is the risk emerging from exposure to environmental pollutants, since chemicals that can mimic the function of estrogens in the human body may account for a considerable number of breast cancer cases (Kortenkamp et al. 2007; Muir 2005; Sasco 2003; Bhatt 2000). Consequently, maintaining a healthy body weight, regular exercise and limiting the exposure to known

carcinogens (including alcohol), are currently the best strategy for every woman to reduce her risk of developing breast cancer (Magne et al. 2011; Kushi et al. 2006). However, these established risk factors are not rare and most women unaffected by the disease also carry them. More precisely, one study showed that 97 percent of cases, but also 96 percent of controls had one or more "traditional" hormone related risk factors for breast cancer, meaning that the effects of these risk factors are quite weak, even when they are found in combination (Millikan et al. 1995; Newman et al. 1995). Indeed, models that are based upon such well known risk factors are unable to predict with acceptable accuracy who will develop breast cancer (Rockhill et al. 2001). Actually, only around half of all breast cancer cases can be attributed to recognised risk factors, including nulliparity or late age of first pregnancy (Madigan et al. 1995), and only a fraction of these again are a result of genetic predispositions (Lichtenstein et al. 2000). Nevertheless, most mammary carcinomas do have one common feature, which will be discussed in the next section.

2.2 Signalling between normal and malignant cells for the transition from in situ to invasive carcinoma

The vast majority of breast cancers originate in the epithelial tissues of the breast, more specifically from a cluster of malignant cells initially confined to the milk ducts (Polyak and Kalluri 2010; Burstein et al. 2004; Radford et al. 1995). At first, these so-called ductal carcinoma in situ (DCIS) are surrounded by normal epithelial cells that form a natural barrier against increased progression of the neoplastic cells (cf. Figure 1). In the early phase of tumorigenesis, this barrier breaks down, probably as a result of signals emitted by the malignant cells, and gives way to invasive progression (invasive ductal carcinoma, IDC). The importance of the integrity of the myoepithelium to function as a barrier was demonstrated already in the 1970s when DeCosse and colleagues (1973 and 1975) showed that a normal mammary microenvironment in co-culture with breast cancer cells was capable of inducing a more differentiated state in the cancer cells and so to revert the malignant phenotype (reviewed by Polyak and Kalluri 2010; DeCosse et al. 1975; DeCosse et al. 1973). Taking these observations further, Hu and colleagues (2008) showed that co-injection of normal myoepithelial cells decreased tumour weights in a xenograft model (mice with human DCIS), whereas injection of cancer cells promoted tumour growth (Hu et al. 2008a). Similarly to the xenograft model, Booth and colleagues (2011) showed that in a mixture of normal mammary epithelial cells with mammary tumour cells, injected into (epithelium-free) mouse mammary, the tumour cells were reverted to normal cells, which even participated in the generation of a

normal, functional mammary gland in the animals (Booth et al. 2011). This suggests that normal epithelial cells are signalling to transformed cells to reverse their malignant fate. The question arises as to the potential for confined carcinoma to transform their microenvironment and to become invasive. There are currently (at least) two slightly different views that explain how the malignant cells, initially confined to the ducts, are able to break through the protective layer of the epithelium. First, the barrier *evasion* model suggests that the first tumour cells promote proliferation of each other and of newly aberrant cells. The malignant cells proliferate until they finally disrupt the myoepithelial cell layer, then degrade the basement membrane and eventually migrate into the stroma. From there on, the tumour cells can invade surrounding tissue or even migrate to distant organs. The second model sees barrier *failure* as the fatal event: tumour cells signal to normal myoepithelial cells in such a way as to disrupt their differentiation, and these cells are lost. Eventually, the epithelium lacks sufficient cells to form the protective barrier, resulting in invasive carcinomas (Polyak and Kalluri 2010).

In both these proposed models, as well as in the studies showing that tumorigenic cells can be re-programmed when they are in a normal microenvironment, the signalling between the normal and the malignant cells has an important role for deciding if a small tumour remains confined, or becomes invasive and consequently more dangerous. The exact signals remain unknown, but paracrine interactions between malignant and normal cells seem likely, such as through cytokines or prostaglandins. Indeed, prostaglandin action, which is mediated by the NFκB pathway, was found to be the target of the crosstalk between normal epithelial and tumour fibroblast cells of the stroma, which has an important role in breast tumour progression (Hu et al. 2009). In particular the signals that increase differentiation and maintain proliferation in normal mammary epithelial cells are vital in this context and are discussed in more depth in the following section.
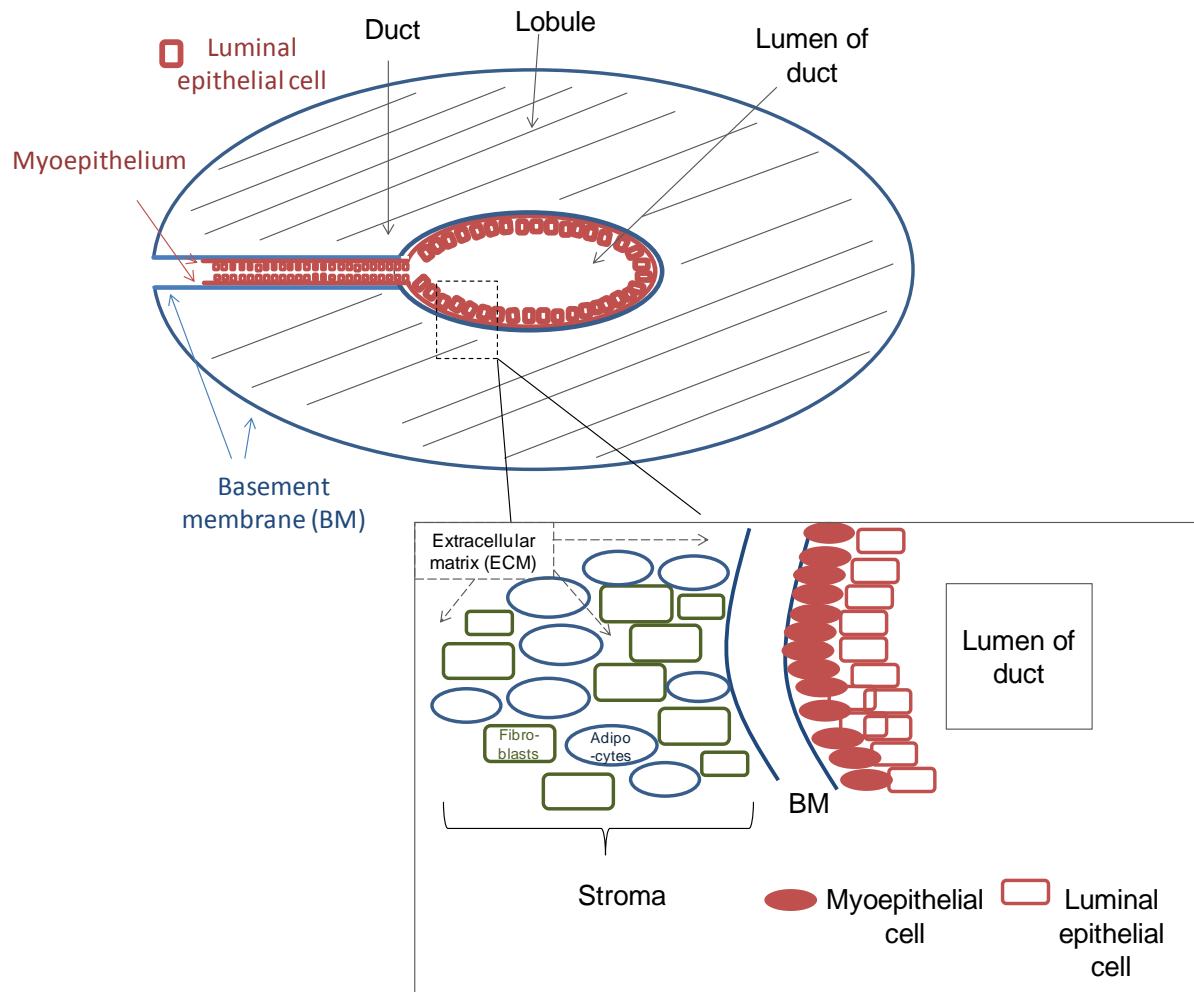
Figure 1 Schematic representation of the different cell types found in the lobules and ducts of the mammary gland lobes

The glandular tissue of the mammary gland consists of separate lobes, each containing several secretory lobules. The ducts are formed by an outer myoepithelial cell layer on the basement membrane (BM) and an inner luminal epithelial cell layer, and are surrounded by the extracellular matrix (ECM) and the stroma. Cells composing the stroma include fibroblasts, myofibroblasts, adipocytes and endothelial cells. The ducts leaving the lobules merge into a single lactiferous duct in each lobe.

3   MAMMARY GLAND EPITHELIUM

3.1   The function of epithelial cells in the mammary gland

The normal development of the mammary gland requires cell proliferation and differentiation, taking place in a tightly controlled manner. Many of these processes are regulated by hormones. Typically, the steroid hormones progesterone and estrogen are found in the mammary gland, and both play major roles for the development of this specialised tissue. The primordial function of epithelial cells in the mammary gland lies in the formation of the milk ducts, which are made up of elongated epithelial cells. This ductal outgrowth is stimulated by estrogens which, during the reproductive cycle, regulate cellular proliferation and turnover (for a recent review about this morphogenesis, see Gjorevski and Nelson 2011). Stimulation of normal ductal elongation and outgrowth by estrogens is transmitted through the estrogen receptor alpha (ERα) found in epithelial and stromal cells, and the loss of ERα expression in these cells results in impaired branching and elongation (Feng et al. 2007; Bocchinfuso et al. 2000; Bocchinfuso and Korach 1997). Thus, estrogens have an impact on cell proliferation in the normal epithelium, but they also strongly increase proliferation in ER positive (ER$^+$) breast cancer cells. It is not entirely clear how the balance between desired proliferative estrogen signalling and repressing aberrant proliferation is maintained in normal cells, and yet this could explain, at least partially, why some cells become overly proliferative and eventually malignant. However, approximately one third of all breast cancers are characterised as estrogen receptor negative (ER$^-$) (Putti et al. 2005; Pervez et al. 1994). ER$^-$ breast cancer cells lack the classical pathway of estrogen-stimulated proliferation. Signalling for their proliferation is mediated through the epidermal growth factor (EGF) receptor (EGFR).

The EGFR (also known as HER or ErbB1) belongs to the ErbB family of receptor tyrosine kinases, which also comprises HER2, as well as ErbB3 and ErbB4. The EGFR is associated with increased proliferation of normal breast epithelial cells. For example, activation of the EGFR is readily detected in extracts of mammary glands of mice at puberty, late pregnancy, and lactation. Conversely, EGFR$^{-/-}$ mice have impaired postnatal ductal development, and are characterized by a reduced proliferation of the mammary epithelium and stroma (Stern 2003). However, it is now also apparent that overexpression of *any* receptor of the ErbB family (or ectopic expression of ErbB agonists) has a role in human cancers (Jin and Esteva 2008; Stern 2003; Yarden and Sliwkowski 2001). Indeed, in ER$^-$ breast cancer cells, the EGFR is found to

be overexpressed, which explains their increased proliferation rate (Biswas et al. 2000; Ma et al. 1998; Fan et al. 1998; Newby et al. 1997). Therefore, simply treating breast cancer with anti-estrogenic compounds to suppress the proliferation of the malignant cells is by far not efficient in all cases. Treatment of breast cancer cells in culture with anti-estrogens even resulted in increased expression of several EGF receptor types. Subsequently, proliferation of such conditioned cells was dependent on EGF related, rather than hormone related pathways (Knowlden et al. 2003; McClelland et al. 2001). As mentioned above, approximately one third of all breast cancer patients display overexpression of the EGFR (ER⁻ tumours), and another 25% overexpress the ErbB receptor HER2. Consequently, inhibitors for the ErbB family have been approved for the treatment of some epithelial tumours that carry specific receptor gene amplifications. However, the efficacy of such therapies has been limited in the case of breast cancer: for example, only 25 to 30% of patients with tumours overexpressing HER2 respond to the classical HER2 targeting agents, trastuzumab and lapatinib (Jin and Esteva 2008).

In order to optimise therapeutic efficacy, it is essential to untangle the complex signalling network in the mammary gland epithelium. Especially a better understanding of the receptor functions and the signals transmitted from the receptors onwards in normal tissue may reveal regulatory elements that may be exploited for developing more targeted therapies. The regulation of proliferation certainly holds a key position in the epithelium, and therefore is discussed in more detail in the next section.

3.2 Signalling for cell cycle progression and proliferation

It has become clear that the signalling pathways that increase differentiation and maintain proliferation in normal epithelial cells are of utmost importance for sustaining the barrier against invasiveness of malignant cells. Proliferation is the result of cells progressing through the cell cycle, which ends with the division of the cell into two daughter cells. The cell cycle is divided into four main stages, the first gap phase (G1), followed by the synthesis (S) phase where the DNA is duplicated, a second gap phase (G2) and finally mitosis (M phase). The progression through the different stages is tightly controlled by so-called cell cycle checkpoints which ensure the fidelity of the cell entity (Murray 1994). Since the G1 phase serves as a period where the cell can grow, the G1/S phase checkpoint may only be passed if the cell has reached a sufficient enough size. The G2 phase checkpoint is required to ensure that the entire genome has been replicated. The mitotic checkpoint, also called the spindle

checkpoint, safeguards the correct assembly of the mitotic spindle and alignment of the chromosomes on the spindle, before onset of cytokinesis.

The work presented here will focus on the events occurring during cell cycle progression out of the quiescent state through G1 into S phase. On its way from G1 into S phase, the cell has to pass the restriction (R) point, where it is decided if the cell is allowed to continue with the cell cycle and divide, or not. This depends on the environmental conditions, and the cell will only progress through the cell cycle if it has received sufficient extracellular growth signals. The R point is lost in most cancer cells, and therefore they proliferate in an uncontrolled fashion. The biochemical mechanism underlying the R point is the hyperphosphorylation of the retinoblastoma protein (pRb), which, in its hypophosphorylated state, suppresses cell cycle progression. Successful hyperphosphorylation is a multistep process, involving many different proteins activated beforehand by mitogen-triggered signalling pathways, such as cyclin D, cyclin E and their respective partner cyclin-dependent kinases (CDK) (Planas-Silva and Weinberg 1997b; Weinberg 1995).

Once the cell passes the R point, it becomes mitogen-independent and is committed to the cell cycle. It will complete the next round of mitosis (unless stopped at one of the subsequent checkpoints for DNA damage repair etc.). Because the R point is a decisive element in the cell cycle, it can be assumed that (growth) factors that activate the R point have a proliferative effect on the cell. Likewise, cells that have a phosphorylated pRb have acquired mitogen autonomy, because all signals required for entry in to S phase must have been received at this point. On the other hand, constitutive phosphorylation of the pRb is regarded as aberrant behaviour: such cells are thought to have lost any dependence on external mitogenic stimuli, and are assumed to proliferate excessively (Weinberg 1995; Pardee 1989; Pardee 1974).

To conclude, these phosphorylation events taking place in G1 around the R point are the result of a finely balanced system of signalling pathways which are not yet fully defined in mammary epithelial cells. The research presented here will focus on a few aspects of these fundamental mechanisms, as is outlined below.

4 AIMS

The paracrine signalling emanating from normal epithelial cells to malignant cells in the mammary ducts holds the potential of suppressing cancer progression at a very early stage. Therefore, the signalling in the mammary microenvironment is under investigation, but progress is slow because the signalling cascades activated in one cell at a time are extremely complex and involve a plethora of different kinases. Even if only one mechanism is examined at a time, the kinase cascades that are activated to achieve for example cell cycle progression are not linear. Research with fibroblast cells has made substantial progress in this regard: one interesting experimental set-up was established by Jones and Kazlauskas (2001) with fibroblasts, which allowed determination of factors that are absolutely necessary and sufficient for cell cycle re-entry (Jones and Kazlauskas 2001). These researchers showed that when fibroblasts were stimulated with growth factors in a discontinuous fashion, the cells were still able to progress through G1 phase, as long as all molecular requirements in terms of temporal availability of specific factors were met. They suggested that it is a general feature of cells that some proteins need to be activated at early times, which set the stage for the subsequent completion of pRb phosphorylation. The responsible signalling cascades are not activated constantly, but in (at least) two distinct waves, thus the external stimuli are required exclusively at these specific times. Intrigued by their so called *two wave model*, we were interested to find out if such a discontinuous experimental set-up could be applied to epithelial cells as well. If so, this would open new possibilities for investigating the signals triggered in the normal mammary microenvironment. Since we wanted to study the signalling events in place for cell cycle progression in normal mammary epithelial cells, the MCF-12A cell line was chosen as a model system. These cells are derived from non-transformed human mammary epithelial tissue obtained during reduction mammoplasty. They immortalised spontaneously after long term cultivation (Paine et al. 1992) and are therefore viewed as a good model for normal epithelial cells of the mammary gland. However, this cell line is delicate to maintain and requires rather complex culture conditions, when compared to other mammary epithelial cell lines, and therefore is not used widely, and comparatively few publications are available.

The first aim was to remove the complex mixture of growth factors present in the serum rich growth medium the MCF-12A cells are usually maintained in, and to find chemically defined (growth) factors that are able to induce cell cycle progression in these cells. Cell cycle

progression was considered successful once cells had reached S phase, as determined by flow cytometric analysis of the combined percentages of S, G2 and M phase cells.

After identification of such specific factors, the second objective was to develop an experimental set-up that applies a discontinuous treatment regimen to the cells. This is imperative because only a discontinuous stimulation would allow first to determine the sequence in which the signalling cascades are triggered, and second to what extent (how long the signalling cascades are kept functional). If there is no succession of cascades, it can be assumed that all signals are triggered at the same time. Consequently, the next objective was to identify these signalling pathways that are triggered for cell cycle re-entry. This includes the identification of the proteins that are activated in the course of these cascades.

Finally, the effect of the endogenous hormone estradiol in the MCF-12A cell line was to be examined. As discussed above, estrogens have an important role in the development of the mammary gland in general, and for mammary epithelial cells in particular. However, the function of estradiol in the MCF-12A cells is not well characterised. Assessing the impact of estradiol on cell cycle progression was therefore another objective of the work presented here. Additionally, we wanted to monitor the influence on the expression of a few genes that are typically regulated by the steroid hormone, including some proliferative genes, such as *PRAD1* (coding for cyclin D1) and *MYC* which is translated into the c-Myc protein transcription factor.

5 THESIS OUTLINE

Chapter 2 describes the material and methods used to carry out the work presented in this thesis.

Chapter 3 covers the methodological issues that had to be addressed at the beginning of the work presented here. First, an appropriate method for cell synchronisation needed to be established and validated. Synchronicity of the cell cultures was monitored with flow cytometric analysis, for which also a suitable protocol was developed. Second, the characteristics of the cell cycle profiles of the cell line used needed to be considered so that the best fitting model for flow cytometric cell cycle analysis could be determined. The reproducibility of data was determined and sources for data variability were discussed. An

appropriate normalisation method for the obtained data was introduced to account for the inter-experimental data variability due to the method chosen for cell synchronisation.

Chapter 4 is dedicated to the experimental establishment of the discontinuous stimulation assay using MCF-12A cells. The parameters that are essential for successful S phase progression are discussed and additionally, the effect of a variety of growth factors utilised in the discontinuous stimulation assay is assessed.

In Chapter 5, the effect of EGF on the regulation of selected genes is presented. The findings are compared with the effect of estradiol on the same set of genes, and are put into context with the observations made on cell cycle progression with these two compounds.

In Chapter 6, some of the signalling cascades triggered for cell cycle progression are revealed; more precisely, the MAP kinase, PI3 kinase and the PLC pathways are investigated in detail. The conclusions about the signalling network are drawn from experiments that illustrate the impact of different kinase and lipase inhibitors on cell cycle progression.

Chapter 7 discusses several proteins that are required for cell cycle progression. First, the activation of the kinases found to be involved in Chapter 6, is confirmed. Secondly, the expression of the transcription factor c-Myc is followed during the discontinuous stimulation assay.

Finally, Chapter 8 summarises the main findings and discusses the relevance of the work presented here.

Chapter 2:

Material and Methods

1 LIST OF CHEMICALS

Table 1 List of chemicals used and suppliers

Chemical	Supplier
17β-estradiol	Sigma
acetic acid	BDH
acrylamide	BioRad
ammonium persulfate	Sigma
bovine serum albumin	Sigma
bromophenol blue	Sigma
charcoal	GE Healthcare
cholera toxin	Sigma
coumaric acid	Sigma
dextrane	GE Healthcare
dimethylsulfoxide	Merck
epidermal growth factor	Sigma
ethanol	Hayman
glycine	BDH
H_2O_2	Sigma
Hank's balanced salt solution	Invitrogen
HCl	Sigma
horse serum	Invitrogen
hydrocortisone	Sigma
insulin	Invitrogen
insulin like growth factor 1	Sigma
iQ SYBR Green Supermix for real time PCR	BioRad
luminol	Sigma
LY294002	Promega

mercaptoethanol	Sigma
M-MLV reverse transcriptase	Promega
molecular size marker for SDS-PAGE	Cell Signaling Technology
Na_2HPO_4	BDH
NaCl	BDH
NaH_2PO_4	Sigma
PD98059	Promega
PDGF-BB	Biolegend
penicillin/streptomycin	Invitrogen
propidium iodide	Calbiochem
PP2	Sigma
protein standard for Bradford assay	Sigma
random primers	Invitrogen
rDNase	Macherey-Nagel
ribonuclease inhibitor (recombinant RNasin)	Promega
RNase A	Sigma
sodium dodecyl sulfate	BDH
TEMED	BioRad
Tris HCl	Sigma
Tris Base	Sigma
Trypsin EDTA	Invitrogen
Tween-20 ®	Sigma
U73122	Calbiochem
ultra pure ethanol	Fisher Scientific Laboratories

Phosphate buffered saline (PBS) was prepared with 155 mM NaCl, 7.7 mM Na_2HPO_4 and 2.3 mM NaH_2PO_4 in 1 litre of UHQ. The pH was adjusted to 7.4. TBS was prepared as a 10x concentrated stock solution with 200 mM Tris base and 137 mM NaCl in UHQ water (pH 7.6). It was diluted to the work solution with UHQ water before use. TBS-T was prepared with 0.05% Tween-20 (v/v) in TBS.

2 ROUTINE CELL CULTURE

2.1 Routine maintenance of cells

MCF-12A cells (from ATCC) were cultured in 75 cm^2 canted neck flasks (T75 flasks, Helena Biosciences, Gateshead, UK) with 12 ml of DMEM/F12 (1:1) medium (Invitrogen, Life Technologies, Paisley, UK), supplemented with 5% horse serum (Invitrogen), epidermal growth factor (EGF, 20 ng/ml), insulin (Sigma-Aldrich Ltd, Gillingham, UK, or Invitrogen, 10 µg/ml), cholera toxin (Sigma, 100 ng/ml), hydrocortisone (Sigma, 0.5 µg/ml) and penicillin/streptomycin (Invitrogen, 5000 µg/ml). This medium is referred to as "complete growth medium".

Flasks were kept in a humified incubator at 37°C with 5% CO$_2$. Cells were media changed every other day and subcultured when cells were around 70% confluent, usually every four to five days.

In order to avoid changes in growth rates based on variations of the serum composition, the same batch of horse serum was used throughout the work for this thesis.

2.2 Media

Several different media were required for various stages of this work, which are described here:

- Basal medium (Phenol red free medium DMEM/F12 (1:1), Invitrogen)

- Freezing medium (complete growth medium with 20% instead of 5% horse serum, and additional 10% (v/v) DMSO)

- Re-suspension medium (complete growth medium with 20% instead of 5% horse serum)

- Starvation medium (Phenol red free medium DMEM/F12 (1:1), Invitrogen, supplemented with 0.5% (v/v) charcoal-dextran treated horse serum)

- Assay medium (Phenol red free medium DMEM/F12 (1:1), Invitrogen, supplemented with 2% (v/v) charcoal-dextran treated horse serum, no addition of EGF)

2.3 Sub-culturing (passaging)

When the cells had reached around 70% confluency in the T75 flasks, they were subcultured, or passaged. For this, the medium was removed from the flask and cells washed once with 10 ml Hank's balanced salt solution (HBSS, Invitrogen). 1-2 ml of 0.05% trypsin EDTA (Invitrogen) was added and cells were incubated for 15-20 min at 37°C, until detached. The cells were then resuspended in 10 ml re-suspension medium. The higher amount of serum present in the re-suspension medium was required to inactivate all enzymatic action of the trypsin, which could have a detrimental effect on the cells. The suspension was pipetted up and down several times to break cell clumps, then centrifuged at 1000 rpm for 5 minutes for removal of the trypsin solution. The cell pellet was resuspended in fresh complete growth medium and cells were plated in new T75 flasks at a ratio of 1:10. Cells were used for no more than 10 passages after resurrection from cryopreservation.

2.4 Cryopreservation and resurrection from cryogenic stocks

Stocks were prepared from low passage cells. After trypsinisation (as before, see above), an aliquot of the cell suspension was counted to determine the total cell concentration. Cells were then centrifuged at 1000 rpm for 5 minutes, the supernatant was removed and the resulting cell pellet re-suspended in a volume of cold freezing medium that ensured the final cell suspension contained 10^6 cells/ml. 1ml aliquots of the cell suspension was transferred into cryogenic vials (Nalgene, through VWR International, Lutterworth, UK). The vial was placed in a freezing container (Nalgene) that cools down the content at a constant rate of 1°C/min when kept in a freezer and stored at -80 °C. After 24 hours, the cryogenic vial was placed in liquid nitrogen for long term storage.

Cells were resurrected from cryopreservation by placing the cryogenic vial into a water bath at 37°C, until the medium was thawed. The cell suspension was then transferred into a centrifuge tube containing 10 ml of pre-warmed re-suspension medium, and centrifuged for 5 min at 1000 rpm. The pellet was resuspended in complete growth medium and cells were plated in a 25 cm^2 canted neck flask. After 72 hours, the cells were passaged and plated into T75 flasks as described above.

2.5 Charcoal-dextran treatment of serum

For some assays, the serum was charcoal-dextran (CD-) treated beforehand. This was necessary because serum contains an undefined mixture of lipids, hormones and other growth factors. In order to obtain a chemically more defined medium with lower amounts of steroidal hormones and other factors that could interfere with our results, the serum was treated with a charcoal/dextran mixture which removes lipophilic components present in the serum. Briefly, a suspension of 5% charcoal and 0.5% dextran T70 (Amersham, GE Healthcare Life Sciences, Little Chalfont, UK) was prepared in a volume of ultra-high quality (UHQ) water equal to the volume of serum to be treated. This was allowed to equilibrate by rolling for 30 min (10 cycles / min) at room temperature (RT) and centrifuged for 10 min at 1000 g. The supernatant was then removed, and the serum was added to the charcoal/dextran pellet and mixed by rolling (10 cycles / min) for 1 hour at RT. The mixture was finally centrifuged for 20 min at 50000 g and then sterilised by filtration. The CD- treated serum was stored at -20ºC.

3 GROWTH FACTORS

Growth factors were kept as powders or stock solutions, as provided by manufacturers, at temperatures specified on the containers. Powders were dissolved as follows:

Epidermal growth factor (EGF, Sigma) was dissolved in 10 mM acetic acid with 0.1% (m/v) bovine serum albumin (BSA, Sigma) to produce a stock concentration of 100 µg/ml. IGF-1 was purchased from Sigma and dissolved into a 1 µg/ml stock solution in UHQ-H_2O. PDGF-BB was purchased from Biolegend (through Cambridge Bioscience Ltd, UK) and dissolved in 10 mM acetic acid with 0.1% (m/v) BSA. Stock solutions of 10 µM 17β-estradiol (Sigma) were prepared in ultra-pure ethanol.

Insulin (Sigma) was kept as provided at 10 µg/ml.

All stock solutions were diluted using basal medium to yield the required final concentrations immediately before use. The concentrations of the stock solutions were chosen in such a way as when the final solutions were prepared, the concentration of ethanol (the solvent used for preparing the stock solutions), did not exceed 0.1% (v/v) in the final medium. This was to ensure that the solvent present in the final solutions was too diluted to have an effect on cell growth or proliferation.

4 INHIBITORS

The inhibitors were kept as powders as provided by manufacturers, at temperatures specified on the containers. Upon reception, an aliquot of each compound was dissolved into stock solutions which were aliquoted and kept at -20°C.

LY294002 (Promega, Southampton, UK) was resuspended in DMSO to produce a stock solution of 50 mM, and was used at a final concentration of 20 µM. PD98059 (Promega) was resuspended in DMSO to produce a stock solution of 20 mM, and was used at a final concentration of 20 µM. PP2 (Sigma) was resuspended in DMSO to produce a stock solution of 20 mM and was used at a final concentration of 25 µM. U73122 (Calbiochem, through VWR International, UK) was resuspended in DMSO to produce a stock solution of 5 mM, and was used at a final concentration of 1 µM.

All stock solutions were diluted using basal medium to yield the required final concentrations immediately before use. The final DMSO concentration never exceeded 0.1% (v/v). This was to exclude any effect of the solvent on cell growth or proliferation.

Before adding the inhibitor solutions, cells were washed twice with HBSS. The inhibitor, diluted in basal medium, was added and the cells were incubated for 20 minutes. The medium was removed and fresh basal medium, containing the inhibitor at the same concentration as before, in addition to the growth factor(s), was added. The cells were then incubated for the time specified for the assay. The time pre-incubating with inhibitors was disregarded for the total release time. Instead, timing for the pulses was started once the growth factor had been added.

5 FLOW CYTOMETRY

5.1 Discontinuous exposure assay

5.1.1 Seeding of MCF-12A cells

MCF-12A cells were seeded in 6-well plates at 10^5 cells/well, with 2ml of complete growth medium per well, and incubated for 24 hours to allow attachment.

5.1.2 Serum depletion for induction of quiescence

After attachment of the cells, the complete growth medium was removed from the wells and cells were washed twice with HBSS, using 2 ml buffer each time. 2 ml of starvation medium was added to each well, and the plates were incubated for 24 hours.

5.1.3 Incubation with growth factors

After the starvation period, the starvation medium was removed and each well was washed twice with HBSS (using 2ml each time). The growth factors to be tested were diluted in basal medium to the concentration required, and 2 ml of that medium was added to each well. The plates were then incubated for 30 minutes (duration of the first pulse). Afterwards, the growth factor containing medium was removed and each well washed twice with HBSS (2 ml each time), and fresh basal medium was added. The plates were then incubated for 3.5 hours until the start of the second pulse. For the second pulse, the basal medium was removed and fresh basal medium containing the growth factors to be tested (prepared immediately before use) was added to the wells. The plates were then incubated for 10 hours (duration of the second pulse). At the end of the incubation period, the medium was removed and all wells washed twice with HBSS (2 ml each time), and fresh basal medium was added and the cells incubated another 4 hours until the end of the assay time.

5.1.4 Incubation with inhibitors

5.1.4.1 Inhibitors tested during the first pulse

When inhibitor compounds were to be tested in addition to growth factors, the cells were pre-incubated with the inhibitor alone: after removal of the starvation medium, followed by two wash steps with HBSS (2 ml each time), 2 ml of basal medium containing the inhibitor to be tested, at the concentration required, was added to each well. The inhibitor solutions were prepared immediately before use. The plates were incubated for 20 minutes, after which the medium was removed and fresh basal medium containing the inhibitor (at the same concentration as before) and the growth factor was added. Countdown of the assay time was started now, and the plates were incubated for 30 minutes (duration of the first pulse). The medium was then removed and the wells washed twice with HBSS (2 ml each time) before addition of fresh basal medium. Cells were incubated for 3.5 hours before the start of the second pulse, which was carried out as described before.

5.1.4.2 Inhibitors tested during the second pulse

After the first pulse (carried out as described before), the cells were incubated with basal medium for 3 hours 10 minutes. The medium was then removed and fresh basal medium with the inhibitor to be tested (solutions were prepared immediately before use) was added to each well. The cells were incubated for 20 minutes, after which the medium was removed and fresh basal medium containing the inhibitor and growth factors was added to the wells, so that the second pulse started at the time point t=4h as before. The plates were then incubated for 10 hours (duration of the second pulse) and the assay completed as described before.

5.2 Sample preparation for flow cytometric analysis

At the end of the assay time, the medium was removed and each well was washed once with HBSS (2 ml). 0.5 ml of trypsin solution was added into each well and cells were incubated, and after detachment centrifuged, as described before (see above). The pellet was resuspended in 2 ml HBSS and centrifuged again at 1000 rpm (5 min) to remove any remaining traces of media. 1 ml of 70% ice cold ethanol was added drop wise to the cell pellet whilst vortexing, and the cells were kept on ice for at least 30 min afterwards to fix them. Cells were either processed immediately for flow cytometric analysis or kept at -20°C (in ethanol) until further treatment.

5.3 Staining of cell DNA

After the incubation on ice, cells were spun down at 7500 rpm for 5 min, and the ethanol was removed carefully to avoid disturbing the cell pellet. 1 ml of cold phosphate buffered saline (PBS) was added to each sample, and the cells centrifuged for 5 min at 6500 rpm. This wash step was repeated once more. After removal of the supernatant, 50 µl of RNase solution (Sigma, 100 µg/ml in PBS) was added to each sample and the cells were incubated for 15 min at room temperature. Following the RNA digestion, 450 µl of a propidium iodide (PI) solution (Calbiochem, 50 µg/ml in PBS) was added and the samples were kept on ice and covered until analysis.

5.4 Analysis on flow cytometer

All samples were analysed on the MACSQuant® Analyzer flow cytometer (Miltenyi Biotec Ltd, Bisley, UK), with the following parameters:

- Flow rate 100 µl/min

- Trigger for detection was 1 µm in FSC

- Excitation with laser at 488 nm

- Emission was detected in channel 4 (FL4), which detected fluorescence between 655 and 730 nm

- A minimum of 10.000 events were detected for each sample

The flow cytometer was calibrated before each use, according to the manufacturer's instructions, using MACSQuant calibration beads (Miltenyi Biotec). All other solutions and buffers required for the flow cytometer were also purchased from Miltenyi Biotec.

5.5 Data analysis with MACSQuantify™ software

Data acquired on the MACSQuant® Analyzer flow cytometer was analysed with the MACSQuantify™ Software, version 2.3.1129.1 (Miltenyi Biotec).

5.6 Data analysis with FlowJo software

Additional data analysis was performed with FlowJo flow cytometry analysis software (free trial software, version 7.6, Tree Star Inc., Ashland, USA) using embedded algorithms.

6 IMMUNOBLOTTING

6.1 Discontinuous exposure assay

6.1.1 Seeding of MCF-12A cells

MCF-12A cells were seeded in Petri Dishes (10 cm). 5×10^5 cells were seeded into each dish, using 10 ml of complete growth medium. Dishes were incubated for 24 hours to allow cells to attach.

6.1.2 Serum depletion, incubation with growth factors and inhibitors

After the attachment period, the cells were processed for starvation, incubation with growth factors and incubation with inhibitors as described before, but for each step, 10 ml of medium (or washing buffer) were used in the Petri dishes.

6.2 Sample preparation for immunoblotting

After the relevant incubation periods, the medium was removed and the wells were washed with cold PBS. To each dish, 350 µl of cold lysis buffer were added and the cells were scraped off. The suspension was immediately boiled for 10 min at 95°C. The lysates were kept at -20°C until further use.

6.2.1 Determination of protein concentration and protein separation with SDS-PAGE

The protein concentration of the lysates was determined using Bradford assay. Absorption was read at 595 nm for each sample. To separate the proteins, SDS-PAGE was used. For this, 1mm space glass plates (Bio-Rad Laboratories Ltd, Hemel Hempstead, UK) were utilised to prepare a running gel with 12% acrylamide (3.3 ml H_2O, 4 ml 30% acrylamide (Bio-Rad), 2.5 ml 1.5M Tris pH 8.8, 100 µl 10% SDS, 100 µl 10% ammonium persulfate, 4 µl TEMED (Bio-Rad)). On top of the polymerised running gel, a layer of stacking gel (2.1 ml H_2O, 0.5 ml 30% acrylamide, 380 µl 1M Tris pH 6.8, 30 µl 10% SDS, 30 µl 10% ammonium persulfate, 3 µl TEMED) was cast over, in which the wells (into which the samples were loaded) were created. Each well had a capacity of maximal 35 µl. The sample with the lowest protein concentration was used to determine the protein load (concentration [µg/µl] x 35 µl) for all samples, which was approximately 1 µg. For the higher concentrated samples, the volumes equal to this protein amount were loaded into the wells. A molecular size marker was added to each gel (Cell Signaling Technology (CST), New England Biolabs Ltd, Hitchin, UK). Proteins were separated by their mass in the running gel by electrophoresis, which was run for 2 hours at 80 Volt, in running buffer (190 mM glycine, 0.1% SDS, 25 mM Tris base, adjusted to pH 8.3).

6.2.2 Transfer

The separated proteins were transferred from the gel onto nitrocellulose membranes (Amersham) in blot sandwiches, kept in cold transfer buffer. The protein transfer was performed at 40 Volt (1 hour).

6.2.3 Incubation with antibodies

After successful transfer of the proteins onto the membranes, the membranes were blocked with 5% (w/v) BSA (Sigma) in TBS-T (0.05% Tween-20 (v/v) in TBS) for 1 hour at room temperature (RT), followed by incubation with the primary antibody at the appropriate

dilution for up to 2 hours at RT, or overnight at 4°C (see Table 2 for incubation conditions for each antibody). Then, the membranes were washed 3x 15 min in TBS-T, followed by incubation with the secondary antibody for 1 hour at RT. All secondary antibodies (anti-mouse HRP-linked, or anti-rabbit HPR-linked, both from CST) were diluted 1:2000 in 5% BSA in TBS-T.

Table 2 Overview of antibodies used for immunoblotting assay

All antibodies were purchased from CST and used under these optimised conditions

target	dilution	dilution medium	incubation time
β-actin	1:2000	5% BSA in TBS-T	overnight (4°C)
Akt	1:1000	5% BSA in TBS-T	overnight (4°C)
phospho-Akt	1:1000	5% BSA in TBS-T	2h (RT)
Erk1/2	1:2000	5% BSA in TBS-T	overnight (4°C)
phospho-Erk1/2	1:3000	5% BSA in TBS-T	2h (RT)
Myc	1:1000	5% BSA in TBS-T	2h (RT)
phospho-Src	1:1000	5% BSA in TBS-T	overnight (4°C)

6.2.4 Protein detection

After incubation with the secondary antibody, the membranes were washed 3x 15 min in TBS-T. Detection of proteins was performed by ECL reaction. The ECL buffer was prepared with 50 µl of luminol solution (250 mM luminol in DMSO), 25 µl of coumaric acid solution (90 mM coumaric acid in DMSO) and 4 µl of H_2O_2 in 10 ml of 100 mM Tris HCl (pH 8.5).

Membranes were incubated for 1 min with ECL buffer, followed by exposure (10 sec to 2 min, depending on signal strength) of hyperfilm (Amersham) to the membranes. To ensure that the developed band was generated from the assumed protein, the position of the bands were compared to the molecular size marker added to each gel.

6.2.5 Re-probing of membranes

Changes in the amount of phosphorylated proteins may be caused by changes in the phosphorylation status or by changes in the amount of total protein. To assess which one was the case in the MCF-12A cells, the total amount of the protein was detected on the same

membrane in addition to the phosphorylated protein. For this, the membranes were stripped of all antibodies after detection of the phosphorylated protein by incubating them for 45 minutes (50°C) in stripping buffer (67.5 ml UHQ-H2O, 20 ml 10% SDS, 12.5 ml 0.5M Tris HCl pH 6.8, 800 µl mercaptoethanol). The membranes were washed 4x 10 min with TBS-T and then blocked again with 5% (w/v) BSA (Sigma) in TBS-T (0.05% Tween-20 (v/v) in TBS) for 1 hour at RT, followed by incubation with the antibodies as described before.

7 QUANTITATIVE REAL-TIME PCR ANALYSIS

7.1 Discontinuous exposure assay

7.1.1 Seeding of MCF-12A cells

MCF-12A cells were seeded in 6-well plates at 10^5 cells/well, with 2 ml of complete growth medium per well, and incubated for 24 hours to let them attach.

7.1.2 Serum depletion for induction of quiescence

The complete growth medium was removed from the wells and cells were washed twice with HBSS, using 2 ml buffer each time. 2 ml of starvation medium was added to each well, and the plates were incubated for 24 hours.

7.1.3 Incubation with growth factors

After removal of the starvation medium, followed by two wash steps with HBSS (2 ml each time), 2 ml of basal medium containing the growth factor(s) to be tested was added to each well. Incubation times were according to the protocol established for discontinuous exposure assay, or for 12 hours continuously.

7.1.4 Incubation with complete growth medium

For the incubation with complete growth medium during the discontinuous exposure assay, all wash steps were included in order to perform the exact same procedure on all samples.

7.2 Sample preparation for rt-PCR analysis

At the end of the incubation time, the medium was removed and each well was washed once with HBSS (2 ml). 0.5 ml of trypsin solution was added into each well and cells were

incubated for 15 min at 37C. After detachment, the cells were centrifuged for 15 min at 0°C, the supernatant was removed and the cells were snap-frozen in liquid nitrogen and kept at -80°C until further analysis.

7.2.1 RNA extraction

For extraction of the RNA, an extraction kit from Macherey and Nagel (NucleoSpin® RNA II) was used according to the manufacturer's protocol:

The frozen cell pellet was left to thaw at room temperature, then a lysis buffer was added. The lysate was transferred to centrifuge columns in eppendorf tubes, and spun down at 11,000 rpm for 1 minute, to separate the cell debris from the cytoplasm. The cytoplasm was centrifuged through another column to bind the RNA. An enzyme to digest the DNA was added, and the RNA was washed several times before elution in RNase-free water.

7.2.2 Determination of RNA concentration

The concentration and purity of the RNA solution was measured on a NanoDrop™ 1000 spectrophotometer (Thermo Scientific, software version 3.7), according to the manufacturer's protocol. The absorbance at 260 nm was measured, and the results of the concentration measurements were used to calculate the amount of the solution that was needed for transcription of 2500 ng RNA into cDNA. The absorbance at 280 nm was also measured to calculate the 260/280 ratio. This ratio was used to assess the purity of the mRNA, and a 260/280 nm ratio of approximately 2 was regarded as acceptable (manufacturer information). All samples used for the work presented here were above this threshold.

7.2.3 Reverse transcription

For reverse-transcription of the extracted mRNA into cDNA, the volume of RNA solution equal to 2500 ng total RNA, 7 µl of 5x buffer, 4 µl of 10 mM dNTP, 1 µl of RNAse inhibitor and 1 µl of hexamer primers was pipetted. The volume was adjusted to 20 µl with RNase and DNase free water, and the samples were incubated in a Mini Thermal Cycler (Bio-Rad) for 10 min at 65°C. The samples were then snap-cooled on ice for 2 minutes and 2 µl of reverse transcriptase (M-MLV RT, Promega) added to each sample before further incubation at 42°C for 90 minutes. The obtained cDNA was stored at -20°C until further use.

7.2.4 Real-time PCR analysis on iCycler iQ Real-Time PCR detection system

cDNA was diluted 1 in 10 in RNase/DNase free water prior to use. For each reaction, 0.8 µl of diluted cDNA, 10 µl of iQ SYBR Green Supermix (Bio-Rad) and the appropriate volumes of primers, as well as water (to give a final volume of 20 µl), were added. The sequences of the primers and the concentrations used are shown in Table 3. All primer concentrations have been optimised previously in our group, to yield between 98 and 100% amplification efficiency. 20 µl of the mix of each sample were pipetted into 96-well plates and analysed on the iCycler iQ Real-Time PCR detection system with the iCycler Software (version 3.1, Bio-Rad).

Table 3 Sequences and concentrations of primers used for PCR analysis

Gene	Primer	Sequence	concentration (nM)
β-actin	Forward	5'-TCAGCAAGCAGGAGTATG-3'	300
	Reverse	5'-GTCAAGAAAGGGTGTAACG-3'	300
BRCA1	Forward	5'-ACATACCATCTTCAACCTCTG-3'	300
	Reverse	5'-CGATGGTATTAGGATAGAAG-3'	300
PRAD1	Forward	5'-TGGAATGGTTTGGGAATATC-3'	200
	Reverse	5'-CCTGGCAATGTGAGAATG-3'	200
MYC	Forward	5'-CCACAGCATACATCCT-3'	200
	Reverse	5'-CTTACGCACAAGAGTTC-3'	200
ESR1	Forward	5'-GCCCTCCCTCCCTGAAC-3'	250
	Reverse	5'-TCAACTACCATTTACCCTCATC-3'	250
PGR	Forward	5'-CACAGCGTTTCTATCAACTTAC-3'	200
	Reverse	5'-GCAGCAATAACTTCAGACATC-3'	200
TFF1	Forward	5'-CCGTGAAAGACAGAATTG-3'	200
	Reverse	5'-CGATGGTATTAGGATAGAAG-3'	200

7.2.5 Determination of threshold cycles

Real-time PCR detects the fluorescence emitted by the SYBR Green molecules which are incorporated into double-stranded DNA during the amplification process. The more cDNA with the same sequence as the primer is present in the sample, the faster this set of DNA is

amplified, and the more fluorescence is detected in a shorter time. Each round of amplification is called a cycle, and the PCR detection system recognises at which cycle number the fluorescence intensity in the sample has exceeded the background fluorescence. The value at which fluorescence in the sample is detected for the first time is consequently called threshold cycle (C_t) and is expressed as a cycle number. Thus, the smaller the C_t value for a target sequence, the more of it was present in the original sample and the higher the expression level of this target gene was in the specimen. For amplification of the cDNA, the protocol provided by the iCycler iQ Real-Time PCR detection system was used, and fluorescence was detected in the exponential amplification phase only. The amplification process was performed with the following parameters: cycle 1 (1 repeat), dwell time 3 min, 95°C; cycle 2 (step 1) 10 sec at 95°C, followed by 45 sec at 55°C (step 2). Cycle 2 was repeated 40 times. Cycle 3 (1 min at 95°C), cycle 4 (1 min at 55°C) and cycle 5 (10 sec at 55°C, repeated 80 times) were performed for generation of the melting curve. The melting curved was used to control that the correct DNA sequence was amplified. If only the DNA sequence specified by the primer is amplified, the melting curve peaks at a single temperature, whereas contaminating amplicons have a different melting curve.

7.2.6 Calculation of expression levels

In order to determine from the C_t value of a target sequence if it was affected by treatment, i.e. if its expression level was up- or down-regulated in the MCF-12A cells as a result of the treatment, the values need to be compared to the C_t value of a gene that is not affected by treatments of the cells. Some genes are always expressed at the same levels. These are called housekeeping genes and are used as markers to which the target genes are normalised to. For the analysis of the MCF-12A cells, β-actin was used as the reference gene. C_t values obtained after treatment were also normalised against values from untreated cells (incubated with ethanol at 0.1% (v/v) in basal medium as the vehicle control). Analysis of the C_t values was carried out according to the *Pfaffl* equation (Pfaffl 2001). The method calculates the ratio between the target gene and the reference (housekeeping gene), taking into account the differences between the treated and the vehicle control samples, and generates the rate of the absolute gene regulation. It uses the following equation:

Equation 1 Calculation of absolute gene regulation with the Ct values from target and reference genes, according to Pfaffl (2001)

Ratio = gene regulation, E = efficiency, target = target sequence, ref = housekeeping reference sequence, Ct = threshold cycle, control = vehicle control sample, treated = sample after treatment

$$\text{ratio} = \frac{(E_{target})^{\Delta Ct\ target\ (control-treated)}}{(E_{ref})^{\Delta Ct\ ref\ (control-treated)}}$$

Chapter 3:
Methodological considerations for cell cycle analysis by flow cytometry

1 PRINCIPLE OF FLOW CYTOMETRY

Flow cytometry is a valuable tool to study a variety of questions in cell biology, including cell cycle analysis (e.g. degree of apoptosis after drug treatment), protein expression (e.g. receptor distribution) or the composition of cell populations (e.g. in blood samples) by analysing various parameters, such as DNA content, surface markers, or incorporated bodies, and this for each individual cell in the population. In this thesis, flow cytometry was used extensively to conduct cell cycle analysis, with the aim of determining the fraction of cells that have entered the cell cycle. Various methods are available for this purpose. The subject of this chapter is to briefly explain the principle of flow cytometry and to carry out a comparative analysis of methods for cell cycle analysis.

By bringing a cell suspension into a hydrodynamically focused fluid, cell after cell passes through a tube into which light is sent. When the light beam hits the cell, part of the light is absorbed by the cells, whereas other photons are deviated. On the other side of the flow tube, the light is captured by a detector, and from the number of photons, and the angle in which these reach the detector, conclusions about the physical characteristics of the cell may be made. The most basic information provided by a flow cytometer is the forward scatter (FSC) and the side scatter (SSC). The FSC or low angle scatter is generated when the light beam hits the cell and is deviated slightly. The FSC is roughly proportional to the size of the cells (e.g. for apoptotic cells, FSC becomes smaller). The orthogonal SSC is caused by intracellular bodies. Therefore, the more granular the cell, the higher the SSC (e.g. granulocytes display a higher SSC than lymphocytes).

Prior to analysis, cell components may be tagged with fluorophores, which in turn may be excited by a laser beam of the appropriate wavelength. The fluorescence emitted is captured by the detectors and translated into a signal which allows conclusions about the cell. For

example, if cell surface markers specific for tumour cells are tagged then the amount of tumour cells in a population can be assessed, whereas measuring the amount of apoptotic cells can be an indicator for the efficiency of an anti-cancer drug. In general, cell cycle analysis is used to study the effects of a treatment on a cell population; conversely, understanding the critical points of cell cycle progression in a specific population creates the possibility to deliver drugs in a more targeted fashion. In the following section, the flow cytometric analysis of the cell cycle, its underlying method and the arising limitations are discussed:

The different phases of the cell cycle are characterised by their different DNA content. In the gap phase 1 (G1), cells possess a single set of DNA (2n), which they duplicate during the synthesis (S) phase of the cell cycle. The DNA quantity (4n) remains stable throughout the second gap phase (G2) before the cells enter mitosis (M phase). Therefore the DNA content is a good marker to assess the cell cycle profile and progression of a cell population.
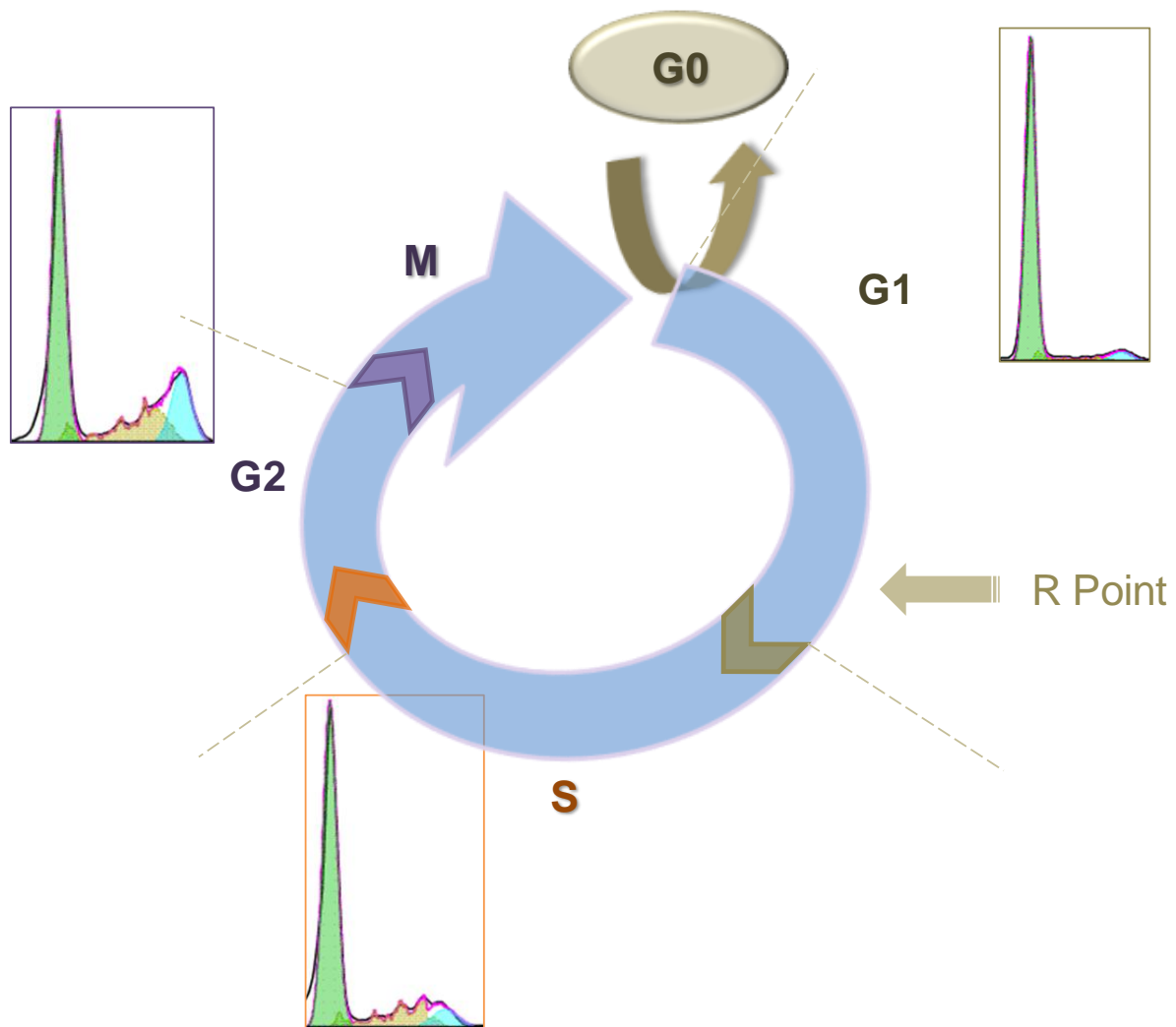
Figure 2 Schematic representation of the cell cycle

The cell progresses through gap phase 1 (G1). Once it has passed the restriction point (R point), it is committed to start DNA synthesis in S phase, followed by a second gap phase (G2) and mitosis (M). The cell can withdraw from the cell cycle (any time between completed mitosis and the R point) into the quiescent G0 phase, which can be induced by changes in culture conditions (cf. page 51). For each cell cycle phase (G0/G1, S and G2/M), a typical flow cytometric histogram is depicted (obtained from MCF-12A cells).

Several different fluorescent dyes are available that stain specifically nucleic acids. Commonly used stains include diaminophenylindole (DAPI), *Hoechst* stains, 7-aminoactinomycin-D (7-AAD) and DRAQ5. Each of these stains binds stoichiometrically to nucleic acids which makes them an excellent use for quantification of DNA. However, it also means that, since both DNA and RNA are tagged, the one nucleic acid that is not of interest

must be removed prior to analysis. The RNA is digested by a specific enzyme (RNase) before adding the stain, so that only DNA is bound.

For the purpose of this thesis, the fluorescent compound propidium iodide (PI) was chosen which intercalates between the bases of double stranded nucleic acids. The maximum of the absorption curve of PI lies at λ_{Ex}=495 nm, therefore an argon laser emitting at 488 nm is used to excite this dye. The maximum of the light emitted by PI is at λ_{Em}=637 nm. Prior to flow cytometric analysis, the cells were fixed in their shape, and the cell membrane is permeabilised before incubation with the DNA stain, followed by flow cytometric analysis (for details of the fixation protocol please refer to Chapter 2, page 19).

Initially, all events (= single cells, stained or unstained) were recorded. A variety of formats is available to display the information gathered from the cell population. The basic representation for unstained samples is a so-called dot plot that displays the SSC over the FSC, shown in Figure 3. Additionally, this heat map illustrates where most cells were accumulated on the dot plot. Red indicates the spot with the highest cell density, and the cooler colours represent the least dense areas. In the example, the cells were concentrated between 300 and 400 AU on the x-axis, and therefore no major difference between the cell sizes existed (the units on the axes are arbitrary for the number of photons). The cells also had a similar granularity, as indicated by the SSC, with only a few events being detected above 600 AU. These events were likely to consist of cell clumps or, further upwards, air bubbles, and should therefore be eliminated from the subsequent analysis. No signals were detected below 300 AU, which would have been indicative for cell debris. The data analysis software lets the user draw manually a gate around the region of interest, and, like in this case, to exclude some events from the subsequent analysis (see the oval in Figure 3). The gate signifies the cells considered for further analysis, and the percentage of the cells within or outside the gate can then be calculated. It is important to assess the FSC as well as the SSC for each experimental set-up before the fluorescence analysis, in order to exclude any noteworthy changes between different cell batches (e.g. significant change in cell size), as well as air bubbles that are recorded as real events and can lead to misinterpretation of the total cell count and consequently the later analysis.
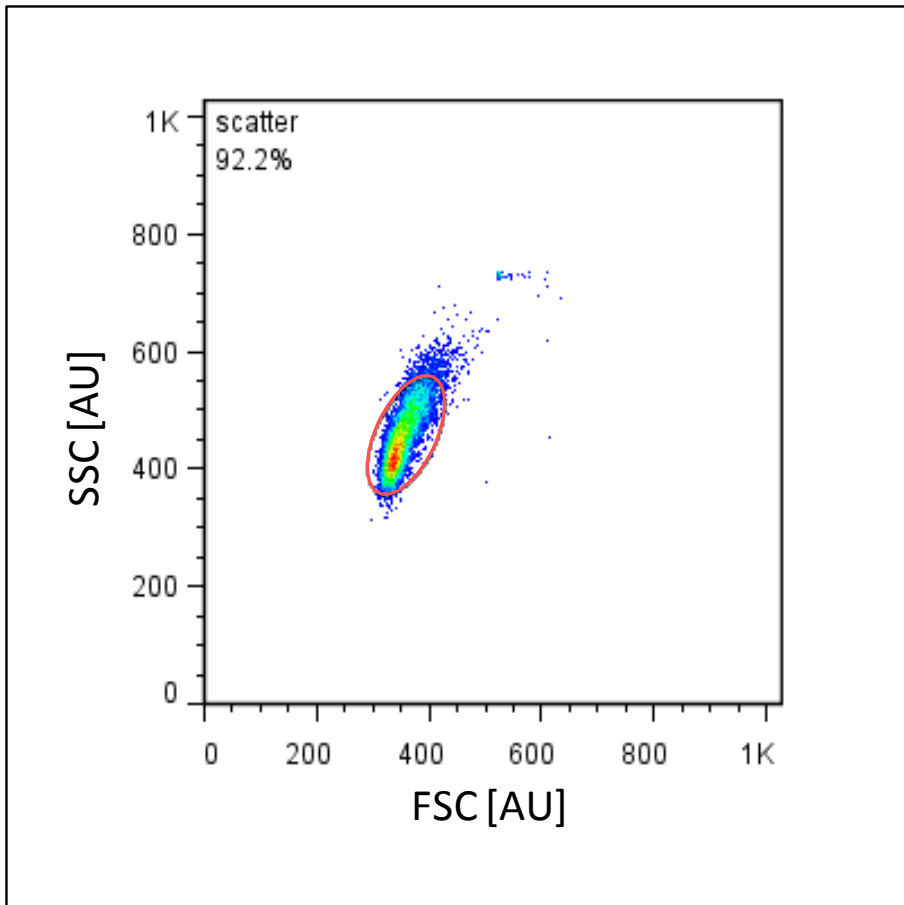
Figure 3 Density scatter dot plot of a sample of MCF-12A cells

The x-axis shows the FSC recorded, which allows conclusions about the size of the cells. On the y-axis, the SSC (intracellular complexity) is shown. The units on both axes are arbitrary for the number of photons (AU). In this flow cytometric analysis all the information was acquired with white light. The dots represent the individual events detected and the heatmap illustrates the amount of events in the respective area with red indicating a high and blue a low number of events. The oval shows the cell population chosen for subsequent analysis; it defines the gate.

When cells are stained with a fluorescent marker prior to cytometric analysis, the fluorescence emission of each single cell is measured and can be shown on both axes in a similar dot plot as the basic version with white light (Figure 3), but this time with the peak height of the fluorescence signal versus the integral of the signal. An example for the detection of PI labelled cells, indicating the DNA content of the analysed cells is shown in Figure 4. If a homogeneous population (in terms of cell type) has been stained evenly (i.e. no gradient in PI concentration), the height of the signal is proportional to the intensity of the signal. Therefore, all events should lie on a diagonal line. Events that show a larger area under the signal, but the same signal height, are generated from cell clumps, whereas events

with increased fluorescence on both axes are polyploid. An increase in signal height, with no changes of the area under the signal, indicates a problem with the staining procedure (e.g. PI concentration gradient).
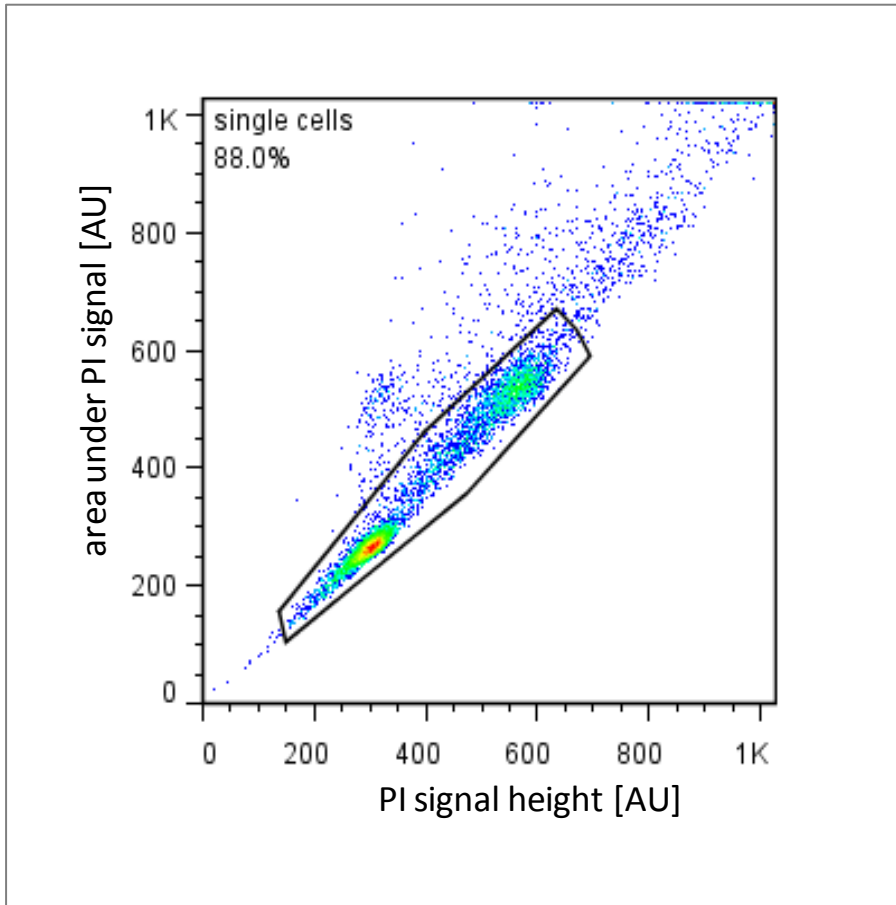
Figure 4 Dot plot of fluorescence signals acquired of PI-stained MCF-12A cells

On the ordinate, the area under the fluorescence signal is shown, whereas the x-axis represents the height of the signal. The sample shown is from MCF-12A cells (serum depleted for 24 hours, fixed with 70% ethanol on ice and stained with PI). The axes show arbitrary units of fluorescence intensity (0 to 1000 AU). The heatmap indicates the concentration of cells in the respective area, with red being the densest spot, and blue showing where fewer events were detected. The polygon drawn around the dot plot shows the cells considered for analysis (the gate).

The cells analysed in the example used in figures 2-8 were accumulated in the G1 phase. Cells in G1 are detected at around 300 AU and indeed a high density of cells was seen at this intensity, as shown by the red colour. Cells that had duplicated their DNA content and were in G2 phase emitted double the amount of fluorescence and were found at roughly 600 AU. Again, unwanted events (cell debris, found in the lower left corner, and agglomerated cells, above the diagonal) were excluded from the subsequent analysis by drawing a gate manually around the region of interest. In Figure 4, the percentage of cells included in the gate (i.e. all events inside the polygon, here referred to as the fluorescence gate) was calculated based on the proportion included in the scatter gate (Figure 3). Thus, 88% found in the fluorescence gate correspond to around 81% of the total number of events recorded initially. The number of cells included for further analysis, even if the gates were drawn automatically (a function available in some software), is variable and strongly dependent on several parameters, such as the cell type, the amount of serum used in the cell culture medium, and the fixative. For instance, cells grown in medium with a high percentage of animal serum tend to clump together more than cells grown in low-serum medium. However, if the proportion of cells detected as single events is stable (within a range), for samples prepared under the same conditions, it indicates that the protocol used is robust.

After the exclusion of all unwanted events by gating them out of the initial population, the data from the remaining cells was used for cell cycle analysis. To this end, the dot plot was transformed into a single parameter histogram, which plots the cell count versus fluorescence intensity recorded for each cell. The fluorescence intensity can represent the height of the signal, the width of the signal, or, more commonly, the area under the signal. The representation in such a frequency histogram allows the user to more easily distinguish between the features of cells in different phases of the cell cycle (Figure 5).
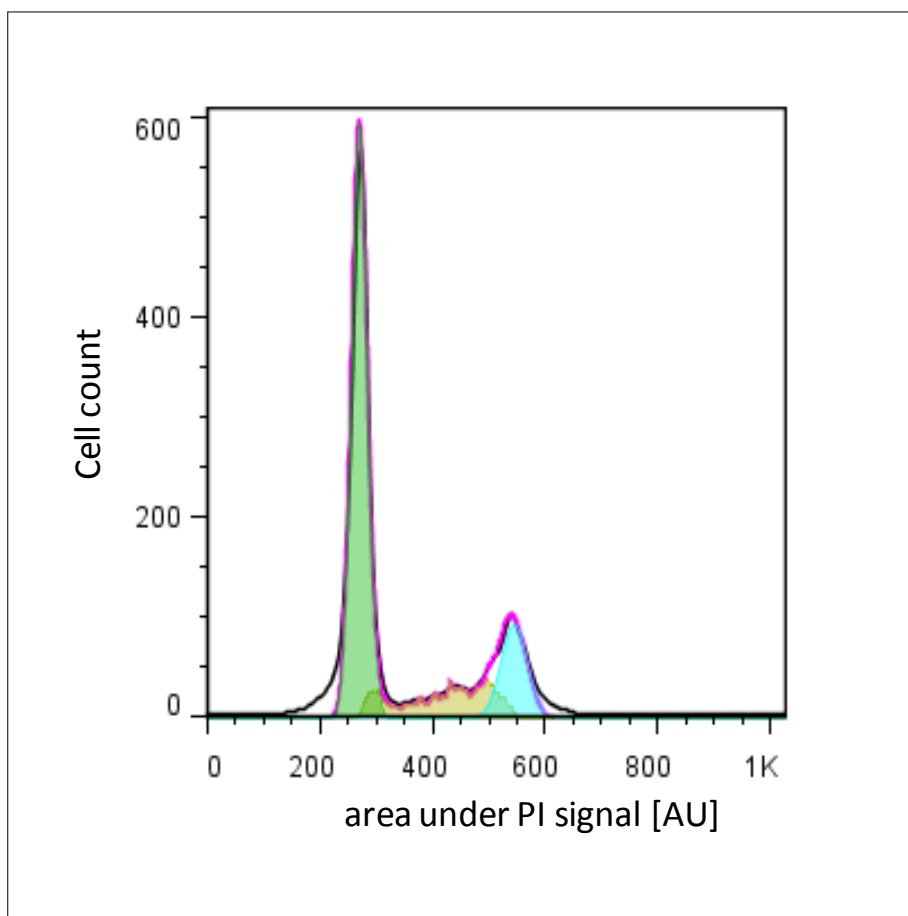
Figure 5 Frequency histogram of fluorescence signals acquired from PI-stained MCF-12A cells

The ordinate shows the number of cells counted for each discrete fluorescence intensity, whereas the x-axis represents the area under the signal acquired at each intensity increment. The x-axis is graduated with arbitrary units of fluorescence intensity (0 to 1000 AU). The sample shown is from MCF-12A cells (serum depleted for 24 hours, fixed with 70% ethanol on ice and stained with PI). The shaded areas were added automatically by the analysis software; the green shading shows the proportion of G1 phase cells, the ochre area shows the distribution of S phase cells, and the blue area stands for the cells in G2+M phase.

The frequency histogram is also the basis for calculating the distribution of cells in the different cell cycle phases. In a frequency histogram, the peak furthest to the left corresponds to cells in G1 with the respective DNA content, whereas the second peak will be found at approximately double the fluorescence intensity, showing the cells in G2 phase (cells that have duplicated their DNA). Since it is not possible to distinguish the G2 phase from the early M phase, because they comprise the same amount of DNA, the second peak is usually referred to as G2+M. In a normally distributed population, a small (low counts), but broad

35

area (equal to many different amounts of DNA per cell) in between the two peaks can be seen, which characterises the cells that are in the process of replicating their genome in the S phase of the cell cycle. The proportions found to the left of the G1 peak and to the right of the G2+M peak are termed sub-G1 and super-G2 respectively. The latter represents an important population in cancer cells, as the super-G2 portion consists of events with more than two copies of the DNA set (> 4n), found in polyploid cells. Accordingly, the sub-G1 population contains cells with less than 2n DNA. Different methods to perform these calculations are discussed in the following section.

2 CELL CYCLE ANALYSIS – CHOOSING THE RIGHT METHODS

Cell cycle analysis is performed by dividing a frequency histogram according to the peaks of the G1, S and G2+M phase. The peaks may be determined by the user, or automatically with the use of specific cytometry software. The differences between these methods, and the parameters that need to be considered when deciding for or against a specific method, are discussed in the following section. Furthermore, the cell cycle distributions of MCF-12A cells according to three different methods are presented and compared to each other, and the deviations between the methods are tested for their significance.

2.1 Cell cycle phase distributions: automated calculation methods vs. manual gating

2.1.1 Mathematical models used for cell cycle analysis

The flow cytometer used in the work described here was the MACSQuant® Analyzer, with the integrated MACSQuantify™ Software for data analysis. This software does not perform automatic cell cycle analysis, but the populations in the different cell cycle phases had to be distinguished visually by the user, followed by manually drawing the gates for each phase. However, the data acquired on the MACSQuant® Analyzer can be exported into a standard file format (flow cytometry standard (FCS) format) and analysed with other cytometry software. Some commercially available cytometer programs allow automatic calculation of the percentages of cells comprised in each peak. As can be seen in the example in Figure 5, in the originally acquired curve it is particularly difficult to decide visually where the S phase starts and ends, because overlaps between the phases occur. In contrast, when analysing the data automatically, the overlaps are taken into account by the mathematical estimations. Many different models have been developed, customized to various research goals. The different models use one or more of the possible model components, such as Normal distribution (used for the G1 and G2+M populations), a broadened rectangle, trapezoid or polynomial to fit the S phase, and exponential curves for the debris.

All models make the assumption that the G1 and G2+M peaks follow the Normal distribution, but they differ in the way in which the S-phase component is calculated. Which component to choose depends on the characteristics of the sample, for example the rectangle component is preferred for histograms generated from solid tumours (Rabinovitch 1994).

It is evident that for the same sample, the results for the percentages will vary with each model, depending on how well the model fits the actual curve. One possibility to decide which algorithm is the most suitable is to determine the values for the root mean of the square (RMS). The RMS value states the gaps that occur where the model does not align with the true curve and therefore the smaller the values for the RMS are, the better the model fits the data. However, the RMS values from one model cannot be compared to the values obtained for a different calculation, and there is no absolute threshold value above which the fitted curve should be rejected. Instead, the RMS values acquired within the same analysis method should be compared to each other and ideally to an internal control sample, and the decision to reject an outlier is at the user's discretion. Secondly, the mathematical curve that is drawn onto the sample curve should be assessed visually and rejected if major discrepancies are noticed. If rejected, the user must assign the peaks manually, or use a different model entirely.

Two of the models that are favoured for cell cycle analysis by most analytical software, the *Dean-Jett-Fox* model and the *Watson* model, will briefly be discussed here.

The algorithm suggested by Dean, Jett and Fox (Fox 1980) fits Normal distributions to the G1 as well as the G2 peak. It has the advantage that in addition to this, it also fits the S phase with a smooth polynomial curve. It is based on the model originally developed by Dean and Jett (Dean and Jett 1974). The original model lays a curve onto the synthesis phase, which was chosen to be very broad in order to account for the spreading of the fluorescence intensity due to staining variability or biological factors. The limitation of this model was that the distributions fit only where a second order polynomial can actually represent the S phase data. This left out many synchronised populations where actual peaks can be observed for the S phase population, depending on the synchronisation method and efficiency. Fox enhanced this mathematical model by adding a single normal curve on top of the polynomial in the S phase region, which should make the function fit more complex S distributions data, such as most synchronised populations. A central issue for this model relates to cases where a large amount of *late* S phase cells dominates the G2+M peak, and therefore the second peak is not easily recognised. In this case, the location of the G2+M peak and its coefficient of variation (CV) must be fixed in relation to the G1 peak. In this case, the CV is forced to be the same as that found for the G1 peak, and the peak location is a constant times the x value for G1 (location of G1 peak maximum on abscissa, x_{G1}). The constant is usually 1.9 for this system,

but the proper value to be used depends on the flow cytometer system being employed, thus must be determined independently by the user.

The model developed by Watson and co-workers (Watson et al. 1987) calculates gap phase peaks in a way similar to Dean, Jett and Fox, but it does not attempt to construct a fit curve for the S phase. Instead, it calculates the probability for finding an S phase cell at each point of the curve. Because of this, it is applicable for most populations and therefore is the more widely used algorithm. It employs the following approach:

The program starts by looking for the highest frequency of cells, where it sets a first, approximate value for the G1 mean and its standard deviation (SD, the width at 60% of the maximal height). Afterwards, a least-square fit is performed between the Normal distribution and the curve from the actual data (cf. *RMS* on page 38). In the next step it computes the mean and SD values for the G2+M peak. The mean for the second peak is assumed to be at 1.75 times the G1 mean, and the SD value is again taken at 60% of the maximal height. Again, a least-square control between the Normal distribution and the real curve is processed. The least-square fit is carried out over a range of -1 to +3 SDs (for the G2+M peak) and -3 to +1 SDs for the G1 peak, respectively, to minimise contributions from the overlapping S phase proportions. Then the model constructs a probability distribution for the S phase cells. Underlying are the two constants kG1 and kG2, which designate the boundary between G1 and S, and between S and G2+M, respectively, where the probability to find an S phase cell is exactly 0.5 each time. The values for the constants are determined in an iterative process, starting from estimates as before. Once the S phase distribution has been estimated, it is subtracted from the total histogram to obtain the plain values for G1 and G2+M. These are cross-checked with the initially computed ones, and if they deviate too much, the values for the mean and the standard deviations are adapted. This iterative process is repeated until a good agreement between the prediction and the actual curve is achieved ($< 2.5\%$ discrepancy between any two pairs) (Watson 1992; Watson et al. 1987).

2.1.2 Variability of cell cycle analysis with the exemplary methods

In order to make a valid decision about which method to employ for the data analysis in this thesis, all samples were analysed for their cell cycle distribution by 3 different means, and the results obtained by the three approaches were compared:

Firstly, the model of *Dean-Jett-Fox* was used for automatic estimation of the percentages for each cell cycle phase. This algorithm places a Normal distribution on the two G peaks, and additionally a polynomial component on the S phase curve.

Secondly, the algorithm according to *Watson* was applied to the samples and the cell cycle phase figures calculated automatically. The Watson model fits a Normal distribution onto the G1 and the G2+M peak, and calculates the S phase proportion by computing the probability to find a S phase cell at every channel (along the abscissa).

The third method consisted of drawing the gates *manually* for the three main phases. This was accomplished by initially analysing one sample that allowed for good visual differentiation between the different cell cycle stages, which was always the negative control sample, i.e. cells that had been serum-depleted for 24 hours and therefore accumulated in the G1 phase. In these samples, the first peak (G1 phase peak) was relatively sharp which facilitated setting the limits. Once the gates had been set on this population, the exact same gates were applied to all other samples in the same experiment (i.e. equivalent batch of cells and preparation for flow cytometry and cytometric analysis on the same day). The gates obtained in this way were only adjusted if major differences in the scatter or the fluorescence dot plots were observed; the latter is the case when the fluorophore : DNA ratio is altered, either due to a sample containing a much higher (or lower) number of cells and / or a significantly different amount of fluorescent dye in the sample, therefore changing the overall number of emitted photons. If the values for the control samples (i.e. a sample that should show the same cell cycle phase distribution for every independent experiment) are comparable between batches, and the analysis is done by the same user, this analysis can be as accurate as a mathematical model. This is true especially if many samples have very differently shaped curves, because in these cases, the model curves set by the automatic system must be adapted yet again manually by the user.

For the following section, one sample was chosen as representative example, with the purpose of demonstrating in more detail the differences between the methods, when applied on the same data set. The representative sample was a negative control, i.e. cells had been serum-starved for 24 hours to accumulate them in G1 phase. The raw data obtained by flow cytometric analysis was used subsequently for analysis by the three different methods described before. The various steps that are taken for the analysis by each approach will be shown in more detail, and the cell cycle phase distributions obtained through each method will be presented. As will become apparent in the following section, the results vary from one

method to the other, and the reason for these differences shall be discussed in more depth, in order to explain the rationale behind the selection of the method, used in the remainder of this thesis.

Figure 6 shows the cell cycle profile of a sample that was chosen for the comparative analysis (MCF-12A cells, 24 hours serum-depleted for accumulation in G1 phase). The data was acquired with a MACSQuant® Analyzer, and was either analysed manually using the integrated software (MACSQuantify™), or transformed from *mqd* format into *fcs* format (cf. page 37) and re-analysed automatically using FlowJo™ software (Tree Star Inc., version 7.6, free trial license) with the embedded algorithms.
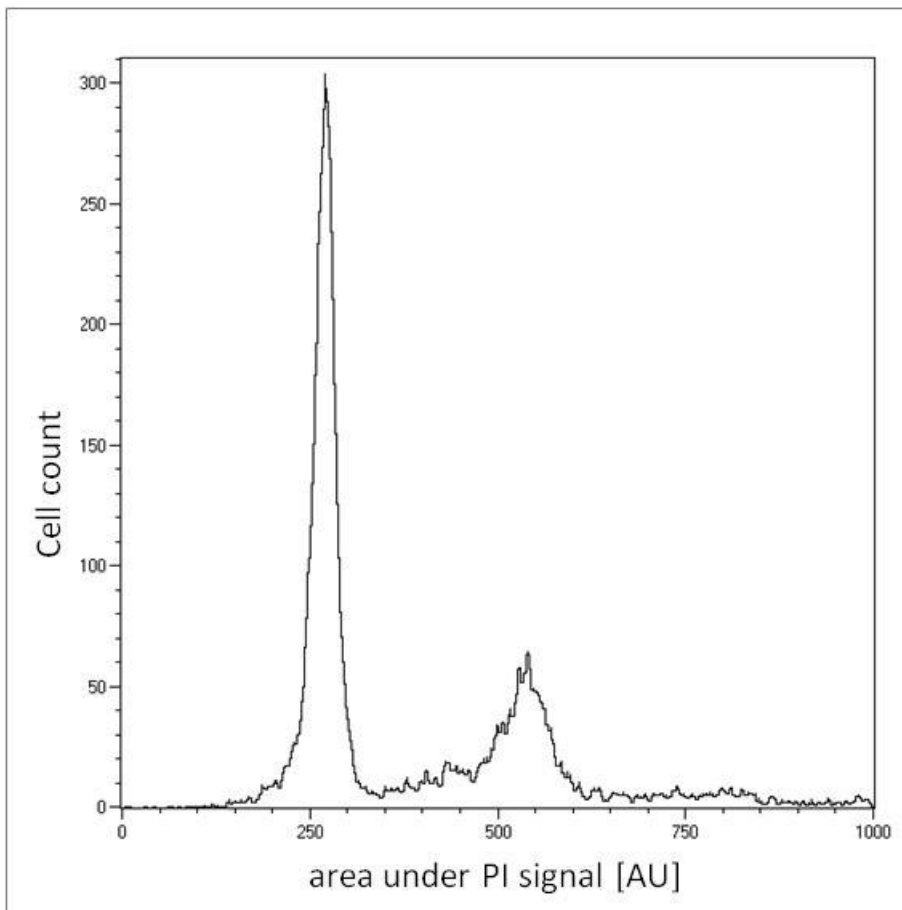
Figure 6 Frequency histogram of fluorescence signals, as acquired on the MACSQuant® Analyzer

Fluorescence signals were acquired from PI-stained MCF-12A cells (serum depleted for 24 hours and fixed with 70% ethanol on ice). The ordinate shows the number of cells counted for each discrete fluorescence intensity, whereas the x-axis represents the area under the signal acquired at each intensity increment. The x-axis is graduated with arbitrary units of fluorescence intensity (0 to 1000 AU).

2.1.2.1 Analysis applying the algorithm based on Dean-Jett-Fox

The pink line in Figure 7 represents the curve as calculated by the Dean-Jett-Fox-algorithm and is fitted onto the acquired data. The Normal distribution for the G1 peak, as estimated by the mathematical model, is shown in green, the Normal distribution for the G2+M peak is coloured in blue, and the ochre area shows the distribution of the S phase cells. For each cell cycle phase, the following percentages were calculated: G1=63.3%, S=12.8% and G2+M=17.5% (RMS=2.4). This algorithm models the S phase by adding a polynomial curve to it, and hence its estimate is not as precise as the actual (experimentally observed) curve shown in black. A difference is also seen for the G2+M peak, since not the entire area is covered by the model.
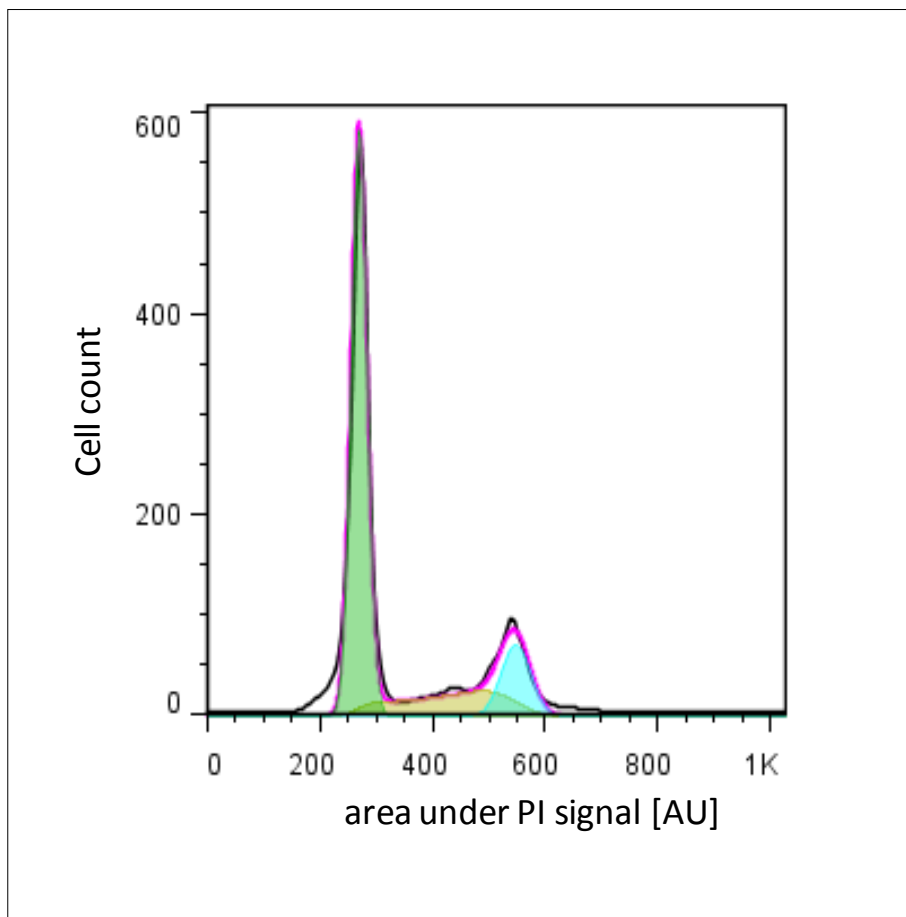
Figure 7 Analysis of frequency histogram based on *Dean-Jett-Fox* model

Example of flow cytometric data represented as frequency histogram and analysed with the Dean-Jett-Fox model: the algorithm (pink curve) is fitted to the experimentally observed curve (black). Green shows the area attributed to the G1 peak, the ochre area represents the S phase population, and blue shows the area of the G2+M peak. Axis labelling: y-axis shows cell count, x-axis shows the fluorescence intensity based on the area under the signal, in arbitrary units (0 to 1000 AU).

2.1.2.2 Analysis applying the algorithm based on Watson

Next, the same sample was subjected to an automatic analysis using the Watson algorithm. For each cell cycle phase, the following percentages were determined by the software: G1=62.5%, S=15.7% and G2+M=15.1% (RMS=2.5). As can be seen in Figure 8, the pink model fits neatly onto the acquired black curve, and the peak of the G2+M phase cells is found at twice the fluorescence intensity of G1. The sub-G1 frequency (5.3%) and super-G2 (2.1%) are also estimated, but no model curve is used for these populations. Simply, everything to the left of the G1 peak is considered as the sub-G1 population, likewise for the super-G2 to the right hand end of the histogram. It will be noticed that the percentages, when added up, exceed 100% because the overlapping areas are not subtracted from each other, as the values derive from estimates for each phase.
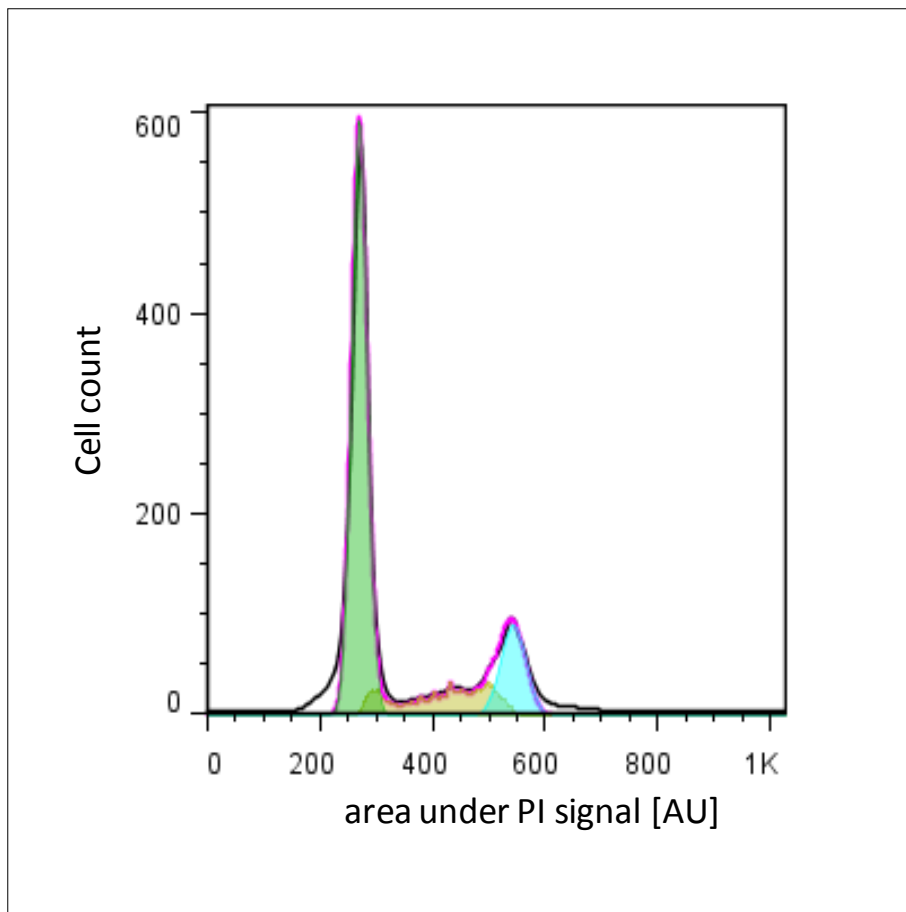
Figure 8 Analysis of frequency histogram based on *Watson* model

Example of flow cytometric data represented as frequency histogram and analysed with the Watson model: the algorithm (pink curve) is fitted onto the actual curve (black). Green shows the area attributed to the G1 peak, the ochre area represents the S phase population, and blue shows the area of the G2+M peak. Axis labelling: y-axis shows cell count, x-axis shows the fluorescence intensity based on the area under the signal, in arbitrary units (0 to 1000 AU).

2.1.2.3 Analysis with manually set gates

Since the sample chosen for this analysis was derived from cells that had been accumulated in the G1 phase, the resulting G1 peak was reasonably sharp and the limits could be set relatively straightforward (Figure 9). However, the border between the S and the G2+M phase was not easily distinguished visually. It was taken into account that the value for the G2+M peak should be calculated from the G1 phase (G2 = 2x G1) and the gate was set accordingly. The frequencies for the sub-G1 and the super-G2 populations were based on visual estimations only. Obviously, these also depended on how narrow the gates for the other peaks were set, but contrary to the main peaks, these were not of interest and variations were neglected. The proportion of cells in S-phase resulted from the gate positioned between the G1 and G2+M gates. Generally, this method underrates the amount of cells in the synthesis phase, because the overlaps between G1 and S, as well as between S and G2+M, cannot be estimated.

The manual analysis yielded the following results for this sample: G1=69.9%, S=8.6%, G2+M=18.8%, sub-G1=1.3%, super-G2=1.4%. Since the boundaries for the different phases are not set overlapping, the total estimates must add up to a total of 100%. This is different for the automated calculations, and an overview of the final results obtained by the three methods is given in Table 4.
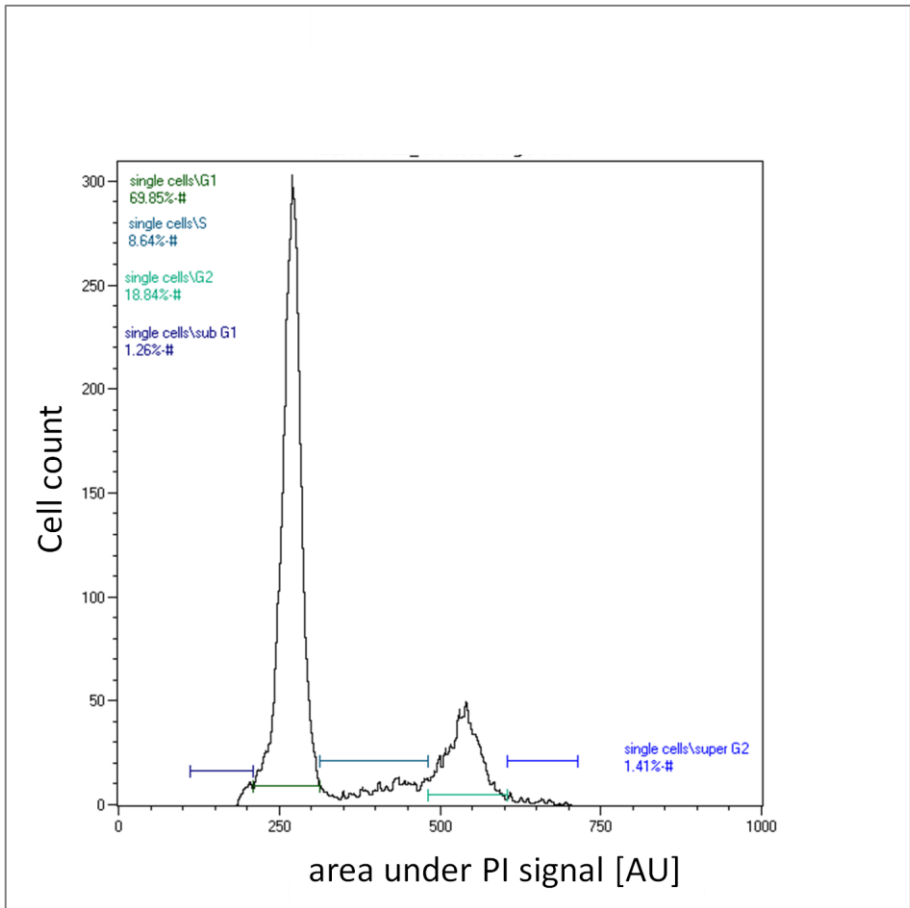
Figure 9 Analysis of frequency histogram based on manual gating

Example of flow cytometric data represented as frequency histogram and analysed with manually drawn gates for each cell cycle phase. Axis labelling: y-axis shows cell count, x-axis shows the fluorescence intensity based on the area under the signal, in arbitrary units (0 to 1000 AU).

Table 4 Overview of results from cell cycle phase calculations

Three different methods were used to analyse the same sample for calculating the percentages for the cell cycle phases.

[%]	Dean-Jett-Fox	Watson	Manual
G1	63.3	62.5	69.9
S	12.8	15.7	8.6
G2+M	17.5	15.1	18.8
sub-G1	-	5.3	1.3
super-G2	-	2.1	1.4
sum	93.6	101.3	100
RMS	2.4	2.5	-

In summary it can be said that analysis with the Watson model resulted in higher S phase percentages than the application of the Dean-Jett-Fox algorithm. The Dean-Jett-Fox model again yielded higher S phase percentages than the manual analysis of the frequency histograms. Based on the results with the one sample chosen as an example, it was important to understand if this was a general feature for similar analyses on the same cell line. More importantly, it should be excluded that the result obtained with one algorithm depended on the cell cycle distribution of the sample. This means, no pattern in the outcome should be seen, e.g. that all samples with a high G1 percentage always yield the highest S phase percentage with the Watson model, but that this is not the case anymore when G1 is lower. Hence, two questions need to be answered:

Is the finding that the sum of S+G2+M phase percentages are highest with the Watson algorithm and lowest with the manual analysis a general feature of this analysis? And if not, does the percentage found with each method depend on the cell cycle distribution of the sample?

In order to answer these questions, a systematic comparison between the three methods of frequency histogram analysis for all samples presented in this work was performed. The findings are discussed in the following section.

2.1.3 Systematic comparison of results obtained by the exemplary methods

Since the results of the work performed for this thesis were expressed by the differences in the number of cells able to progress into the cell cycle, i.e. to leave G1 phase, the sum of the percentages found for S and G2+M phase was calculated. Thus it was more useful to document the differences between the samples in terms of this *sum*, rather than to compare the absolute values for each phase of each sample, for evaluating the three different methods for cell cycle phase analysis. In order to compare the methods, the differences between the sums of S+G2+M phase for all analysed samples were calculated. In total, 511 samples analysed with flow cytometry are presented here. Table 5 gives an overview of how many samples were found to be different from each other through the different methods, and to what extent. It was decided to assess the number of samples different for each method *in relation to the manual* method, because with the user-based approach, the gates for the distinct phases were set manually solely on the negative control (i.e. serum-depleted, G1 phase accumulated cells), and these very gates were then applied to all other samples.

Therefore this method provided a good origin for comparisons between the negative control and treated samples.

Table 5 Overview of the total number of samples found to be different for the three approaches for cell cycle analysis

The sum of the percentages obtained for S, G2 and M phase was calculated for each sample, for each analysis method. The difference between the sums obtained with the three different methods was calculated for each sample.

difference in the percentages of the sum of S+G2+M	number of samples found to be different		
	S+G2+M (Watson) – S+G2+M (manual)	S+G2+M (Dean-Jett-Fox) – S+G2+M (manual)	S+G2+M (Watson) – S+G2+M (Dean-Jett-Fox)
<-10%	19	96	33
<-5 to -10%	28	20	43
<-0.1 to -5%	55	45	137
from 0 to 5%	222	168	171
>5 to 10%	118	96	36
>10 to 15%	51	40	14
>15%	18	46	77

The automated analyses were performed subsequently with the aim of possibly increasing the significance between negative controls and treated cells, because the manual method often underestimates the S phase. Since this was the phase of outmost importance for the work presented here, a model that takes this phase into account more precisely was preferred. The differences between the approaches mainly arise from the overlaps between S and G1 phase, which could not be taken into account with the manual method. This is a clear disadvantage of the manual approach, and another reason for preferring an automated calculation for the final analysis. The overview in Table 5 was generated in order to evaluate precisely which of the two models was more suitable. The majority of samples (340 out of 511) analysed using

the Watson model included no more than 10% more cells in S+G2+M phase than the original results ("original" refers to the values obtained with manual gating). Surprisingly, for some samples (102 samples), the Watson model calculated less cells in S+G2+M phase than the manual method. However, this was still less often the case than with the Dean-Jett-Fox model. The finding that this other automated calculation underestimated more often the amount of cells in S+G2+M phase had already been suspected, because when looking at the modelled distributions, they did not match well the true curve, as seen in Figure 7. Nevertheless, a systematic analysis of the *deviations between the methods* was performed. Firstly, a comparison of the sum of S+G2+M phase percentages was carried out by performing a Student's *t*-test for all 511 samples, analysed by the three methods, which showed that no significant difference exists between the results obtained by the distinct methods (Table 6).

Table 6 Overview of the differences between the three methods analysed

The mean was calculated for the sum of S+G2+M phase percentages obtained with each analysis method for 511 samples. The differences between the methods are not statistically significant (Student's *t*-test, P=0.01).

	mean [%]	SD
manual gating	29.7	±16.3
Watson algorithm	33.2	±17.4
Dean-Jett-Fox algorithm	34.0	±18.2

Next, the samples were analysed based on the differences between two methods. Albeit not statistically significant, as presented in Table 6, it must be excluded that these differences occurred following to a trend, since clearly this would bias the choice of the best suited method. Notably, the deviation must not be generated according to the cell cycle distribution (since this was the parameter by which samples were distinguished). First, the deviation between the manual and the Watson method was assessed. To this end, all samples were expressed as the difference in the sum of S+G2+M phase between manual analysis and analysis with the Watson algorithm. Then, these values were divided into three groups. Group 1 consisted of the samples with the majority of cells in G1 phase (319 samples), group 2 included the samples were S phase cells were predominant (107 samples), and the samples with mostly G2+M phase cells were in group 3 (77 samples). (The division was based on the original results obtained with the manual gating analysis.) A Student's *t*-test was then

performed between two groups. It was expected that no statistical significance between the mean values of the groups was found, because only then could be excluded that the deviation between the analysis methods was due to the cell cycle phase distribution. Indeed, the difference between the mean values of all possible comparisons between the groups (group 1 with group 2, group 2 with group 3 and group 1 with group 3) was statistically not relevant, as shown in Table 7. The same analysis was then performed for the deviations between the Dean-Jett-Fox model and the manual gating method, also shown in Table 7. Here it was seen that for the samples that were found to be in G2+M phase, the difference in the cell cycle analysis between the Dean-Jett-Fox algorithm and the original method was statistically significant, meaning that the outcome for each method was highly dependent on the phase distribution. This is due possibly to the shape of the frequency histogram which makes it difficult to find the correct cut off between the S phase and the G2+M phase peaks. The reason why such an important difference is found between the manual and the Dean-Jett-Fox method, but not with the Watson model, lies in the mode in which the two algorithms generate the models on the actual curves. The Dean-Jett-Fox algorithm fits a polynomial curve on the S phase distribution which is especially problematic with samples having a large number of (late) S phase cells, as discussed before (cf. section 2.1.1 of this chapter). In contrast, the Watson algorithm calculates the probability of finding an S phase cell at each point and therefore provides a model much closer to the actual curve.

Table 7 Overview of the differences between the methods

Samples were expressed as the difference in sum of S+G2+M phase percentages obtained with manual or Watson or Dean-Jett-Fox method, respectively. The values obtained were divided into 3 groups according to the cell cycle distribution of the sample and a Student's *t*-test was performed between the groups. Shown are the mean values of the differences for each group (standard deviation in brackets). The value that is statistically different from the other groups is marked with ******* (P=0.01).

	sum S+G2+M (Watson - manual)	sum S+G2+M (DeanJettFox - manual)
group 1 (G1 phase samples)	4.02% (±7.6)	1.45% (±17.4)
group 2 (S phase samples)	3.70% (±8.5)	-0.87% (±17.4)
group 3 (G2+M phase samples)	3.59% (±10.1)	-8.75% (±25.7)*******

2.1.4 Summary of results obtained by the exemplary methods

Since it is preferable to eliminate subjective analysis of samples, generated during the gating applied by the user, the aim was to find an automated algorithm for cell cycle analysis of the MCF-12A cells. Due to the method of manual gating, differences between this method and an automated analysis were found, as expected. It was important, however, to assure that this was not a systematic error, for example depending on the cell cycle phase distribution. Hence, a systematic analysis of the differences was performed. The deviations between the results obtained with manual gating and the model according to Dean-Jett-Fox were caused by the method underlying the automated algorithm and resulted in a systematic error when the frequency histogram displayed a large number of G2+M phase cells. Therefore, this algorithm was not suitable for cell cycle analysis of the MCF-12A cells. In contrast, the differences between manual gating and the Watson model were not significant and in good agreement with each other. Besides, this model generates curves very close to the true data because of the theory underlying the algorithm (discussed above in section 2.1.1 of this chapter).

2.1.5 Discussion

All the results presented in this thesis were initially analysed manually with the MACSQuantify™ Software, i.e. the software generated a frequency histogram in which the gates for the cell cycle phases were positioned. In each batch, the negative control samples were analysed in this way first, and then the gates were applied to the remaining samples of the same batch. However, this software was developed specifically for analysing clinical blood samples with a focus on population studies. Furthermore, the algorithm by which this software transforms fluorescence signals into a frequency histogram is not well suited for subsequent cell cycle analysis (personal communication from manufacturer). Additionally, the data analysis requires manual input from the user, resulting in possibly significant inter-experimental variations.

In order to pool data acquired in independent experiments, automatic analysis is preferable. The commercially available Flow Jo software was specifically developed for cell cycle analysis and was suitable to apply with the data acquired from MCF-12A samples. Therefore a second stage of analysis was performed, where all samples were subjected to an automated calculation with the FlowJo software (version 7.6). Two different mathematical models were explored for the analysis, one based on Dean-Jett-Fox, and one according to Watson (Watson

et al. 1987; Fox 1980). In general, both automatic calculations yielded higher numbers for the S phase than the manual system, the main reason being that all phases are shown in an overlapped manner in the histogram, which cannot be estimated visually, whereas the mathematical models take these portions into account to some extent. However, the same problem may persist even when an automated approximation is used, as was found in a comparative review of many models carried out by Baisch and colleagues (Baisch et al. 1982). The methods they compared yielded reasonably accurate numbers for each cell cycle fraction (relative error between 10 and 20%), but also here, mostly the G1 part tended to be overestimated, and the S phase value to be underestimated. In addition, variations in the shape of the S phase distribution caused considerable errors. These can be corrected by the user but not automatically, which is a clear advantage of the manual method.

With the samples analysed for the present work, it was noticed that with the Dean-Jett-Fox calculations, the G2+M peak had to be adapted quite often by the user. This was due to the fact that this model assumes the G2+M peak at 1.9x the cell number corresponding to the G1 value (cf. page 38) hence the proportion of the second peak became much greater. However, it was more appropriate to place the second peak at 2x the G1 peak. This was one reason for deciding against the Dean-Jett-Fox model. The second reason was the fact that it models the S phase populations. Since this was the fraction of outmost interest, the model according to Watson was more appropriate because it actually calculates (iteratively) the percentage contained in this population. Indeed, by visual comparison, the curves proposed by the Watson approach seemed to fit better the original data. Thus, the Watson model was preferred over the Dean-Jett-Fox model. Furthermore it was decided to present the findings as calculated by the automatic software, according to the Watson model, rather than the results found with the manually drawn gates in order to eliminate variations emerging from the user. When a difference $>\pm10\%$ was noted, the histogram was assessed visually to detect the reasons for such major discrepancies between the original curve and the model, and the model distributions were subject to manual corrections, if appropriate.

2.2 Methods for synchronisation of human normal mammary epithelial cells (MCF-12A cell line)

To evaluate the effect of a treatment on cell cycle progression and to make it comparable to untreated controls, the cell populations under investigation should be at the same point of "departure" in the cell cycle. To achieve this, it is crucial to synchronise the populations

beforehand, so that the results obtained at the end of the treatment are comparable to each other without bias. To minimise the variability of cell synchronicity and make the results comparable within and between experiments, an effective synchronisation method had to be determined for the cell lines in use for this work.

The synchronisation of a cell population may be achieved by different means. One example is the method of the mitotic shake off, which takes advantage of the fact that cells round up shortly before and during mitosis and therefore are less attached to the cell culture dish. This method, first described in the 1960s (Terasima and Tolmach 1963), is suitable for all adherently growing cell types, but yields only very low numbers of mitotic figures, because mitosis represents a very short process within the total length of the cycle, so that only a small number of cells are found in M phase at any given time in unsynchronised cultures. More efficient are protocols that halt the onset of specific cell cycle phases and so accumulate the population in the previous phase. For example, in mammalian cells, the nucleoside thymidine interrupts DNA synthesis, when added in excess to the culture. As a result, the cells are blocked at the boundary between G1 and S phase, with very high efficiency (Puck 1964). However, if the events that are taking place in the G1 phase are to be studied, this method may be less suitable.

A method of choice for reversibly blocking cells before the onset of G1 is serum depletion. Cells in culture usually require relatively high amounts of serum in the culture medium for healthy growth and proliferation. Serum provides many factors essential for cell growth and proliferation, such as hormones and cytokines, and for cells in suspension it also provides some protection against shear stress. When the cells are depleted of serum for a long enough time (usually 24 to 72 hours), because of nutrient starvation they will withdraw from the cell cycle and go into the quiescent G0 phase. Upon addition of serum, the starved cells will resume the cell cycle and progress through G1 phase. The efficiency of this method depends on several parameters, mainly the reduction in serum concentration, the duration of serum depletion and the ability of the studied cells to survive under these conditions. The lower the percentage of serum contained in the culture medium, the higher synchronicity is achieved, but a compromise must be found between the highest amount of serum sufficient for G0 accumulation, and the lowest amount tolerated by the cells over a longer period. Greater synchronicity may also be achieved by extending the depletion period, although a starvation period of one full cell cycle length should be sufficient for maximal G0 blocking. A high degree of G0 accumulation might also come at the cost of fewer cells being able to re-enter

52

the cell cycle. When decreasing the amount of serum in the culture medium and choosing the duration of starvation, the characteristics of the cell line need to be considered. Generally, tumour lines tolerate well the complete removal of serum for up to 3 days, whereas cells derived from normal tissue are more delicate and require a minimal amount of serum at all times for survival. For these, a starvation period of 24 to 48 hours is often sufficient for synchronisation.

The synchronicity achieved is also a fair indicator of the overall health of the cell culture, and of potential variations in the following cell cycle progression: it is possible to synchronise the same cell line to approximately the same degree (more or less), but when one batch shows a substantially higher rate of synchronisation (for example, 90% vs. usually 80%), this surge could indicate a problem within the culture (e.g. a higher rate of apoptotic cells that were counted towards the G1 population). The differences from one batch to the other could also lead to a slower cell cycle progression, or to a lower amount of cells that are able to leave the quiescent state (consequences for the outcome are cell-type specific). In order to screen for such deviations, it is important to include control samples in the analysis. Therefore, in every batch analysed for this thesis, a negative control sample (serum-depleted cells synchronised in G1 phase), a positive control sample (cells stimulated to leave G1 phase and allowed for release until they reached a specific point in the cell cycle), and a growth control sample (asynchronous population) were included to monitor if the cell batch used was proliferating healthily.

2.3 Variability of synchronicity in MCF-12A cells and the need for normalisation

For this thesis, the MCF-12A cell line was used. The primary cells were derived from normal epithelial tissue obtained during mammary reduction surgery. When put into culture, the cells immortalised spontaneously, and the MCF-12A cell line was generated. For the cell cycle progression studies performed for the work presented here, the focus was on the progression through the G1 phase, and therefore, the serum depletion method for synchronisation in the G0 phase was applied. The reduction of the amount of horse serum in the culture medium from 5% to 0.5% (v/v) over 24 hours resulted in approximately 70% of cells being in the G0 phase. However, this percentage was subject to variation, with the yields for G0 ranging from just over 60% to almost 90% between experiments, whereas the samples within one experiment showed comparable synchronisation rates. In order to be able to compare data

from different batches and / or days, and to allow for pooling the results from different experiments, this variability needs to be accounted for in the subsequent analyses. The approach for this normalisation is explained in this section.

To allow for a quantitative comparison of flow cytometric results acquired from different batches, it is essential to normalise the results to a control value: cell sizes may be different from batch to batch, and for fluorescence tagged samples, the amount of fluorescent molecules per cell may differ, due to the several steps involved in sample preparation. However, these were minor variations that could be neglected. With the human mammary cell line MCF-12A, the largest batch-to-batch variations seen resulted from differences in the efficiency of the synchronisation and of the ability of the cells to re-enter the cell cycle, as monitored by the release with a positive control (as mentioned in the previous section). Therefore, normalisation of the acquired data to an internal control is crucial to account for these variations.

For the work with the MCF-12A cell line, the objective was to study the effect of various treatments on the progression of cells from the quiescent G0 state through the G1 stage into the S phase. The efficiency of a substance to induce cell cycle re-entry can be derived from the fraction of cells that were able to leave the G0 block, so the sum of cells in S and G2+M phase should be measured. In our experimental approach, the cells were accumulated in the G0 stage by incubating them with 0.5% of serum over 24 hours; this treatment successfully blocked around 70 to 80% in the desired phase. However, this result also meant that at least around 20% of all cells continued to cycle, i.e. were present in S and G2+M. Thus, the effect of a treatment was expressed as the *increase* in S and G2+M phase percentages in relation to the quiescent control sample. As the aim was to study the effects of the treatments, the variations introduced by different synchronisation efficiencies between experiments had to be eliminated. This was achieved by setting the S+G2+M fraction of the (negative) control sample with serum-depleted cells to 1 and normalising the results from treatments and positive controls accordingly.

The importance of normalising the acquired data to a control value for the work presented here becomes clearer by considering the following example: the data in Figure 10 shows on the y-axis the sum of the percentages of cells found in S+G2+M phase, as calculated by the cytometry software using the Watson model after data acquisition with flow cytometry. Three different samples were analysed, a negative control sample (serum-starved, G1 accumulated cells), a positive control (mitogen-stimulated, S+G2+M accumulated cells), and one treated

sample. This assay was repeated two more times independently, on different days, so that a total of three independent repeats was obtained. As can be seen, the differences between the experiments, although not very pronounced for the negative control samples, were considerable in the positive controls, as well as for the treatment. For representative purposes, the original histograms acquired for each sample are shown in Figure 11.

In order to assess the reproducibility of the results, as well as the significance of the effects of the treatment, taking into account all independent repeats, the data had to be pooled. However, the raw data varied too much and could not be pooled. For this reason, the data had to be normalised before pooling. The normalisation was conducted by setting one of the control samples to 1, and setting the other samples from the same experiment in relation the control. This normalisation was based on the assumption that the *proportion* of each phase remains the same for the same treatment, although the absolute reading may vary between experiments. The variation in synchronisation is introduced for example by different cell densities. In order to eliminate these inter-experimental variations, the S+G2+M fractions of the treatment and of the positive control were normalised to their corresponding negative control sample. Either positive or negative control may be chosen as the baseline sample, but for the purpose of this thesis, the use of the negative control was more appropriate, as outlined above. As shown in Figure 12, this elimination of the variation introduced by the different synchronisation efficiency on the three different days decreased the variation between the treatments considerably. Finally, the data normalised in this way could be pooled and was suitable for further statistical analysis (Figure 13). For an overview of the range of percentages found in the different experiments of which the results are usually presented normalised to the negative controls, please refer to Appendix Table i found in the appendices' section.
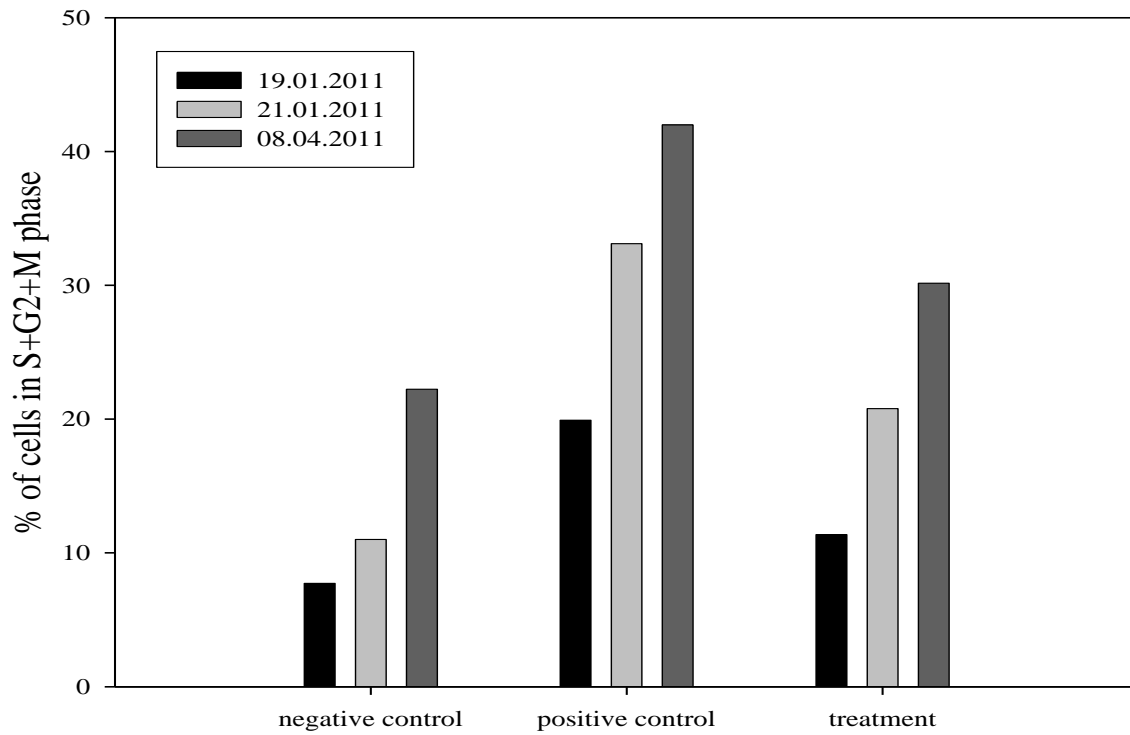
Figure 10 Example for variations in cell cycle distributions in 3 independent experiments

Sample treatment, preparation for analysis and data acquisition and analysis was performed according to protocol. Results of three independent experiments are shown to illustrate the inter-experimental variations obtained. Negative control = serum depleted cells (G0 accumulated); positive control = cells released into S+G2+M phase.
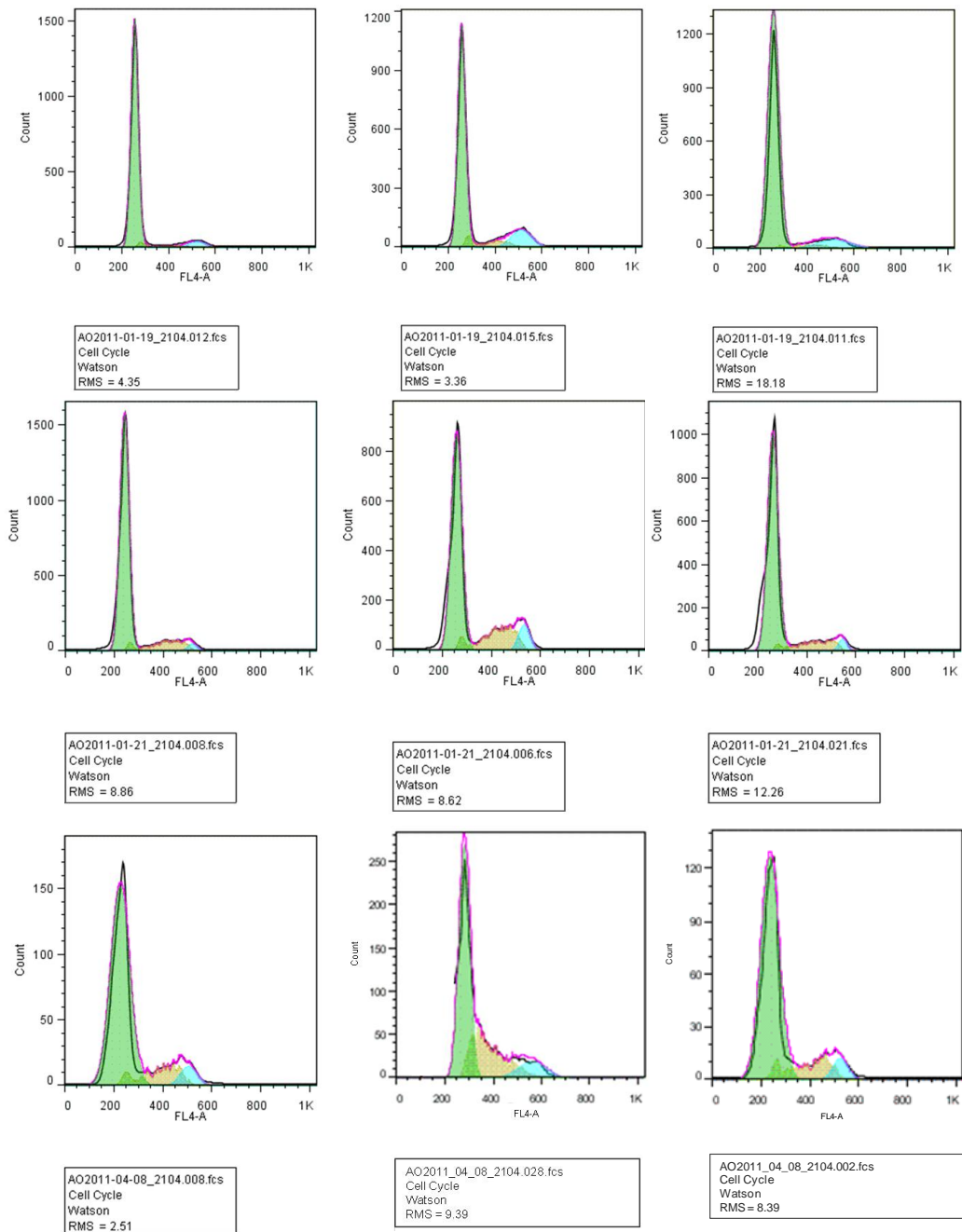
Figure 11 Examples for variation in cell cycle histograms in 3 independent experiments

Flow cytometric histograms of samples after identical treatments are shown to illustrate the variations between independent experiments (results of S and G2+M percentages are shown in Figure 10). The MCF-12A cells utilised for these samples are from two different batches (batch 1 used for 01/2011, batch 2 for 04/2011). Beneath each histogram, the sample ID, the analysis mode ("Cell Cycle"), the analysis model ("Watson") and the RMS is shown.

Table 8 Results of flow cytometric analysis of 3 samples from 3 independent experiments

The percentages for each cell cycle phase for the 3 different samples presented in Figure 10 and Figure 11 are shown to illustrate the inter-experimental variability of the flow cytometric results.

sampled ID	treatment	Freq. G1	Freq. S	Freq. G2/M
AO2011-01-19_2104.012.fcs	negative control	87.5	5.17	5.9
AO2011-01-21_2104.008.fcs	negative control	82.2	9.4	2.93
AO2011-04-08_2104.008.fcs	negative control	92.9	17.2	8.05
AO2011-01-19_2104.015.fcs	positive control	71.7	10.1	15.3
AO2011-01-21_2104.006.fcs	positive control	67.8	22.7	8.71
AO2011-04-08_2104.028.fcs	positive control	58.01	34.17	7.82
AO2011-01-19_2104.011.fcs	treatment	88.19	4.81	7.01
AO2011-01-21_2104.021.fcs	treatment	78.6	14.1	3.81
AO2011-04-08_2104.002.fcs	treatment	67.9	20.2	12
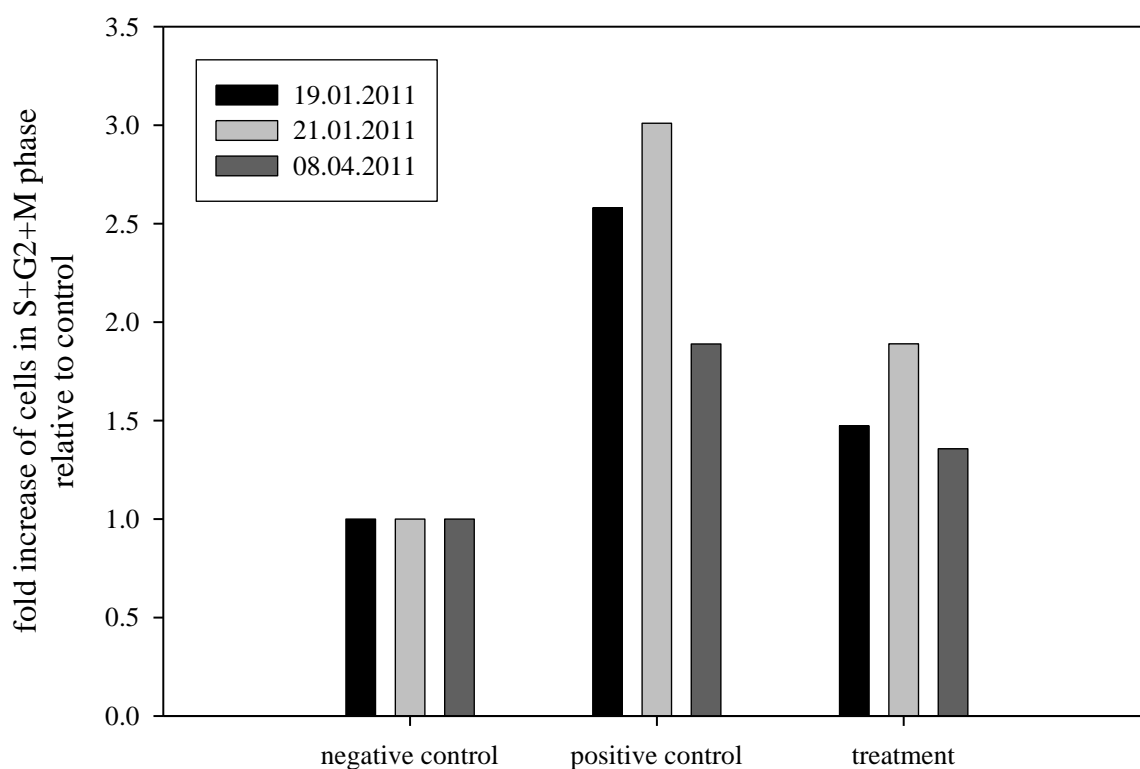
Figure 12 Normalised cell cycle data

The data presented in Figure 10 (results from three independent experiments) was normalised to the respective negative control value, which was set to 1.
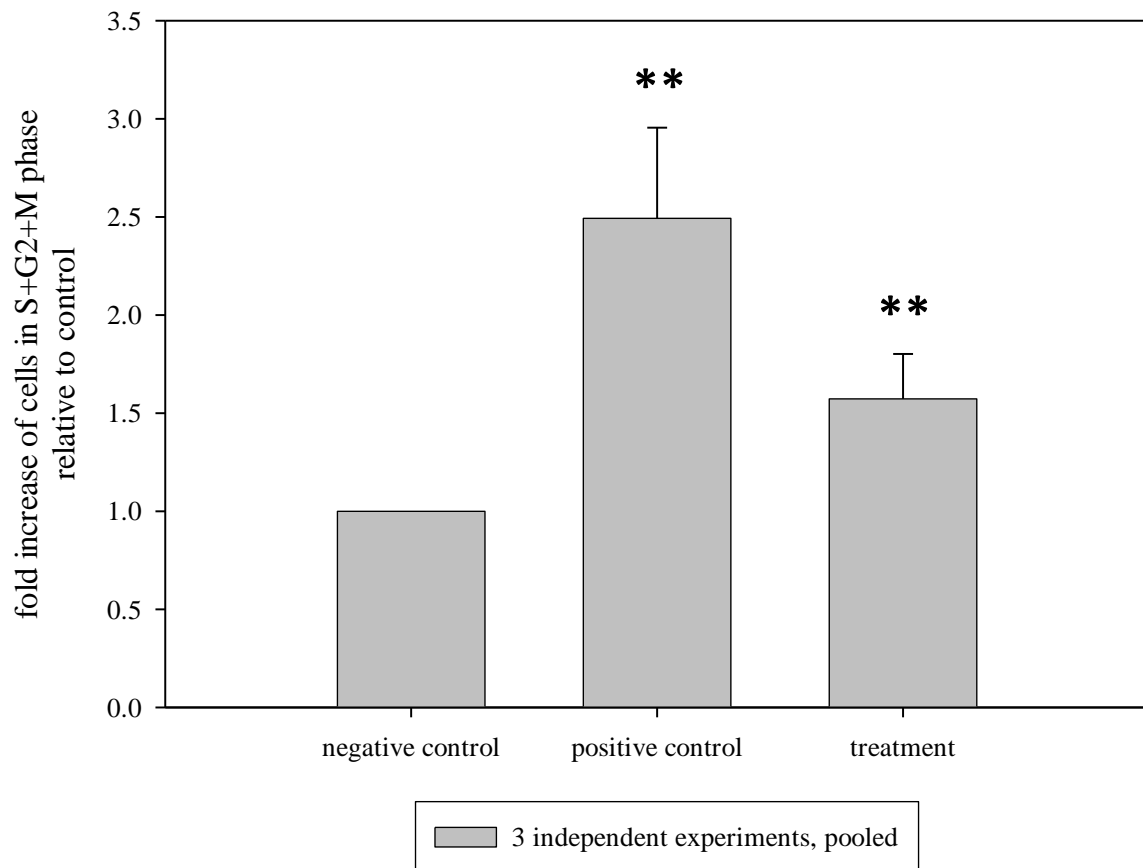
Figure 13 Normalised data pooled from three independent experiments

The normalised data presented in Figure 12 were pooled together; values shown are the mean of the three independent experiments; error bars show SEM. Student's *t*-test was performed for significance testing, samples marked with ** (P=0.05) are significantly different from the negative control.

3 SUMMARY

All data presented in this work was acquired on the MACSQuant® Analyzer. The raw data files were transformed into the flow cytometry standard file format for data analysis. The method for cell cycle phase analysis was chosen to be the algorithm as proposed by Watson. The software to perform these calculations was FlowJo™ (Tree Star, Inc., version 7.6, free trial licence) with the embedded algorithm. The analysis was performed in unconstrained modus (no modification by the user), unless the peaks could not be detected by the algorithm. In this case, the user set a fixed number for the G1 peak (if visual estimation was possible), and forced the G2+M peak to be at 2.0 times x_{G1}.

For pooling the data and to compare treatments, as well as to account for differences in synchronisation efficiency, samples were normalised to the internal negative control (cells accumulated in G1), unless otherwise stated. This might occur in specific cases, as for some samples (depending on the treatment and the purpose of the analysis), it might be more suitable to normalise to the positive controls.

Chapter 4:

Implementing the discontinuous exposure assay with MCF-12A cells

1 INTRODUCTION

Cell proliferation is a fundamental process that ends in a cell dividing into two daughter cells, by going through one round of the cell cycle. The description of the phases of the cell cycle (Figure 2) by Howard and Pelc in 1953 (Howard and Pelc 1953) was followed by a surge of research on cell cycle kinetics in normal and cancer tissue culture (for example, Sisken and Morasca 1965; Quastler 1960; and references herein).

Identifying the substances (hormones, growth factors) that are responsible for cell cycle progression is rendered difficult by the presence of serum that is usually added to cell cultures in order to maintain them at their optimal health. Different cell types require specific sera, but they all have in common that these are undefined mixtures of hundreds of components, such as proteins, electrolytes, lipids, carbohydrates, hormones and enzymes. Serum also supplies factors for growth, proliferation, differentiation and attachment. Adjusting the concentration of the serum is a convenient method to control the proliferation rate of fibroblast cells (Holley 1975). Culturing cells in completely serum-free and / or a chemically defined medium has been attempted many times since the very early beginning of cell culture research (Eagle 1955), in order to identify the strictly necessary substances, to better understand what enables (cancer) cells to proliferate (Hutchings and Sato 1978), or to discover new growth factors (Karey et al. 1989; Eastment and Sirbasku 1978). Also for production of therapeutic products from (mammalian) cells, serum-free cultures are preferred (for an overview, see Jayme et al. 1997).

When nutritional conditions are not optimal, cells can go into a quiescent state, with slowed down or completely halted growth. Cells survive well in this state, as demonstrated by their ability to resume proliferation upon re-addition of serum to the medium. The quiescent state can also be induced by amino acid starvation or increased levels of cAMP, as shown in

Chinese Hamster Ovary (CHO) cells (Rozengurt and Pardee 1972), and through high cell density, although this is mediated by contact inhibition rather than nutrient deprivation.

Evidence that the quiescent state means a slowing down of metabolism to endure suboptimal environmental conditions, rather than a simple arrest somewhere in the G1 phase, was first given by Arthur Pardee (Pardee 1974). Using fibroblasts he showed that the quiescent state, induced by any nutrient deprivation or cAMP augmentation, stopped the cells at the same point of the cell cycle, since the transit time until induction of DNA synthesis was the same for all means of quiescence. This "lag time" stayed unchanged when the cells were kept under the inhibitory conditions for a prolonged time. The effect (and therefore the mechanism) was different when non-physiological methods were tested for cell cycle arrest such as hydroxyurea (stops cells in S phase because it inhibits ribonucleotide reductase) or colchicine (stops cells in mitosis because it inhibits attachment of tubulin to the microtubules).

The concept of a "switch" in the cell, from either being committed to the cell cycle or from staying in the non-proliferating state, had been described some few years earlier by Howard Temin in chicken fibroblasts (Temin 1971). Temin also recommended a further division of the G1 phase into several critical stages, but Pardee suggested for the first time the term *restriction point* (R point) for the specific time in the cell cycle at which their switch back into the normal cell cycle occurs. The importance of this observation was acknowledged immediately, since Pardee suggested at the same time that malignant cells may have lost the control mechanism of such a restriction point, resulting in excessive proliferation.

The return to normal cell cycle progression is achieved by restoring optimal nutrition (re-addition of serum to the culture medium). Interestingly, the nutritive effect of serum could be divided into two functions, each provided for by a distinct fraction of the serum, the first function being to maintain cell viability, the second to induce replication (Paul et al. 1971). A similar idea evolved from work with Balb/c3T3 fibroblast cells, that saw the transition of quiescent cells into the cell cycle divided into at least two different stages, each under the control of a different set of mitogens (Pledger et al. 1977). For fibroblasts which had been depleted with platelet-poor plasma, Pledger et al. showed that upon addition of platelet extract, the cells resumed DNA synthesis, and cell replication took place again. Moreover, the percentage of stimulated cells was linear to the platelet concentration. But interestingly, to bring 100% of the cells into S phase, the concentration of the platelet-poor plasma had to be increased as well, showing that the platelet extract and the depleted plasma act synergistically

for maximum DNA synthesis. Inspired by these observations, Pledger and his co-workers were the first to introduce the concept of *competence* versus *progression*: the addition of platelet extracts to quiescent (contact-inhibited) cells rendered them competent to enter the cell cycle, i.e. to pass the R point, and this competent state lasted for several hours, but if no plasma was added afterwards for progression, the cells lost their ability to pass the R point. The rate of entry into S phase depended on the concentration of the plasma. Hence, this work was a first indication towards the later discovery that a sequence of signals has to be activated in an orderly fashion to promote cell cycle progression, and that these signals may be triggered by different factors.

Much work in this field has been done using fibroblasts, where growth factors such as the platelet derived growth factor (PDGF) have been identified to be a major contributor to cell cycle progression (Balciunaite and Kazlauskas 2002; Jones and Kazlauskas 2000; Balciunaite et al. 2000; Jones et al. 1999; Simm et al. 1998; Harrington et al. 1987). Especially Kazlauskas' group attempted to identify the signalling events that mediate the effect of PDGF. Taking further the discoveries made by Pledger and colleagues in 1977, Jones and Kazlauskas developed a discontinuous treatment assay that allowed the conclusion that growth factors commit cells to the cell cycle by using distinct sets of signals or pathways, at distinct times, and that these are not interchangeable (Jones and Kazlauskas 2001; Pledger et al. 1977). These observations suggested that the transition from quiescence into S phase is composed of (at least) two segments, the accomplishment of both depending on growth factor stimuli. A new terminology was proposed accordingly, with the early G1 phase ($G1_E$) that follows when cells are enabled out of quiescence (and which is still poorly defined), and the late G1 phase ($G1_L$) where cells are ready to be driven into S phase.

To identify if such a segmented G1 phase is existent in human breast epithelial cells was one of the aims of this thesis. To address this issue, it is important to understand which factors are able to induce cell cycle progression in epithelial tissue, not least because most breast cancers originate from epithelial cells with a few excessively progressing cells. Normal cells can form a barrier to stop the aberrant cells from spreading. In this chapter the focus was on identifying growth factors that provide competence and progression to the human mammary epithelial cell line MCF-12A.

2 OBJECTIVES

The signalling pathways that are activated for proliferation in normal breast epithelial cells are not well known. In order to study these pathways, our aim was to investigate the applicability of the two-wave concept to human mammary epithelial cells. To achieve this aim, a discontinuous exposure assay for the MCF-12A cell line had to be set up. The specific objectives for this part of the project were

- To find a suitable serum depletion protocol for synchronising these cells in the quiescent G0 phase
- To identify the time point when the cells enter S phase, once they have been released from the starvation block
- To eliminate the serum from the releasing medium in order to use a chemically defined medium
- To test various growth factors for their mitogenic properties in this cell line
- To establish a (time) protocol for a discontinuous release in order to be able to study the R point in this cell line

3 METHODOLOGICAL CONSIDERATIONS

3.1 Establishing a synchronisation protocol

Several methods are described in the literature for synchronising cells derived from breast tissue and tumours in various stages of the cell cycle:

- Mitotic shake off
- Thymidine block and double-thymidine block
- Contact inhibition
- Serum-depletion

The method of the mitotic shake off, takes advantage of the fact that cells round up shortly before and during mitosis and therefore the cells detach more readily. This method, first described in the 1960s (Terasima and Tolmach 1963), is suitable for all cell types, but yields only very low numbers of mitotic figures, because mitosis covers only a short period in the cell cycle, so that only a small number of cells are found in M phase at any given time. An

often used protocol is the addition of thymidine to the culture medium for up to 24 hours (a "thymidine block"). In a double thymidine block this method is used with a recovery period in between two exposures. The method was first mentioned by Puck more than 40 years ago (Puck 1964). Thymidine specifically interrupts the DNA synthesis, and when given in excess to mammalian cells, it arrests the cells that are in G2 phase, mitosis, or G1 at the G1/S phase boundary (Tobey et al. 1966).

Serum-depletion or simply nutrient starvation forces the cells out of the cell cycle into a quiescent stage, the G0 phase, where they can survive for a prolonged period of time, and from where they can also re-enter the cell cycle when sufficient nutrients are available again. However, if the nutrient-depleted state lasts too long, cells will undergo apoptosis. In MCF-7 cells, starvation for 72 hours was shown to yield a high synchronicity of 80-85%, with no apparent apoptosis (Yoon et al. 2004).

Contact-inhibited cells accumulate in the G1 stage, and the mechanism by which this is induced is different from the other methods: when cells have grown to complete confluency in the culture vessel, physical contact between them triggers membrane proteins to signal that the cell should stop growing.

The purpose of the work presented here was to study how a cell line of human breast epithelial cells (MCF-12A cell line) becomes committed to the cell cycle; therefore cells caught in the quiescent state were considered the most suitable material to begin with, and serum-depletion seemed the appropriate method to achieve G0 synchronicity.

For all assays, the complete serum was replaced by charcoal/dextran (CD-) treated serum. This treatment removes lipophilic components and endogenous steroid hormones and results in a chemically more defined serum.

3.2   Release of cells from G0 block

3.2.1 Continuous exposure of cells for release from G0 block

The ability of cells to leave the quiescent state was monitored after addition of mitogens following the starvation period, either in the form of serum (the starvation medium was replaced with fresh complete growth medium), or as chemically defined growth factors (the starvation medium was replaced with fresh starvation medium supplemented with growth factors at various concentrations). To assess efficiency in cell cycle progression, the

percentages of the cells in S and G2+M phase were normalised to the respective negative control samples (G0 blocked sample).

3.2.2 Determination of the intervening time between administration of the two pulses in the discontinuous exposure assay

The possibility of stimulating cells in a discontinuous regime with two pulses only, instead of continuously with mitogens, provides a valuable tool to study the events that lead to cell cycle progression. The incubation time for the first pulse was based on published results which showed that an initial burst of signalling factors is triggered after no more than 10 minutes of contact with a growth factor in hepatocytes (Balciunaite et al. 2000) and 30 minutes in fibroblasts (Jones and Kazlauskas 2001). The length of the second pulse, as well as the gap phase between the two incubations, needed to be determined specifically for the MCF-12A cells. Between 4 and 10 hours were tested for the length for the gap phases, and these times were iterated from previously published data, obtained in fibroblasts:

- A gap of 12 hours was too long for the second exposure to be efficient (Temin 1971), but 8 hours between the two administrations were tolerated.
- The small G protein Ras showed a biphasic pattern of activity in serum stimulated cells: it peaked very early (after 30 min), dropped and was elevated again at the time points between 2 and 4 hours after exit from quiescence (Gille and Downward 1999). This information was important to be considered because Ras is a key molecule for activating mitogenic signals in all cell types.

3.2.3 Determination of growth factors to be tested

The effect of different growth factors on cell cycle progression was tested. The growth factors chosen (PDGF, EGF, IGF-1, insulin) are known to be strong mitogens in many different cell lines, and some of them are contained in the growth medium used for the MCF-12A cell line.

3.2.3.1 Platelet-derived growth factor (PDGF)

A growth factor initially discovered through the use of platelet-enriched serum and platelet extracts, the PDGF exists as a heterodimer (PDGF-AB) and as AA- and BB- homodimers (Eastment and Sirbasku 1978; Westermark and Wasteson 1976). It is one of the best studied growth factors, extensively used for studies on proliferative pathways, with strong mitogenic properties for fibroblasts and other cell lines, of different species (Ross et al. 1986). PDGF

was also used for discontinuous exposure of NIH3T3 cells to study the signalling pathways activated for G1 to S phase transition in these mouse embryonic fibroblasts (Jones and Kazlauskas 2001; Jones et al. 1999).

3.2.3.2 Epidermal growth factor (EGF)

During studies on nerve growth factors (NGF), Stanley Cohen isolated a protein from the submaxillary gland of mice, which showed to accelerate teeth eruption and eyelid opening in newborn mice (Cohen 1962). This protein turned out to be a growth factor for epithelial cells, and was termed epidermal growth factor (EGF). Later, urogastrone was isolated from urine, and identified as the human equivalent to EGF (Gregory and Willshire 1975; Gregory 1975). The corresponding receptor was also described by Cohen for the first time (Cohen et al. 1980). EGF is contained in the culture medium of the MCF-12A cell line and essential for its maintenance in prolonged culture. Therefore it may be assumed that this growth factor is important for cell cycle progression.

3.2.3.3 Insulin and insulin-like growth factor type I (IGF-1)

Insulin and IGF-1 stimulate pathways that mediate G1 / S phase transition: in MCF-7 cancer epithelial cells, insulin increased the rate of DNA synthesis after long-term exposure (12 hours), but protein synthesis was increased after only 1 hour of incubation with insulin, and the cell cycle progression was also markedly accelerated (Mawson et al. 2005; Rillema and Linebaugh 1977). Insulin is also part of the complete culture medium for the MCF-12A cell line. Therefore it may be assumed that this hormone has a role in supporting cell growth and / or proliferation.

4 RESULTS

Before setting up a discontinuous exposure assay, it was important to find a suitable protocol for serum-depletion that allowed good yields for synchronisation as well as release from the serum-depleted state. The results from these cytometric experiments are presented as percentages for each cell cycle phase, in order to determine at which time point(s) the percentage for S phase cells is maximal. Once a suitable depletion and release regime was found, it was attempted to eliminate the serum gradually from the medium; subsequently, instead of the serum, various growth factors were tested for their effect on the cells. For these assays, cells were analysed always at the same, previously determined time point, and the

cytometric results from then on were normalised to the negative control samples, in order to have a standardised basis on which results from independent experiments are compared to each other. A schematic overview of the sequence of experiments to be performed to achieve a discontinuous exposure with defined growth factors is given in Figure 14. As discussed in the previous chapter, flow cytometry was performed on a MACSQuant® Analyzer. The acquired data was transformed into flow cytometry standard files and cell cycle analysis was performed using FlowJo™ analysis software based on the *Watson* algorithm (cf. Chapter 3, page 50). All these results are presented in the following sections.

```
┌─────────────────────────────────────┐
│      Induction of quiescence        │
│          (Fig. 15+16)               │
└─────────────────────────────────────┘
                  ⇓
┌──────────────────────┬──────────────────────────┐
│                      │  48h/72h serum depletion  │
│  24h serum depletion │          and              │
│                      │ different concentrations  │
│                      │  of serum were tested     │
└──────────────────────┴──────────────────────────┘
                  ⇓
┌───────────────────────────────────────────────────┐
│ Release cells from quiescence with complete growth │
│  medium (continuously) over 27 hours to monitor S  │
│                   phase entry                      │
│                                                    │
│ 18 hours after release was determined as time point│
│           of S phase entry (Fig. 17+18)            │
└───────────────────────────────────────────────────┘
                  ⇓
┌───────────────────────────────────────────────────┐
│ Test continuous exposure to defined growth factors │
│ (in starvation medium); at18 hours of continuous   │
│              stimulation (Fig. 19)                 │
├──────────────────┬──────────────────┬──────────────┤
│ Concentration of │ Test discontinuous│ Insulin and  │
│ 20 ng/ml EGF was │ stimulation with  │ IGF-1 with   │
│ determined       │ 20ng/ml EGF for   │ little effect │
│ (App. Fig. i)    │ cell cycle re-entry│ on cell cycle│
│                  │ (Fig. 20)         │ re-entry     │
└──────────────────┴──────────────────┴──────────────┘
                  ⇓
┌───────────────────────────────────────────────────┐
│ Initial stimulation of 30 minutes + distinct second│
│ incubation (after intervening time of 4 hours) is  │
│    sufficient for successful cell cycle re-entry    │
│ 2nd pulse = 14 hours (resulting from intervening   │
│    time and total assay time of 18 hours)          │
└───────────────────────────────────────────────────┘
                  ⇓
┌───────────────────────────────────────────────────┐
│ Different growth factors were tested in the first  │
│          and the second incubation period          │
│                                                    │
│ Combination of EGF in the initial exposure,        │
│ followed by EGF + insulin in the second exposure → │
│   successful cell cycle re-entry (Fig. 22)         │
└───────────────────────────────────────────────────┘

┌───────────────────────────────────────────────────┐
│ Assay to shorten the second exposure (Fig. 23)     │
└───────────────────────────────────────────────────┘
                  ⇓
┌───────────────────────────────────────────────────┐
│ Optimal discontinuous exposure assay, used routinely│
│   for the remainder of the work presented          │
│              (Fig. 24+ff.)                         │
└───────────────────────────────────────────────────┘
```

Figure 14 Schematic overview of experimental design for the discontinuous stimulation of MCF-12A cells

The schema depicts the sequence of experiments necessary to test the hypothesis that discontinuous stimulation of MCF-12A cells with defined growth factors is sufficient to induce cell cycle re-entry. After induction of quiescence, the cells were stimulated with complete growth medium and monitored over an entire cycle in order to determine the time at which synthesis phase starts. This time point was the end point for all following assays. Subsequently, the stimulation was performed in two distinct pulses, and the serum-containing medium was replaced by defined growth factors.

4.1 Cell synchronisation in the G0 phase through serum depletion

Around 70% of the MCF-12A cells accumulated in the G0 phase after 24 hours of serum depletion, whereas a longer starvation period did not increase the number of cells blocked in G0, as seen in Figure 15. The cells that were not found to be in the quiescent state were distributed to equal parts in the other two cell cycle phases distinguishable by flow cytometry (S phase or G2+M phase). The lower G0 count after 48 hours of starvation very likely was from cells that were able to continue the cell cycle despite the low amount of growth factors available. In order to confirm this, cells were released into basal medium after 48 hours of depletion. It was expected that cells would be unable to further progress into the cell cycle, once all mitogens remaining from the starvation medium had been washed out. Indeed, the results, presented in Figure 16, confirmed this explanation, since it was observed that the percentages found for each phase did not change considerably over time.
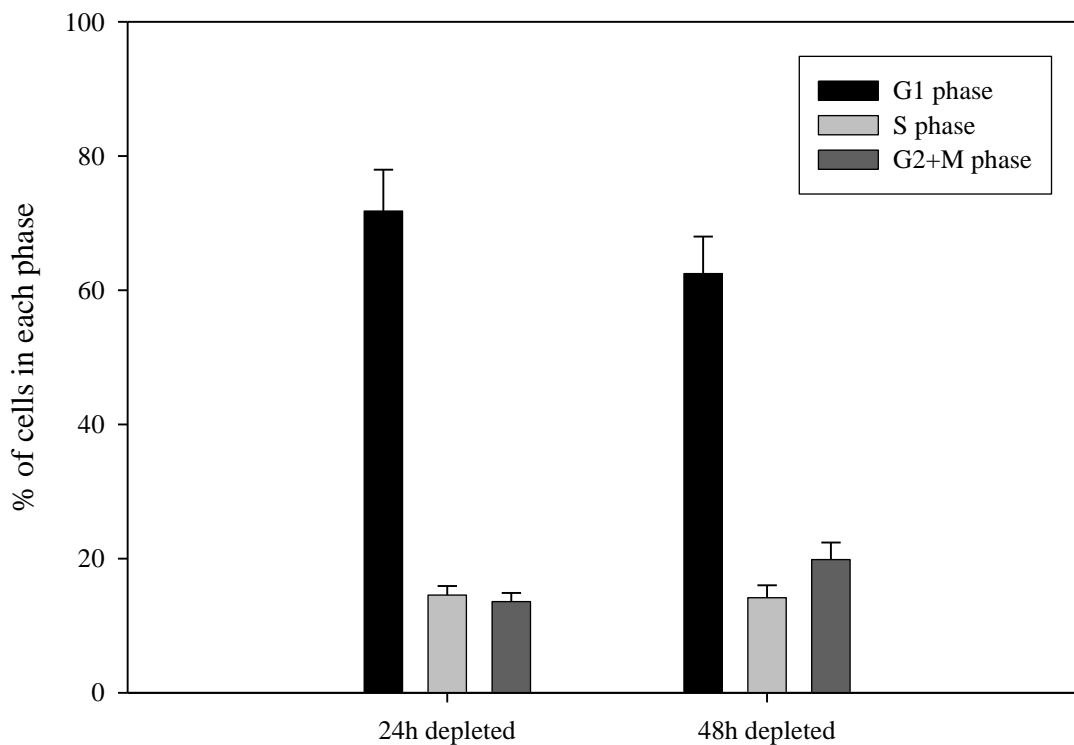
Figure 15 Efficiency of serum depletion on MCF-12A cells for G0 accumulation

Cells were incubated with 0.5% CD-treated horse serum for the times shown, and analysed by flow cytometry after DNA staining with propidium iodide (PI). Values are the mean of 5 independent experiments and error bars show SEM.

70
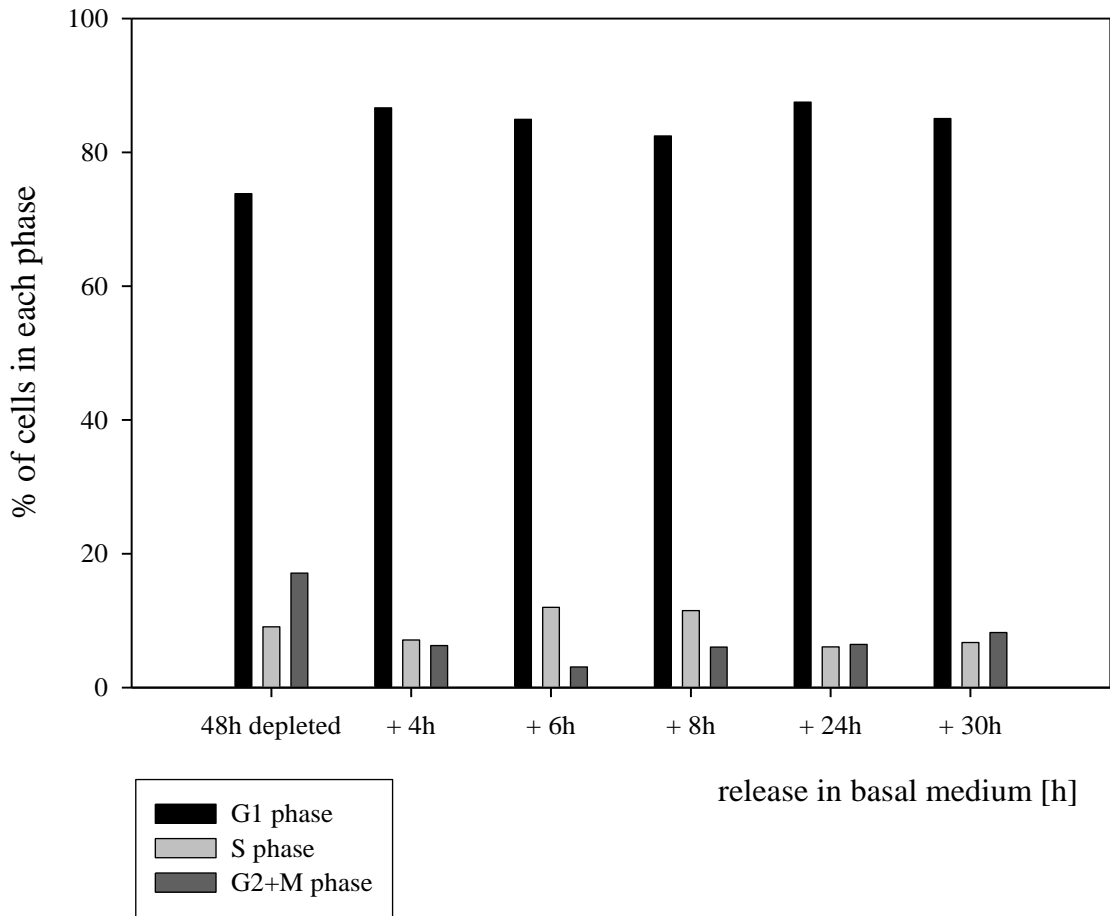
Figure 16 Release of MCF-12A cells into basal medium after 48 hours of serum-depletion

After a serum-depletion period of 48 hours, starvation medium was removed and cells were incubated with basal medium for the times shown. Cell cycle analysis was performed by flow cytometric analysis after DNA staining with PI. The results of one representative experiment are shown.

4.2 Release of cells from G0 block

4.2.1 Release with complete growth medium

It had been shown previously in our laboratory [1] that MCF-12A cells progress in approximately 18 to 21 hours out of the G0 blocked state into the synthesis phase. Nevertheless, the timeline of the MCF-12A cell cycle needed to be confirmed beforehand, as the work presented here was carried out using a different batch of this cell line. After starving the cells for 24 hours with 0.5% charcoal/dextran treated horse serum (CD-HS), complete culture medium was added to facilitate release from the G0 block. As shown in Figure 17, the maximum number of cells in S phase was reached after 21 hours of release. However, the percentage after 18 hours was almost as high, and since the overall aim of the project was to determine the requirements for pushing cells past the R point, which occurs several hours before the start of DNA synthesis, the early S phase at 18 hours from G0 onwards was regarded as a suitable endpoint for all subsequent assays.

---

[1] Alonso Gonzalez, C.: Interactions between multiple growth factors and hormones in cell cycle progression; Centre for Toxicology, 10.07.2010
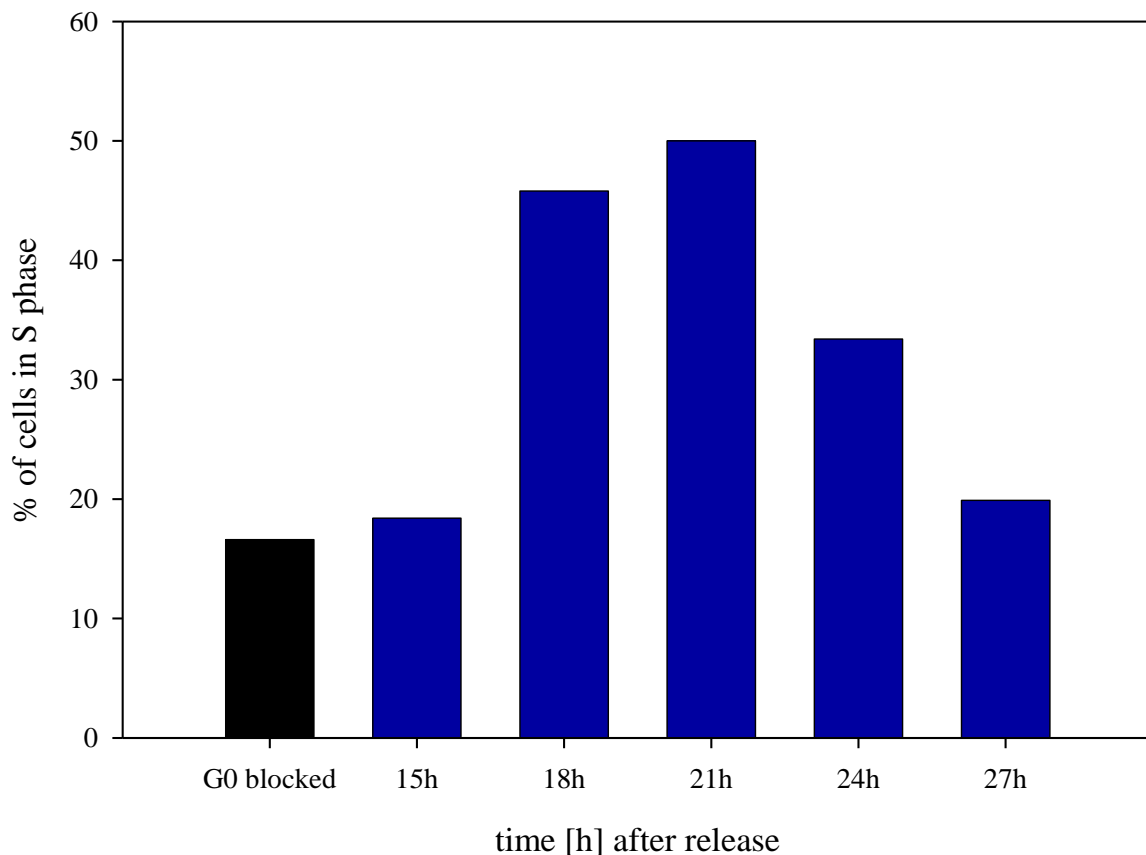
Figure 17 Fraction of MCF-12A cells in S phase after release into complete growth medium following 24 hours of serum-depletion

G0 accumulation was induced with serum-depletion for 24 hours (0.5% CD-HS), after which the starvation medium was removed and complete medium was added. Cell cycle analysis was performed by flow cytometry carried out after staining of DNA with PI. Shown are the results of a representative experiment.

4.2.2 Replacement of complete medium by starvation medium plus EGF

As mentioned above, the complete growth medium for MCF-12A cells contains several growth factors. In order to establish which of these factors are necessary and sufficient for proliferation, they were tested in addition to the starvation medium.

Firstly, the mitogenic properties of EGF alone were tested. To this end, G0 blocked cells were treated with EGF (20 ng/ml) in starvation medium (= 0.5% CD-HS in basal medium) to see whether this combination of growth factors was sufficient to drive the cells into the cell cycle. As shown in Figure 18, the pattern of accumulation of S phase cells was very similar to the one seen when cells were released with complete growth medium. Cells started to enter S

phase at 18 hours after release from block, and DNA synthesis required approximately 6 hours. At 27 hours, cells had already begun to exit S phase. The concentration of EGF had been chosen according to preliminary results (cf. Appendix Figure i in the appendices' section).
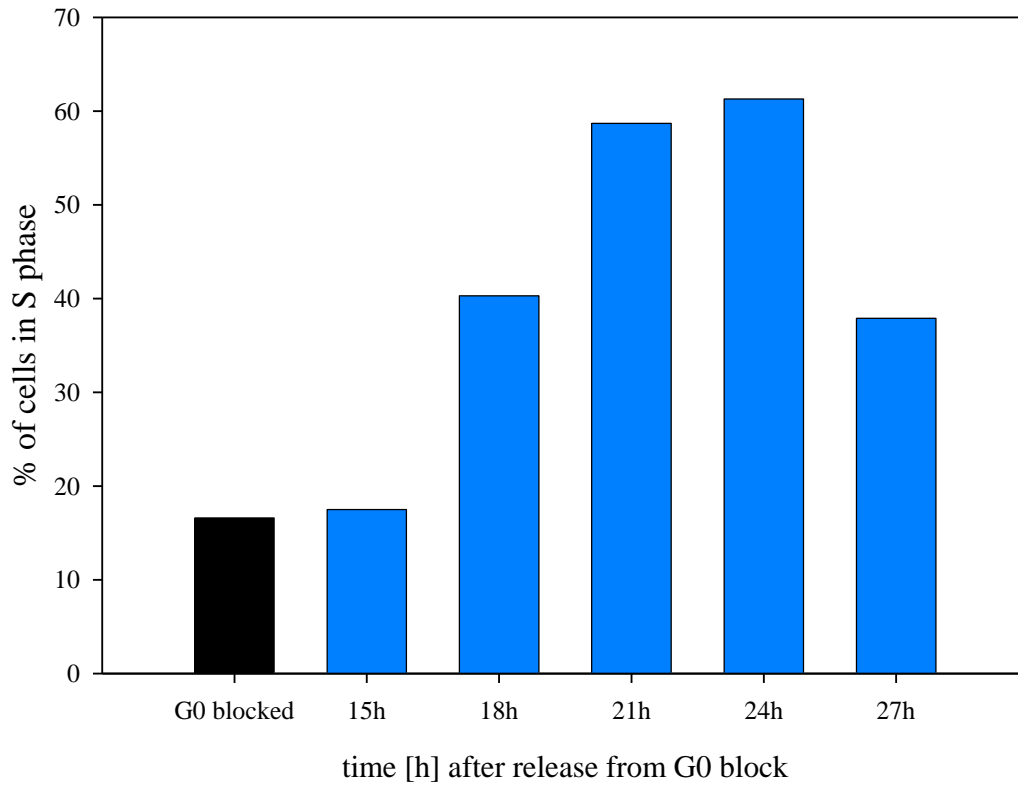
Figure 18 Fraction of MCF-12A cells in S phase after release into starvation medium with EGF following 24 hours of serum-depletion

G0 accumulation was induced with serum-depletion for 24 hours (0.5% CD-HS), after which the starvation medium was removed and EGF (20 ng/ml) in fresh starvation medium was added. Cell cycle analysis was performed with flow cytometry after staining of DNA with PI. Shown are the results of a representative experiment.

4.2.3 Other growth factors in starvation medium

We tested if the addition of growth factors other than EGF would yield similar results in terms of cell cycle progression. Insulin, IGF-1, and a combination of insulin with EGF were chosen. The results are presented as fractions normalised to the negative control sample. The addition of EGF, alone or together with insulin, in starvation medium had by far the strongest effect on cell cycle progression (Figure 19). Insulin or IGF-1 as the sole growth factor did not significantly induce progression in these cells.
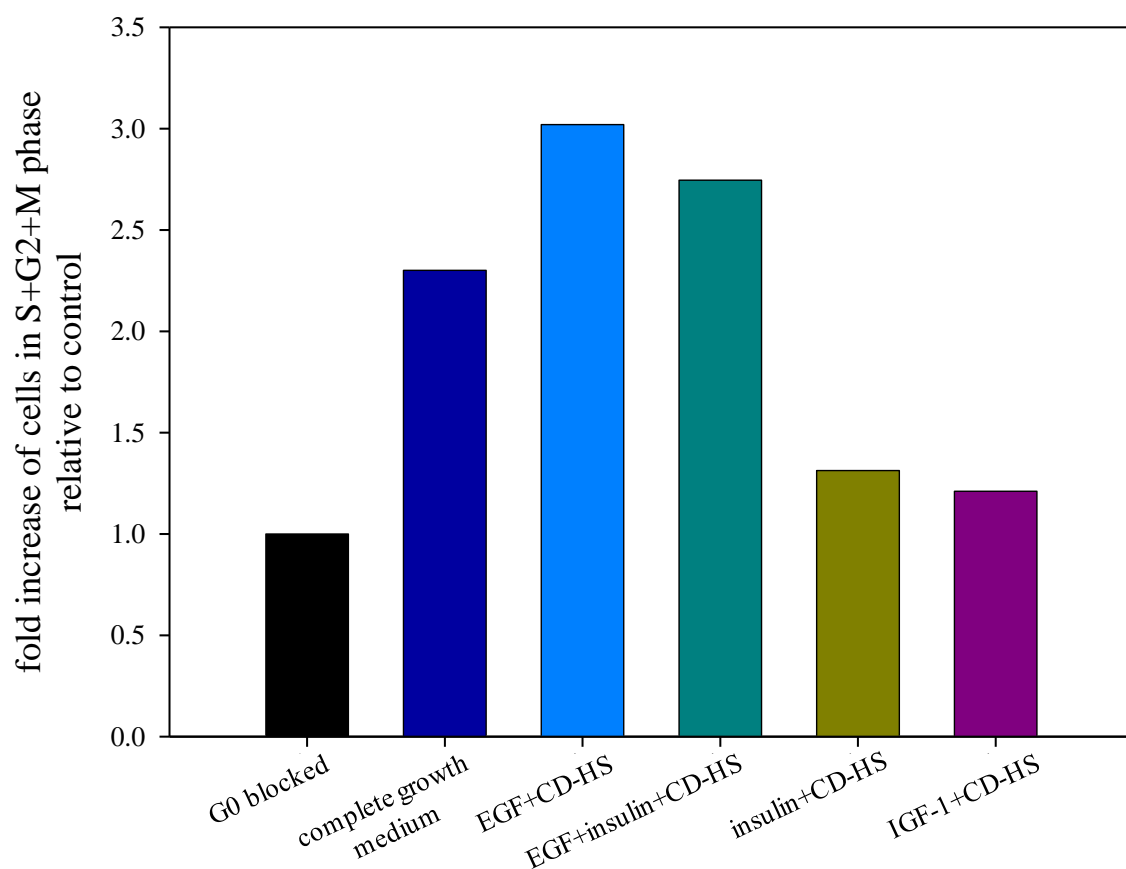
Figure 19 Proportion of MCF-12A cells re-entering the cell cycle 18 hours after release into starvation medium supplemented with various growth factors

G0 accumulation was induced with serum-depletion for 24 hours (0.5% CD-HS). Cells were released with EGF (20 ng/ml), EGF+insulin (20+100 ng/ml), insulin (100 ng/ml), IGF-1 (20 ng/ml), each in in fresh starvation medium, or complete growth medium (= positive control). Incubations lasted for 18 hours before flow cytometry analysis was performed after staining of DNA with PI. Values were normalised to negative control (G0 blocked sample) which was set to 1. Shown are the results of a representative experiment.

4.3 Varying the intervening time between administration of the two pulses

Next, it was necessary to test if a discontinuous exposure regimen, with two pulses of administration of growth factors would be sufficient to stimulate cell cycle re-entry of MCF-12A cells. To this end, we utilised an experimental set-up where the G0 blocked cells were incubated during two distinct pulses of different duration with EGF (20 ng/ml) in starvation medium. The length of the first pulse (30 minutes) had been established from published reports (Jones and Kazlauskas 2001), but the gap phase between the two incubation times needed to be determined empirically. The results are presented in Figure 20. An intervening time of 4 hours from the start of the release to the start of the second exposure (meaning an actual waiting time of 3.5 hours after the end of the first incubation), was optimal for recovering most of the cells from the G0 phase into the S phase. Prolongation of the gap phase beyond 4 hours to 6, 8 or 10 hours led to fewer cells entering the cell cycle. The positive control (C+) was a sample that was incubated continuously with 0.5% CD-HS and EGF (20 ng/ml).
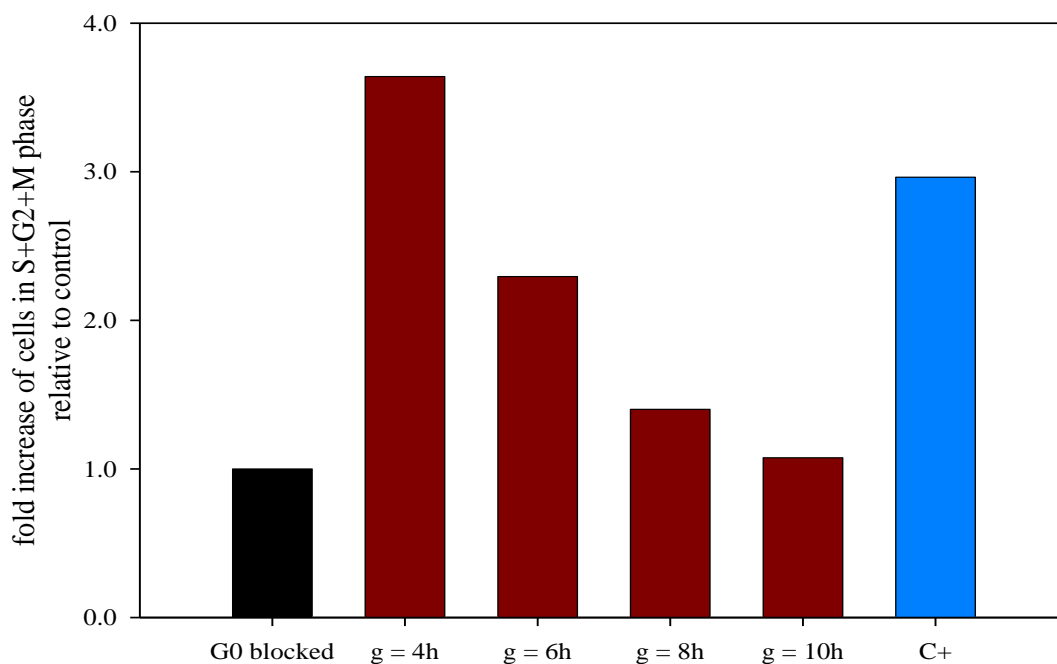
Figure 20 Proportion of MCF-12A cells re-entering the cell cycle 18 hours after discontinuous exposure to EGF in starvation medium

G0 accumulation was induced with serum-depletion for 24 hours (0.5% CD-HS). Cells were released with EGF (20 ng/ml) in fresh starvation medium. Incubation was carried out at two distinct times; the gap phase (g) between the two exposures was varied from 4 to 10 hours. Flow cytometric analysis was performed after staining of DNA with PI. Values were normalised to negative control (G0 blocked sample, set to 1), positive control (C+) is from cells that were continuously exposed. Shown are the results of a representative experiment.

4.4 Omission of serum from culture media

The complete omission of serum, from both exposure pulses, was important for all subsequent assays. The effect of the tested growth factor may be assessed properly only if interference from serum factors can be excluded. It was decided to remove the serum initially only from the first pulse, before removing it completely.

To compensate for the removal of serum during the first pulse, the cells were treated with higher concentrations of EGF (50 ng/ml), while serum was included during the second pulse, with 20 ng/ml EGF plus 0.5% CD-HS (Figure 21). The number of cells able to re-enter the cell cycle upon discontinuous stimulation remained virtually the same when the initial pulse consisted of EGF only, when compared to the cells that were treated with serum containing medium both times.
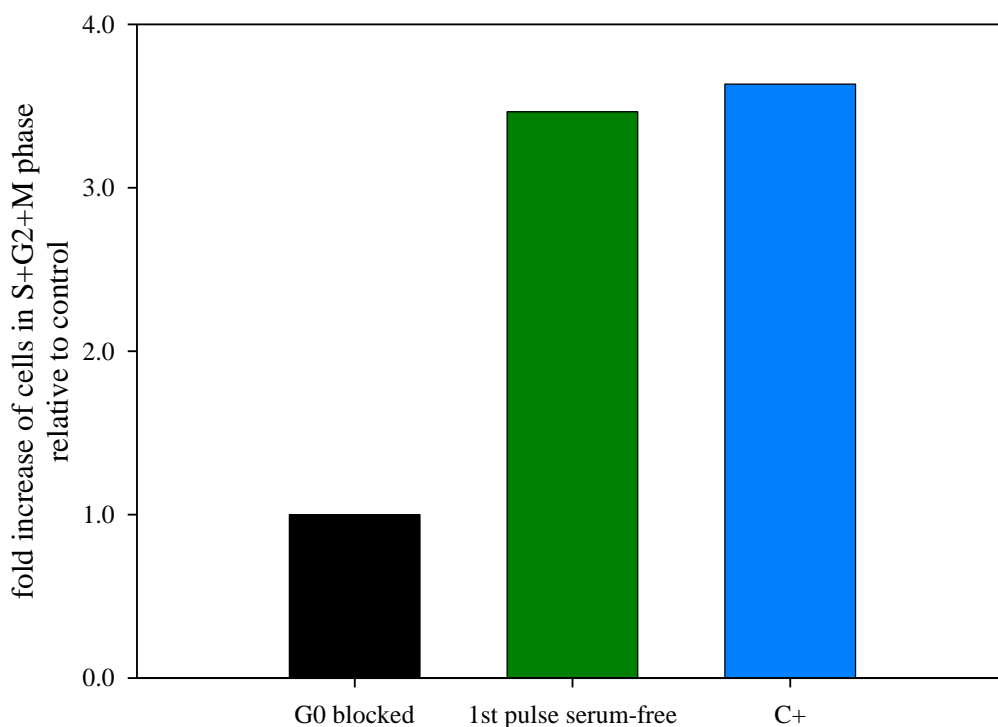
Figure 21 Proportion of MCF-12A cells re-entering the cell cycle with EGF in basal medium (first pulse)

G0 accumulation was induced with serum-depletion for 24 hours (0.5% CD-HS). Incubation for release was carried out at two distinct times. Cell cycle analysis was performed 18 hours after start of release. Values were normalised to negative control (G0 blocked sample, set to 1), positive control (C+) shows results from cells that were exposed to 0.5% CD-HS + 20 ng/ml EGF in both pulses. Complete omission of CD-HS during the first pulse after serum-depletion, instead cells received EGF alone (50 ng/ml) in the first pulse, and 0.5% CD-HS + 20 ng/ml EGF in the second pulse. The results shown are from one representative experiment.

For the subsequent experiments the serum was left out during both pulses. In all these experiments, EGF (50 ng/ml) was administered during the first pulse and the effect of different growth factors in the second pulse was tested. The investigated combinations are listed in Table 9.

Table 9: Growth factor combinations tested in the discontinuous exposure assay

Overview of the combinations of growth factors tested in the discontinuous experimental set-up in order to eliminate gradually the serum from both pulses.

growth factor in 1st incubation	concentration	growth factor in 2nd incubation	concentration
EGF	50 ng/ml	EGF	50 ng/ml
EGF	50 ng/ml	insulin	100 ng/ml
EGF	50 ng/ml	EGF + insulin	20 + 100 ng/ml
positive control:			
EGF	50 ng/ml	EGF + CD-HS	20ng/ml + 0.5% (v/v)

The results, obtained by flow cytometry as percentages for each cell cycle phase, were normalised to the negative control (which was set to 1) as before and are shown in Figure 22. As can be seen, two samples without serum showed a very similar amount of cells in the cell cycle after the total release time of 18 hours to the positive control, namely the one that received EGF only, and the sample exposed to EGF together with insulin. It is obvious that the MCF-12A cells did not require serum for entering S phase after arrest in G0.
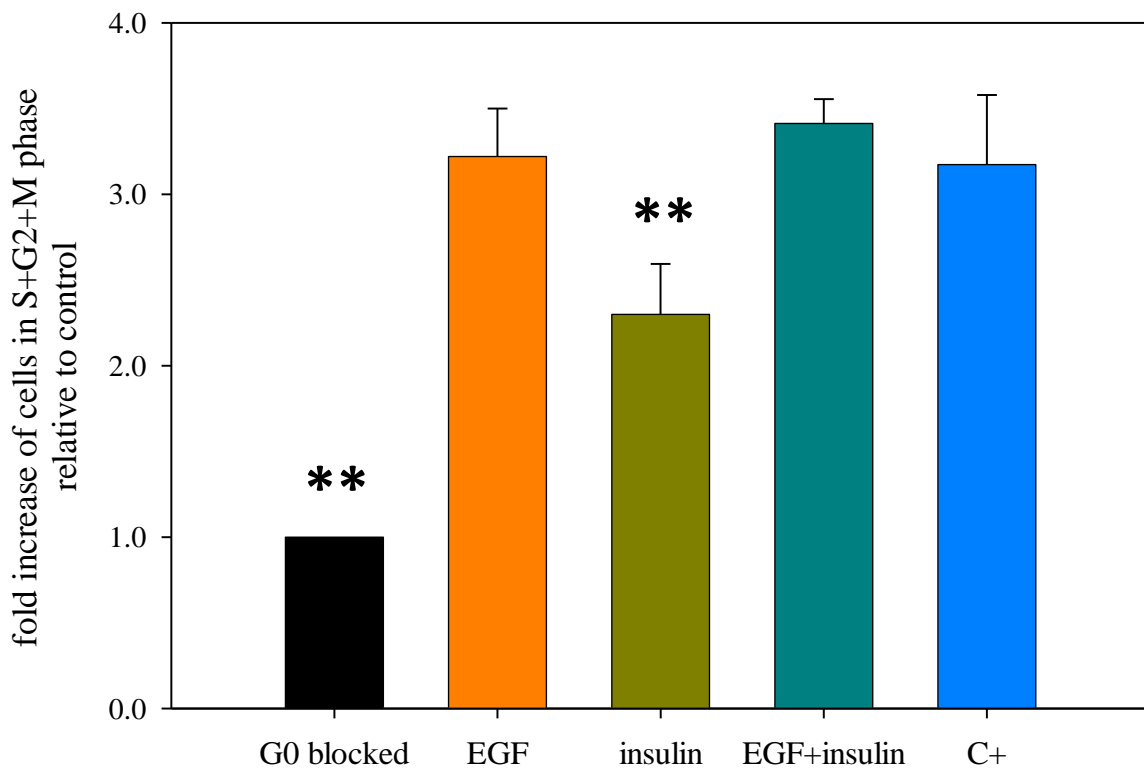
Figure 22 Proportion of MCF-12A cells re-entering the cell cycle with defined growth factors

G0 accumulation was induced with serum-depletion for 24 hours (0.5% CD-HS). Incubation for release was carried out at two distinct times, and cell cycle analysis was performed 18 hours after start of release. Values were normalised to negative control (G0 blocked sample, set to 1). Cells were incubated with EGF (50 ng/ml) in the first pulse, and the named growth factors in the second pulse; positive control (C+) was exposed to EGF in the 1st pulse and EGF+CD-HS in the 2nd pulse (cf. Table 9). Values show the mean of three independent experiments; error bars show SEM. Student's *t*-test was performed for significance testing, samples marked with ** (P=0.05) are significantly different from the positive control (C+).

4.5   Varying the length of the second pulse

The discontinuous exposure regimen established thus far for MCF-12A cells has the following features:

During 24 hours, cells received a reduced amount of serum of 0.5% (v/v) (instead of 5% (v/v) in the complete growth medium) which led to accumulation in G0. Subsequently, the cells were incubated for 30 minutes with 50 ng/ml EGF in basal medium, then washed out with aqueous buffer and left in basal medium for three and a half hours, before treatment with 20 ng/ml EGF and 100 ng/ml insulin in basal medium. The cells were incubated until the end of the assay, which was determined by the length of the total release time, 18 hours, where S phase percentages peaked. The second incubation therefore lasted for 14 hours. Since the overall aim of this project was to study the signals important for inducing cell cycle entry, past the R point before the start of S phase, we next investigated the influence of shortening the duration of the second incubation. The purpose was to find out whether a shorter second pulse would be sufficient, in terms of yielding the same S phase figures as before, if the overall release period of 18 hours remained unchanged. To this end, the length of the second cycle was varied to last between 4 and 14 hours. When the 2nd incubation was shorter than 14 hours, the cells were incubated afterwards with basal medium once more in order to give them sufficient time to progress into S phase, until completion of the total release time of 18 hours. The intervening time between the two distinct exposures was not changed (4 hours between the start of the 1st and the start of the 2nd incubation); hence the duration of the final cycle in basal medium was variable. It was found that a second pulse of 8 hours was sufficient to bring most cells past the R point (Figure 23). However, for practical reasons, a 10 hour incubation was chosen as the standard protocol. The diagram (Figure 24) gives a summary of the standard protocol and its timing. This protocol was used for in-depth studies in the subsequent chapters of this thesis.
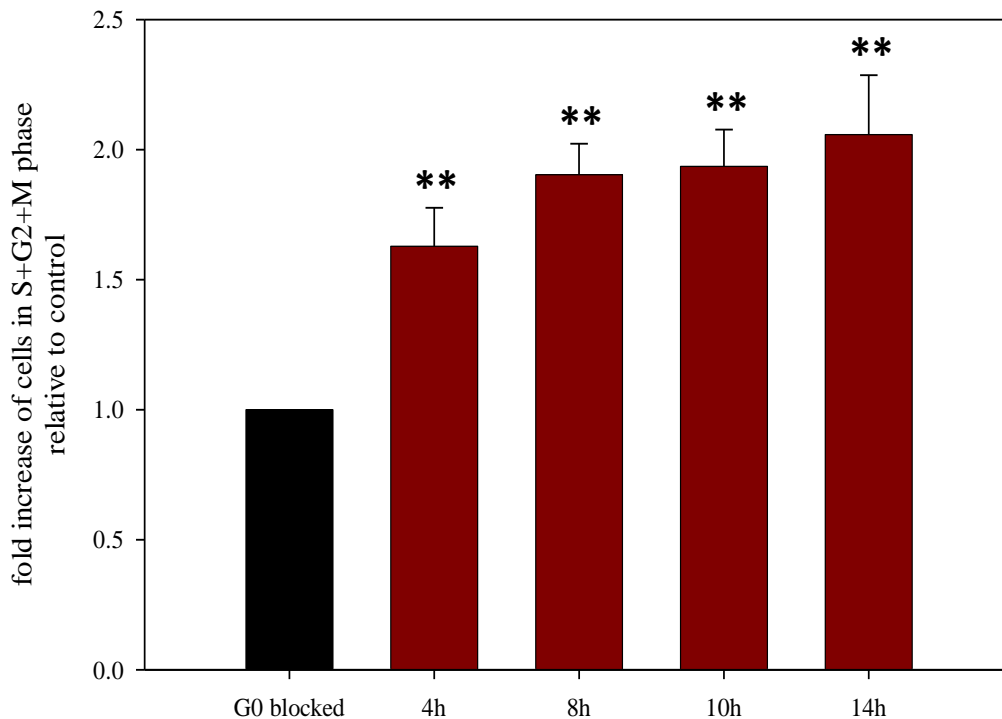
Figure 23 Varying the duration of the second pulse for release of MCF-12A cells

G0 accumulation was induced with serum-depletion for 24 hours (0.5% CD-HS). Incubation for release was carried out at two distinct times. Cells were incubated with EGF (50 ng/ml) in the first pulse, and EGF (20 ng/ml) plus insulin (100 ng/ml) in the second pulse. The length of the 2nd pulse was varied. Flow cytometry was performed 18 hours after start of release. Values were normalised to negative control (G0 blocked sample, set to 1). Values show the mean of three independent experiments; error bars show SEM. Student's *t*-test was performed for significance testing, samples marked with ** (P=0.05) are significantly different from the negative control (G0 blocked). The pulsed samples are not significantly different from each other.

Figure 24 Schematic representation of the discontinuous regime

The incubation times applied in the discontinuous exposure assay as used for the routine exposures for the remainder of the work presented here.

It was important to confirm that the discontinuous exposure regimen as established above, truly reflects the distribution of the cell cycle phases as would be obtained with the complete growth medium (shown in Figure 17). To this end two assays were performed in parallel, one where cells were treated continuously with complete growth medium, the second where cells were stimulated according to the discontinuous exposure assay, under otherwise exactly the same conditions (same seeding densities, attachment and starvation period). Cells were analysed at different time points after the initiation of S phase. The results are shown in Figure 25. For better legibility, the cell cycle phases are illustrated in 2 bars only, one that represents the cells in G0/G1 phase, the other bar showing the percentage of cells that re-entered the cycle, i.e. the sum of the percentages obtained for S, G2 and M phase. It can be seen that the fraction of cells to be found in S+G2+M phase at each time point after discontinuous stimulation did not differ significantly from the continuously exposed cells. Accordingly, the bars representing the G1 phase cells reached very similar heights with either treatment. This allowed the conclusion that the pulsed regimen did not alter the cell cycle, but that it induced the same cell cycle activities as did continuous treatment with complete growth medium. Therefore, the discontinuous treatment provided a good method for studying the influence of specific growth factors on cell cycle re-entry in these cells.
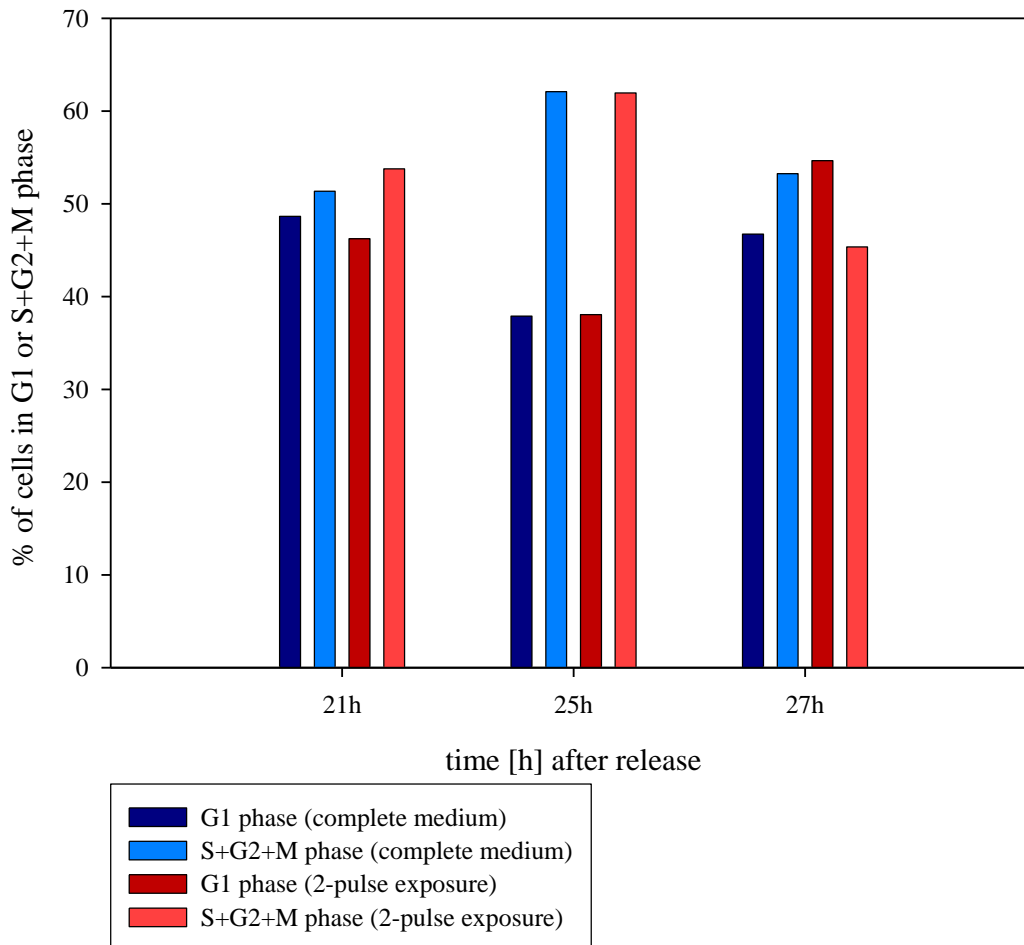
Figure 25 Comparison of cell cycle progression in MCF-12A cells released from cell cycle arrest by treatment with complete growth medium or by using the discontinuous exposure regimen

G0 accumulation was induced with serum-depletion for 24 hours (0.5% CD-HS). Cell cycle analysis was performed after release with continuous exposure to complete growth medium (blue bars) or with two distinct exposures to mitogens (EGF (50 ng/ml) in the first pulse, and EGF (20 ng/ml) plus insulin (100 ng/ml) in the second pulse, red bars). Results are from a representative experiment.

4.6 Investigating the influence of omitting the 1st pulse

Since the first pulse was so much shorter than the second pulse, its contribution to enable the cells to enter the cell cycle was unclear. The relevance of the 1st pulse for cell cycle entry was investigated by omitting it completely (Figure 26). The total number of cells able to enter the cell cycle was significantly reduced when the first round of EGF was omitted. However, in approximately one third of all cells, the second incubation period seemed to activate sufficient signals that allowed them to pass the R point.
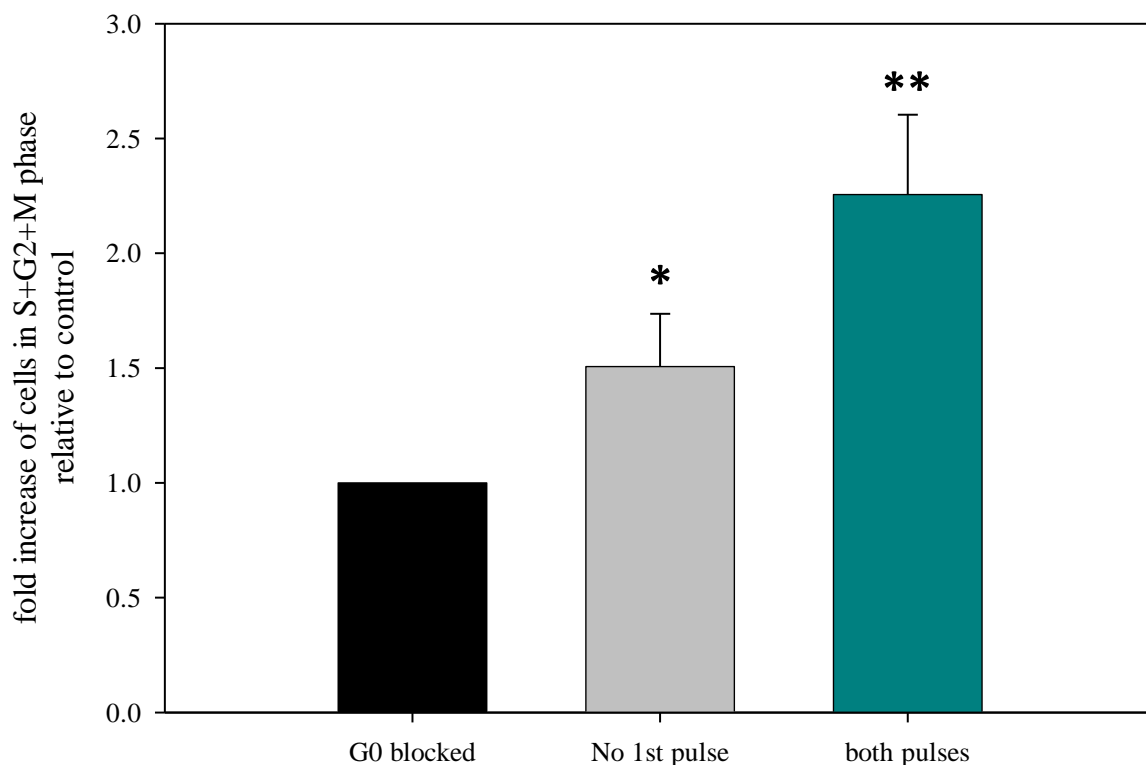
Figure 26 Comparison of cell cycle progression in MCF-12A cells released with or without the first pulse

G0 accumulation was induced with serum-depletion for 24 hours (0.5% CD-HS). Cell cycle analysis was performed 18h after start of release with two distinct incubation times (EGF (50 ng/ml) in the first pulse, EGF (20 ng/ml) plus insulin (100 ng/ml) in the second pulse), or with the second pulse only. Values were normalised to the negative control (G0 blocked sample, set to 1). Values show the mean of five independent experiments; error bars show SEM. Student's *t*-test was performed for significance testing, both pulsed samples are significantly different from the negative control (G0 blocked; ** (P=0.01); * (P=0.1)), but they are not significantly different from each other.

4.7 Combinations of growth factors in each pulse

Apart from the routine combination of EGF and insulin (cf. Figure 24), it was of interest to assess other combinations of growth factors for their ability to facilitate cell cycle entry of MCF-12A.

4.7.1 EGF as the sole growth factor

As EGF in combination with a small amount of serum had such a positive effect on cell cycle re-entry (as seen in Figure 18 in comparison to Figure 17), EGF alone was tested in both exposures, but replacing the combination of EGF + insulin in the second pulse by a higher dose of EGF alone (50 ng/ml). The efficiency of this combination of EGF was as high as that of the positive control, shown in Figure 27.

4.7.2 Insulin

Next, the effects of the hormone insulin in each pulse were assessed. As seen in the same figure (Figure 27), some cells were able to leave the G0 block when they received insulin instead of EGF in the first pulse, but the effect was not as strong as in the positive control where cells were treated with EGF in the first pulse (and a combination of EGF with insulin in the second pulse). When insulin alone was added in the second pulse, its effect was even lower and closer to the percentages of the negative control, independently of which growth factor the cells received during the first pulse (EGF or insulin). Interestingly, the slight stimulation effect by insulin in the second pulse seemed to be dose-dependent, as demonstrated in Figure 28.
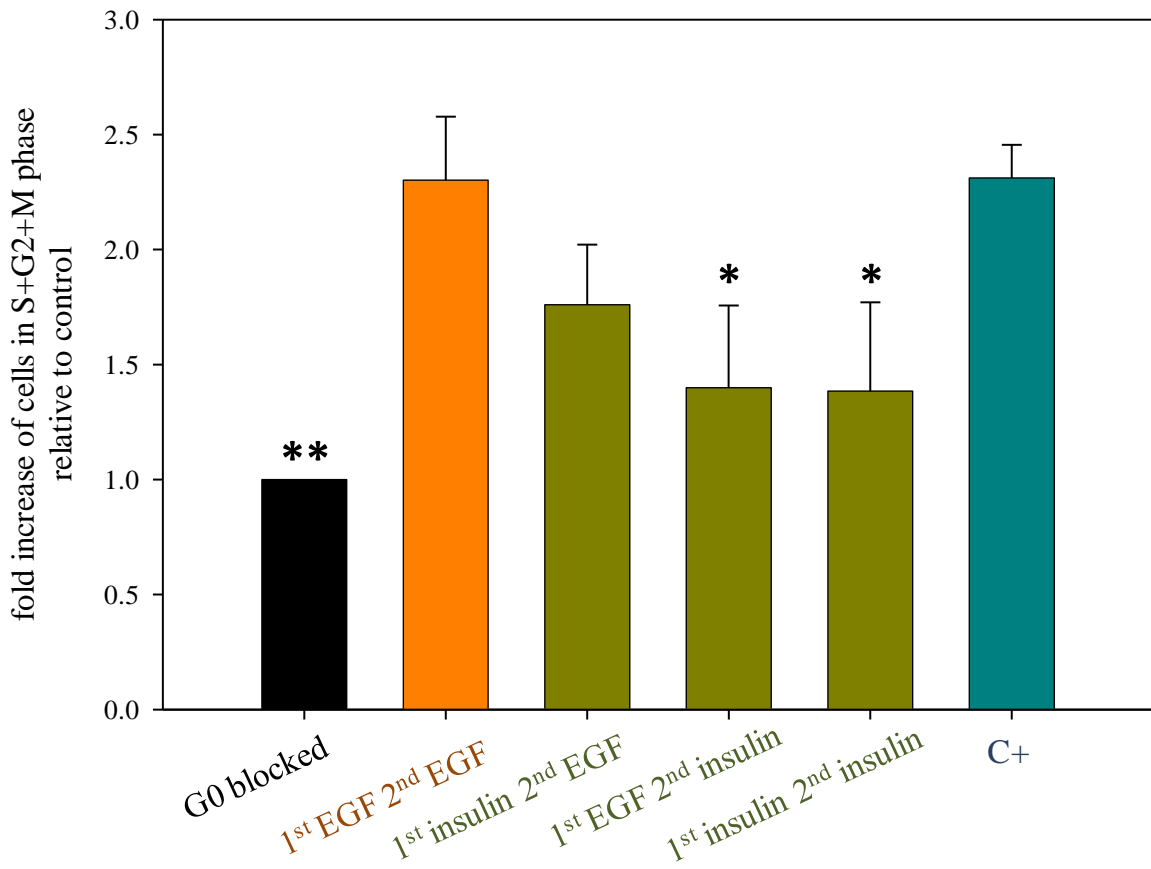
Figure 27 Effect of different combinations of growth factors on cell cycle re-entry of MCF-12A cells

G0 accumulation was induced with serum-depletion for 24 hours (0.5% CD-HS). Cell cycle analysis was performed 18h after start of release with two distinct incubation times. Cells were incubated with the combinations shown for each bar (concentrations used were: insulin=200ng/ml; EGF=50ng/ml). Positive control sample (C+) was incubated with the routine combination (1ˢᵗ pulse EGF (50ng/ml), 2ⁿᵈ pulse EGF+insulin (20+100ng/ml), Figure 24). Values were normalised to the negative control (G0 blocked sample, set to 1). Values shown are the mean of at least three independent experiments; error bars show SEM. Student's *t*-test was performed for significance testing, samples marked with ** (P=0.05) and * (P=0.1) are significantly different from the positive control (C+).
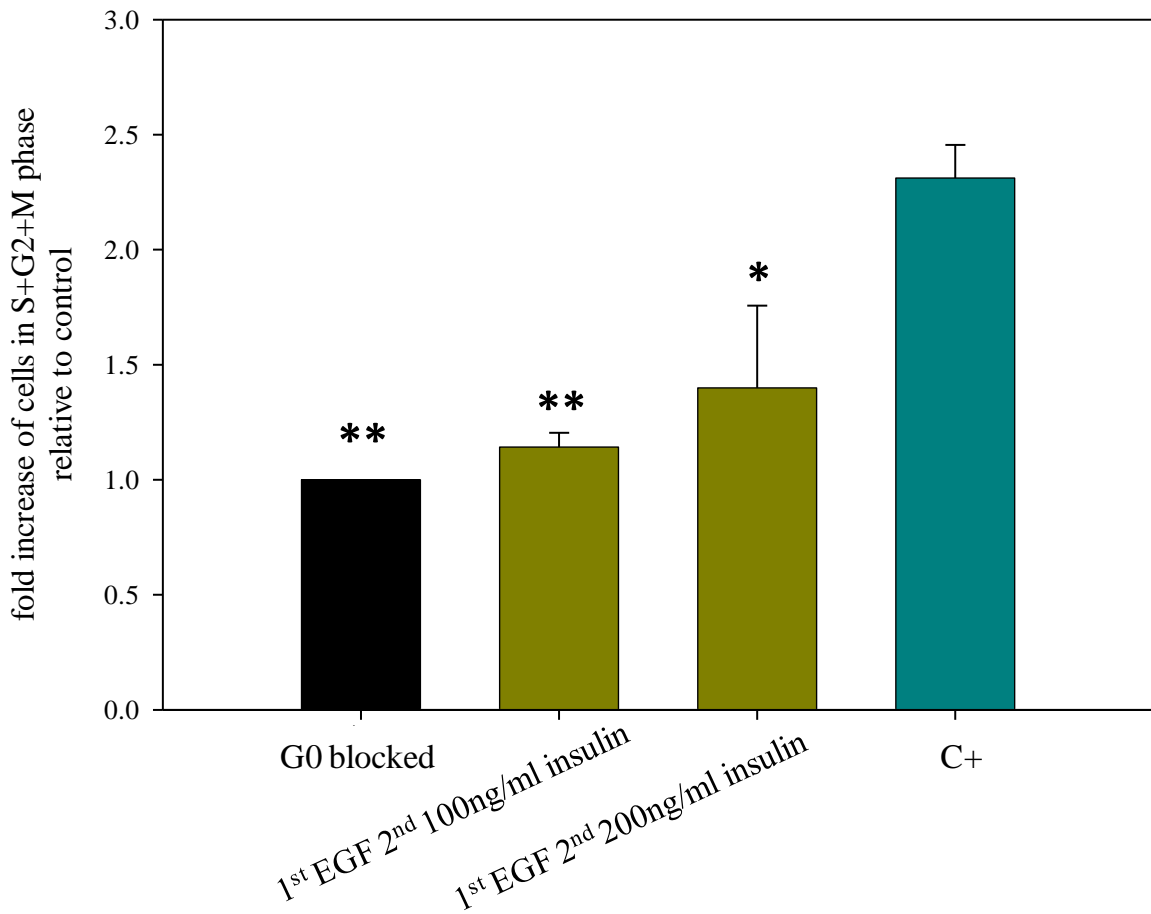
Figure 28 Effect of different concentrations of insulin on cell cycle progression of MCF-12A cells released with the discontinuous exposure assay

G0 accumulation was induced with serum-depletion for 24 hours (0.5% CD-HS). Cell cycle analysis was performed 18h after start of release with two distinct incubation times. Cells were incubated with the combinations shown for each bar (EGF=50ng/ml). Positive control sample (C+) was incubated with the routine combination (1st pulse EGF (50ng/ml), 2nd pulse EGF+insulin (20+100ng/ml), Figure 24). Values were normalised to G0 blocked sample which was set to 1. Values show mean of four independent experiments, except from the sample with insulin=100ng/ml (n=2); error bars show SEM. Student's *t*-test was performed for significance testing, samples marked with ** (P=0.05) and * (P=0.1) are significantly different from the positive control (C+).

4.7.3 PDGF

PDGF was tested for its ability to promote cell cycle progression the discontinuous exposure assay, and the findings of this set of experiments are presented in Figure 29. Similar to insulin, PDGF was able to stimulate the cells slightly when administered during the 1st pulse, followed by EGF in the second pulse, but no effect was observed compared to the G0 blocked sample when it was added in the second pulse, or in both incubation periods.
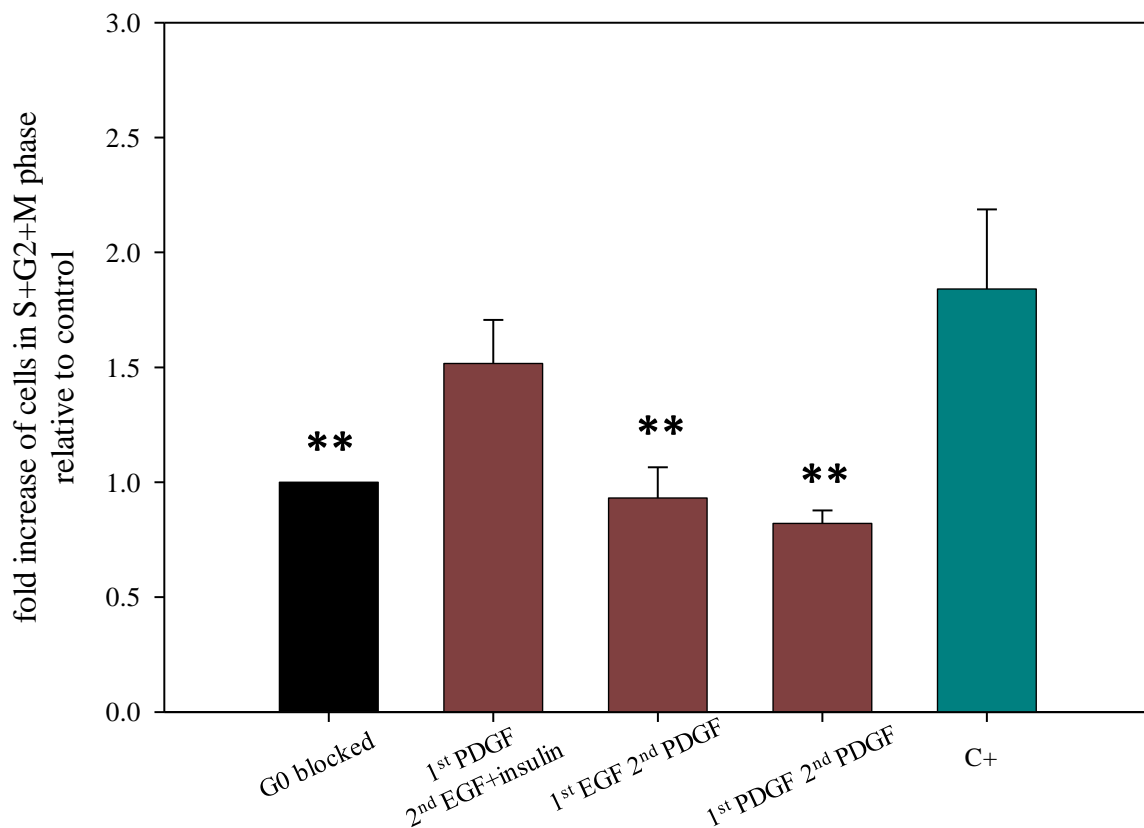
Figure 29 Effect of different combinations of PDGF on cell cycle progression of MCF-12A cells

G0 accumulation was induced with serum-depletion for 24 hours (0.5% CD-HS). Cell cycle analysis was performed 18h after start of release with two distinct incubation times. Cells were incubated with the combinations shown for each bar (concentrations used were: PDGF=50 ng/ml; EGF=50 ng/ml; EGF+insulin= 20+100 ng/ml). Positive control sample (C+) was incubated with the routine combination (1st pulse EGF (50 ng/ml), 2nd pulse EGF+insulin (20+100 ng/ml), Figure 24). Values were normalised to G0 blocked sample which was set to 1. Values show the mean of three independent experiments; error bars show SEM. Student's t-test was performed for significance testing, samples marked with ** (P=0.05) are significantly different from the positive control (C+).

4.7.4 Estradiol

Finally, the effect of the endogenous hormone estradiol (E2) was examined. Clearly, E2 was unable to promote cell cycle progression in quiescent MCF-12A cells (Figure 30). Administration during the second pulse resulted in no difference of S phase percentages from the negative control sample. The percentages were slightly higher when E2 was added during the first pulse, but not significantly when compared to the positive control.
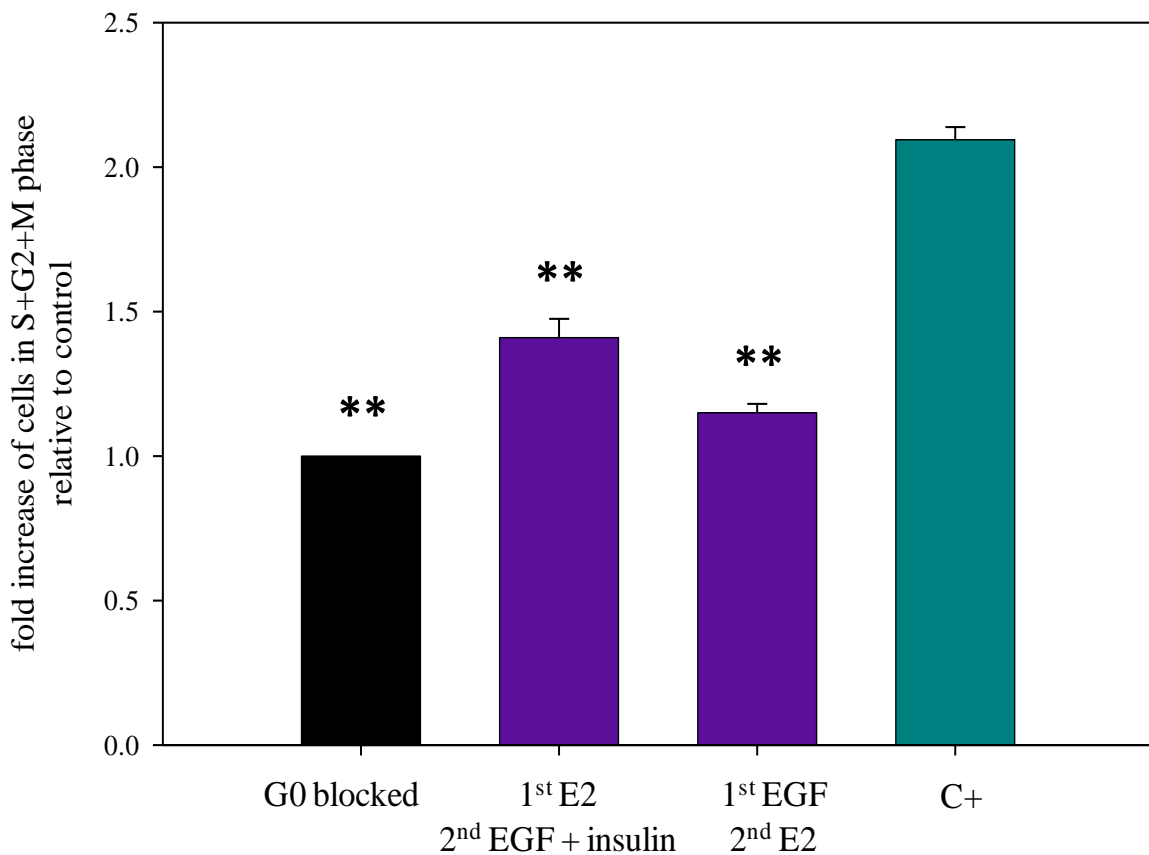
Figure 30 Effect of E2 in the discontinuous exposure assay on cell cycle progression of MCF-12A cells

G0 accumulation was induced with serum-depletion for 24 hours (0.5% CD-HS). Cell cycle analysis was performed 18h after start of release with two distinct incubation times. Cells were incubated with the combinations shown for each bar (E2=10nM; EGF=50ng/ml; EGF+insulin=20+100ng/ml). Positive control sample (C+) was incubated with the routine combination (1st pulse EGF (50ng/ml), 2nd pulse EGF+insulin (20+100ng/ml), Figure 24). Values were normalised to the negative control (G0 blocked sample, set to 1). Values show mean of four independent experiments; error bars show SEM. Student's *t*-test was performed for significance testing, samples marked with ** (P=0.05) are significantly different from the positive control (C+).

5 DISCUSSION

5.1 Cell synchronisation

The human breast epithelial cell line MCF-12A was well synchronised when the amount of serum in the culture medium was reduced from 5% of full serum to 0.5% of CD-treated horse serum for 24 hours, which resulted in more than 70% of cells arrested in the G0 phase of the cell cycle. The remainder of the cells (approximately 30%) was able to progress through the cell cycle when only 0.5% of CD-HS was available, but extended starvation periods did not result in higher synchronicity and even led to the loss of cells through induction of apoptosis. In general, serum starvation never renders all cells quiescent, but for some cells it only slows down the process of cell division. This emphasizes once more the importance of normalising the flow cytometric results to the negative control (G0 blocked cells), which was discussed in the previous Chapter 3 (page 53).

5.2 Cell cycle re-entry with continuous stimulation

The cells could be released from quiescence by replacing the starvation medium with complete growth medium. The majority of cells reached S phase 21 hours later. The complete culture medium contained a variety of growth factors, originating from the horse serum used for supplementation, as well as from separate additions, namely cholera toxin, EGF, hydrocortisone and insulin. Essentially the same results were achieved when the complete medium was replaced with EGF in the presence of 0.5% CD-HS. However, the number of cells in S phase stayed high for longer (3 hours longer compared to the release with complete medium), indicating that the progression through S phase was slowed down. An explanation for this may be that EGF+0.5% CD-HS did not elicit the same mitogenic signalling pathways as the combination of several growth factors present in the complete growth medium. Then the rate of DNA synthesis would be slowed down compared to a fully stimulated population. This explanation is backed up by the fact that the maximal number of S phase cells is higher with EGF in starvation medium (in Figure 18) than with complete growth medium (in Figure 17), because the probability of finding a S phase cell at any point of the analysis is greater, the longer the process of accumulating replicated DNA takes (cf. Chapter 3, page 37).

Insulin, when tested alone to replace EGF, was ineffective in inducing cell cycle progression in MCF-12A cells. This was surprising, given the pronounced effects of this compounds on

various other cell lines (Tamm and Kikuchi 1990; Straus 1984), including malignant human mammary epithelial cells (Dufourny et al. 2000), and considering the presence of insulin in the complete growth medium for the MCF-12A cells. It is possible that insulin exerted proliferative properties only in conjunction with hydrocortisone (which was included in the complete growth medium), as was reported for MCF-7 cells (Linebaugh and Rillema 1977). Also, the MCF-7 cell line slightly over-expresses the insulin receptor (Oleksiewicz et al. 2011), which might account for its more pronounced effect, and which may not be the case for the normal MCF-12A cells. Indeed, in rat normal mammary cells low expression of the insulin receptor (IR) was observed (Hvid et al. 2011). To better assess the results, an examination of the expression profile of the relevant receptors would be useful.

5.3 The discontinuous exposure assay

All observations so far were made after the cells had been stimulated continuously. Taking the assay further, the cells were subjected to a discontinuous stimulation with EGF+0.5% CD-HS. The length of the incubation periods and the intervening time between the two pulses was determined firstly on the basis of published methods (Jones and Kazlauskas 2001; Balciunaite et al. 2000; Pledger et al. 1977; Temin 1971), and then refined empirically. Subsequently, the serum present during both pulses was removed, and a routine experimental set-up, as shown in Figure 24, was established.

The length of the first pulse (30 minutes) had been based on observations that kinases essential for mitogenesis were activated within 10 minutes of serum stimulation, and that their initial activity was required for no more than 30 minutes (Stacey and Kazlauskas 2002; Jones et al. 1999; Gille and Downward 1999). The length of incubation was sufficient to make a significant contribution to cell cycle re-entry, although a remarkable number of cells were able to leave the quiescent state upon incubation with the 2nd pulse only. This was in disagreement with reports from fibroblasts, where the omission of the 1st pulse resulted in completely unsuccessful cell cycle re-entry (Jones and Kazlauskas 2001). This difference can be explained with the competence / progression system assumed to be underlying cell cycle re-entry: cells need to receive a first input from growth factors which pushes them out of G0 and so they become competent for the subsequent stimulation, which will result in progression through G1, followed by passing the R point. If the cells do not receive a first stimulation, but if the second pulse is strong enough (strength would possibly be determined by the time span that mitogens are available), the second incubation may be sufficient to

91

provide for all necessary signals. To test this possibility, quiescent cells could be incubated with the second pulse only (omission of 1st pulse), but for a shorter period of time. A decrease in the number of cells in S phase after a shorter second pulse compared to a population exposed to both pulses (but also with a shorter second pulse, cf. Figure 23) would be expected. The differences in responsiveness may be attributed to variances in physiological factors, such as the number of receptors expressed on the membrane.

The suggestion that the mechanism of competence and progression is in place in MCF-12A cells was supported by the finding that the intervening time between the two pulses could not be stretched beyond 6 hours, which is in good agreement with the time line suggested by others (Jones and Kazlauskas 2001; Temin 1971).

5.4 Assessment of growth factors

Having established a discontinuous experimental set-up, which allowed quiescent MCF-12A cells to re-enter the cell cycle upon incubation with only insulin and EGF (presented in Figure 24), it was attempted to find other growth factors that would have a similar effect on cell cycle progression.

The most pronounced effect in terms of the percentage of cells brought into S phase was observed when the MCF-12A received first EGF, followed by EGF combined with insulin. However, application of EGF during both pulses gave nearly as strong a result, which provokes the question as to the actual role of insulin. It has been reported for malignant mammary epithelial cells, that insulin's effect on proliferation was stronger when added in combination with EGF (van der Burg et al. 1988), possibly because crosstalk between insulin receptors and EGFR occurred, and also in combination with hydrocortisone (Linebaugh and Rillema 1977). That insulin indeed contributed to the progression of MCF-12A cells could be seen when it was given alone in the second pulse, and its effect became more pronounced with a higher concentration. The dose-dependent effect of insulin may be explained by considering that EGF alone triggers signals more potently; therefore a higher concentration of insulin was needed to compensate for the missing EGF and to activate pathways to the same extent. Interestingly, a similar pattern was observed in fibroblast cells: insulin given in the first pulse did not contribute to initiating DNA replication, but when used as the 2nd mitogen, it was very powerful (Jones and Kazlauskas 2001). This points towards the concept already developed in the 1970s (Pledger et al. 1977), namely, that quiescent cells needed a first input to render them competent, followed by a second stimulus that enabled the competent cells to

actually progress in G1 phase. From this point of view, insulin seemed to be more of a progression factor than a competence factor, independently of the cell type.

As PDGF was extensively used in fibroblast cells, it was also tested on the MCF-12A, with very little effect on cell cycle re-entry when used during the 1st pulse, and no effect when used during the 2nd pulse. It was suspected that the MCF-12A cell line did not express sufficiently the appropriate receptor, and therefore PDGF was unable to elicit mitogenic signalling pathways in these cells. The minor effect of PDGF during the first cycle may be explained by the three-dimensional structure of the isoform PDGF-BB used here. It shows some resemblance to the structure of the transforming growth factor-β (TGF-β). TGF-β is a potent ligand for the EGFR, therefore an activation of the EGFR by PDGF-BB could not be ruled out entirely (Heldin and Westermark 1999). More likely, however, is that here again, some cells received sufficient signals during the second incubation period for passing successfully the R point, as has been considered before (cf. page 91).

Finally, the effect of the endogenous hormone estradiol (E2) was assessed. This was of special interest as estradiol plays a crucial role in the development and differentiation of the mammary gland, in particular of the luminal compartment (for a recent review see Bussard and Smith 2011) from which the MCF-12A cell line is derived. E2 increases proliferation through binding to the estrogen receptor alpha (ERα). The activated ER can either localise to the nucleus to activate proliferative genes, or act directly on mitogenic signalling pathways (Moriarty et al. 2006). E2 triggers cell proliferation in MCF-7 (ER+) cells (Karey and Sirbasku 1988; van der Burg et al. 1988), although the degree to which E2 promotes proliferation also depends on the culture condition, i.e. other factors present in the culture medium (Ruedl et al. 1990; Najid et al. 1989; Katzenellenbogen et al. 1987; Soto and Sonnenschein 1985).

The MCF-12A cells express the ERα, and therefore, a positive impact of E2 on the transition from the G0 block into S phase was expected. Surprisingly, no significant effect of E2 was observed when added instead of growth factors during the discontinuous assay (Figure 30). This is in apparent contrast to the physiological situation where mammary gland epithelial cells are reliant on the input of estrogens for growth and branching. The MCF-12A cells used here are immortalized non-transformed cells that may well have lost their sensitivity to estradiol (despite the presence of the ERα). This view is supported by reports that these cells display very different transcriptional activities and phenotypes when cultured in a three-dimensional context (contrary to our two-dimensional populations) which is closer to the

93

original environment *in vivo* (Polyak and Kalluri 2010). On the other hand, the effect of E2 on MCF-12A cell proliferation may also depend on the expression of other, not estrogen-related receptors. Such a dependency has been shown in MCF-7 cells: Hamelers and colleagues (2003) studied three different strains of this cell, each displaying a different sensitivity to estrogens, despite their similar ER expression activity levels (Hamelers et al. 2003). It was found that induction of proliferation by E2 was dependent on IGF-1R activation, and this was blocked by antibodies for the IGF-1R, in both E2-sensitive cell lines. Similarly, Surmacz and Burgaud (1995) reported that overexpression of the principal substrate for the IGF-1R, IRS1, reduced the requirement of MCF-7 cells for E2 for growth. Furthermore, induction of IRS1 facilitated the cells' growth in soft agar, which is a measure for malignant transformation (Surmacz and Burgaud 1995). Thus, sensitivity of breast epithelial cells to estrogens may be regarded as a feature of transformation to malignancy, as has been suggested already more than two decades ago (Nenci et al. 1988). This would support the opinion that the lack of effect of E2 in the MCF-12A cells indeed reflects their original phenotype.

6 CONCLUSIONS

It is intriguing that MCF-12A cells responded to a variety of growth factors in terms of transition from quiescence into S phase only if these were administered in a specific sequence. This raises several questions:

First, what is the role of the estrogen receptor in the MCF-12A cells, if exposure to the ligand estradiol does not result in cell cycle progression? And secondly, what is the nature of the signalling pathways during the different pulsed exposures? Are similar pathways activated at the distinct incubation times, or do the cells employ different signalling cascades at different time points? These issues will be addressed in the following chapters.

Chapter 5:

Regulation of genes by estradiol compared to EGF in MCF-12A cells

1 INTRODUCTION

As was shown in the previous Chapter 4, the endogenous hormone estradiol (E2) did not have a pronounced effect on cell cycle progression of MCF-12A cells when it was applied instead of a growth factor, during the discontinuous exposure assay. This was unexpected, since the hormone has a major function in the development of the mammary gland, from which the MCF-12A cell line was derived, and these cells express the ERα on a transcriptional and translational level. As such, the role of this receptor for these cells is unclear. In order to better define its function, the mRNA levels of genes normally controlled by the receptor were investigated after incubation with E2. The genes to be investigated were chosen according to their role in MCF-7 cells, which is the correspondent malignant line to the MCF-12A cells. Additionally, to compare the effect of this hormone with a truly mitogenic compound (in the context of MCF-12A cells), cells were treated with EGF, which was shown to have a positive impact on proliferation in MCF-12A cells.

The roles of E2 and the expression of genes affected by ERα are described in this section:

E2, together with its metabolites estrone (E1) and estriol (E3), belongs to the estrogen group of steroid hormones. Estrogens are involved in the development, growth and homeostasis of many different tissues, but their best known effects are observed in mammalian reproduction and the mammary gland. In contrast to most other organs, the development of the human mammary gland occurs mainly postnatally. Its completion requires the action of estrogens appearing cyclically during adulthood. The mammary epithelial cells even necessitate the high levels of estrogens produced only during a full term pregnancy for differentiation and resulting full maturation of the duct system (Polyak and Kalluri 2010).

E2 does play a critical role *in vivo*, but for obvious reasons is mainly studied *in vitro*. In many human breast cancer cell lines, the hormone induced proliferation (Papendorp et al. 1985; Soto and Sonnenschein 1985; Darbre et al. 1983). The proliferative effect of estrogens is mediated through specific receptors (Katzenellenbogen 1996), of which to date, three different types are known, the estrogen receptor (ER) alpha (ERα), ERβ and the G-protein coupled estrogen receptor (GPER or GPR30). ERα and ERβ are members of the large family of nuclear receptors, whereas GPR30 is a transmembrane receptor. Compared to ERα, ERβ has a limited expression pattern and is found mostly in the ovaries, while ERα is abundant in the breast and other target organs (Couse et al. 1997). In mammary epithelial cells ERα action is required for the normal development of the milk ducts in the gland because it signals for ductal elongation (Bocchinfuso et al. 2000). Thus, we will focus on the function of ERα.

In the absence of a ligand, the receptor is held in an inhibitory complex in the nucleus of the target cell. Upon binding of the hormone, the ERα forms a homodimer, and translocates towards a specific sequence in the DNA, the estrogen responsive element (ERE). EREs are found in the promoter region of a gene and thus enhance the transcription of their target (Means and O'Malley 1972; O'Malley et al. 1968). The target is often a gene with proliferative characteristics, but depending on the cell, the DNA-bound receptor also can exert a suppressive effect on the expression of such a target gene, or bind completely different types of genes, such as the pro-apoptotic *BCL2*. The different effects (inducing or inhibitory) may be explained either in terms of the final conformation that the ERs take after ligand binding or in terms of the cell's or promoter context, i.e. the multiple molecular factors present in each cell which might interact with the ligand-receptor complex, thus changing the ability of the complex to interact with the ERE (Ciocca and Fanelli 1997).

A few genes with perfect ERE palindromes, i.e. a high affinity for binding the ERα, have been identified, but the ERα also binds to and induces transcription through an imperfect responsive element. Examples of genes controlled by imperfect ERE include the *TFF1* and the *BCL2* genes (Bourdeau et al. 2004; O'Lone et al. 2004). In some cases a half-ERE site is located in proximity to a so called Sp-1 site (the Specificity Protein (Sp-) 1 is a transcription factor). Binding of the activated receptor to an ERE may even be omitted completely when the ERα engages in protein-protein interactions instead (so-called tethering), such as with the activating protein 1 (AP-1) complex. AP-1 is a dimeric transcription factor composed of Fos and Jun, and both proteins are strong promoters of cell cycle progression and proliferation. Since these many different mechanisms of action of the ERα on the genome exist, the effects

of ERα ligand binding are diverse and differ according to cell type. The information available to date about the impact of estrogens on specific target genes is provided mostly by estrogen-sensitive cancer cell lines, whereas data from normal cells is scarce.

1.1   Genes coding for nuclear steroid receptors (ESR1 and PGR)

Evidence from ERα-competent cell lines such as MCF-7 shows that the genes first and foremost affected by the endogenous hormone estradiol include *ESR1*, coding for ERα, which contains three ERE half-sites in its promoter region, and the gene *PGR*, coding for the progesterone receptor (PR). Together with estradiol, progesterone signalling is crucial for the normal development of the mammary gland: studies with *PGR* knockout mice suggested that progesterone is responsible for the formation of the lobes, whereas estrogens drive the ductal elongation in the gland. The effect of E2 on the *PGR* is mediated by binding of the activated ERα to estrogen-responsive regions (half ERE sites) located in proximity to a Sp-1 binding site in the regulatory region of the *PGR* gene (O'Lone et al. 2004; Kastner et al. 1990). The *PGR* is one of the best studied estrogen-dependent targets and a recognised marker for studying estrogen action (Graham and Clarke 1997), and also has been recognised to have a role in tumorigenesis (reviewed byAnderson 2002).

In MCF-7 cells the *ESR1* is down-regulated as a result of negative feedback provided by E2, whereas E2 has a highly up-regulating effect on the *PGR* (Silva et al. 2010; Bourdeau et al. 2008; Cho et al. 1991; Berkenstam et al. 1989; May et al. 1989; Nardulli et al. 1988), and a similar gene expression pattern is expected to be found in MCF-12A cells after E2 stimulation.

1.2   Target gene TFF1 (trefoil factor 1)

In MCF-7 cells, stimulation with E2, as well as with EGF increased *TFF1* mRNA levels to a similar extent. This effect became even stronger when E2 was added together with EGF (El-Tanani and Green 1997). The *TFF1* gene codes for a secreted protein of the trefoil class, pS2, which can act in a growth factor-like manner, promoting cell survival and motility (Prest et al. 2002) and even oncogenic transformation (Radiloff et al. 2011). The pS2 protein is found at a higher expression level in aberrant tissue compared to normal breast epithelium (Poulsom et al. 1997), and for these reasons can be considered a proto-oncogene. The role of this protein on cell cycle progression and proliferation is less clear, since it was shown to induce the expression of the *PRAD1* gene (coding for cyclin D1, required for G1 progression).

However, it can also delay the G1 to S phase transition (Perry et al. 2008; Bossenmeyer-Pourie et al. 2002). As mentioned above, the *TFF1* gene contains an imperfect palindromic ERE in its promoter region, and is therefore up-regulated by the ligand-bound, activated ER in estrogen-sensitive cells (Henry et al. 1990).

1.3   The breast cancer susceptibility gene BRCA1

Other genes that have been investigated in the context of mammary carcinoma include the breast and ovarian cancer susceptibility (*BRCA1*) gene, and the *PRAD1* gene, coding for the cyclin D1 protein. *BRCA1* encodes a transcription factor, which contributes to DNA repair functions (Scully et al. 1997), preventing aberrant DNA from being passed on to daughter cells and thus helping to prevent carcinogenesis (Deng 2006). Reduced levels of wild-type BRCA1 protein have been detected in a large percentage of sporadic breast tumours in the absence of mutations in the *BRCA1* gene, suggesting that disruption of BRCA1 expression may contribute to the onset of mammary carcinogenesis (Wilson et al. 1999; Thompson et al. 1995). The transcription of *BRCA1* is regulated by diverse extracellular stimuli including mitogenic compounds, and provides a feedback control that monitors the growth effects of estrogen in hormone-responsive cells. In ERα competent cells, such as MCF-7, expression of *BRCA1* is controlled through the binding of the receptor to an alternative ERE and an AP-1 site in the promoter region of the gene (Jeffy et al. 2005; Xu et al. 1997). In MCF-7 cells, *BRCA1* was induced after E2 treatment (Silva et al. 2010; Jeffy et al. 2005; Spillman and Bowcock 1996; Gudas et al. 1995), and an increase of *BRCA1* mRNA levels would be expected in the non-transformed MCF-12 cells due to the effects of activated ERα on the *BRCA1* promoter.

1.4   Target gene PRAD1, coding for cyclin D1 (CCND1)

The protein cyclin D1, encoded by *PRAD1*, occupies an important role in all cell types for cell cycle progression, as its expression needs to be highly increased for successful transition from the G1 into S phase. In non-transformed cells, *PRAD1* is one of the genes that assess the mitogenic potential of the cellular environment during cell-cycle entry from quiescence, and therefore cyclin D1 acts as a control protein (the importance of cyclin D1 for cell cycle progression is discussed in more length in Chapter 7). During cellular transformation, such controls are lost, and correspondingly the *PRAD1* gene is found to be overexpressed in a number of cancers, including breast cancer. In MCF-7 cells, cyclin D1 was shown to be

induced as a result of estrogen stimulation, at the mRNA level as well as in terms of protein expression levels (Silva et al. 2010; Sabbah et al. 1999; Prall et al. 1997; Planas-Silva and Weinberg 1997a; Foster and Wimalasena 1996). Both mRNA and protein level increases were suppressed in the presence of the ERα antagonist ICI182780, confirming that the ERα was involved in the transduction of the proliferative signals. Several mechanisms of action for inducing the gene expression are suggested, such as binding of the estrogen receptor to the AP-1 (Albanese et al. 1995), the CREB or the Sp-1 consensus site in the *PRAD1* promoter (Klein and Assoian 2008).

All the genes discussed so far (*TFF1*, *PGR*, *ESR1*, *PRAD1* and *BRCA1*) have been extensively studied in the MCF-7 cell line by our group (Silva et al. 2010), and since this is the correspondent malignant line to the non-transformed MCF-12A cells, we were especially interested in investigating the effects of E2 on these same targets in the normal epithelial cells. In addition to the targets mentioned, the *MYC* gene is an important endpoint to be considered as well.

1.5 Transcription factor MYC

MYC codes for the Myc protein, which is a transcription factor, known to have a function in normal cell cycle progression. In non-transformed cells, *MYC* mRNA levels are up-regulated upon mitogen stimulation, followed by an increase in Myc protein expression (Dean et al. 1986; Kelly et al. 1983). Aberrant cells display high copy numbers of the *MYC* gene, and such cells are prone for increased proliferation rates (Wasylishen and Penn 2010). In ERα[+], G1 blocked MCF-7 cells, treatment with E2 resulted in a significant accumulation of c-Myc mRNA (Dubik and Shiu 1988; Dubik et al. 1987), which is a prerequisite for cell cycle progression and proliferation, and we expected to find an up-regulation of the *MYC* gene in normal cells after mitogen stimulation as well.

2 OBJECTIVES AND METHODOLOGICAL CONSIDERATIONS

The aim in this chapter was to examine MCF-12A cells more closely in terms of the effects of E2 in controlling the expression of representative genes normally regulated by ERα in cell lines such as MCF-7. These studies were motivated by our observation of a lack of proliferative effects of E2 in MCF-12A cells. This seemed paradoxical, considering that MCF-12A cells contain the ERα. The hypothesis to be explored was that ERα signalling in

these cells might be set up differently from MCF-7 cells, such that the ERα lacks the ability to control expression of ER regulated genes. The genes to be analysed were carefully chosen according to information available about their expression in the malignant epithelial cell line MCF-7 (*ESR1*, *PGR*, *TFF1*, *BRCA1*, and *PRAD1*) which reacts to E2 exposure with cell proliferation. The direction of gene regulation (up- or down-regulation) can then be compared to the effect of E2 reported for the transformed cells. However, since the endogenous hormone had no cell cycle promoting properties in MCF-12A cells we also wished to compare the effect of E2 in these cells with those of an established mitogenic compound, EGF, on the same target genes. To this end, MCF-12A cells were incubated for 12 hours with E2 or EGF, and these expression profiles compared.

In addition to the aforementioned targets, which are genes classically influenced by the endogenous hormone E2, the *MYC* gene was also monitored. The incubation time and the genes chosen as targets had been determined beforehand with preliminary experiments (cf. Appendix Figure ii and Appendix Figure iii in the appendices' section).

In order to remove any estrogenic compound from the medium which could overshadow the effect of the added E2, cells were incubated in medium deprived of estrogens by charcoal-dextran (CD) stripping (phenol-red free medium with CD-treated horse serum, here referred to as "assay medium") for 24 hours prior to the start of the assay. The subsequent incubation with E2 (10 nM) or EGF (100 ng/ml) for 12 hours was performed in assay medium as well. A detailed description of the entire procedure is given in the material and method's section (Chapter 2).

3 RESULTS

3.1 Effect of E2 on gene expression

The gene expression levels seen after incubation of MCF-12A cells with E2 (10 nM) over 12 hours were normalised to a sample incubated with the solvent for the same duration, here termed solvent control (set to 1 (dotted line) in Figure 31). Surprisingly, E2 failed to stimulate the expression of *BRCA1*, *PRAD1* and *TFF1* that would be expected to occur in ERα competent cells. There was also no indication of a down-regulation of the mRNA coding for the ERα which is also normally seen in ERα competent cells after exposure to E2. The mRNA levels of *BRCA1*, *PRAD1*, *ESR1* and *TFF1* remained very close to the levels

monitored in the solvent control samples. The *MYC* gene was slightly induced, however, due to the variation between the independent experiments (as seen from the error bars), the difference to the vehicle control were too small to be detected as statistically significant. The strong induction of the *PGR* gene usually observed in MCF-7 cells also did not occur in MCF-12A cells. Instead, the *PGR* gene seemed slightly down-regulated. In summary, the differences between the E2-treated samples and the solvent control samples were not statistically significant for any of the genes detected, and the expression pattern typical for other ERα competent cells was not observed.

3.2   Effect of EGF on gene expression

Incubation with EGF altered the gene expression profile more dramatically than did E2. EGF strongly induced *BRCA1* and *PRAD1* (both show an approximately 4 fold induction over the control). The between-experiment variation of the results obtained for *BRCA1* were considerable, therefore the statistical test performed (Student's *t*-test) did not indicate statistically significant differences to the control sample. *PRAD1*, on the other hand, was induced by EGF, and the differences in mRNA levels to solvent control reached statistical significance (P=0.05). The genes coding for the steroid receptors (*ESR1* for ERα and *PGR* for PR) were detected below the control level, however, the differences were not significant. The *MYC* gene was slightly increased to an extent similar to that observed with E2, but again this induction was statistically not significant. Although expressed in the MCF-12A cells (as seen from the results with solvent- and E2-treated samples), the *TFF1* gene was not detected in the samples exposed to EGF. This suggested a considerable down-regulation of this target.
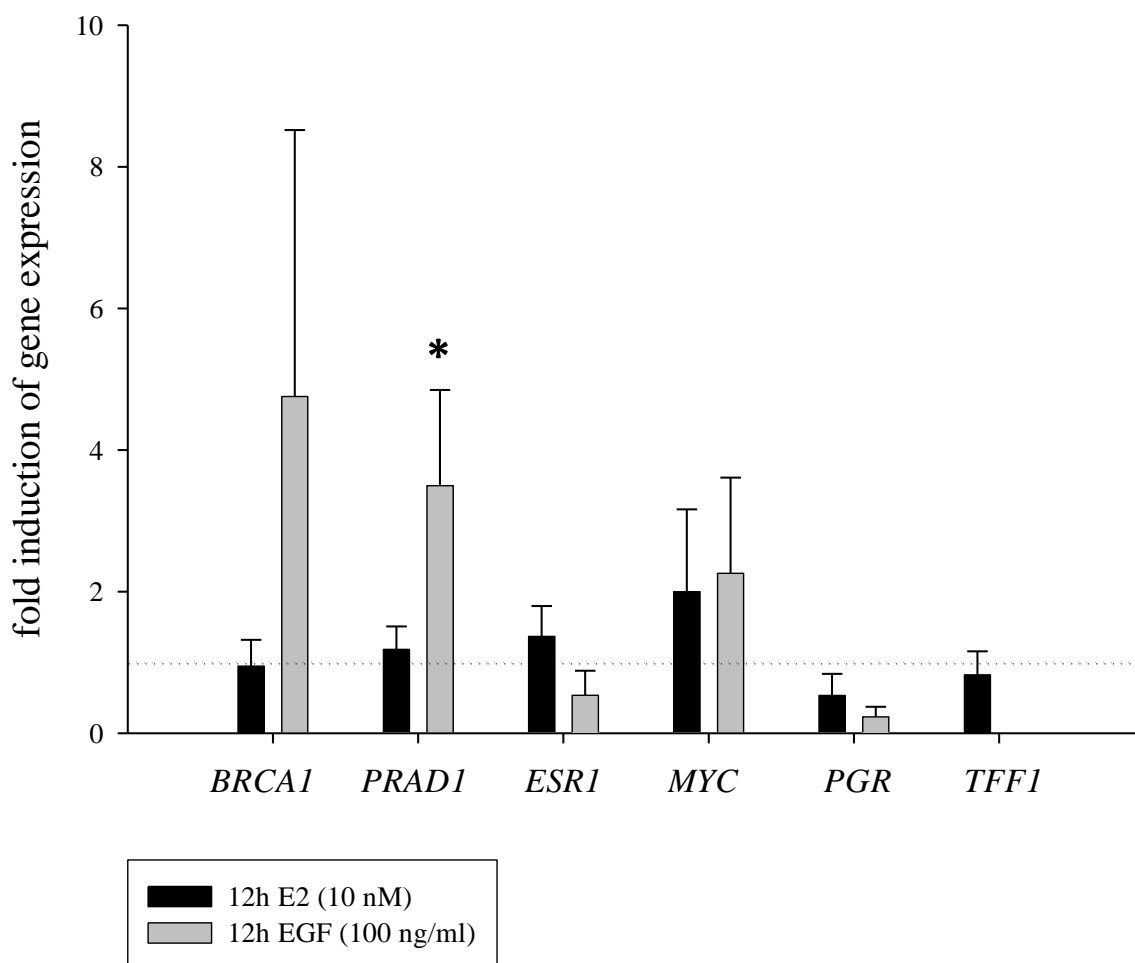
Figure 31 Effect of E2 (10 nM) or EGF (100 ng/ml) on gene expression in MCF-12A cells

Samples were taken after a 24h serum-depletion period, followed by 12 hours of incubation with E2 (10 nM) or EGF (100 ng/ml), and PCR analysis was performed. Values are means of 4 independent experiments, error bars show SEM. The gene expression in the solvent control sample ("G0 blocked) was set to 1 (dotted line) and used as the control value against which all other results were normalised. Student's *t*-test was performed for significance testing. The sample marked with * is significantly different (P=0.05) from the E2 treated sample and from the negative control (set to 1). None of the other samples was statistically significantly different from negative control (G0 blocked). *TFF1* was not detected after treatment with EGF.

4 DISCUSSION

4.1 The role of E2 for gene expression

By assessing the expression of genes that in breast cancer epithelial cells such as MCF-7 are regulated by ERα in the wake of activation by E2 we investigated the signalling roles of the receptor in MCF-12A cells. In contrast to breast cancer epithelial cells, MCF-12A cells did not progress into the cell cycle after exposure to E2. In numerous studies with MCF-7 breast cancer epithelial cells, *BRCA1*, *PRAD1, PGR* and *TFF1* were shown to be strongly induced upon E2 treatment. The *ESR1* gene is typically down-regulated in response to E2.

It came to a surprise to us that the endogenous hormone E2 did not significantly alter the expression of any of the genes monitored in this study. Since E2 did not have an impact on cell cycle progression in MCF-12A cells, it may be argued that proliferative genes such as *MYC* or *PRAD1* should not be altered by exposure to the hormone. The receptor ERα for which E2 is a ligand, however, can be expected to be affected in any case when the ligand is present. Treatment with an estrogen should result in a decline of the receptor mRNA level, caused by a negative feedback loop. Such a feedback is mediated directly by the ligand-bound, activated receptor which associates with an ERE in the promoter domain of the receptor gene, and has been shown in MCF-7 and other breast cancer cells (Silva et al. 2010; Bourdeau et al. 2008; Cho et al. 1991; Berkenstam et al. 1989). It is noteworthy though that an increase of *ESR1* mRNA levels has also been reported, albeit not in human tissue (Ing 2005). Clearly, in the MCF-12A neither such regulation occurred. The receptor is expressed in this cell line (E.Silva, personal communication), yet apparently did not react with the target sequence in the promoter region of the *ESR1* gene. This would suggest that either E2 did not bind sufficiently its target receptor, which is highly unlikely, or that the receptor was not activated by the bound ligand. If the latter is the case, then the function of the ERα for the MCF-12A cells is still unclear.

Similar to E2, the endogenous hormone progesterone also plays an important role for normal development of the mammary gland. The effects of the hormone are mediated through the nuclear progesterone receptors of which two isoforms exist, which differ only by one amino acid. Interestingly, estrogens are required to induce the expression of PR, and mammary epithelial cells that express PR also express ERα (Lange 2008). Similar to the ERα, the ligand-activated PR dimerizes and then associates with target sequences in the DNA

(progesterone response elements, PRE), more specifically in the promoter region of target genes, to regulate their expression (Scarpin et al. 2009). Both mRNA and protein expression of PR were shown to be induced as a result of E2 treatment in the rat uterus (Kraus and Katzenellenbogen 1993), and even more significantly in malignant MCF-7 mammary epithelial cells (Silva et al. 2010). Also the amount of receptor protein was markedly increased in all cell types (Kraus and Katzenellenbogen 1993; Cormier et al. 1989; Welshons and Jordan 1987). However, the direction of the gene regulation may also depend on the cell type, e.g. in vaginal epithelium E2 up-regulated *PGR*, whereas in uterine epithelium it resulted in down-regulation (Kurita et al. 2000). Thus, the observation that E2 did not alter the expression of the *PGR* gene was surprising considering the observations made with the other cell types. As was speculated above, the process usually triggered by ligand-binding on the ERα seems to be disrupted, and the lack of effect of E2 on *ESR1* may explain the outcome of E2 exposure on *PGR* regulation.

Similar to the *PGR* gene, E2 had no effect on the expression of the *TFF1* gene. This is in contrast to observations reported from other breast epithelial cell lines: in neoplastic human epithelium, the *TFF1* gene was found to be highly expressed (Poulsom et al. 1997), and in MCF-7 mammary carcinoma cells expression was increased under E2 induction (Prest et al. 2002). *TFF1* was also found in normal breast tissue, albeit at lower expression levels than in the aberrant tissue (Poulsom et al. 1997). In fact, all *TFF* genes (1, 2 and 3) are considered classical estrogen-regulated genes, and their gene expression profile is used to assess estrogenicity of compounds. The up-regulation of *TFF1* through E2 exposure in breast cancer cells can be mediated through the ERE site found in the *TFF1* promoter region, providing a docking site for the ligand-activated ERα, but also through an AP-1 site found in the *TFF1* sequence (reviewed by Perry et al. 2008). The AP-1 site allows the ER to trigger additional genes that do not contain ERE site and thus cannot be activated directly by the receptor. When signal transduction through the MAPK pathway is involved, AP-1 is the preferred site to achieve *TFF1* activation (Espino et al. 2006), but crosstalk between the kinase and receptor signalling has also been reported (Barkhem et al. 2002). Hence the endogenous hormones may employ several mechanisms to act on *TFF1*, and so the lack of an up-regulation presented here was therefore very surprising, but underlined once more the unusual role of this hormone in the MCF-12A cells.

The BRCA1 protein is an important product needed to balance proliferation and repair mechanisms, and is switched on when mitogenic factors act on the cell. Although E2 was not

significantly mitogenic in the MCF-12A cells, the lack of effect of the hormone on *BRCA1* induction was surprising, since estrogens are known to induce maximal mRNA levels of *BRCA1* in human breast cancer (MCF-7) cells (Spillman and Bowcock 1996). Yet Chen and colleagues (1996) detected the highest expression in S phase (Chen et al. 1996), which was certainly not reached after 12 hours after which the PCR analysis of the MCF-12A was performed, others have reported that the *BRCA1* gene expression peaked in late G1 phase (Gudas et al. 1996; Vaughn et al. 1996), and some even observed significant mRNA accumulation as early as 5 hours after addition of E2 (Marks et al. 1997) (all in MCF-7 cells). Although the hormone did not have an effect on cell cycle progression (cf. Chapter 4, page 89), the stimulation of the MCF-12A with E2 lasted for 12 hours, so the question why no change of *BRCA1* was seen with E2, remained. The mode of action of E2 on *BRCA1* gene regulation provides a possible explanation. It was found that estrogen does not regulate the gene directly, but in an indirect fashion: in several breast cancer cell lines, Marks and co-workers (1997) showed that the induction of the *BRCA1* is dependent on accumulation of synthesised DNA. When ERα$^+$ MCF-7 cells were stimulated with the mitogenic factors EGF or IGF-1 instead of E2, the *BRCA1* gene was also induced, suggesting that the effect of E2 on the genes only occurs as a result of E2 being a mitogenic stimuli. Evidence pointing the same direction exists for retinoic acid (RA). RA, a mitogen for MCF-7 cells, but no other cell line (as demonstrated by an increase of cells in S phase), induced *BRCA1* only in the cell line where it also stimulated cell division (Marks et al. 1997). Relating these findings to the observations made in MCF-12A cells, we suggest that E2 did not increase *BRCA1* mRNA levels in MCF-12A cells because it failed to induce DNA synthesis sufficiently, whereas a strong mitogenic compound should induce *BRCA1*.

E2 also failed to induce the *PRAD1* gene, coding for cyclin D1. Cyclin D1 is a protein whose expression is classically increased before the onset of S phase, resulting from input from growth factors, and the cyclin-dependent kinase complexes are important for phosphorylation of several key substrates involved in cell cycle progression and proliferation. Treatment of ERα$^+$ breast cancer cells with E2 was reported to result in an increase of *PRAD1* mRNA levels within less than an hour (Castro-Rivera et al. 2001, and references herein). Albeit the *PRAD1* promoter does not display an estrogen responsive element, its expression is thought to be enhanced as a direct outcome of the association of the translocating ERα with the transcription factors AP-1, Sp-1, and CREB (Silva et al. 2010; Castro-Rivera et al. 2001; Sabbah et al. 1999). The observations made in the MCF-12A on *PRAD1* suggest once more,

that the receptor is not enabled to exert is functions observed in the malignant epithelial cells upon ligand activation.

The sole target that seemed to be induced upon E2 treatment was the gene coding for the transcription factor Myc, however, the analysis results varied between experiments, therefore the induction was statistically not significant when compared to the negative control, treated with the vehicle only. Similar to *PRAD1*, *MYC* is induced upon stimulation with mitogenic factors, and the expression of the Myc protein, a transcription factor, is crucial for successful cell cycle progression. The regulatory region of the *MYC* gene contains an ERE, which potentially can be bound by the ligand-activated estrogen receptor (Dubik and Shiu 1992). The finding that this gene was not induced by stimulation of the cells with E2, despite the presence of a signal enhancing element, is in line with the observations made on other genes in this cell line.

4.2   Impact of EGF on gene expression

Thus far, the results obtained with E2 on the expression of the target genes chosen were assessed in relation to the effects of E2 reported for the correspondent malignant cell line MCF-7. To understand better the signalling in MCF-12A cells, we sought to investigate a reference case, where a growth factor strongly induces cell cycle progression and proliferation. We compared the results obtained from the studies with E2 to those with EGF, a growth factor shown to have proliferative effects on MCF-12A cells.

The steroid receptors *ESR1* and *PGR* were both detected at very low levels after incubation with EGF; however, the downregulation was not statistically significant. The observation made with *ESR1* is more or less in line with results from MCF-7 cells, where a decrease of ERα expression as a result of EGF action has been reported, on a transcriptional and translational level (Silva et al. 2010; Stoica et al. 2000; Cormier et al. 1989). However, in order for EGF to decrease the expression of the receptor gene, the ERα itself must have been activated first. Bunone et al. (1996) examined extensively the mechanism by which EGF could act on the nuclear receptor, and found that ER stimulation by EGF targeted the activation function 1 (AF-1) domain in the receptor, and more specifically its serine residue Ser118. Exactly this residue is phosphorylated by MAP kinases. The role of the MAPK pathway for activation of ERα was confirmed with a dominant negative Ras mutant which significantly reduced the efficiency of EGF to trigger ERα (Bunone et al. 1996). Possibly, the

same signalling pathway was in place in the MCF-12A cells. The MAP kinases were shown to be strongly up-regulated upon treatment with EGF in these cells (discussed in Chapter 7), and could then phosphorylate ERα. Subsequently, the activated receptor would bind the ERE domain in its target, resulting in a decrease of receptor gene expression. It should be noted though that Stoica and coworkers (2000) found that the regulation of ERα by EGF (in MCF-7 cells) was mediated rather through the protein kinase B (Akt) than the MAP kinase (Stoica et al. 2000). In order to verify the assumption that in the MCF-12A the MAPK pathway was triggered, assessment of *ESR1* mRNA levels after incubation with a specific MAPK inhibitor, which would be expected to disrupt the down-regulation of the receptor, would be necessary.

The progesterone receptor was also under investigation in the study by Stoica and colleagues (Stoica et al. 2000). Using the same concentration of EGF (100 ng/ml), they found that expression of the *PGR* in MCF-7 cells was induced after 6 hours, but to a smaller degree than with E2, whereas others report no effect of EGF on *PGR* expression (after 24 hours) (Silva et al. 2010). It seems that also in the MCF-12A cells, *PGR* is not under the control of mitogenic pathways (triggered by EGF), and since EGF was the stronger mitogen for MCF-12A cells than E2, the lack of effect of E2 is also conceivable. Possibly, *PGR* mRNA levels are regulated by other signals, because the receptor does have a function in non-transformed cells.

Analysis of the *TFF1* gene came as a surprise, since in none of the samples treated with EGF, it was detectable. In all other samples (control and E2-treated) it was expressed at rather low levels (compared to the expression levels of the housekeeping gene β-actin), so its disappearance suggested a down-regulation, although this assumption could not be analysed statistically, for obvious reasons. Usually, a positive correlation between mitogenic stimulation with EGF and *TFF1* expression is found. For example, up-regulation of *TFF1* upon EGF incubation has been observed in MCF-7 breast epithelial cells (Silva et al. 2010; El-Tanani and Green 1997), and inhibition of the tyrosine kinase activity of the EGFR resulted in a reduction of the *TFF1* mediated growth in kidney cancer epithelial cells (Rodrigues et al. 2003). Additionally, induced overexpression of the *TFF1* gene led to an increase in S phase numbers of MCF-7 cells, suggesting a role for *TFF1* in cell cycle progression (Amiry et al. 2009). Since the MCF-12A cells relied heavily on EGF for cell cycle progression, the downregulation of *TFF1* with this growth factor was surprising, even more so since *TFF1* and EGFR signalling share functions such as migration, increased proliferation and anti-apoptotic features (Emami et al. 2004). On the other hand, the finding

that EGF did not induce *TFF1*, although the growth factor promotes cell cycle progression in MCF-12A, confirms the result with E2, underlining once more that E2 is unable to promote cell cycle progression in the normal breast epithelial cells because it fails to induce proliferative genes.

Looking at the treatment with EGF strictly as a purpose for comparing the effect of E2 with an actual growth factor, the characteristics of *BRCA1* are in line with *TFF1*, in the sense that in the MCF-12A cells, EGF has more impact on the expression of genes that are classically under the control of pro-proliferative factors, than does E2. Although the variation between the independent experiments was relatively high, so that the increase in mRNA levels was actually not statistically significant, the mean value of all results indicates that there was an increase in mRNA levels. In fact, it seemed to be the strongest induced target, or at least the difference between E2 and EGF treatments was most pronounced with *BRCA1*.

Nevertheless, the only significant increase in mRNA levels produced by EGF was observed with the gene coding for cyclin D1, *PRAD1*. As has been mentioned above (cf. section 1.4 of this chapter), cyclins are established key regulators of the cell cycle, and cyclin D1 has been shown to be essential for successful progression from G1 phase into S phase. Since EGF promoted cell cycle progression (as seen from the flow cytometric results in Chapter 4), the increase of *PRAD1* mRNA levels by EGF was quite expected, and is in agreement with numerous reports about the link between growth factor stimulation and cyclin D1 induction (Klein and Assoian 2008; Rieber and Rieber 2006; Chou et al. 1999; Lavoie et al. 1996; Sutherland et al. 1993).

Finally, the effect of EGF on mRNA levels of *MYC* was very similar to the lack of impact of E2 on this gene. Although the level of *MYC* expression does not vary in cells that are continuously exposed to serum (Rabbitts et al. 1985; Thompson et al. 1985), it is virtually undetectable in quiescent cells, followed by a rapid rise in mRNA levels upon growth factor stimulation (Facchini and Penn 1998; Ran et al. 1986; Bravo et al. 1985; Curran et al. 1985). Therefore, it may be expected to see an induction of *MYC* as a result of the EGF exposure. However, the cells were analysed after an incubation period of 12 hours, which may be too late for detection of *MYC* induction, since it has been reported that mRNA levels peak 2 to 4 hours after stimulation, and decline subsequently (Handler et al. 1990; Dean et al. 1986). In order to assess the true impact of EGF on *MYC* regulation in MCF-12A cells, samples need to be analysed at earlier time points after addition of the growth factor. However, since the aim

of EGF exposure in this assay was to compare it to the effect of E2 treatment, this was not performed here, but is presented in Chapter 7 below.

4.3 E2-triggered signalling in MCF-12A versus MCF-7 cells

Although only a handful of targets were monitored, we were able to conclude from the assays performed with E2 in comparison to EGF that the non-transformed MCF-12A epithelial cells are entirely differently affected by E2 than the malignant cell line MCF-7. Not only did E2 not stimulate the cells to continue their cycle, as discussed in the previous Chapter 4, but also its impact on genes that are well known to be regulated by the hormone in MCF-7 cells, was absent in all targets. This may be regarded as a feature of normal epithelial cells, and in reverse, lead to the conclusion that responsiveness to E2 is characteristic for transformed cells. This thought has been discussed in the literature, with a particular focus on the role of cyclin D1, for several reasons. Firstly, it was noticed that cyclin D1 is overexpressed in primary breast cancer cells which were in a very early stage of malignancy (Weinstat-Saslow et al. 1995). Secondly, it was observed in MCF-7 cells that their ability to overcome a G1 block depended on estrogen induced cyclin D1 transcription (Wilcken et al. 1997). The ability of estrogens to drive cyclin D1 expression is thus considered crucial for the proliferation of ER$^+$ breast tumours, and although *PRAD1* lacks an ERE, the effect of the hormone is probably transmitted through an AP-1 site in the promoter of the gene (Wisdom et al. 1999; Planas-Silva et al. 1999 and references herein; Brown et al. 1998). In line with these observations, it has been established that the presence of an ER *per se* is not sufficient to promote proliferation as a result of estrogen stimulation (Zajchowski et al. 1993; Jiang and Jordan 1992). On the other hand, it was shown that in normal human breast tissue, proliferating cells are sparse among those cells expressing an ER (which accounted for only around 15% of all cells), whereas in mammary tumours, the majority of ER$^+$ cells were dividing (Clarke et al. 1997).

Taken together, these findings indicate that ER$^+$ cells responsiveness to estrogens, by increasing cyclin D1 transcription or, ultimately, by proliferating, is a feature of aberrant cell behaviour. In this respect, the insensitivity of the MCF-12A cells (which do express the ERα) to E2 emphasises their non-transformed character. The quite different, but crucial role of EGF for cell cycle progression was underlined by its impact on *PRAD1*.

5 CONCLUSIONS

The first and foremost aim of this chapter was to clarify the role of the endogenous hormone E2 in the MCF-12A cells. E2 did not have a significant effect on cell cycle progression when used instead of a growth factor in the discontinuous exposure assay (Chapter 4). Therefore, a closer examination of the mRNA levels of typically estrogen-regulated genes was decided. Two proliferative genes, *PRAD1* and *MYC*, which were significantly induced upon the pro-proliferative incubation with EGF, were assessed after E2 stimulation. Additionally two genes that are classically up-regulated upon E2 stimulation, *BRCA1* and *TFF1*, were also examined, as well as two genes coding for estrogen-sensitive receptors (*ESR1* and *PGR*).

The conclusion from the flow cytometric analysis, that E2 did not have a proliferative effect on MCF-12A cells, was confirmed by the analysis of *PRAD1* and *MYC*, which were both not significantly up-regulated, in contrast to stimulation with EGF. The lack of mitogenic properties of E2 in MCF-12A cells was further supported by the results on the *BRCA1* gene.

In summary, the results found with E2, in comparison to EGF, at the two different endpoints, S phase evaluation by flow cytometry and mRNA analysis of mitogen-dependent genes, were consistent with each other. The results on the usually mitogen-independent, but estrogen-regulated targets *ESR1*, *PGR* and *TFF1*, suggest an atypical role for E2 in the MCF-12A cells, when compared to the correspondent malignant cell line MCF-7, but are in line with the hypothesis that E2-responsiveness indicates transformation, whereas normal cells do not react to hormone stimulation, despite the presence of estrogen receptors.

In the following chapter we will further explore the impact of EGF, which did not only induce the proliferative gene *PRAD1*, but more importantly promoted cell cycle progression very strongly. In particular the signalling pathways that are triggered by EGF to achieve cell cycle progression will be examined more closely.

Chapter 6:
Signal transduction for cell cycle re-entry

1 INTRODUCTION

Having established a discontinuous assay scheme that allows quiescent MCF-12A cells to re-enter the cell cycle upon two distinct exposures to defined growth factors, the next stage of the investigations was to find out which signalling pathways were activated during these pulses and which of these were decisive in advancing the cell cycle. The discontinuous exposure consisted of a 30 minutes pulse with epidermal growth factor (EGF), followed by a 3.5 hour resting period and a second pulse of 10 hours, with administration of EGF in combination with insulin. It yielded good results in terms of the percentage of cells advancing into the S and G2+M phases after a total release time of 18 hours. This set-up was used throughout the next series of experiments presented in this chapter, where specific kinase and lipase inhibitors were added during the exposures, together with the respective growth factor(s), in order to determine which of the targeted enzymes were involved in the G1 to S phase transit.

To develop criteria for the selection of appropriate inhibitory agents, we first had to establish which kinases are activated by EGF and insulin in epithelial cells. Growth factors are ligands for their specific receptors which relay the message from outside the cell into intracellular compartments. Both EGF and insulin act through cell surface receptor tyrosine kinases (RTK), which are transmembrane proteins: on their extracellular domain, they bind specific (growth) factors, and the intracellular domain encodes the tyrosine kinase which propagates the signal. The superfamily of RTKs comprises a variety of different subclasses. The human EGF receptors (HER) 1 to 4, also called ErbB receptors, are part of the type I receptors of the superfamily. The type II receptor family members consist of the insulin receptors. The receptors of type I and II have in common that they have leucine-rich (L) and cysteine-rich (CR) domains which have a role in ligand binding and stabilisation. They are distinguished by their form of appearance on the membrane: type I receptors exist as monomers, whereas type II receptors are found as disulfide linked dimers. In total, there are more than a dozen of

family members, including also receptors for factors such as vascular-endothelial growth factor (VEGF) and the platelet-derived growth factor (PDGF). The common feature of the RTKs, as the name suggests, is that they phosphorylate various intracellular substrates on their tyrosine residues.

In the following sections, the mode of actions of EGF and insulin on their respective receptors will be discussed in more detail.

1.1 Epidermal growth factor (EGF) and its receptor, EGFR

1.1.1 Structure of the receptor

During his studies on the nerve growth factor, Stanley Cohen isolated a protein from the salivary gland of mice which he injected into newborn animals. This resulted in remarkable anatomical changes: both tooth eruption and eyelid opening occurred much (several days) sooner, but weight gain was slowed down (Cohen 1962). The protein was characterised as epidermal growth factor (EGF) a few years later (reviewed by Gill et al. 1987). His work on this growth factor also led him to discover the corresponding receptor (Cohen et al. 1980), and for these major findings he received the Nobel Prize in 1986.

The EGFR, also known as ErbB1 or HER1, is a 180 kDa large glycoprotein and possesses one trans-membrane domain, the extracellular ligand-binding domain and on the intracellular side its kinase binding domain and a long C-terminus with several tyrosine residues as phosphorylation targets (Figure 32). The ectodomain consist of 4 domains named L1, L2, CR1 and CR2, but only the first two are the targets for ligand binding, and the major binding domain seems to be L2. CR1 mediates dimerisation of the receptor molecule, whereas CR2 is responsible for stabilising it (Walker et al. 2004). The transmembrane domain extends into the juxtamembrane region and primarily serves as a site for the shutdown loop, through negative feedback by the extracellular signal-regulated kinases (Erk) and protein kinase C (PKC) (Wells 1999). The C-terminal (intracellular) domain provides the tyrosine residues.
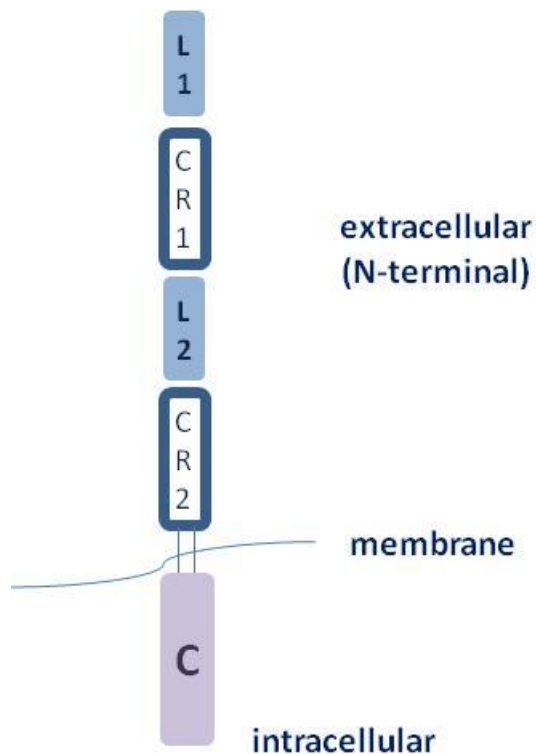
Figure 32 Schematic representation of EGFR monomer

The leucine-rich (L) and cysteine-rich (CR) domains are found on the extracellular site of the receptor and are responsible for binding of the ligand. The tyrosine kinase is found on the C-terminal site (adapted from Ward et al. 2007).

1.1.2 Mode of action of EGF on its receptor (EGFR):

To date, seven ligands of the EGFR have been identified, but only the interactions with EGF will be discussed here. The EGFR is activated upon binding of a ligand molecule. The receptor then dimerises to form either a homodimer or a heterodimer with another HER, preferably with the ErbB2, and phosphorylates itself.

Each molecule of EGF is clamped between the L1 and L2 domains from the same EGFR molecule, so that it is in contact with only one receptor in the dimer. For optimal activity of the dimer, the EGFR requires direct protein-protein interactions between the C-terminus of one kinase and the N-terminal domain of the other kinase (Figure 33), so that this asymmetric conformation displays an elongated shape compared to a symmetric dimer (Hubbard 2006). The receptor that bound first the ligand molecule then activates the second monomer (Jura et al. 2009).

113
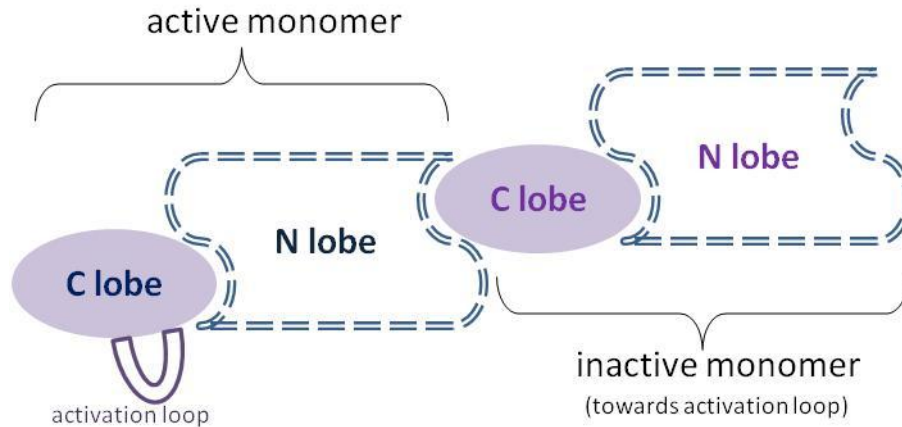
Figure 33 Schematic representation of dimerised EGFR

Signalling by the EGFR requires interaction between the kinase domains of two receptor monomers, whereby one activates the other. The ligand bound monomer pushes the inactive monomer towards its activation loop for full activity of the dimer (adapted from Hubbard 2006).

It should be noted that the EGFR can form heterodimers with other members of the ErbB family, so that ligands not specific for the EGFR can still incite signal transduction. On the other hand, no ligand is known thus far for the ErbB2, but when this receptor forms a heterodimer with EGFR, it provokes the strongest mitogenic response of all dimers possible (Yarden and Sliwkowski 2001).

1.1.3 Mechanisms of signal transduction by the EGFR

The autophosphorylated and activated EGFR provides docking sites for SH2 domains, and attracts different linker proteins to these sites. One possible linker to begin with is the adaptor protein Grb2, which contains several Src homology (SH) domains, one SH2 and two SH3 domains. The SH2 domain of the Grb2 protein will bind directly to the EGFR and provides a link between the receptor and the transducer molecule Sos (Rozakis-Adcock et al. 1993). A group of factors termed <u>S</u>ignal <u>T</u>ransducer and <u>A</u>ctivator of <u>T</u>ranscription factors (STATs) also contain SH2 domains that enable them to link to the EGFR; the activated STAT translocates to the nucleus where it can bind to a variety of target genes (Quesnelle et al. 2007). The Shc protein was identified as a <u>S</u>rc <u>h</u>omology (SH2) <u>c</u>ontaining proto-oncogene that complexed with, and was phosphorylated by, the activated EGFR (Pelicci et al. 1992).

114

However, more recently it became clear that Shc binds to the receptor preferably via its phosphotyrosine-binding (PTB) domains, subsequently bringing in the adaptor protein Grb2 (Ravichandran 2001). Finally, the Src protein, which contains a SH3 and SH2 domain, followed by the catalytic (tyrosine kinase) domain and a regulatory tyrosine phosphorylation site on its C-terminal end, may associate with the EGFR (Luttrell et al. 1994).

It is interesting to note that Grb2 may connect to the receptor in two different ways: firstly, the by direct binding of the adaptor to the receptor on its residues Y1068 and Y1086, and secondly, via the Shc protein, which is associated to the EGFR through different residues (Y1173 and Y992). It is not completely understood yet if these different modes of attachment result in distinct functional roles, or if the recruitment modus is cell-type specific (Jorissen et al. 2003; Batzer et al. 1994).

1.2   Insulin and the insulin receptors

1.2.1 Structure of the receptor

Insulin has been discovered much earlier than EGF. It was isolated in 1922 (Banting and Best 1922), and thirty years later, it became the first protein to have its primary amino acid structure sequenced, for which Frederick Sanger received the Nobel Prize in 1958.

Insulin is a ligand to several receptors: the family of insulin receptors comprises the insulin receptor (IR), the receptor for insulin-like growth factor / type I (IGF-1R), and the insulin receptor related receptor (IRR). The IR exists in two isoforms (IR-A and IR-B) (Lee and Pilch 1994). All three receptor types usually exist as homodimers, although hybrids between the IR and the IGF-1R were found in cells that express both receptor types, but their physiological role is unknown (De 2004). Since the highest affinity of insulin is for the IR, the focus will be on this receptor type.
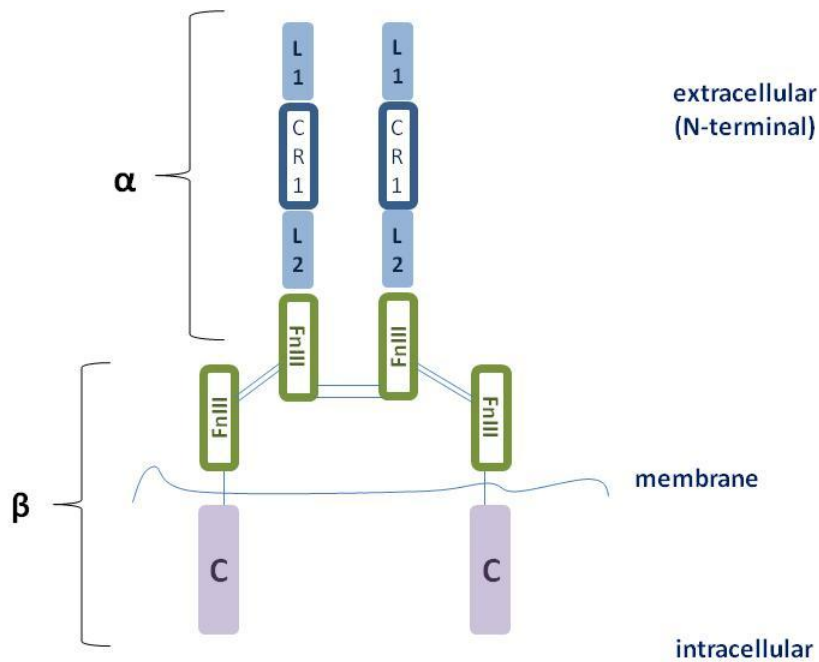
Figure 34 Schematic representation of the IR

Similar to the EGFR (see Figure 32), the IR has leucine-rich (L) and cysteine-rich (CR) domains on the extracellular side for ligand binding, but the IR is present as a stable heterotetramer on the cell surface (adapted from Ward et al. 2007).

The IR consists of an α-chain (130 kDa of size), which is entirely extracellular and contains the insulin-binding site, and a β-chain (95 kDa of size) that is composed of an extracellular region, a single transmembrane domain and a cytoplasmic region (Figure 34). The two chains are disulfide-linked, and in turn two of these heterodimers are held together by disulfide bonds at the α-chains. Thus, unlike other RTK, the insulin receptor is present on the cell surface as a stable dimer. Binding of an insulin molecule results in a conformational change of the β-chains so that they can initiate autophosphorylation. The ectodomain consist of 6 domains, named L1, L2, CR and the fibronectin (type III) domains FnIII-1 to -3. L1, CR, L2 and FnIII-1 are parts of the α-chain, whereas the fibronectin domains 2 and 3 belong to the β-chain. The transmembrane domain consists entirely of the β-chain. The intracellular region of the IR contains the kinase domain neighboured by two regulatory regions (the juxtamembrane region and the C-tail) that contain phosphotyrosine-binding sites for signalling molecules.

116

1.2.2 Mode of action of insulin on its receptors

The IR and the IGF-1R are homologous kinases that bind both, insulin and IGF-1, albeit with different affinities (insulin attaches to the IR with high affinity, whereas the affinity of IGF-1 is low for the IR). Interestingly, the IR-A (but not IR-B) binds the type II insulin like growth factor with an affinity similar to that of the IGF-1R. High-affinity binding is accompanied by structural compaction of the receptor and not by extension as in the case of the EGFR.

For the IRR, no ligand is known so far, and its physiological function is unknown, although the generation of triple gene knockout mice showed that the complete receptor family is required for male sexual differentiation (Nef et al. 2003).

1.2.3 Mechanisms of signal transduction by the IR and the IGF-1R

In contrast to the EGFR and most other RTKs which form stable complexes directly with their effectors through their SH2 domains, the mechanism by which the IR transmits its signals is biochemically different. The process of autophosphorylation of the IR exposes binding sites for the PTB domains of the insulin receptor substrates (IRS). The IRS are members of a small family of docking proteins, with IRS-1 and IRS-2 as the main substrates. These substrates are then available for binding with SH2 containing proteins. However, it has been shown that the activated IR can also complex with the Shc protein as its substrate, which itself contains a SH2 domain and through this can bind the adaptor molecule Grb2 (Sasaoka and Kobayashi 2000). The insulin receptor also phosphorylates the multisite docking protein Grb2-associated binder-1 (Gab-1) and -2. Thus, Gab-1 and Gab-2 are also considered as members of the IRS family, which means they can transmit signals from the IR towards several kinase pathways (Lehr et al. 2000; Holgado-Madruga et al. 1996).

1.3 Signalling pathways triggered through activation of the EGFR and IR

The pathways mainly implicated in cell growth and proliferation are the MAP kinase and the PI3 kinase pathways. Both are triggered upon RTK activation, and therefore will be discussed in more detail. Furthermore, PLC was shown to be a substrate for the EGFR, and may function as a co-activator of the other mentioned kinases, therefore the PLC/PKC pathway also will be considered here.

1.3.1 The mitogen-activated protein kinase (MAPK) pathway

A key player for signal transduction from the RTKs is the adaptor molecule Grb2. Grb2 is a 23 kDa small protein, consisting of a sequence of three Src homology domains, SH3-SH2-SH3. The SH2 domain binds to specific domains on the activated receptors, whereas with its SH3 domain it is constitutively bound to the guanine nucleotide exchange factor Sos (Rozakis-Adcock et al. 1993; Buday and Downward 1993). Sos exchanges GDP for GTP on the small G protein Ras (Batzer et al. 1994). Active in its GTP-state, Ras binds to the N-terminus of Raf-1 (Vojtek et al. 1993), a serine/threonine-specific protein kinase and an activator of the MAPK kinases (MEK), which in turn activate the MAP kinases Erk 1 and Erk2. Erk1 and 2 catalyse the phosphorylation of nuclear transcription factors, ultimately resulting in enhanced proliferation. Stable overexpression of Grb2 enhances insulin-induced activity of the ERKs, but not when the SH2 domain binding properties are affected by point mutations, demonstrating the importance of the integrity of this adaptor protein (Skolnik et al. 1993). Upon EGF stimulation, overexpression of Grb2 was shown to increase the amount of Ras in the GTP-bound state (Kazlauskas 1994).

The MAP kinase pathway may also be triggered through a slightly altered mechanism, namely through the Src tyrosine kinase. It was shown that the Src protein is tightly connected to the EGFR. Firstly, overexpression of the Src enhances EGF-mediated proliferation in epithelial cells (Luttrell et al. 1988), and conversely, inhibition of the Src protein blocks EGF-mediated DNA synthesis (Roche et al. 1995). This allows the assumption that Src is a signal transducer located downstream of the EGFR. The Src protein attracts adaptor proteins such as Grb2 for activating Sos, resulting in the activation of the Ras molecule, which again triggers the MAP kinase cascade. Docking of Gab is also considered essential for activation of the MAPK pathway because it targets Shp2 to its appropriate location for its key substrate Ras (Gu and Neel 2003), and Shp2 is required for full and sustained activation of Ras (Neel et al. 2003).

1.3.2 The phosphatidyl-inositol-3-kinase (PI3K) pathway

There are four classes of PI3 kinases, with the enzymes of class I being the most abundant, and the best studied ones. Class I PI3Ks are heterodimeric proteins, with a 110 kDa catalytic subunit (p110) and the regulatory subunit of 55-85 kDa of size (called p85). Several mechanisms of PI3K activation exist:

The p85 contains a p110 binding site between two SH2 domains, and an additional SH3 domain. These domains allow the PI3 kinase to be recruited either directly or indirectly to the receptors (Foster et al. 2003; Fry 1994). The direct binding of the p85 is only possible in an EGFR heterodimer: the EGF receptor (ErbB1) can form a heterodimer with a receptor from the same family, namely ErbB3. It is the latter that then binds p85 which is the regulatory subunit of the PI3 kinase and therefore activates the whole enzyme (Soltoff et al. 1994). The EGFR as well as the ErbB2 lack the p85-SH2 recognition domain which is necessary for binding the regulatory adaptor protein. Nevertheless, the p85 subunit can bind indirectly, through Grb-2, to the RTKs: first, the adaptor protein Grb2 binds to the EGFR, then the Gab-1 molecule (Grb2-associated binder) is recruited. The Gab family are docking proteins that lack enzymatic activity, but they provide binding sites for SH2 domain containing proteins. In fact, Gab provides a major route for PI3K activation in all mammalian systems, especially for receptors lacking a p85 binding site, and has been shown to link the EGFR with the PI3 kinase pathway (Wohrle et al. 2009a; Wohrle et al. 2009b; Gu and Neel 2003; Gu et al. 2000).

The Src protein is equally responsible for activating the PI3K pathway, because Src can recruit the p85 subunit, whose binding leads to completion of the PI3-kinase and its activation (Fry 2001).

Thus, the PI3K pathway may be triggered through activation of both, the EGRF and the IR. The phosphatidyl-inositol kinases target proteins which contain a lipid recognition module; from these, the activated PI3K produces inositol lipids which recruit proteins with a pleckstrin homology (PH) domain. The best known example for such a protein, and the best studied PI3K substrate, is the Akt kinase (also called protein B kinase, PKB). The PI3K signalling can be stopped by phosphatases, and the strongest termination reaction is mediated by the tumour suppressor gene product PTEN. Indeed, PTEN was found to be down-regulated in some human cancers. In quiescent cells, PI3K activity increases in two waves following growth factor stimulation. Inhibition of PI3K up to 2 hours before entry into S phase reduced c-Myc (a protein important for S phase progression) levels for several hours afterwards, and also the number of cells able to enter S phase (Kumar et al. 2006). This report confirmed previous findings by Kazlauskas' group (Jones and Kazlauskas 2001; Jones et al. 1999).

1.3.3 The phospholipase C (PLC) pathway

Phospholipase C and D are both substrates for the activated epidermal growth factor receptor. In mammalian tissues, 5 different groups of phospholipase C have been identified (PLCβ, γ, δ, ε, ζ), each group consisting of several isoforms. The PLCs contain SH2 domains, through which they are bound to the tyrosine residues 992 and 1173 of the EGFR upon mitogen stimulation. The binding results in relocalisation of the usually cytosolic PLCγ1 and γ2 to the membrane, where they catalyse the hydrolysis of inositol phospholipids (phosphatidyl-inositol 4,5-diphosphate) into inositol-triphosphates (IP$_3$) and diacylglycerol (DAG) (Nishizuka 1995). PLC gamma possibly also gets activated through the Grb2 protein, notably the binder Gab-1 which provides docking sites for the SH2 domain of the PLC (Gu and Neel 2003).

DAG is the co-factor for the protein kinase C (PKC) which is an activator of MAP kinases, both the JNK pathway and the Erk pathway. However, different studies suggest that several isoforms of PKC may be involved in the activation of these distinct MAPK pathways, depending on the stimulus and the cell type (Pysz et al. 2009; Koivunen et al. 2006; Hagemann and Blank 2001). IP$_3$ on the other hand mediates release of calcium from the cell, affecting Ca^{2+} dependent pathways and potentiates the PKC activation. Downstream targets of PKC are the Erk1/2 kinases, the glycogen synthase kinase 3 (GSK3) and NFκB (nuclear factor kappa beta) whose constitutive activation is associated with inflammatory diseases as well as some cancer forms (Kim et al. 2006). Thus, the signalling towards the phospholipid metabolism through EGFR is also linked to (increased) proliferation, as is the more direct activation of the classical MAPK cascade (Koivunen et al. 2006; Nishizuka 1995)

1.4 Key mechanisms for the transition from G0/G1 into S phase

There are numerous biochemical processes taking place in the cell, at different levels after the stimulation with growth factors, which need to be completed successfully in order to achieve progression through the G1 phase into synthesis state. The key mechanisms in this multistep process will be discussed in this section, and are depicted schematically in Figure 35.

1.4.1 The restriction point and its role in controlling proliferation

The restriction point (R point) is the point in the cell cycle where processes are initiated that lead to the assessment of the cell's ability to successfully undergo the next round of replication. If the assessment is positive, the R point represents the point of no return, because

the cell will complete one full cycle, even if environmental conditions change during the completion, e.g. when growth factors are withdrawn. Hence, the R point is also defined as the time point when the cell acquires serum independence. However, the R point is not a mere additional checkpoint in the cell cycle, since its function is different from that of a checkpoint. During a checkpoint, the cell ensures that its genome is intact, and that the previous steps of the cell cycle have been executed properly. If this is not the case, the cell is stopped at this control point until the genome has been repaired, and if repair is not possible, the cell will undergo apoptosis. In contrast, the R point can be passed if sufficient external signals have been received, and if this was not the case, the cell will withdraw from the cell cycle into a quiescent state. Importantly, this state can be left again when the cell is exposed to specific growth factors over an extended time, and the full round of cell cycle phases will be completed.

The activation of the MAPK pathway is essential for allowing a cell to pass the restriction point. In quiescent NIH3T3 cells, the activity of the Erk1/2 kinases must be sustained until late G1 for successful S phase entry. Inhibition of this pathway, even shortly (2 hours) before the onset of S phase, resulted in abandonment of DNA replication (Yamamoto et al. 2006). However, the activity of the Erk kinases declined quickly after entry into S phase and was not required for completion of DNA replication. This is in agreement with previous findings that put the R point up to a few hours before synthesis, but the exact onset of it seems to be cell type dependent. In the following sections, the signalling events that are taking place around the R point are presented and put into context with each other.

1.4.1.1 Elevation of the transcription factor c-Myc

The c-Myc protein is often overexpressed in human cancers. The role of c-Myc as an oncoprotein is supported by the observation that cell cycle arrest as a consequence of mitogen withdrawal (or another growth-inhibitory signal) can be overcome through ectopic expression of c-Myc. This protein has a pivotal role in cell cycle progression. Its activation is sufficient to induce cell cycle entry, even in the absence of growth factors, and conversely treatment of quiescent cells with growth factors increases c-Myc expression (Kelly et al. 1983). Expression of c-Myc is important for accumulation of the cyclins, which themselves are essential for G1 to S phase transition (discussed below): c-Myc is able to induce expression of D-type cyclins (Perez-Roger et al. 1999), and also helps to remove the inhibitory proteins $p27^{Kip1}$ and $p21^{Cip1}$ by inducing labile forms of those proteins (Hermeking et al. 1995). Hanson et al. (1994) demonstrated the importance of the transcription factor with c-myc

heterozygous cells in which they observed a clear delay in cyclin E expression during G1. Consequently, Rb phosphorylation, which follows the expression of cyclin E, was also delayed. The same result was obtained whether the cyclin protein or the RNA levels were analysed. All effects in the heterozygous cell line were reversed when transfected with a c-myc transgene (Hanson et al. 1994).

c-Myc is also a phosphorylation substrate for MAP kinases (English et al. 1998; Alvarez et al. 1991). In fibroblasts, signalling to Erk1/2 and induction of c-Myc expression were both necessary for cell cycle progression (Jones and Kazlauskas 2001). Erk1/2 directly enhanced the stability of the c-Myc protein by phosphorylating a specific serine residue (Ser62) (Sears et al. 2000). One target of the PI3K effector Akt is the glycogen synthase kinase 3 (GSK3). This protein kinase is constitutively active in unstimulated cells and phosphorylates c-Myc and cyclin D to keep them inactive. Phosphorylation of GSK3 by Akt turns off the catalytic activity of this enzyme, resulting in the activation of pathways that are normally repressed by GSK3. Conversely, specific PI3K inhibitors block growth factor induced elevation of c-Myc, in various cell types (Schild et al. 2009; Li et al. 2008; Chanprasert et al. 2006; Liang and Slingerland 2003; Chen and Sytkowski 2001).

1.4.1.2 Elevation of levels of cyclin dependent kinases

Cyclins were discovered as key regulators of the cell cycle in sea urchin eggs and fission yeast by Tim Hunt and Sir Paul Nurse, who shared the Nobel Prize 2001 for this work together with Leland H. Hartwell.

In mammalian cells, there are two types of cyclins important for the cell cycle stages from G1 to S phase, the D-type and the E-type cyclins. G1 progression depends on the sustained expression of D-type cyclins, which, in turn, depends on mitogenic stimulation, so that cyclins provide a link between mitogen signalling and the cell-cycle machinery. The overexpression of D-type cyclins in fibroblasts led to an accelerated progression through the G1 phase, with a premature entry into S phase (Quelle et al. 1993), and overexpression of cyclin D1 is also a feature of several human cancers (Arber et al. 1996a; Arber et al. 1996b).

The cyclins represent the regulatory part of the binary system of cyclin-dependent kinases (CDKs), which is completed by a catalytic subunit, the kinase. In mammalian cells, two types of CDKs exist that are important for the G1 to S transition:

Firstly, the CDK4 and CDK6 that are related to D-cyclins (D1, D2 and D3). These complexes are activated at mid-G1, their primary target being the Retinoblastoma protein (pRb), whose phosphorylation process they initiate (Ewen et al. 1993). Secondly, CDK2, which is activated

with cyclin E; this complex is slightly delayed compared with the CDK4/6 and acts at the G1/S transition.

1.4.1.2.1 The MAPK pathway and the cyclin dependent kinases

To further reveal how the MAP kinases support G1/S transitions, different links upstream and downstream in this pathway have been examined. For example, the small G-protein Ras upstream of MAPK and MEK strongly phosphorylates Erk1/2, therefore its role in cell cycle progression was assessed: an inducible dominant negative Ras mutant in NIH3T3 was used to show that if Ras expression is delayed after stimulation with EGF, the cells are unable to leave the G1 phase. This was the case even if the negative Ras was induced up to 3 hours after the addition of EGF (Takuwa and Takuwa 1997). The Ras mutant also inhibited downregulation of p27^{Kip1} which is an inhibitor for the cyclin-dependent kinases. On the other hand, increased activation of Ras induced significant overexpression of cyclin D1, shown in fibroblasts as well as mouse mammary gland epithelial cells (Liu et al. 1995; Filmus et al. 1994), and shortened the time necessary for G1 completion (Winston et al. 1996).

Direct links between the MAP kinase cascade and cyclins have been studied as well: e.g. the activation of Erk1/2 was found to be necessary for transcriptional induction of the cyclin D1 gene (Lavoie et al. 1996), and in addition, this activation needed to be sustained in order to accumulate sufficient cyclin D1. Inhibition of Erk1/2 up to 4 hours after the addition of the mitogen resulted in G1 arrest (Weber et al. 1997).

1.4.1.2.2 The PI3K pathway and the cyclin dependent kinases

The substrate of the PI3 kinase, Akt, was shown to up-regulate cyclin D1 expression in mammary epithelium, thus linking this pathway directly to cell cycle progression (Hutchinson et al. 2001). Growth factor stimulation of quiescent MCF-7 cells led to increased cyclin D1 synthesis, which was blocked with specific PI3K inhibitors, but not with a MEK1 inhibitor (Dufourny et al. 1997). The increase in protein levels was the result of cyclin D1 mRNA with an extended half life. Again, the stabilisation of the mRNA could be reversed with a specific PI3K inhibitor, but the MEK1 inhibitor had no effect (Dufourny et al. 2000). The same was reported for colon carcinoma and fibroblast cells (Muise-Helmericks et al. 1998).

1.4.1.3 Decrease of p27^{Kip1} and p21^{Cip1}

Cyclins are regulated by specific inhibitors, the proteins p21^{Cip1} and p27^{Kip1} (reviewed by Bartek and Lukas 2001; and by Ekholm and Reed 2000). p27^{Kip1} transcription and protein levels are maximal in G0 and early G1, and high p27^{Kip1} is required for the G1 arrest induced by growth factor deprivation. p27^{Kip1} levels fall abruptly with exit from quiescence and during G1 progression (Hengst and Reed 1996). Cyclin D1 is able to sequester p27^{Kip1} from the nucleus into the cytoplasm, thus making cyclin-dependent kinase 2 (CDK2) available for binding with cyclin E (Perez-Roger et al. 1999). CDK2 is inhibited in the nucleus by p27^{Kip1}, and the amount of this protein in the nucleus must drop below a certain level to release a sufficient amount of the kinase for formation of CDK2. The CDK2 complex itself phosphorylates again p27^{Kip1}, leading to whose further degradation (Philipp-Staheli et al. 2001; Albrecht et al. 1999). p21^{Cip1} also needs to be decreased, as shown in liver cells of p21$^{Cip1-/-}$ mice where complete removal of the inhibitor resulted in accelerated G1-progression (Albrecht et al. 1998). Conversely, accumulation of p21^{Cip1} leads to binding to and inactivation of CDKs in the G1 phase.

1.4.1.3.1 The MAPK pathway and the inhibitors p21^{Cip1} and p27^{Kip1}

One key element for the progression of cells through the cell cycle are the inhibitory proteins p27^{Kip1} and p21^{Cip1}. These must be decreased below a certain threshold for successful transition from G1 to S phase. It has been suggested that the Ras/Erk1/2 signalling pathway is directly involved in the mitogen-induced downregulation of p27^{Kip1} because inhibition of MEK1 prevented the reduction of p27^{Kip1} protein and its mRNA, whereas direct activation of ERK (through a constitutively active form of MEK) led to a reduction of p27^{Kip1} protein and mRNA, demonstrated in smooth muscle cells (Sakakibara et al. 2005). Similar observations were made in a malignant breast epithelial cell line MCF-7 that overexpressed the ErbB2: the presence of this receptor reduced p27^{Kip1} and increased cyclin D1 (Lenferink et al. 2001). This is because Erk1 and Erk2 phosphorylate p27^{Kip1} and so make it a target for degradation. The same was shown for p21^{Cip1}. In non-malignant breast epithelial cells, this inhibitory protein was phosphorylated, thus target for degradation, following the activation of the MAP kinase (Timms et al. 2002).

1.4.1.3.2 The PI3K pathway and the inhibitors p21^{Cip1} and p27^{Kip1}

The Cdk inhibitor p27^{Kip1} is phosphorylated for its degradation upon growth factor induced stimulation of the PI3K pathway, as was demonstrated with the specific inhibitor LY294002 in intestinal epithelial cells (Sheng et al. 2001), in several breast cancer cell lines (Motti et al. 2004) and in renal epithelial cells (Kim et al. 2009).

1.4.1.4 Hyperphosphorylation of the retinoblastoma protein

The retinoblastoma protein (pRb) represents the critical factor in determining the timing of the restriction point: in its partially (hypo-) phosphorylated state pRb suppresses cell cycle progression. These inhibitory properties are lost when the protein becomes phosphorylated and therefore inert. The R point is passed once the Rb protein has been hyper-phosphorylated, and this happens in two steps. First, the phosphorylation of the protein is initiated by the complex of the cyclin-dependent kinases (CDK) 4 and 6, which beforehand must become activated through cyclin D1 (CCND1). The second phase of phosphorylation is achieved through the CDK2 (which has to be cyclin E-activated earlier). The phosphorylation of pRb disrupts its association with E2F transcription factor family members, starting off the transcription of genes required for DNA replication in synthesis phase (Bracken et al. 2004; Harbour and Dean 2000; Weinberg 1995). Generally speaking, the inactivation of Rb family proteins and CDK inhibitors creates positive feedback loops and reduces the cell's dependency on mitogens, eventually leading to the irreversibility of the S phase entry.

1.4.1.4.1 The MAPK pathway and the Retinoblastoma protein

The Ras kinase, the upstream activator of the MAP kinase, is linked directly to the cell cycle via the retinoblastoma protein, as Rb$^{-/-}$ mouse embryonic fibroblasts (MEFs) had a reduced requirement for Ras to start DNA synthesis. The same observation was made by Peeper and co-workers (1997) in two different cell lines, both Rb$^{+/+}$, where Ras elimination led to G1 arrest, whereas in Rb$^{-/-}$ lines, DNA synthesis still took place, despite the lack of Ras. The specificity of the Rb dependence for Ras was confirmed by successful induction of a G1 arrest with different means (Cdk inhibitors) in both cell types (Rb positive and negative). These results suggest that the inactivation of pRb is one of the functions of Ras signalling that promotes cell proliferation. Interestingly, the relationship between Ras and pRb is bidirectional, as demonstrated by Lee et al. (1999) in MEFs: the Rb$^{-/-}$ cells displayed increased levels of Ras, which were lowered when pRb was reconstituted (Lee et al. 1999; Peeper et al. 1997; Mittnacht et al. 1997). Assays involving directly the MAP kinase and the

retinoblastoma protein as targets showed in human melanoma cells with constitutively active Erk1 and 2, that the inhibition of the MEK1 (upstream of the MAP kinases) resulted in hypo-phosphorylation of the retinoblastoma protein (Kortylewski et al. 2001).

1.4.1.4.2 *The PI3K pathway and the Retinoblastoma protein*

Dufourny et al. (1997) found that IGF-1 stimulates DNA synthesis and proliferation in MCF-7 cells, and after 16 hours of stimulation, the pRb was markedly increased. This could be reversed by the specific PI3K inhibitor LY294002, but not by an MEK1 suppressor, indicating the specificity of the signal mediated by IGF-1 for the PI3 kinase (Dufourny et al. 1997).

1.4.2 *Phospholipase pathways*

Since PLC acts upstream of PKC, which activates the MAP kinases Erk and JNK, it is conceivable that all implications of the mitogen-activated pathway for the processes in the G1 to S phase transition are also applicable to the phospholipase pathways. This is supported by the finding that RNAi mediated knockdown of several different PLC groups resulted in abandoned proliferation of fibroblast cells, because DNA synthesis was affected (Kaproth-Joslin et al. 2008).

Evidently, the MAP kinase and the PI3 kinase both have crucial roles in triggering events necessary for the transition from G1 into S phase. Thus, the disruption of either pathway most likely will provide valuable information about the signalling network activated in the MCF-12A cells. Additionally, the use of a PLC inhibitor may reveal if the PKC feeds into those two major pathways as well.
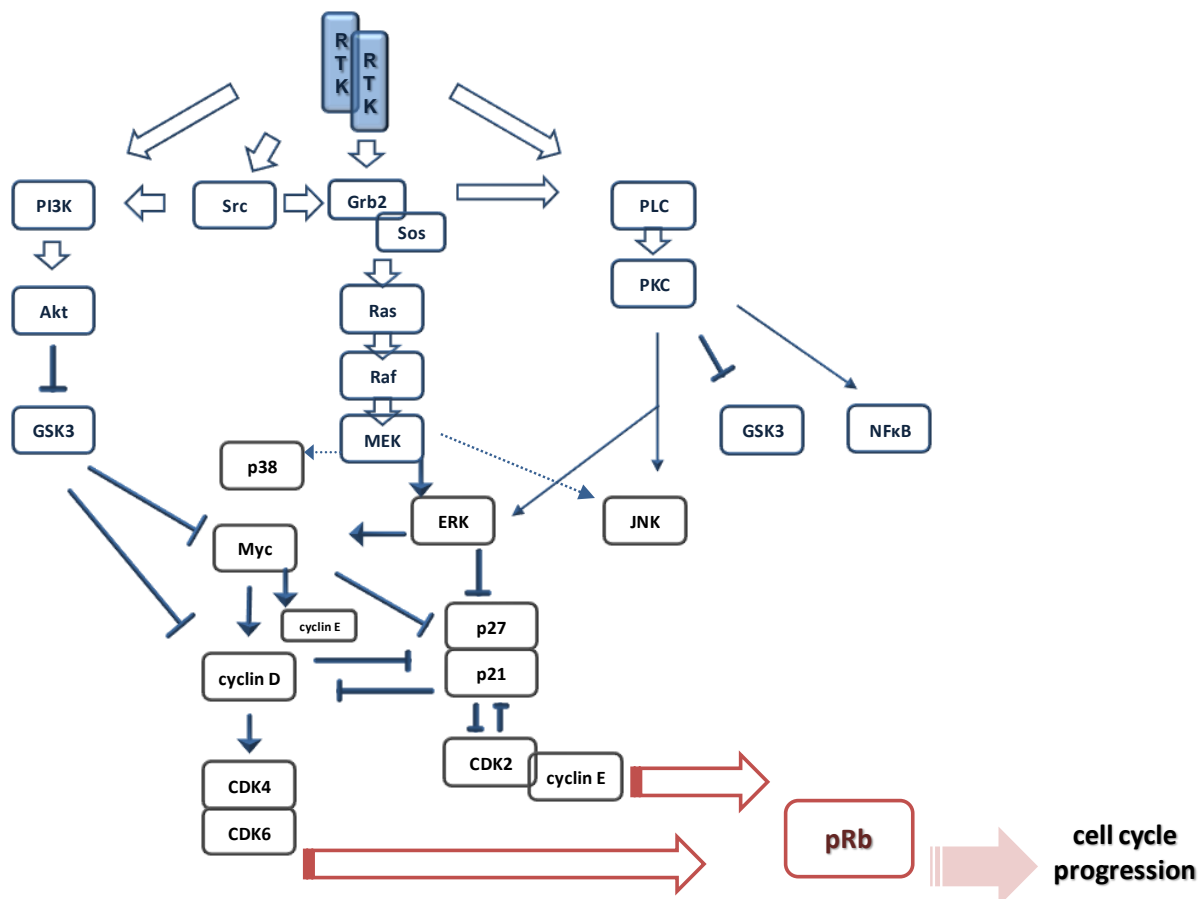
Figure 35 Schematic overview of molecular mechanisms involved in cell cycle progression

The key molecular mechanisms responsible for successful cell cycle progression, as described in detail in the section 1.4 of this chapter, are initiated by dimerisation of the receptor tyrosine kinases (RTK), induced by binding of a ligand. Kinases and lipases may be activated directly by the dimerised RTK, e.g. the Src and PI3 kinases and the phospholipase C (PLC), or through an adaptor protein, such as Grb2. The signals triggered by the ligand are propagated via different pathways, resulting in activation of the Myc transcription factor and the cyclin D/CDK4 (CDK6) and cyclin E/CDK2 complexes. These complexes are responsible for hyperphosphorylation of the retinoblastoma protein (Rb), commencing cell cycle progression.

2 OBJECTIVES AND METHODOLOGICAL CONSIDERATIONS

The aim of this part of the work is to investigate the signalling networks in MCF-12A cells that have a role in promoting cell cycle progression within the framework of the discontinuous exposure assay. On the basis of information about the kinases that are activated downstream of EGFR and IR, the objective was to characterise their involvement in cell cycle progression from G1 to S. Of particular interest was to analyse which signalling events are critical during the first and the second pulse of exposure, and if several pathways are

triggered at the same time. If so, is one pathway more prominent than the other, or are all of equal importance during the first and second pulse? If, for example, EGF is administered during the first pulse of growth factor stimulation, is only the EGFR activated, and if so, does this receptor trigger multiple cascades, or is its action more restricted?

Considering the importance of the three pathways discussed above for cell cycle progression, we selected inhibitors that target critical elements of these pathways. The features of the chosen inhibitors, their mode of action and important considerations for experimental design are discussed below.

PD98059 binds selectively to MEK1 (a MAPKK) and so prevents its activation by the upstream located Raf-1 kinase. Therefore, the effectors Erk1/2 (which are MAP kinases) will not be phosphorylated (Cowley et al. 1994).

LY294002 is a highly selective inhibitor of PI3K, and also blocks the PI3 kinase-dependent Akt phosphorylation and kinase activity (Vlahos et al. 1994).

The pyrazolo-pyrimidines PP1 and the related compound PP2 were the first inhibitors found for the Src family kinases, and PP2 is still the most selective inhibitor for Src available (Hanke et al. 1996). For this reason it was selected for our studies.

Finally, U73122 inhibits selectively receptor-coupled PLC dependent processes, but is not specific for a subclass of the PLC lipases; instead, it inhibits all isotypes of the phospholipases C (β, γ δ, etc.).

For every experimental procedure presented in this chapter, the MCF-12A cells were pre-incubated with the inhibitor alone (in basal medium, 20 minutes, at the concentrations specified in the material and methods' section (Chapter 2)), before addition of fresh basal medium containing the growth factor(s). This medium also contained the inhibitor at the same concentration as during the pre-incubation period, so that the total exposure to inhibitors lasted 50 minutes (in case of the first pulse) or 10h 20min (for the second pulse). The pre-incubation step was important as to occupy and block the receptors on the cell surface before the presence of the growth factors, since triggering of signalling pathways by ligand binding is a very fast mechanism. If the inhibitors were added at the same time with the growth factors, it is likely that the receptor was activated before the inhibitor reached the cell surface. The concentrations of the inhibitors to be used had been established beforehand in our laboratory, with the exception of the PLC inhibitor U73122. Its optimal concentration for our use (1 μM) was experimentally assessed, based on suggestions from the supplier.

The percentages of cells in the various cell cycle phases were normalised to the negative control sample (G0 blocked cells), as described before (Chapter 3, page 53). The positive control samples were from cells that had received both pulses with the growth promoting factors, but no inhibitors. Instead of the pre-incubation times, these samples were exposed to basic medium for 20 minutes, in order to compensate for any stress-induced effects from the washing steps. The data obtained by flow cytometry were subjected to a Student's t-test to determine significant differences between the treatments with inhibitors and the control samples. It was expected that incubation with inhibitors would hinder the cells from re-entering the cell cycle. Thus, the significance test was performed as a comparison to the positive control. A significance test in relation to the negative control is less suited, because it cannot be assumed that the inhibitors cancel out completely the effect of growth factor stimulation on cell cycle progression.

3 RESULTS

First, the effects of inhibiting specific kinases or a lipase during the first pulse of growth factor administration was examined. In this set of experiments, the inhibitors were present for a total of 50 minutes only (20 minutes pre-incubation in basal medium, followed by the first pulse of 30 minutes with EGF and the respective inhibitor). Three out of the four inhibitors tested had a marked effect on S phase progression (Figure 36). The strongest disruption was observed with the MEK1 inhibitor PD98059 (20 µM), which reduced the number of cells found in S+G2+M phase significantly compared to the positive control, almost to the level of the G0 blocked sample. Of comparable magnitude were the effects of the PLC inhibitor U73122 (1 µM), although with this compound, the variation between experiments was higher than with the MEK1 inhibitor, as seen from the size of the error bar, so that the reduction of the S phase percentage was less significant when compared to the positive control. Administration of the PI3K inhibitor LY294002 (20 µM) during the first pulse also decreased the number of cells found in S+G2+M phase at the end of the assay, whereas the Src inhibitor PP2 (25 µM) did not have any effect at this time.
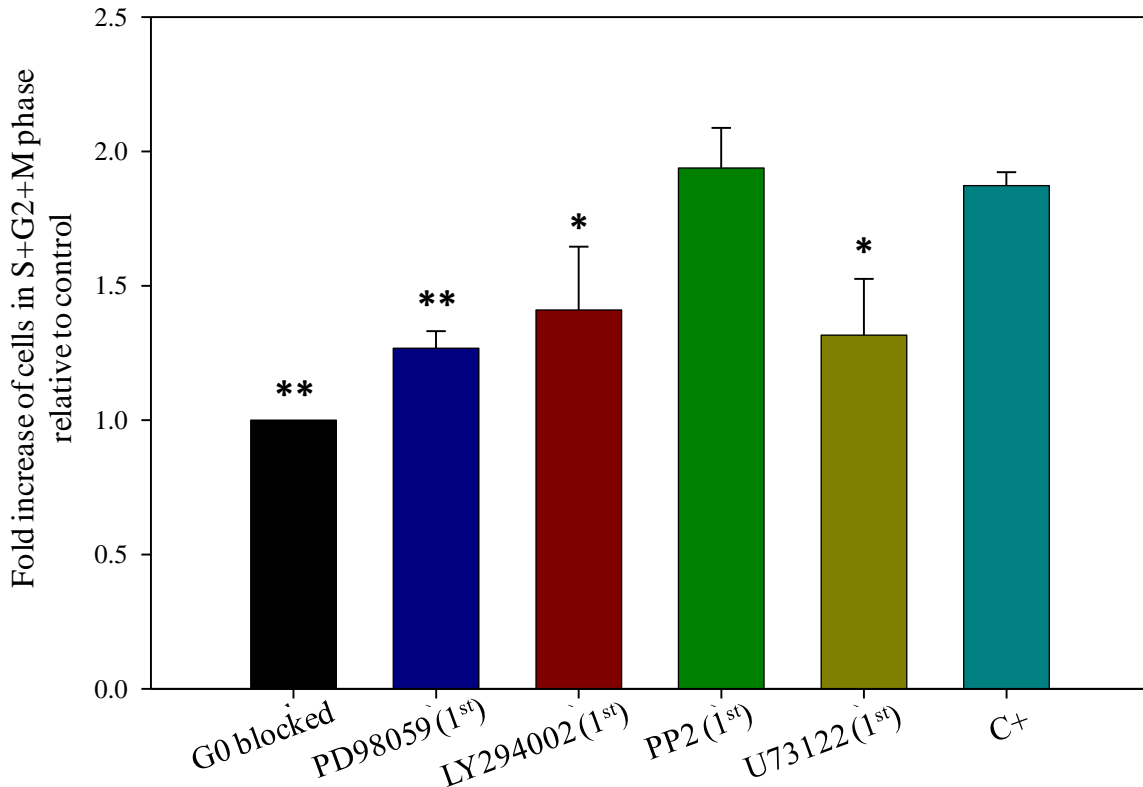
Figure 36 Effect of specific inhibitors administered during the first pulse on cell cycle progression of MCF-12A cells

Effect of MEK1 inhibitor (PD98059, 20 μM), PI3K inhibitor (LY294002, 20 μM), Src inhibitor (PP2, 25 μM) or PLC inhibitor (U73122, 1 μM) when added in the first pulse of growth factor administration in the discontinuous exposure assay. All samples were treated with the second pulse of growth factors and were analysed after a total release time of 18 hours. Percentages obtained with flow cytometry were normalised to the negative control (G0 blocked sample, set to 1). Values show the mean of 4 independent experiments, error bars show SEM. Student's t-test was performed for significance testing, samples marked with * (P=0.1) and ** (P=0.05) are significantly different from the positive control (C+). Positive control: 1st pulse (30min) = 50 ng/ml EGF, 2nd pulse (10h) = EGF + insulin (20 + 100 ng/ml).

Next, we examined whether any of these inhibitors would interfere with cell cycle progression when administered during the second pulse of growth factor exposure. As seen in Figure 37, the MEK1 inhibitor PD98059 (20 µM) was again able to significantly reduce the fraction of cells that progressed into the S phase, when compared to the positive control. This compound reduced the number of S phase cells to a similar level as when it was administered during the first pulse. However, the strongest reduction was seen with the PI3K inhibitor LY294002 (20 µM): under its impact, no cells were able to leave the quiescent state. Equally strong was the effect of the Src inhibitor PP2 (25 µM). The mean fraction of cells treated with the PLC inhibitor U73122 (1 µM) that had progressed to S phase was decreased compared to the positive control, but again, as with the sample treated during the first pulse, the variation between experiments was considerable. As a consequence, the difference was not statistically significant, as seen from the size of the error bars.
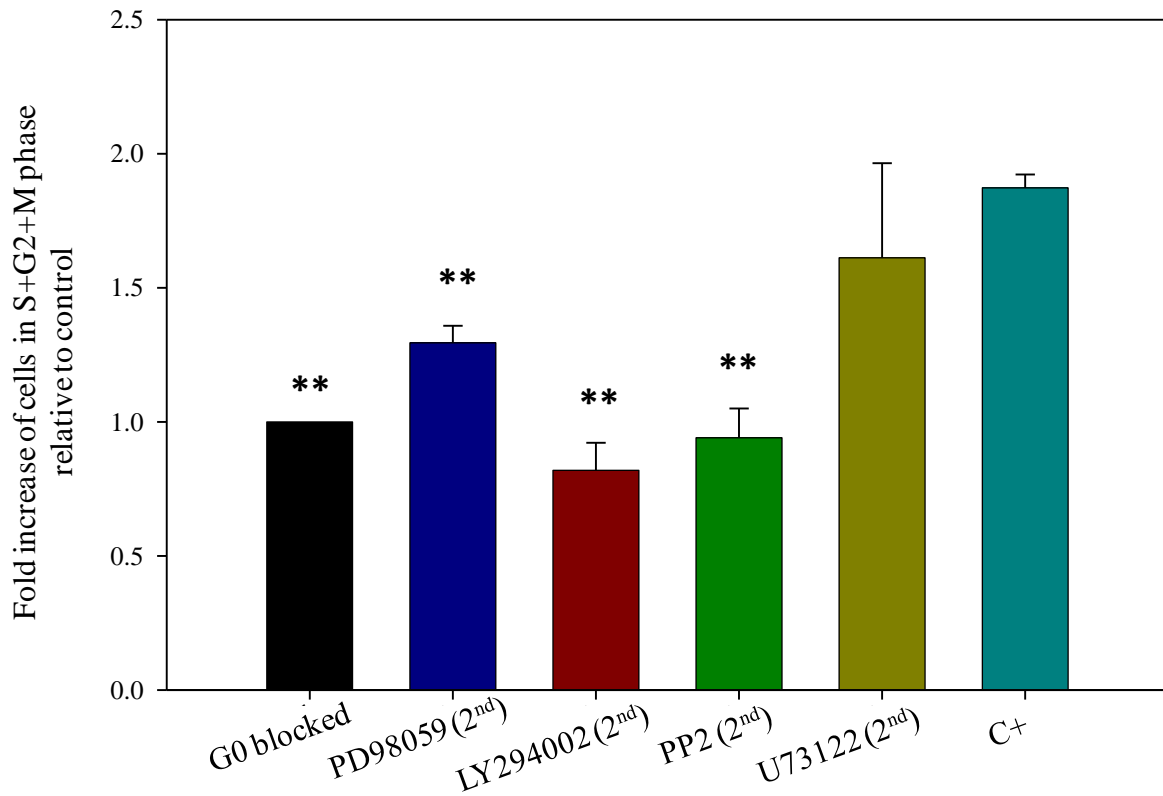
Figure 37 Effect of specific inhibitors administered during the second pulse on cell cycle progression of MCF-12A cells

Effect of MEK1 inhibitor (PD98059, 20 μM), PI3K inhibitor (LY294002, 20 μM), Src inhibitor (PP2, 25 μM) or PLC inhibitor (U73122, 1 μM) when added in the second pulse of growth factor administration in the discontinuous exposure assay. All samples were treated with a first pulse of EGF and were analysed after a total release time of 18 hours. Percentages obtained with flow cytometry were normalised to the negative control (G0 blocked sample, set to 1). Values show the mean of 4 independent experiments, error bars show SEM. Student's *t*-test was performed for significance testing, samples marked with **are significantly different from the positive control (P=0.05). Positive control (C+): 1st pulse (30min) = 50 ng/ml EGF, 2nd pulse (10h) = EGF + insulin (20 + 100 ng/ml).

The marked reduction in S phase progression with both the MEK1 and PI3K inhibitors indicates that both pathways, the MAP and the PI3 kinase pathways, were activated through the combined action of EGF + insulin, but that the inositol dependent pathway played a more important role at this stage of the cell cycle. It was therefore interesting to see if the addition of both the MEK1 inhibitor PD98059 (20 μM) and the PI3K inhibitor LY294002 (20 μM) together during the first pulse would be able to decrease further the number of cells in S

phase, or perhaps even to inhibit cell cycle progression completely. Administration of both inhibitors was then repeated for the second pulse, and the results are shown in Figure 38. The combined action of the two inhibitors during the first period of incubation did not decrease further the progression through G1 into S phase. The percentages of cells that were found in S+G2+M phase were very similar to the results obtained with cells that were incubated with each inhibitor separately. Treatment with both inhibitors together during the second pulse did reduce the fraction of cells that progressed into the cell cycle to the levels observed in growth arrested controls, but the effect was not different from that seen with the PI3K inhibitor individually which already decreased this number to the lowest level possible, equal to the G0 blocked sample.
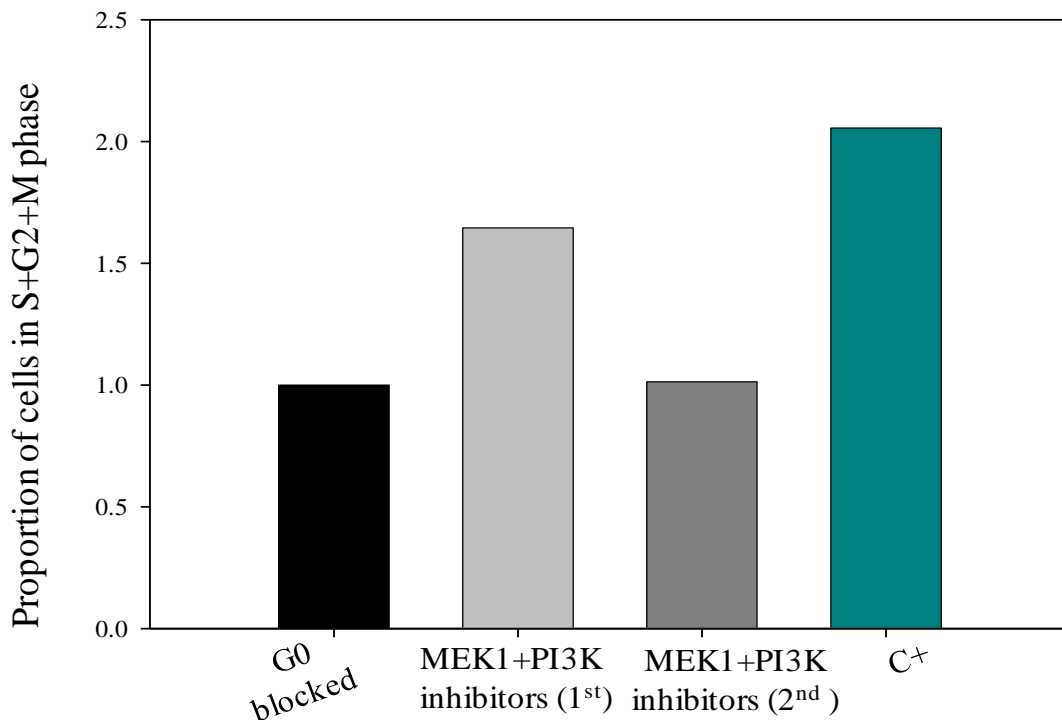
Figure 38 Effect of combined inhibition of MEK1 and PI3K on cell cycle progression of MCF-12A cells

Effect of the combination of the MEK1-inhibitor PD98059 (20 μM) and the PI3K-inhibitor LY294002 (20 μM) when added either in the first or the second pulse of growth factors in the discontinuous exposure assay. All samples were analysed after a total release time of 18 hours. Percentages obtained with flow cytometry were normalised to the negative control (G0 blocked sample, set to 1). Positive control (C+): 1st pulse (30min) = 50 ng/ml EGF, 2nd pulse (10h) = EGF + insulin (20 + 100 ng/ml). Results are from a representative experiment.

4 DISCUSSION

This series of experiments was aimed at studying the pathways that are activated in MCF-12A cells upon treatment with the discontinuous exposure assay, representing a combination of growth factors at two discrete time points, both necessary for cell cycle re-entry. The use of several inhibitors, specific for three different kinases and one lipase, revealed the sequence in which the MAP kinase, the PI3 kinase and the phospholipase pathways are activated upon growth factor stimulation, as well as details about the adaptor molecules involved. An overview of the signal cascades activated by the two investigated growth factors, EGF and insulin, is given in Figure 39 and Figure 40.
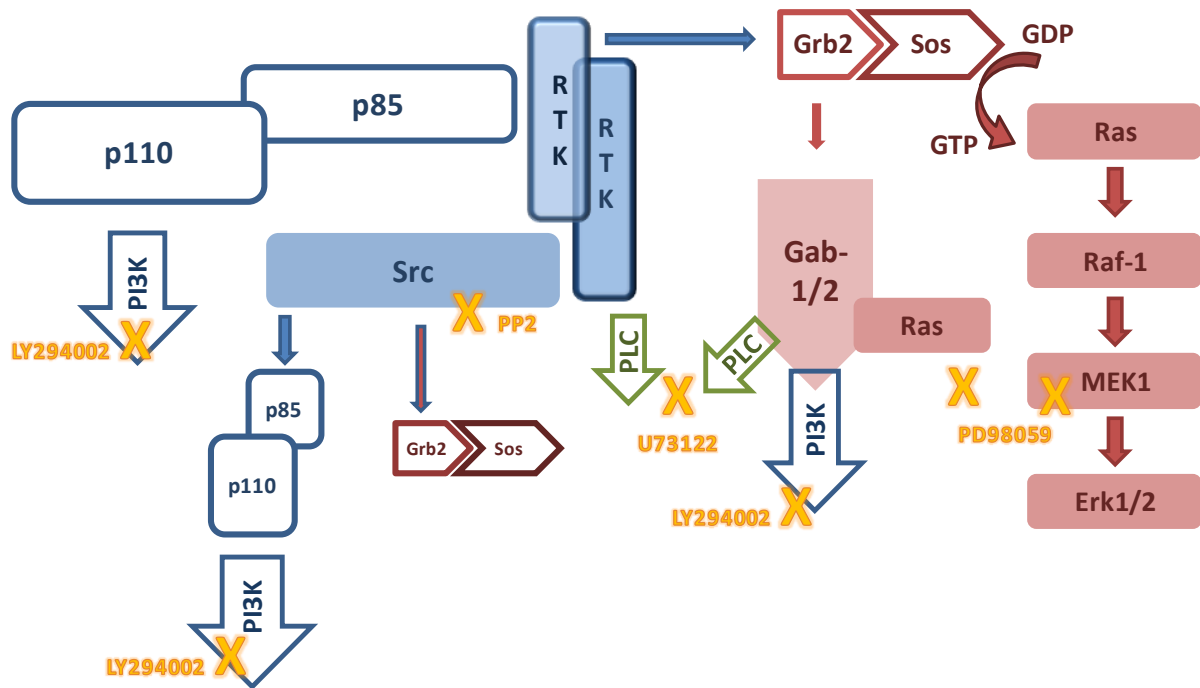
Figure 39 Overview of cascades downstream of EGRF involved in cell cycle progression in MCF-12A cells

The EGRF is a receptor tyrosine kinase which, once dimerised, associates with a multitude of molecules to trigger the PI3K, MAPK and PLC pathways. For more details please refer to the relevant sections 1.1.3 and 1.3 in the introduction of this chapter. The sites of action of the inhibitors used are marked with X.
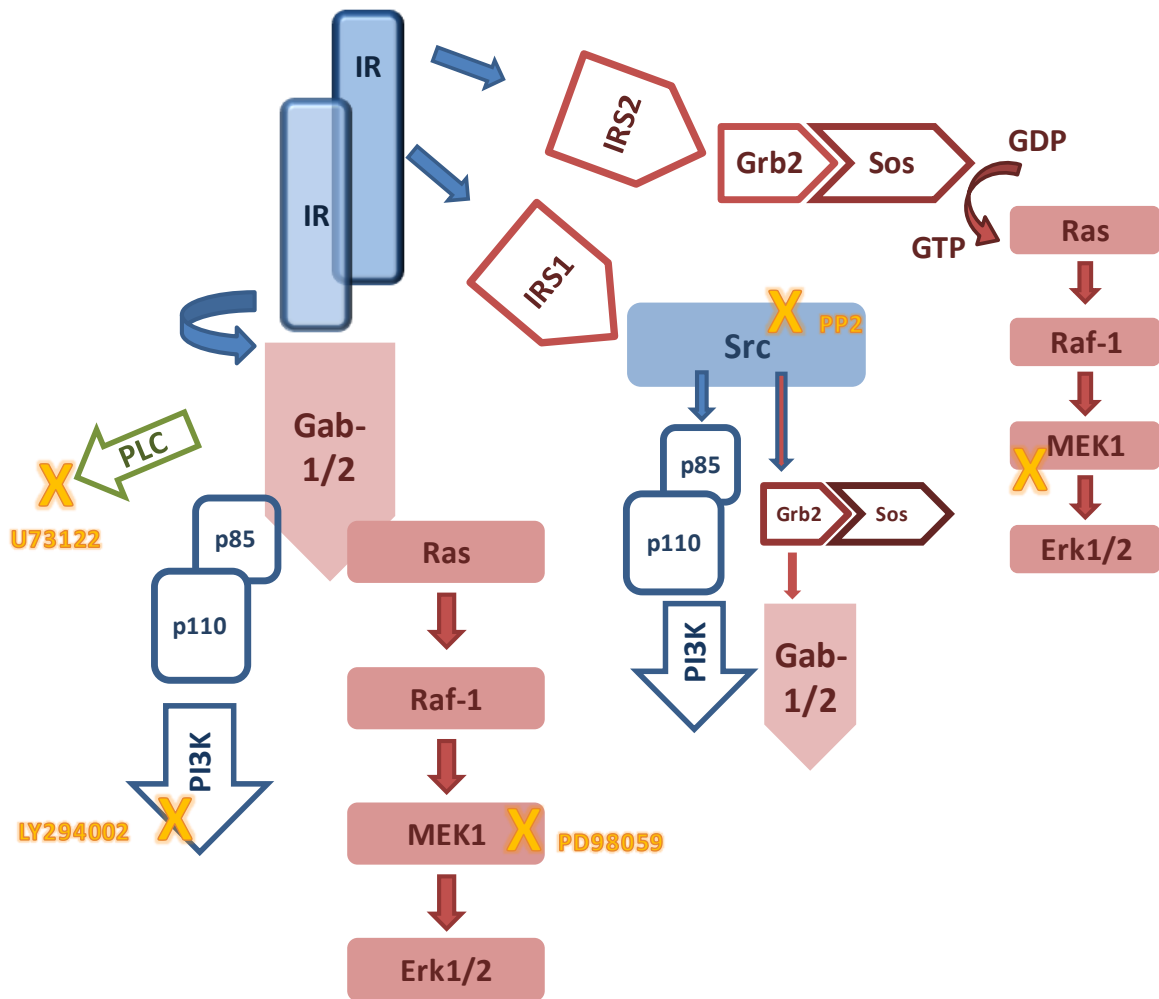
Figure 40 Overview of cascades downstream of IR involved in cell cycle progression in MCF-12A cells

The IR is present as a stable heterotetramer on the cell surface and binds to insulin receptor substrates 1 and 2 (IRS1 and IRS2), as well as the adaptor molecules Gab-1 and Gab-2, which are also considered receptor substrates. Different signalling cascades are triggered at the level of the receptor substrates. For details, please refer to the relevant sections 1.2.3 and 1.3 in the introduction of this chapter. The sites of action of the inhibitors used are marked with X.

4.1 First pulse of growth factors (EGF)

S phase progression was markedly disrupted with inhibitors for MEK1 and PI3K in the first pulse. This suggests that the first incubation with EGF triggered two pathways, the MAP kinase and the PI3 kinase mediated pathways. Both seemed to be equally important, because with the specific inhibitors, the cell cycle progression was affected to the same extent. The effects observed were similar to those where the growth factor was omitted completely from the first pulse (cf. Figure 26), thus equivalent to the maximal achievable suppression at this

time point. It is important to note that the effects observed cannot be explained in terms of residual inhibitory molecules remaining in the culture dishes after the first pulse, because after removal of the culture medium, the cells were washed twice with buffer before addition of fresh basal medium. Therefore, any remaining inhibitor would be present at a much diluted concentration only.

It is conceivable that two independent pathways were set in motion as a result of the activation of one type of receptor tyrosine kinase: the dimerised receptor provides docking sites for molecules that contain a SH2 domain, and for that reason attracts an array of proteins. These proteins include the non-receptor tyrosine kinase Src, the adaptor molecules Grb2 and Shc, and the regulatory protein p85. Firstly, p85 is the regulatory unit of the phosphatidyl-inositol-3 kinase (PI3K), hence upon binding of the subunit to the EGFR, the PI3 kinase may have become activated. The adaptor molecules Grb2 and Shc do not have catalytic properties themselves, however, they are essential for transducing signals from a receptor to the kinases located further downstream, namely the PI3 kinase (through Gab-1 which binds p85) and the mitogen-activated protein kinase (through the exchange factor Sos that activates Ras). Finally, the Src kinase phosphorylates a multitude of substrates, including focal adhesion proteins, structural proteins such as tubulin, the phospholipase Cγ and the protein kinase Cδ, and the molecules Shc and p85. The last two evidently connect the Src with the main pathways of PI3 and MAP kinases, as reviewed in detail by Thomas and Brugge in 1997 (Thomas and Brugge 1997). However, Src was apparently not involved in the signalling generated by EGF in the first instance, because the specific Src inhibitor PP2 was unable to prevent cell cycle progression. When rendered inactive through reversible inhibition, Src can be effectively bypassed through direct activation of Shc and Grb2 by EGFR (see Figure 39 and 40). Based on these observations it was concluded that in quiescent MCF-12A cells, EGF stimulated activation of both PI3 and MAP kinases was mediated entirely through the adaptor molecules Shc and Grb2.

The Src kinase is an activator of the MAP and PI3 kinase, situated much further upstream in the signalling cascades. As an alternative to this tyrosine kinase, it was tested if an inhibitor of a lipase, also located further upstream than the previously investigated MEK1 and PI3 kinases, would hinder cell cycle progression. PLC indirectly acts on PKC, as it provides co-factors necessary for PKC activity. PKC phosphorylates different types of MAP kinases (Erk1, Erk2 and JNK). PLC itself is activated directly by the dimerised EGFR, as it is able to bind to the receptor via a SH2 domain. In the light of these interconnections, it was

136

speculated that in the MCF-12A cells, the PLC inhibitor targeted another relatively far upstream activator, exclusive to the MAPK cascade. Indeed it was observed that the PLC inhibitor hindered cell cycle progression to an extent similar to the kinase inhibitors. Hence three different pathways were activated by dimerisation of the EGFR, PI3K, PLC and Ras/Raf-1/Erk1/2, and all of them were equally important for promoting cell cycle re-entry.

4.2   Second pulse of growth factors (EGF and insulin)

4.2.1 The MAPK and PI3K pathways and mediation of signalling through Src kinase

The MAPK and the PI3K pathways were activated also during the second pulse, with consequences for cell cycle progression. At this time, the PI3 kinase pathway seemed to be more important in terms of cell cycle progression, considering that the fraction of cells hindered from cell cycle entry was larger upon administration of the PI3K inhibitor than with the MEK1 inhibitor. The mean value for the S+G2+M phase percentages was even below the percentages found for the cells blocked in G0 after treatment with the PI3K inhibitor LY294002 suggesting that disruption of the PI3K pathway alone during the second pulse was able to keep additional cells in quiescence. The combination of both the PI3K and MEK1 inhibitors was not able to reduce the number of escaped cells further than to the negative control level (G0 blocked cells).

Another important finding was that inhibition of PLC during the second pulse had very little impact on hindering cell cycle entry. This is in contrast to the situation during the first pulse, where administration of the PLC inhibitor U73122 significantly disrupted cell cycle progression.

Further differences were seen in relation to Src. The specific inhibitor PP2 reduced the numbers of cells found in S phase to the same extent as the PI3K inhibitor. This suggests that the activation of the PI3 kinase pathway during the second pulse seemed to be mediated mainly through the Src kinase. In contrast, during the first pulse, Src signalling was found to be redundant.

The Src kinase is indeed involved in a range of signal transductions that control cell growth and proliferation, as well as apoptosis. Interestingly, this kinase is not only activated by receptors, but can itself modulate RTKs (Bromann et al. 2004). The relationship between the non-receptor tyrosine kinase Src and the RTK was first shown with the PDGF receptor to

which Src bound through its SH2 domain (Mori et al. 1993). The binding of Src releases it from its autoinhibited, membrane bound state by opening the intramolecular loop of the domains; the tyrosine residues are then phosphorylated, and the kinase site is active. The importance of the association of Src with the receptor was demonstrated in quiescent fibroblasts: upon stimulation with PDGF, those cells showed an increased Src kinase activity. Moreover, this also correlated with higher levels of active PI3 kinase (Kypta et al. 1990). The implications of this relationship for cell cycle progression were assessed by Courtneidge et al. (1993): fibroblasts with a catalytically inactive form of the Src kinase were incapable of progressing through the cell cycle under growth stimulation (Courtneidge et al. 1993). Their inability to leave the G1 phase was a result of failed DNA synthesis, but this was rescued when the transcription factor Myc was injected (Barone and Courtneidge 1995).

Of special interest in this context is that the EGFR is often overexpressed together with Src in mammary tumours (Muthuswamy et al. 1994), and that the Src kinase has been shown to physically associate with the EGFR and HER2 receptor in breast cancer cells (Biscardi et al. 1998). The malignant cells that overexpressed both kinases also showed a stronger increase of DNA synthesis upon stimulation with EGF, further underlining the importance of the communication between Src and EGFR for proliferation (Biscardi et al. 1998). The Src kinase is not only mediating EGFR signalling, but it even potentiates the effect of the receptor on proliferation, because it phosphorylates the receptor again on a different residue, as shown in fibroblast cells (Biscardi et al. 2000; Tice et al. 1999). Increased Src activity led to loss of cell-cell adhesion and increased invasiveness in malignant cells. In normal epithelial cells, increased Src resulted in loss of adherence junctions. Underlying this effect of the Src was an overly induced PI3 kinase (Kotelevets et al. 2001). Taken together, these observations suggested that overexpression of Src contributes to tumour progression.

In normal breast epithelial cells (MCF-10A cell line), the overexpressed Src kinase also stimulated proliferation, in cooperation with the Grb2-associated binder 2 (Gab-2) (Bennett et al. 2008). Gab-2 serves as a linker between a receptor and the PI3 kinase (by binding p85) or the MAP kinase, by binding Shp 2. Likewise, in mouse mammary epithelium, Src ablation disrupted cell cycle progression and cyclin expression, elevating at the same time the expression of Cdk-inhibitors (Marcotte et al. 2011).

Clearly, the Src kinase plays an important role for transducing growth promoting signals from the receptor to the downstream kinases, and especially the EGF receptor acts in tune with this

kinase. From the results presented in this chapter, it was concluded that a similar strong relationship between these two kinases also existed in the MCF-12A cells. However, it is somewhat surprising that the predominantly activated pathway was the PI3 kinase cascade, because signalling through the EGFR is classically associated with the MAP kinase cascade. When the Erk1/2 pathway was disrupted, S phase progression was significantly hindered, but the effect was not as strong as with the PI3K- and the Src-inhibitors. Obviously, with the experimental set-up employed here, it was not possible to distinguish the effects of the two different growth factors in the second incubation period, but the potential role of insulin and its receptor IR needs consideration here:

One of the proteins shown to interact with IRS-1 after insulin stimulation is the Src family member Fyn (Sun et al. 1996). This interaction is possible through the SH2 domain of Fyn. Viewed in the context of the results presented here, it would suggest that MCF-12A cells utilized the Src family member Fyn for signalling. Fyn is also actively inhibited by PP2, the molecule that was used for the inhibitory experiments shown here. However, according to Thomas and Brugge (1997), no difference in Fyn kinase activity has been observed after insulin treatment (Thomas and Brugge 1997). More recently, however, insulin was shown to cause Src activity in muscle cells, and physical association of the kinase with the IR. At the same time, the Src inhibitor PP2 disrupted insulin-induced phosphorylation of the IR (Rosenzweig et al. 2004). Crosstalk between IRS and Src for phosphorylation of focal adhesion proteins was reported in CHO cells (El et al. 2001). On the other hand, insulin receptor tyrosine kinase substrates (IRTKs) are important for cell motility; migration of malignant fibroblasts was enhanced with high, Src-induced phosphorylation of IRTKs (Chen et al. 2011). Although these observations were made in different systems, the possibility that a similar relationship between the insulin receptor and the Src kinase existed also in the breast epithelial cells cannot be dismissed.

However, one needs to bear in mind that insulin was not absolutely required for cell cycle progression of the MCF-12A cells. In Chapter 4, it was shown that the cells were able to re-enter the cell cycle after serum-depleted induced G0 block when EGF only was administered in both incubation times. Such an exposure regime resulted in almost the same fraction of cells in S+G2+M phase than seen with the positive control treatment. On the other hand, insulin is also able to induce MAP kinase signalling, which is initiated through the binding of the Grb2 adaptor to the IRS:

4.2.2 Crosstalk between the pathways that are triggered through EGF and insulin

Without a doubt, there are many similarities between the cascades that are triggered by activation of the EGFR and the IR. It is not evident if these pathways, when triggered in the same cell, are attenuated by each other, signal completely independent of each other, or even reinforce each other through crosstalk mechanisms. To know which of these three possibilities is most likely in place in MCF-12A cells is important for assessing the effect that the growth factors EGF and insulin had on the epithelial cells. Published work about crosstalk between mitogenic signalling pathways mainly handles overlapping functions between the estrogen receptor (ER) and the IGF-1R, because the ER activity plays an important role in breast cancer, and the signals of the IGF-1R and the ER have been found to enhance each other. Therefore it might be of importance to attenuate both receptors for the treatment of the disease (Hamelers and Steenbergh 2003). Comparatively little work has been done to systematically investigate the overlaps between the cascades triggered by the EGF and the IGF-1R, and even less for the EGFR with IR. In colon carcinoma cells, EGFR activation was found to be downstream of the IGF-1R, because an inhibitor for the PI3K (activated by IGF-1R) resulted in loss of EGFR activation (Hu et al. 2008b). Both activities, originating from EGRF and IGF-1R, also target the pro-apoptotic protein BAD, but their downstream pathways phosphorylate BAD in different residues, thus enhancing each other's effect (Gilmore et al. 2002). In HepG2 (human liver hepatocellular carcinoma) cells, EGF was able to activate IGF-1R. This transactivation was mediated by the Src kinase: EGF stimulated the tyrosine phosphorylation of Src, and induced its association with the IGF-IR. EGF induced IGF-1R activation could be repressed by the specific inhibitor PP2. EGF also induced phosphorylation of IRS-1 and IRS-2, pointing towards the possibility of a heterodimer in these cells (Hallak et al. 2002). This different kind of crosstalk between the receptor types indeed happens: both the ErbB-family receptors and the IGF-1R and the IR have been found to form heterodimers with each other, even between families, with full cellular functionality, which could mediate resistance to anticancer therapies (Jin and Esteva 2008).

4.2.3 The phospholipase pathway

The phospholipases are bound to growth factor receptors (PDGFR and EGFR) upon growth-factor induced activation of the receptors, and mediate mitogenic signalling through offering an additional docking site for Grb2 with their associated Ras/Raf-1 signalling. The PLCs

therefore link the MAP kinase pathway in an additional way to the EGFR. The disruption of the lipase presented a somewhat more direct inhibition of the EGF-mediated MAP kinase signalling, than the MEK1 inhibitor, because at this point of inhibition, crosstalk between two or more pathways may already have taken place, at a higher level of signal transduction (at the stage of Grb2, because this adaptor spreads to both cascades). Unfortunately, the PLC inhibitor during the second pulse yielded mixed results: in one exposure experiment, cell cycle progression was clearly impaired with the lipase inhibitor, but in the second assay, this result was not seen. The experiment was carried out four times in total, but the percentages for the S phase fraction were highly variable, so that the difference between the treated and the control samples was statistically not significant.

5 CONCLUSIONS

It is concluded that the activation of the EGFR through EGF in the first pulse was propagated via the Erk1/2 kinases, through two different mechanisms, first the activation of PLC, and secondly through binding of adaptor molecules that transduce the signal via the Ras/MEK1 pathway. The latter mechanism then also relayed signals towards the PI3 kinase pathway, and both cascades seemed to be equally important during the first pulse. Bearing in mind the function of the restriction point (which is to ensure that the signals thus far received are sufficient to induce and pursue transcription), it seems conceivable that these two pathways converge further downstream, for one single purpose, which is to induce transcriptional activity leading to cell cycle activation.

The second pulse of growth factors (EGF combined with insulin), triggered several pathways through the EGFR and the IR. In contrast to the first pulse, the Src kinase was strongly involved in signal transduction leading to cell cycle progression. Since Src is mainly associated with the EGFR, it seemed that EGF participated to a greater extent to activating downstream signals, than did insulin. One could be inclined to interpret that insulin indeed has a weak but measurable role in promoting PI3K activity, because when the PI3 kinase was inhibited, the percentage of S phase cells was slightly more reduced than with the Src inhibitor. In order to assess the contribution of each single receptor-bound transducer (Src, IRS), further experimentations are necessary, which employ more specific inhibitors, e.g. as to interrupt Grb2 and its associated binders. Additionally, repetitions of the assay with the lipase inhibitor during the second pulse would be of interest, especially in the light of the

findings by Choi et al. (2005) in kidney cells (HEK cells), where Grb2 association with PLCγ resulted in negative regulation of the EGFR-mediated cell signalling (Choi et al. 2005).

It is now necessary to seek molecular explanations for the observations made in this chapter by investigating the identity of the signalling molecules present after the first and the second pulse of growth factor administration. What is the nature of the signals triggered during the first pulse, and how are these signals taken forward to promote cell cycle entry during the second pulse? These topics will be addressed in the subsequent chapter.

Chapter 7:
Regulation of gene and protein expression for G1/S transition

1 INTRODUCTION

An array of diverse processes needs to take place in an orderly fashion for cells to be able to successfully progress out of the quiescent state through G1 into S phase. For MCF-12A cells, an experimental set-up was developed where, after serum-depletion for accumulation in the G0 phase, the cells received different growth factors in a discontinuous fashion at two distinct time points. This discontinuous stimulation was sufficient to bring the cells back into the cell cycle, as demonstrated by elevated numbers of S phase cells at the end of the assay. In the previous Chapter 6 we employed specific kinase inhibitors to develop hypotheses about the kinases involved in S phase induction during the two distinct pulses in the discontinuous exposure assay. However, the use of kinase and lipase inhibitors is an indirect method of investigation which cannot reveal which signalling molecules are indeed activated by the various growth factors during the discontinuous exposure assay. Here, immunoblotting of cell lysates against specific kinase antibodies was conducted, firstly to establish the identity of the enzymes activated during cell cycle progression, and secondly the specificity of the inhibitors used. In addition to these two aspects, molecular explanations for the observations made in the previous Chapter 6 were sought. To realise this aim, it was necessary to analyse other targets as well. A review of the signalling molecules considered for this part of the work is given in the following section.

1.1 Exploring the molecular basis of cell cycle progression – selection of targets

1.1.1 Signalling kinases Src, Akt, Erk1/2

The general association of external growth factors with intracellular signalling was discussed in the previous Chapter 6. The importance of the kinases Src, Akt and Erk1/2 is recapitulated briefly in this section, with a focus on the importance of activating these kinases for cell cycle progression.

The Src kinase is not immediately involved in the induction of gene and protein expression. However, it provides a link between growth factor receptors and intracellular signalling molecules and triggers several pathways that have pivotal roles for the positive regulation of transcription factors and the transition from the quiescent state into S phase (Thomas and Brugge 1997). Thus the activity levels of the Src kinase were monitored by immunoblotting.

Akt is phosphorylated by the PI3 kinase, which can be activated either by the Src kinase, or by associating directly with ligand-bound receptors. Phosphorylation of Akt, which is synonymous with activation of the PI3K pathway, in the G1 phase is essential for subsequent initiation of DNA synthesis induced by growth factors. Together with the MAPK pathway it ensures a rapid increase in c-Myc expression (Liang and Slingerland 2003). The role of the transcription factor c-Myc was detailed previously (cf. pages 99 and 121).

The mitogen-activated protein kinase (MAPK) cascade is the best studied signalling pathway in mammalian cell lines; the involved kinases transduce signals from extracellular, receptor-bound growth factors into the cell, eliciting growth and proliferation. The cascade may be triggered by several molecules situated between the MAPK kinase (MEK) and the dimerized receptor. The MAP kinases include the ERK1, ERK2, the p38 MAP, and the JNK kinases. These are phosphorylated by the MAPK kinases such as MEK1 and MEK2. MEKs in turn are activated by Raf, which needs to be phosphorylated beforehand by the small G-protein Ras (Ramos 2008). In fibroblast cells, the Ras protein was shown to be required for S phase initiation, in response to serum stimulation, and – in a sufficiently high concentration – promoted DNA synthesis also without the addition of serum (Mulcahy et al. 1985).

1.1.2 Transcription factor c-Myc

The link between the growth factor stimulation and the transcription factor Myc has been established at numerous levels, as well as the role of Myc in cell cycle progression. Most of these investigations were carried out in quiescent fibroblast cells, which were also used to show the following:

- the stimulation with PDGF for a few hours resulted in a significant increase of *MYC* RNA levels, and the amount of RNA found was in direct correlation to the concentration of the growth factor (Kelly et al. 1983).
- Inhibition of DNA synthesis by a Src antibody was rescued with constitutively expressed Myc (Barone and Courtneidge 1995),

144

- but MEK induced DNA synthesis was shown to be also dependent on the activation of the PI3K pathway (Treinies et al. 1999).

- The Ras and Myc proteins both have been identified as critical components which are key for the control of normal cell growth: as shown by Leone and colleagues (1997), overexpression of Myc alone or constitutive activation of Ras alone was insufficient for Cdk activity in G1 phase, but co-expression of Myc together with activated Ras induced S phase (Leone et al. 1997).

- When Ras expression was delayed after stimulation with EGF, cells were unable to leave the G1 phase. This was the case even if a dominant negative Ras mutant was induced up to 3 hours after the addition of EGF (Takuwa and Takuwa 1997).

- The ability of the Raf kinase to induce Myc was severely impaired after addition of the inhibitor PD98059, providing a direct correlation between MEK1 and the transcription factor (Sears et al. 1999). Additionally, the MAP kinases Erk1 and 2 directly enhanced the stability of the Myc protein by phosphorylating a specific serine residue on it (Ser62), and this residue was also important for proper degradation of the protein, providing a switch for keeping the balance between activation and disassembly of Myc (Sears et al. 2000; Sears et al. 1999).

- These stability enhancing properties of the kinases could be important for the overall role of the transcription factor, because it is very unstable: the level of Myc was shown to be very low in quiescent cells, but peaked within 2 hours of stimulation, followed by a rapid decline to half-maximal levels. This is in agreement with reports of a very short half-life (< 1 hour) of the protein in growing cells. On the other hand, the degradation of Myc was slowed down by activating the Ras pathway (Sears et al. 1999).

- In different fibroblast cell lines, the activity of the Erk1 and Erk2 together with the induction of Myc expression were both necessary for cell cycle progression (Jones and Kazlauskas 2001).

Because of these correlations between growth factor stimulation, the activation of Src, Ras, PI3 and MAP kinase cascades and the transcription factor during cell cycle progression, the expression pattern of Myc was examined in the MCF-12A cells during the discontinuous exposure, at two different levels: transcription of the gene coding for c-Myc was monitored and compared to its expression in quiescent cells, and cell lysates were assayed for the protein product.

1.1.3 Cyclin D1

Cyclins are now established as key regulators of the cell cycle. There are two types of cyclins in mammalian cells important for the transition from one cell cycle stage into the other, the D-type and the E-type cyclins. Cyclin D1 has been shown to be essential for successful progression from G1 phase into S phase. The mitogen-activated protein kinases Erk1 and Erk2 were found important for inducing the transcription of the cyclin D1 gene in early G1 phase in response to growth factor stimulation, and its expression must be continuous for successful cell cycle progression. The relationship between growth factor activated cascades and the cyclins was examined at different levels in numerous studies:

− The transcription factor Myc protein induced expression of D-type cyclins (Perez-Roger et al. 1999)

− The Ras protein and the MAP kinase both activated cyclin D1 transcription (Albanese et al. 1995; Filmus et al. 1994)

− The induction of cyclin D1 was controlled by the activation of the MAP kinases Erk1 and Erk2 (Lavoie et al. 1996), and the addition of the MEK1 inhibitor PD98059 at several hours after exposure to a mitogen in serum-starved cells (PDGF in the case of fibroblasts) resulted in a significant decrease in the expression of cyclin D1, both at the protein and the mRNA level. The continued expression of cyclin D1 was disrupted after the inhibition of the MAP kinase compared to uninhibited control cells, demonstrating a requirement for sustained MAPK activation throughout G1 for the positive regulation of cyclin D1 (Weber et al. 1997).

− However, overly enhanced activity of the cyclins is not desired since the overexpression of D-type cyclin protein led to a shorter G1 phase (faster progression through G1) and a premature entry into S phase (Liu et al. 1995; Quelle et al. 1993).

− In line with these reports is the observation that the gene coding for cyclin D1 was found to be overexpressed in many human cancers (Arber et al. 1996a; Arber et al. 1996b).

It was important to investigate relationships between mitogen stimulation of quiescent cells and the expression of cyclin D1 also in the mammary epithelial cell line MCF-12A. Because induction of cyclin D1 is dependent on transcription factors such as c-Myc, and because translation and synthesis may take several hours, with the protein product being detectable only at the very end of the discontinuous exposure assay, cyclin expression was examined at

the gene level only: the transcription into mRNA of the gene coding for cyclin D1 (*CCND1* or *PRAD1*) was monitored during the discontinuous exposure assay and compared to cells that were exposed continuously to serum. The regulation of the genes that code for the cyclin D1 was an interesting endpoint for the discontinuous exposure assay, because if this gene was elevated in the MCF-12A cells following two distinct pulses of mitogens, this would confirm that the cells did not require a constant input from growth factors.

2 OBJECTIVES

In the previous chapter, the flow cytometric results revealed that inhibition of the Src kinase, MEK1, PI3K and PLC each affected cell cycle re-entry, but to different extents at different times. For example, inhibition of MEK1 during the first administration of growth factors reduced markedly the percentage of cells that arrived in S phase. Although MEK1 may be activated through the Src kinase, the inhibitor for Src (PP2) had no effect on cell cycle re-entry. Thus, the MAPK pathway did not seem to be activated via the Src kinase.

Blocking of MEK1 activity during the second administration of growth factors also resulted in a decrease of S phase numbers, and the same was observed with the PI3 kinase inhibitor. This could mean that both these kinases (MEK1 and PI3K) are required for cell cycle re-entry. However, the Raf-1 kinase may also be triggered by PI3K, which puts the MAP kinase pathway under the control of PI3K. Hence, it is possible that only activation of the PI3K pathway is required to trigger all other signals necessary for cell cycle re-entry.

The aim of the work presented in this chapter was to uncover the proteins that are important for cell cycle re-entry of MCF-12A cells, or at least to identify the proteins that are not decisive for cell cycle entry, by a negative exclusion approach. To achieve this, the kinases affected by the inhibitors tested previously were investigated more closely by assaying for their phosphorylation status over time during the discontinuous exposure assay. Keeping in mind the possible crosstalk between pathways, the phosphorylation events were also investigated under the effect of different specific enzyme inhibitors, to reveal the relationships between different kinases. A kinase was considered not to be decisive for cell cycle progression if it was phosphorylated whilst cell cycle progression was not successful.

Additionally we wished to verify the status of key transcription factors that are required for successful cell cycle progression, also as a function of suppressed kinase activity. We were

especially interested in monitoring the c-Myc protein, which was shown to be crucial for cell cycle re-entry of fibroblast cells (Jones and Kazlauskas 2001).

In detail, the objectives of this chapter were

    i.   To confirm the expression of specific key genes and proteins in the MCF-12A cells, as a consequence of the discontinuous exposure to growth factors. The endpoints chosen were:

- The expression of the genes coding for the transcription factor c-Myc and cyclin D1. These were determined by reverse transcription (RT) real-time PCR at different time points in the discontinuous exposure assay.
- Changes in the levels of c-Myc protein expression were assessed by immunoblotting at different time points in the discontinuous exposure assay.
- The phosphorylation state of kinases Src, Erk1/2, and Akt (as the downstream effector of PI3K), at different time points in the discontinuous exposure assay.

    ii.   To confirm that the expression or phosphorylation of these key genes and proteins was indeed a result of the activation of the pathways that had been established before (MAPK, PI3K and PLC pathway), the same endpoints were assessed after treatment of cells with specific inhibitors for MEK1, PI3K or PLC. These specific kinase and lipase inhibitors were added either during the first or the second pulse, and the protein targets described above were assayed. Since activation of the PLC pathway during the second pulse was not necessary for S phase entry (its inhibition did not interfere with cell cycle progression), the impact of the PLC pathway for the second pulse was not examined further.

3 METHODOLOGY

In order to monitor the events that seemed most relevant, the following approach was taken: Cells were rendered quiescent, and then released from the G0 block with the discontinuous stimulation assay, as before. To test the effect of the inhibitors, the cells were pre-incubated with inhibitors in basal medium for 20 minutes at 37°C and then stimulated with the growth factor during each pulse, in the presence of inhibitor. For the analysis of Src, Akt and Erk1/2 kinase activation as a result of the first administration of growth factors, the routine first pulse

of EGF (50 ng/ml) for 30 minutes was not carried out in full length, but lysates were produced 10 min after the addition of the growth factor, in order to assess the early phosphorylation events. Accordingly, the positive control sample (quiescent cells incubated with 50 ng/ml EGF in basal medium) was also lysed after 10 minutes of incubation with EGF. To analyse the phosphorylation status as a result of the second pulse, lysates were produced at different time points after the addition of EGF and insulin. For the positive control sample, cells were lysed at the 6 hour time point (equal to 2 hours after the start of the 2nd pulse).

For the assessment of c-Myc expression, different time points were chosen. These were determined based on the immunoblots where c-Myc was detected over the full length of the discontinuous exposure assay. Since c-Myc is not expressed immediately, the positive control lysate was produced 2 hours after the start of the incubation (when the effect of inhibitors during the first pulse was to be determined), and 6 hours after the start of the incubation in the case where inhibitors during the second pulse were assessed.

To ensure that the bands in the blots were derived from the proteins under investigation, the position of the bands was compared to the molecular size marker added to each gel (cf. Chapter 2). All assays were performed in three independent experiments, but only representative immunoblots are shown.

In parallel to the immunoblotting samples, for each independent experiment one additional sample was incubated according to the standard discontinuous exposure regime (cf. Figure 24) and analysed with flow cytometry as described before. This was performed as an internal control in order to monitor the cell cycle phase distributions when assessing the expression and phosphorylation of aforementioned proteins at the earlier time points. No changes in the percentages of G1 and S+G2+M phases were observed after 18 hours.

4 RESULTS

4.1 Detection of Erk1/2 activity

4.1.1 Activation of the mitogen-activated protein kinases Erk1 and Erk2

As seen in Figure 41, the mitogen-activated protein kinases Erk1 and Erk2 were strongly phosphorylated within 10 minutes of addition of the growth factor EGF during the first pulse of administration. The phosphorylated state lasted for more than 30 minutes, but after 2 hours the activity of the kinases decreased markedly, presumably because the levels of EGF had decreased considerably. Upon incubation with the second set of growth factors (EGF + insulin) at 4 hours after the start of the assay, the kinases were again strongly phosphorylated, but then the activity receded slightly for about two hours. After 7 hours, the kinases showed a sustained activity for several hours, before levelling off towards the end of the incubation.
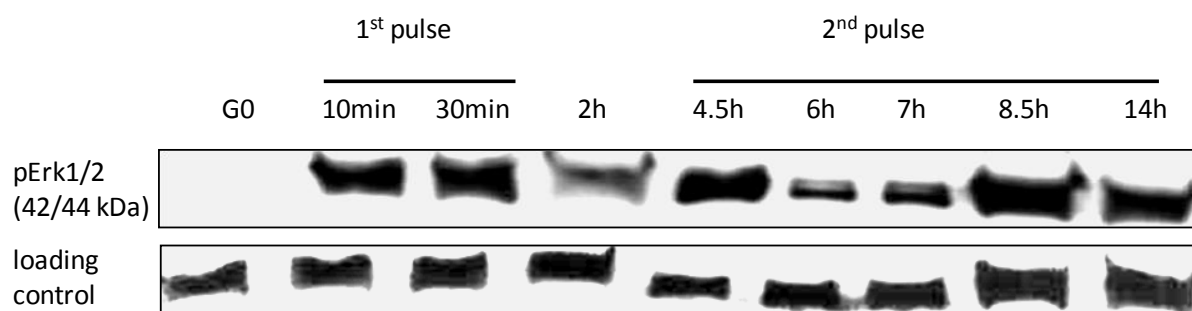
Figure 41 Detection of phosphorylated Erk1/2 over time in the discontinuous exposure assay

Immunoblots of MCF-12A cell lysates were obtained at different time points during the discontinuous exposure assay EGF (50 ng/ml) from 0 to 30 min, EGF + insulin (20 + 100 ng/ml) from 4h to 14h) and assayed against phosphorylated Erk1/2 (upper row). Equal loading of protein was monitored by probing against β-actin (bottom row). "G0" was the negative control sample from quiescent cells, and Erk1,2 activity was not detected in this sample.

4.1.2 Inhibition of MEK1, Src, PLC and PI3K and the impact on Erk1/1 activation

During the first pulse of EGF treatment, application of the inhibitors PD98059 and PP2 led to a complete disruption of Erk1/2 phosphorylation, whereas the inhibitor for the PI3 kinase (LY294002) did not induce diminutions of Erk1/2 phosphorylation (Figure 42). When using U73122, an inhibitor for the phospholipase C, contradictory results were obtained. In one experiment, the effects on Erk1/2 were negligible (Figure 42), but in another independently repeated experiment phosphorylated Erk1/2 could not be detected after administration of the PLC inhibitor (shown in Figure 43).
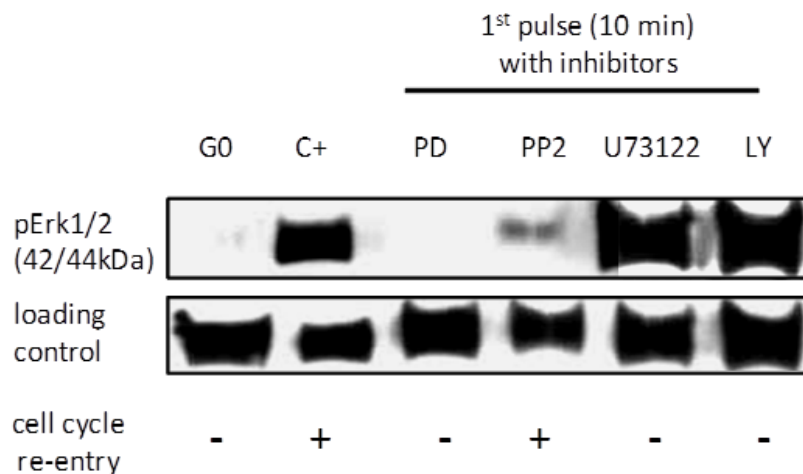
Figure 42 Detection of phosphorylated Erk1/2 after incubation with inhibitors during the first pulse

Immunoblots of MCF-12A cell lysates obtained 10 minutes after the addition of EGF (50 ng/ml) (positive control C+), or EGF in combination with an inhibitor (MEK1 inhibitor PD98059 (PD) at 20 μM, Src inhibitor PP2 at 25 μM, PLC inhibitor U73122 at 1 μM, or PI3K inhibitor LY294002 (LY) at 20 μM). Lysates were assayed against phospho-Erk1/2 (upper row). Equal protein loading was monitored by probing against total Erk1/2 (middle row). "G0" was the negative control sample from quiescent cells where no Erk1,2 phosphorylation could be detected. The bottom row recapitulates the results from the previous Chapter 6 and indicates the effect of the inhibitors on cell cycle re-entry (- = no cell cycle progression, + = successful cell cycle progression).
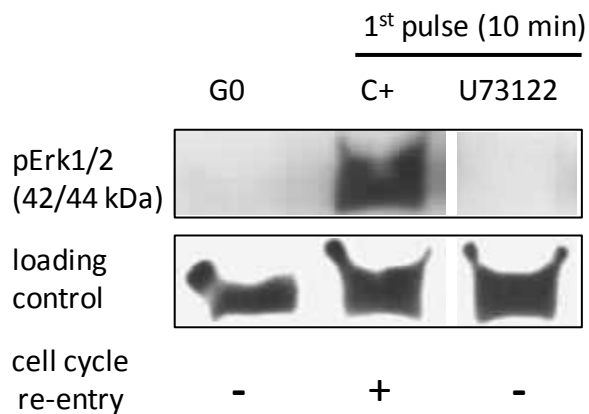
Figure 43 Detection of phosphorylated Erk1/2 after incubation with PLC inhibitor during the first pulse

Immunoblots of MCF-12A cell lysates obtained 10 minutes after the addition of EGF (50 ng/ml) (positive control C+), or EGF in combination with the PLC inhibitor (U73122 at 1 μM). Lysates were assayed against phospho-Erk1/2 (upper row). Equal protein loading was monitored by probing against β-actin (bottom row). "G0 blocked" was the negative control sample from quiescent cells.

During the second exposure to PP2 (Figure 44), when the Src kinase was inhibited, Erk1/2 phosphorylation was not strongly suppressed, but it was lowered considerably at the 7 hour time point. When the PI3 kinase was disrupted with LY294002, phosphorylation of Erk1/2 was weaker throughout the entire exposure time, but still more pronounced than in the quiescent control sample.
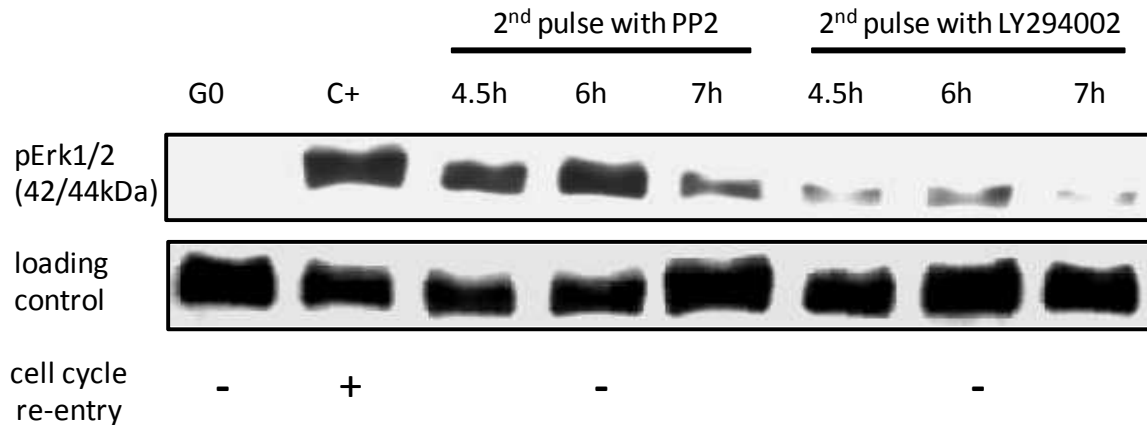
Figure 44 Detection of phosphorylated Erk1/2 after incubation with inhibitors during the second pulse

Immunoblots of MCF-12A cell lysates obtained at several time points after the release from serum-depletion with the discontinuous exposure assay (1st pulse with EGF (50 ng/ml), 2nd pulse with EGF + insulin (20 ng/ml and 100 ng/ml), positive control C+). During the 2nd pulse, the cells were additionally incubated with an inhibitor (Src inhibitor PP2 at 25 μM, or PI3K inhibitor LY294002 at 20 μM). Lysates were assayed against phospho-Erk1/2 (upper row). Equal protein loading was monitored by probing against β-actin (middle row). "G0 blocked" was the negative control sample from quiescent cells. The bottom row recapitulates the results from the previous Chapter 6 and indicates the effect of the inhibitors on cell cycle re-entry (- = no cell cycle progression, + = successful cell cycle progression).

4.2 Detection of Akt kinase activity

4.2.1 Activation of the phosphatidyl-inositol-3 kinase effector protein kinase B (Akt kinase)

The phosphatidyl-inositol-3 kinase (PI3K) phosphorylates directly the Akt kinase, therefore Akt was considered a useful target for monitoring the activity of PI3K. Akt was strongly phosphorylated after the first incubation with EGF, but its activity disappeared completely 2 hours after the start of the incubation (Figure 45). Following the second addition of growth factors at 4 hours, Akt was again phosphorylated strongly, and this activity level was maintained throughout the total exposure time.
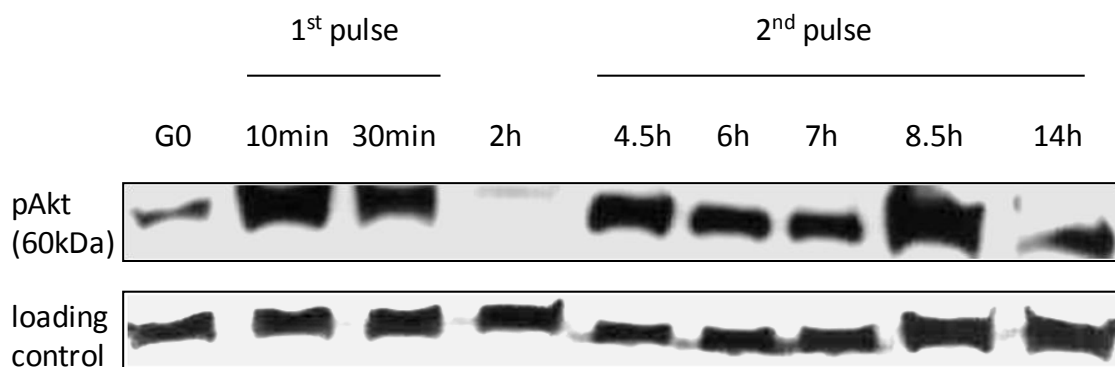
Figure 45 Detection of phosphorylated Akt over time in the discontinuous exposure assay

Immunoblots of MCF-12A cell lysates obtained at different time points during the discontinuous exposure assay (EGF (50 ng/ml) from 0 to 30 min, EGF + insulin (20 + 100 ng/ml) from 4h to 14h). Lysates were assayed against phosphorylated Akt kinase (upper row). Equal loading of protein was monitored by probing against β-actin (bottom row). "G0 blocked" was the negative control sample from quiescent cells.

4.2.2 Inhibition of Src and PI3K and its impact on Akt kinase activity

The phosphorylation of the Akt enzyme during the first incubation with EGF was completely abolished by inhibition of the Src and the PI3 kinases with PP2 or LY294002, respectively (Figure 46). It should be noted that the level of Akt phosphorylation detected in the quiescent cells in some cases was almost as high as in the positive control sample (seen in Figure 46), also in other immunoblots prepared with lysates from independently performed experiments. During the second pulse with mitogens (Figure 47), activation of the Akt kinase could be suppressed by the PI3K inhibitor, but not to levels seen in negative controls, whereas inhibition of the Src kinase did not have a strong effect on Akt phosphorylation at these later time points.
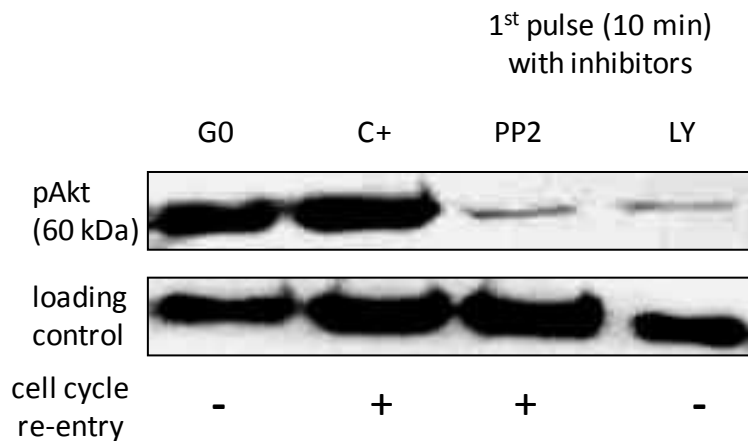
Figure 46 Detection of phosphorylated Akt after incubation with inhibitors during the first pulse

Immunoblots of MCF-12A cell lysates obtained 10 minutes after the addition of EGF (50 ng/ml) (positive control C+), or EGF with one inhibitor (Src inhibitor PP2 at 25 μM or PI3K inhibitor LY294002 (LY) at 20 μM). Lysates were assayed with phospho-Akt antibodies (upper row). Equal protein loading was monitored by probing against total Akt (middle row). "G0 blocked" was the negative control sample from quiescent cells. The bottom row recapitulates the results from the previous Chapter 6 and indicates the effect of the inhibitors on cell cycle re-entry (- = no cell cycle progression, + = successful cell cycle progression).
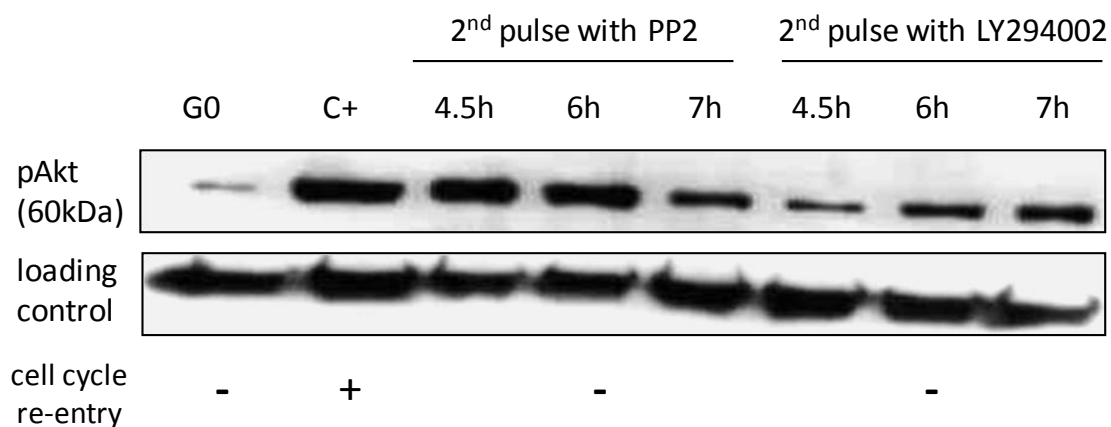
Figure 47 Detection of phosphorylated Akt after incubation with inhibitors during the second pulse

Immunoblots of MCF-12A cell lysates obtained at several time points after the release from serum-depletion with the discontinuous exposure assay (1st pulse with EGF (50 ng/ml), 2nd pulse with EGF + insulin (20 ng/ml and 100 ng/ml), positive control C+). During the 2nd pulse, the cells were additionally incubated with one inhibitor (Src inhibitor PP2 at 25 μM, or PI3K inhibitor LY294002 at 20 μM). Lysates were assayed against phospho-Akt (upper row). Even protein loading was monitored by probing against total Akt (middle row). "G0 blocked" was the negative control sample from quiescent cells. The bottom row recapitulates the results from the previous Chapter 6 and indicates the effect of the inhibitors on cell cycle re-entry (- = no cell cycle progression, + = successful cell cycle progression).

4.3 Detection of Src kinase activity

4.3.1 Activation of the tyrosine kinase Src

As seen in Figure 48, the Src kinase was found to be activated shortly after the addition of EGF in serum-depleted cell populations, and although the phosphorylation decreased after EGF had been washed out, a low level of activated Src kinase was maintained almost throughout the entire experiment. When the second pulse of growth factors was added, the kinase was not strongly phosphorylated immediately, but a significant increase in band intensity after 6 hours was observed (corresponding to 2 hours after the start of the second pulse). The loading of the sample of the following time point (7h) was somewhat reduced, therefore a more pronounced increase at this time cannot be excluded completely. This immunoblot was repeated twice, but the bands were even fainter both times, however, the only bands where an increase compared to the G0 blocked cells was definitely observed in those blots were the 10 min and 6 h time points.
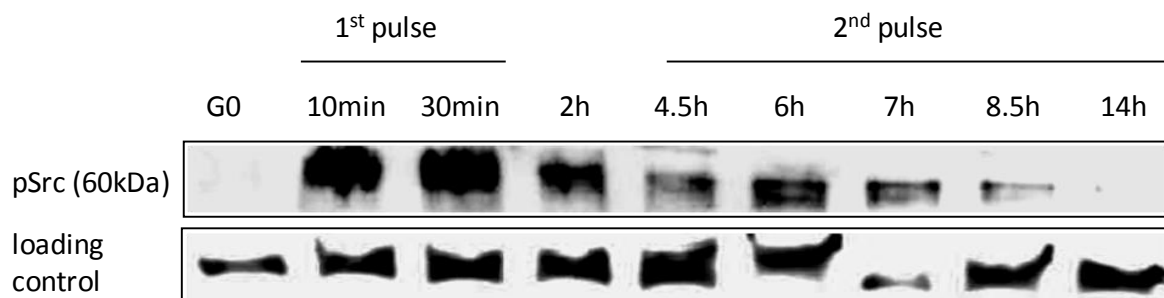
Figure 48 Detection of phosphorylated Src over time in the discontinuous exposure assay

Immunoblots of MCF-12A cell lysates obtained at different time points after the release of cells from serum-depletion with the discontinuous exposure assay (EGF (50 ng/ml) from 0 to 30 min, EGF + insulin (20 + 100 ng/ml) from 4h to 14h). Lysates were assayed against phosphorylated Src kinase (upper row). Equal loading of protein was monitored by probing against β-actin (bottom row). "G0 blocked" was the negative control sample from quiescent cells.

4.3.2 Inhibition of Src and PI3K and its influence on Src kinase activity

Although activation of the Src kinase was detected with EGF (Figure 48), no impact of Src kinase inhibition in the first pulse was seen with flow cytometric analysis of S phase progression (Chapter 6, page 129). Therefore immunoblotting for the Src kinase with inhibitors was carried out only with samples produced during the second pulse of growth factor exposure. The results are shown in Figure 49. When using antibodies against phosphorylated Src, the background was relatively strong in all blots, making interpretation of the results difficult. Nevertheless, it was concluded that the Src kinase was inhibited efficiently by the inhibitor PP2. It was assumed that the slight increase in Src kinase detected after 6 hours despite the presence of PP2 was due to the higher protein amount loaded. But this also demonstrated that the Src kinase was not completely disrupted by its specific inhibitor. With the PI3 kinase inhibitor LY294002, Src kinase activity was not detected at the beginning of the 2nd incubation, but a considerable band appeared at the 6h time point, which disappeared again within one hour.
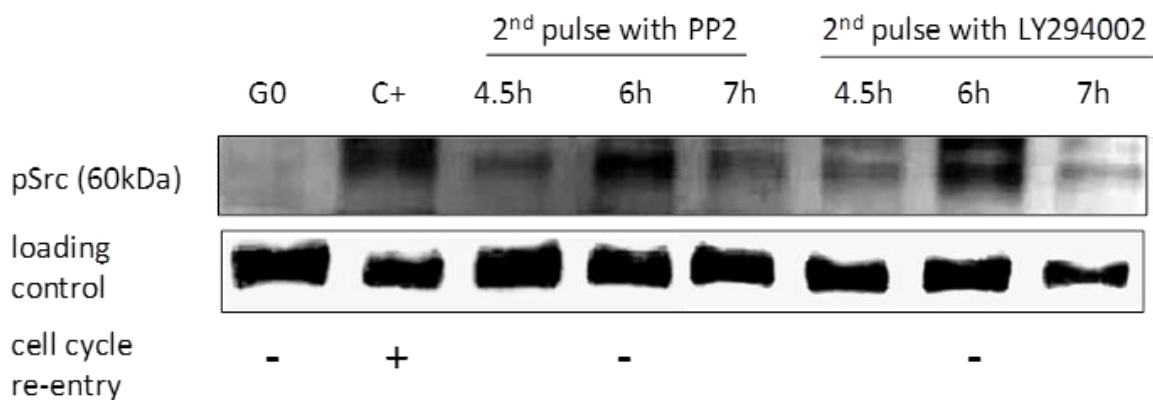
Figure 49 Detection of phosphorylated Src after incubation with inhibitors during the second pulse

Immunoblots of MCF-12A cell lysates obtained at several time points after the release from serum-depletion with the discontinuous exposure assay (positive control (C+) = 1st pulse with EGF (50 ng/ml), 2nd pulse with EGF + insulin (20 ng/ml and 100 ng/ml). During the 2nd pulse, the cells were additionally incubated with an inhibitor (Src inhibitor PP2 at 25 μM, or PI3K inhibitor LY294002 at 20 μM). Lysates were assayed against phospho-Src (upper row). Even protein loading was monitored by probing against β-actin (middle row). "G0 blocked" was the negative control sample from quiescent cells. The bottom row recapitulates the results from the previous Chapter 6 and indicates the effect of the inhibitors on cell cycle re-entry (- = no cell cycle progression, + = successful cell cycle progression).

4.4 The transcription factor Myc

4.4.1 Detection of c-Myc during the discontinuous exposure assay

The protein Myc was detected 2 hours after the release of the cells from the G0 block (Figure 50). This time point coincided with the time when the cells did not receive any growth factors, but when they were kept in basal medium. The amount of synthesised protein then diminished, but was elevated again two hours after the addition of the second growth factor (at the 6 hour time point), and was detected to a similar extent for at least 2.5 hours after administration of growth factors EGF and insulin. However, after ten hours of exposure (during the 2nd pulse), the amount of protein declined again to the negative control levels, despite the fact that growth factors were still present at this moment.
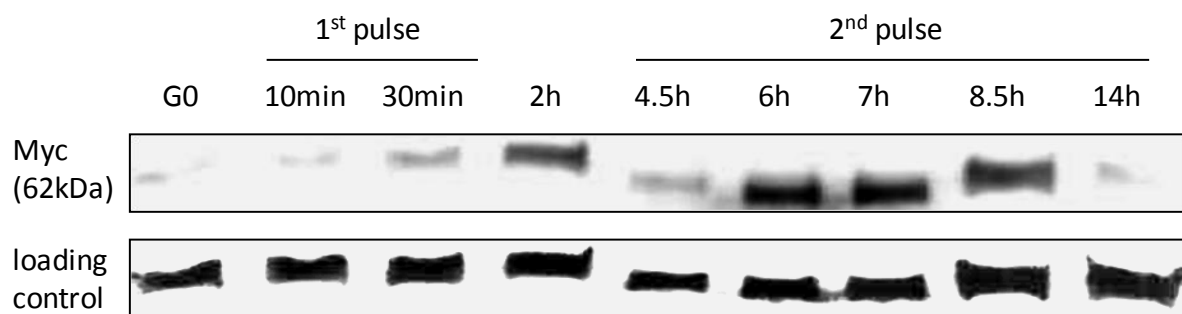
Figure 50 Detection of c-Myc over time during the discontinuous exposure assay

Immunoblots of MCF-12A cell lysates obtained at different time points after the release of cells from serum-depletion with the discontinuous exposure assay (1st pulse with EGF (50 ng/ml), 2nd pulse with EGF + insulin (20 ng/ml and 100 ng/ml)). Lysates were assayed using anti-Myc antibodies (upper row). Equal loading of protein was monitored by probing against β-actin (bottom row). "G0 blocked" was the negative control sample from quiescent cells.

4.4.2 Influence of kinase inhibitors on c-Myc levels

During the first pulse, the synthesis of the c-Myc protein was disrupted with all of the inhibitors tested, PD98059 (PD), PP2, LY294002 (LY), or U73122 (Figure 51). The strongest disruption was seen with the Src inhibitor PP2, followed by LY294002 and U73122, which inhibited c-Myc expression to a similar degree. The weakest effect was observed with PD98059, however, in other immunoblots prepared (assays with all inhibitors were carried out in three independent experiments), it inhibited c-Myc more strongly, as seen in Figure 52.
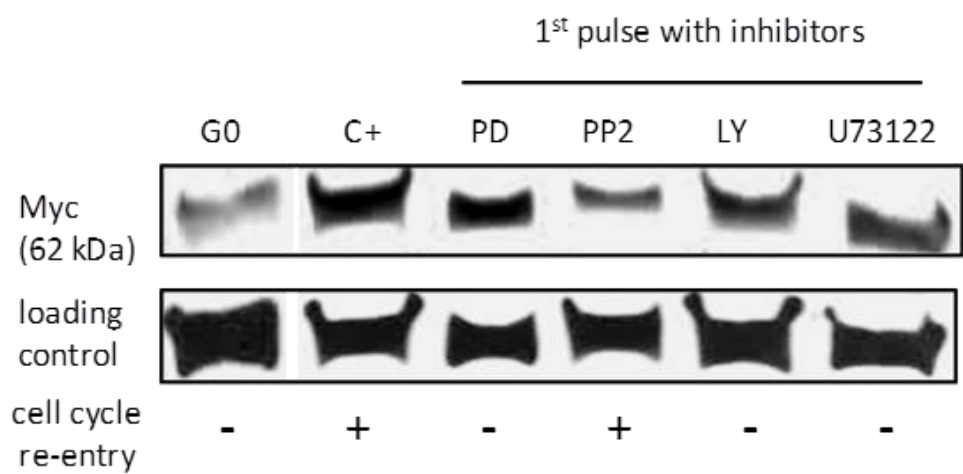
Figure 51 Detection of c-Myc after incubation with inhibitors during the first pulse

Immunoblots of MCF-12A cell lysates obtained 2 hours after the release of the cells from serum-depletion (EGF (50 ng/ml) from 0 to 30 minutes (positive control C+), or with additionally one inhibitor (MEK1 inhibitor PD98059 (PD) at 20 μM, Src inhibitor PP2 at 25 μM, PI3K inhibitor LY294002 (LY) at 20 μM, or PLC inhibitor U73122 at 1 μM). Lysates were assayed against c-Myc (upper row). Even protein loading was monitored by probing against β-actin (middle row). "G0 blocked" was the negative control sample from quiescent cells. The bottom row recapitulates the results from the previous Chapter 6 and indicates the effect of the inhibitors on cell cycle re-entry (- = no cell cycle progression, + = successful cell cycle progression).

Figure 52 Detection of c-Myc after incubation with inhibitors during the first pulse

Immunoblots of MCF-12A cell lysates obtained 2 hours after the release of the cells from serum-depletion (EGF (50 ng/ml) from 0 to 30 minutes (positive control C+), or with additionally one inhibitor (MEK1 inhibitor PD98059 (PD) at 20 μM). Lysates were assayed against c-Myc (upper row). Even protein loading was monitored by probing against β-actin (middle row). "G0 blocked" was the negative control sample from quiescent cells. The bottom row recapitulates the results from the previous Chapter 6 and indicates the effect of the inhibitors on cell cycle re-entry (- = no cell cycle progression, + = successful cell cycle progression).

During the second pulse only inhibitors for the Src and the PI3 kinase were tested, shown in Figure 53, because these were the pathways demonstrated to be most important at these time points. However, neither inhibitor reduced significantly the amount of c-Myc synthesised at the time where it could be detected first (6h, cf. Figure 50). On the other hand, with both inhibitors tested, the bands at the 7h time point were already weaker, compared to the positive control (C+) and compared to the bands observed at 7h and 8.5h without any inhibitor (cf. Figure 50).
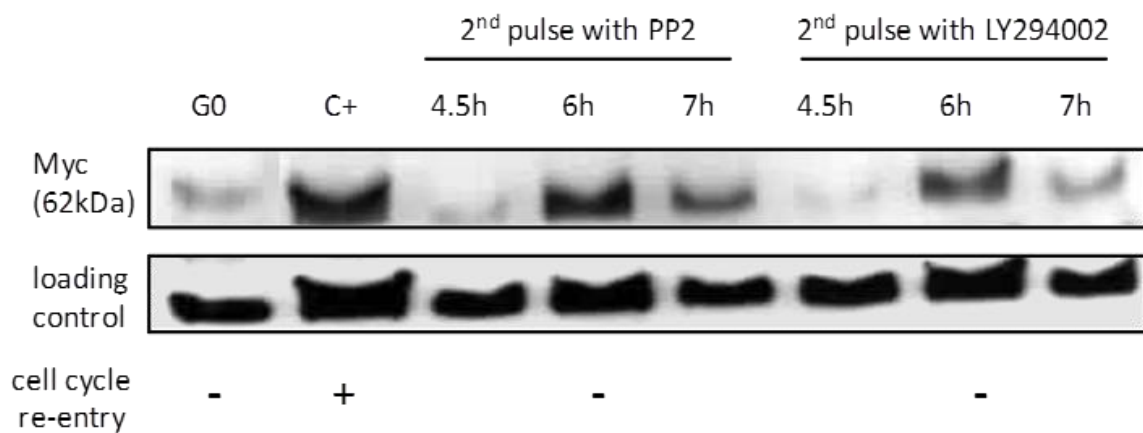
Figure 53 Detection of c-Myc after incubation with inhibitors during the second pulse

Immunoblots of MCF-12A cell lysates obtained at several time points after the release from serum-depletion with the discontinuous exposure assay (1st pulse with EGF (50 ng/ml), 2nd pulse with EGF + insulin (20 ng/ml and 100 ng/ml), positive control C+). During the 2nd pulse, the cells were additionally incubated with one inhibitor (Src inhibitor PP2 at 25 μM, or PI3K inhibitor LY294002 at 20 μM). Lysates were detected with anti-Myc antibodies (upper row). Even protein loading was monitored by probing against β-actin (middle row). "G0 blocked" was the negative control sample from quiescent cells. The bottom row recapitulates the results from the previous Chapter 6 and indicates the effect of the inhibitors on cell cycle re-entry (- = no cell cycle progression, + = successful cell cycle progression).

4.5   Regulation of genes for transition from G1 phase to S phase

4.5.1 Detection of gene coding for transcription factor Myc

Cells were accumulated in the G0 phase through serum-depletion as before, and stimulated to re-enter the cell cycle. This was achieved by adding either complete growth medium to the cells and exposing them continuously (continuous serum stimulation), or with isolated growth factors, added at two distinct times (i.e. by the discontinuous stimulation assay, as described previously). After exposure, RNA was extracted for detection of gene expression. The detected levels were analysed by using Student's *t*-test to determine if they are significantly different from the levels observed in the negative control (G0 blocked cells). Samples that were significantly different from the negative control (G0 blocked sample) are marked with * (P=0.05). As seen in Figure 54, already after the first pulse, the *c-MYC* gene was expressed at levels four times higher than in the quiescent cells. However, this strong induction receded relatively quickly. At 2 hours into the release time, the expression of the gene was not different from the negative control, and at the later time points, the expression was even lower than in quiescent cells. The mode of treatment did not have an influence on *c-MYC* expression; since with continuous serum stimulation, the pattern of gene induction was the same as with the discontinuous exposure assay, except from the 2 h time point, where the gene expression was still slightly increased in serum stimulated cells.
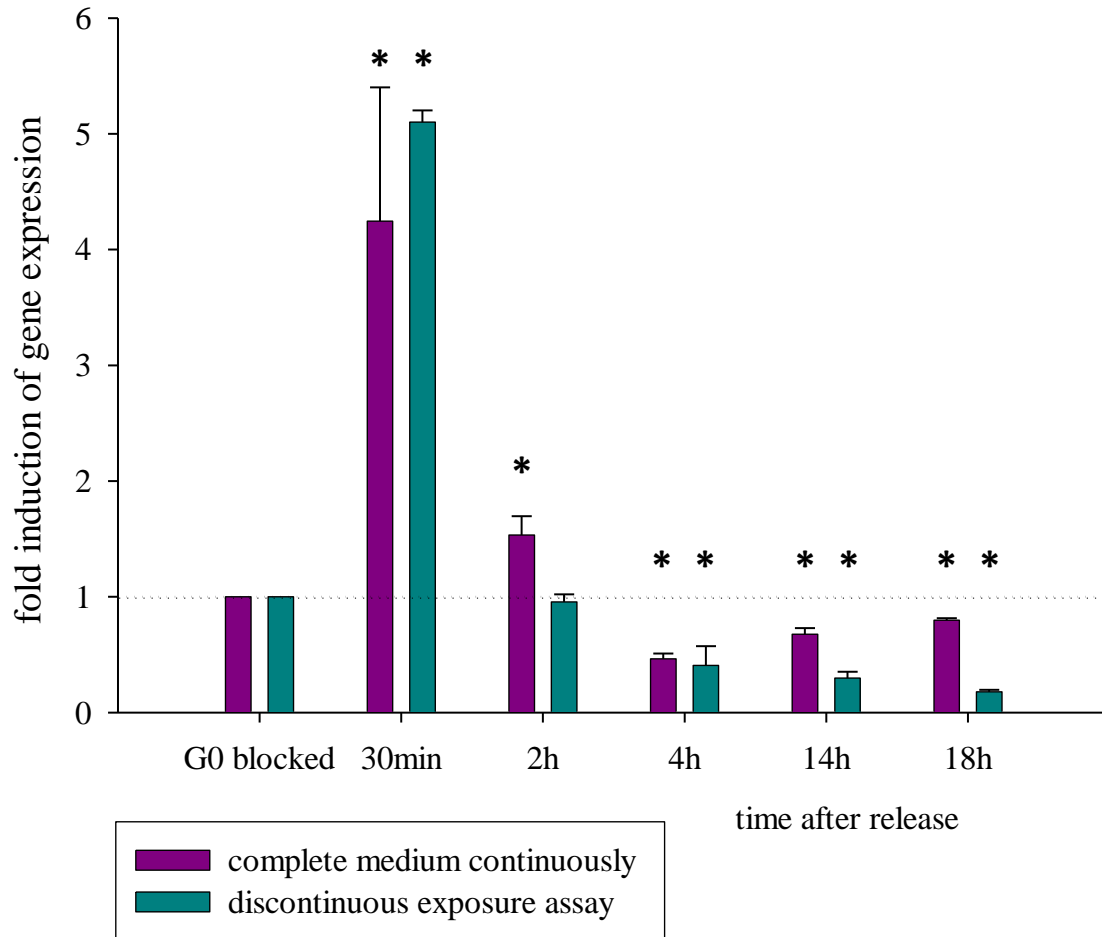
Figure 54 Regulation of the gene coding for Myc protein in MCF-12A cells over time in the cell cycle

Samples of cells were taken at different time points after release from serum-depletion. The gene expression in the negative control sample ("G0 blocked) was set to 1 (dotted line) and used as the control value against which all other results were normalised. Values shown are the mean of three independent experiments; error bars show SEM. Student's *t*-test was performed for significance testing. Samples marked with * are significantly different from negative control (G0 blocked) (P=0.05).

4.5.2 Expression patterns of PRAD1

Expression of the *PRAD1* gene (coding for cyclin D1) showed higher variation between the different time points and between serum stimulated, growth factor stimulated, or quiescent cells than expression of *c-MYC*. Differences between the mRNA levels were tested for their statistical significance with a Student's *t*-test. Samples that were significantly different from the negative control (G0 blocked sample) are marked with * (P=0.05). The induction of *PRAD1* in cells stimulated according to the discontinuous exposure assay became significant after 4 hours, where expression levels four times higher than in quiescent cells were seen. They remained elevated until the end of the assay at 18 hours. Although for the 14 h time point the variation between experiments was high, and therefore the gene expression level was not statistically different from the negative control, a higher absolute mean value than in quiescent cells was observed. In contrast, the continuously stimulated cells showed highly induced expression of *PRAD1* over the entire time, except from the 2h time point, where the mRNA level was not different from quiescent cells. A peak of nine fold induction was reached at the end of the assay (18 hours).

PRAD1
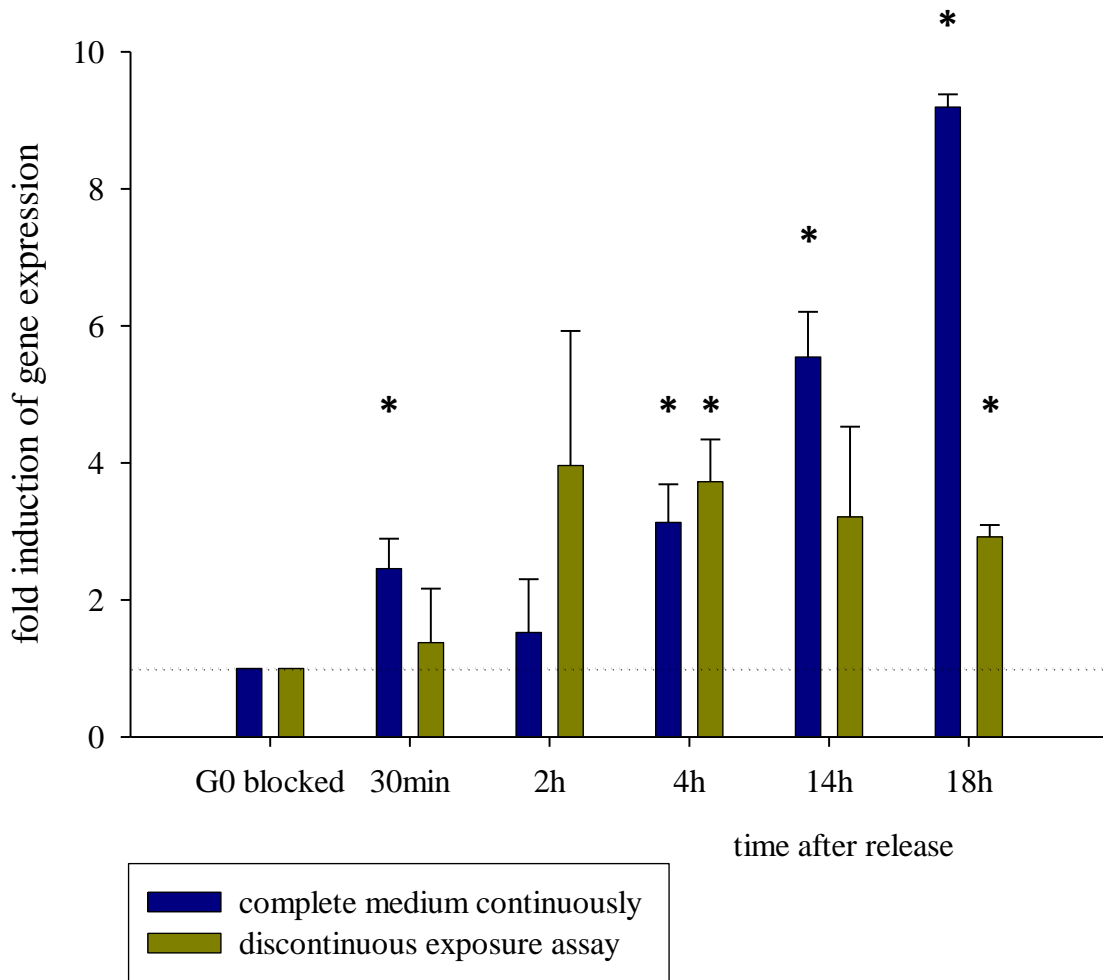
Figure 55 Regulation of the gene coding for cyclin D1 protein in MCF-12A cells over time in the cell cycle

Samples of cells were taken at different time points after release from serum-depletion. The gene expression in the negative control sample ("G0 blocked) was set to 1 (dotted line) and used as the control value against which all other results were normalised. Values shown are the mean of four independent experiments; error bars show SEM. Student's *t*-test was performed for significance testing. Samples marked with * are significantly different from negative control (G0 blocked) (P=0.05).

5 DISCUSSION
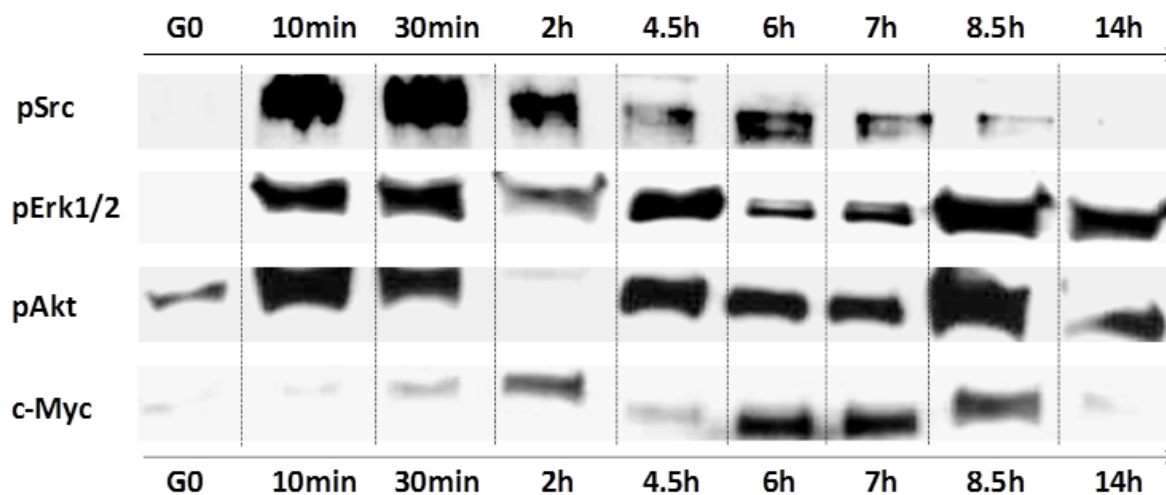
Figure 56 Overview of protein expression and phosphorylation over time in MCF-12A cells

Immunoblots of MCF-12A cell lysates obtained at several time points after the release from serum-depletion with the discontinuous exposure assay (1st pulse with EGF (50 ng/ml), 2nd pulse with EGF + insulin (20 ng/ml and 100 ng/ml), positive control C+). Lysates produced were assayed for the phosphorylation status of Src kinase, Erk1/2 and Akt kinase, or for expression of c-Myc protein. This figure consists of the immunoblots shown in Figure 41, Figure 45, Figure 48 and Figure 50.

5.1 Protein activities during the first pulse of stimulation

The results obtained in this chapter are recapitulated in Table 10, together with the observations made on S phase entry in the previous chapter. The aim of the investigations was to reveal which of the targets examined (pErk1/2, pAkt, pSrc or c-Myc) was decisive for cell cycle progression.

During the first pulse of stimulation, cell cycle re-entry was prevented by the MEK1 inhibitor (PD98059), but does this mean that MEK1 activity was absolutely required for S phase progression? MEK1 activity was also strongly inhibited by the Src inhibitor PP2, but disruption of Src during the first pulse did not prevent cells from entering S phase. From these observations it can be concluded that pErk1/2 was not decisive for cell cycle re-entry. If

it were, then inhibition of Src by PP2 should also have blocked the cells from cell cycle progression.

The links between the different targets observed so far and presented in this and the previous chapter are discussed in detail in this section. The aim was to draw conclusions regarding which proteins are required for cell cycle progression in MCF-12A cells during the first pulse. Alternatively, signalling molecules which can be excluded as being decisive for cell cycle progression were to be pinpointed. A similar matrix was established for the proteins monitored during the second pulse, which is presented further below.

Table 10 Impact of specific kinase and lipase inhibitors during the first pulse on expression and phosphorylation of proteins and cell cycle re-entry

Overview of the results obtained with flow cytometry (transferred from chapter 3) for cell cycle re-entry, and with immunoblotting for the phosphorylation status of Erk1/2, Akt and Src kinase, and the expression of c-Myc, after incubation with specific kinase and lipase inhibitors (MEK1 inhibitor PD98059, PI3K inhibitor LY294002, Src inhibitor PP2, PLC inhibitor U73122) during the first pulse of growth factor administration. nd = not determined.

impact of inhibitor (1st pulse) on:	PD98059	LY294002	PP2	U73122
cell cycle progression	↓	↓	↔	↓
pErk1/2	↓	↔	↓	↔
pAkt	nd	↓	↓	nd
pSrc	nd	nd	nd	nd
c-Myc	↓	↓	↓	↓

5.1.1 The mitogen-activated protein kinases Erk1 and Erk2

The activation of Erk1 and Erk2 was assayed by immunoblotting, and it was shown that they are phosphorylated rapidly after the addition of the growth factors, at both times of stimulation. The initial increase in phosphorylation, after the first pulse, was not sustained, but decreased after 2 hours. The activity during the first pulse (first 30 minutes of incubation) was efficiently suppressed by PD98059, an inhibitor specific for MEK1, which is the main activator of Erk1/2, as well as by PP2, the Src kinase inhibitor. Disruption by PD98059 was

expected, since the MAP kinase kinase MEK1 activates Erk1/2 by phosphorylation of the threonine and tyrosine residues within their activation loop (Pearson et al. 2001). The observation that the Src kinase inhibitor PP2 had a suppressive effect on levels of phosphorylated Erk1/2 became interesting when viewed in the light of the results shown in Chapter 6 where PP2 had little impact on cell cycle progression. Both results taken together mean that the Src kinase had a considerable role in the phosphorylation of Erk1/2, but at the same time, inhibition of Src did not hinder S phase entry. These observations allow the conclusion that phosphorylation of Erk1/2 is not decisive for cell cycle progression in MCF-12A cells. They also suggest that activated Src is not required for cell cycle re-entry. But there are alternative pathways relevant for the transition from G1 into S phase; these other options include the activation of the PI3K and the PLC pathway (both can be activated directly through the dimerised RTK, not involving the Src kinase). Both alternatives are conceivable, when taking into account the results shown in the previous Chapter 6 and Table 10, where inhibition of these pathways during the 1st pulse reduced considerably the number of cells entering S phase. Only the protein kinase B (Akt), being the pivotal member of the PI3K pathway, was investigated with the immunoblotting assays, and the results are discussed in detail below.

5.1.2 The phosphatidyl-inositol-3 kinase effector protein kinase B (Akt kinase)

The expression of the protein kinase B, also termed Akt kinase, was monitored because this kinase is the main effector of the PI3 kinase. The PI3K is activated by receptor tyrosine kinases and holds a key function for triggering cascades that signal for cell cycle progression. Activated PI3 kinase induces cyclin D1 transcription (a key regulator of the G1/S phase transition), mediated by the serine/threonine kinase Akt (Gille and Downward 1999). Additionally, Akt inhibits glycogen synthase kinase 3 (GSK3β), which in turn is an inhibitor of cyclin D1 (van Weeren et al. 1998). When the activation of Akt was assayed with immunoblotting, it showed strong phosphorylation within 10 minutes of addition of EGF. The activity disappeared when the growth factor was removed at the end of the 1st pulse. This means that PI3K was rapidly activated by the EGFR while the receptor was dimerized, and that its activity receded when the ligand was washed out. Phosphorylation of Akt was prevented completely by the PI3K inhibitor LY294002, which was to be expected because signalling from RTKs towards Akt is transmitted predominantly through PI3K. Since inhibition of PI3K with LY294002 hindered substantially cell cycle re-entry (shown by flow

cytometry, as did inhibition of MEK1 with PD98059), it seemed that this pathway was necessary for cell cycle progression; however, inhibition of the Src kinase with PP2 during the first pulse (30 minutes with EGF) disrupted Akt phosphorylation as well, but when the number of cells arriving in S phase was assessed (cf. Chapter 6), no effect of Src inhibition during the 1st pulse had been observed. Thus, these findings reflect the results with the Src inhibitor on Erk1/2 phosphorylation, and also demonstrate that phosphorylation of Akt was not decisive for S phase entry.

It must be mentioned that Akt may be phosphorylated independently of the Src kinase, by binding of the p85 subunit to the EGRF, either directly or via Grb-2, with subsequent activation of PI3K. However, if this activating mechanism was in place during the first pulse in MCF-12A cells, the Akt kinase should have been detected in its phosphorylated state, despite the inhibition of Src.

5.1.3 The Src kinase

The Src kinase was chosen as an endpoint because it is usually associated with the EGFR, and generally mediates signals from RTKs to a multitude of downstream pathways. Assessment of the protein assays for the Src kinase was difficult because of the strong background compared to the bands of interest. Nevertheless, a clearly increased phosphorylation of the Src kinase was observed after 10 minutes of addition of EGF, and the activated state was maintained until the end of the first incubation period, followed by a decrease in activity, albeit not to negative control levels. However, the activity of the kinase at this time seemed of no importance in terms of cell cycle progression, because inhibition of Src during the first pulse had no effect on progression.

5.1.4 The transcription factor c-Myc

c-Myc is a protein important for proliferation and growth, since it increases the expression of proliferative genes, and their transcription into the gene products. This protein was found to be essential for driving fibroblast cells out of quiescence in a discontinuous experimental set-up (Jones and Kazlauskas 2001), and therefore it was of interest to assess its expression in the epithelial breast cells as well. The protein was expressed 2 hours after the start of the assay. Although EGF had already been washed out at this time, it is highly likely that the c-Myc increase was the direct result of the first pulse, because expression of this transcription factor requires at least one hour after growth stimulation. Hence, the timeline found in the MCF-

12A cells for the c-Myc increase is in good agreement with publications from other cell lines (Waters et al. 1991). It also means that the MCF-12A cells did not require constant stimulation with mitogens to produce c-Myc.

During the first pulse of growth factor administration, expression of c-Myc was disrupted by all kinase and lipase inhibitors tested, albeit to different degrees and never to the same extent as seen with serum starvation. The most pronounced effect was observed with the Src kinase inhibitor. Since Src kinase inhibition did not prevent cell cycle progression, this observation suggests that expression of c-Myc after the first pulse was not critical. The inhibition of c-Myc with the PI3K and PLC inhibitors (LY294002 and U73122, respectively) mirrored the results from the cytometric experiments: both inhibitors reduced S phase numbers, but did not prevent progression entirely; likewise, they reduced the expression of c-Myc, but never to negative control levels. In this assay, the smallest effect was seen with the MEK1 inhibitor PD98059, which was unexpected when considering the flow cytometric results (where PD98059 was shown to have the strongest effect on disrupting cell cycle progression). An explanation for the discrepancy between the impact of the MEK1 inhibitor on S phase numbers and on c-Myc expression could be that c-Myc was not the sole transcription factor triggered by the MAPK pathway. Moreover, c-Myc is not induced exclusively by Erk1/2, but also by the PI3K pathway, as well as the PLC pathway.

As with the observation made in the presence of the Src inhibitor, with the other kinase inhibitors it was concluded that expression of the transcription factor after the first pulse is not decisive, although it cannot be excluded that residual activity of the transcription factor was sufficient to induce S phase entry. These deductions may be substantiated by either immunoblotting for the presence of other transcription factors, such as activator protein (AP-1) or STATs, which may be activated by the dimerized EGFR, and by inhibiting c-Myc directly and monitoring S phase entry with flow cytometry.

5.2   Protein activities during the second pulse of stimulation

Table 11 shows an overview of the results obtained with the use of inhibitors during the second administration of growth factors. The impact of the inhibitors on cell cycle re-entry (presented in Chapter 6) as well as on the phosphorylation and expression of the target proteins is shown. The conclusions drawn from our observations are discussed in detail in

this section, with the focus on excluding the proteins from the matrix that are not decisive for cell cycle progression.

Table 11 Impact of specific kinase and lipase inhibitors during the second pulse on expression and phosphorylation of proteins and cell cycle re-entry

Overview of the results obtained with flow cytometry (transferred from chapter 3) for cell cycle re-entry, and with immunoblotting for the phosphorylation status of Erk1/2, Akt and Src kinase, and the expression of c-Myc, after incubation with specific kinase and lipase inhibitors (MEK1 inhibitor PD98059, PI3K inhibitor LY294002, Src inhibitor PP2, PLC inhibitor U73122) during the second pulse of growth factor administration. nd = not determined.

impact of inhibitor (2nd pulse) on:	PD98059	LY294002	PP2	U73122
cell cycle progression	↓	↓	↓	↔
pErk1/2	nd	↓	↔	nd
pAkt	nd	↓	↓	nd
pSrc	nd	↔	↓	nd
c-Myc	nd	↓	↓	nd

5.2.1 The mitogen-activated protein kinases Erk1 and Erk2

During the second incubation period, the Erk 1/2 activity was maintained until the end of the assay, although a slight decrease was observed at 6 and 7 hours. The following time points (8.5 and 14 hours) seemed to feature another (minor) increase in kinase activity, but this may also have been caused by a slightly higher amount of total protein loaded. Only one representative immunoblot is shown, but in every immunoblot performed, the kinase activity was seen strongest directly after the addition of the growth factors in the second pulse, and most likely diminished gradually during the 10 hours of incubation. It is noteworthy that Erk1/2 was reported to be degraded rapidly at the beginning of S phase (Meloche 1995), but in the assays presented here, even at the 14 hour time point (end of second pulse), the kinases were still more phosphorylated than in the negative control.

Several studies documented that upon continuous mitogen stimulation of fibroblast cells, the activation of these kinases is taking place in a biphasic manner, therefore the fact that phosphorylation of Erk1/2 in two distinct waves (Erk1/2 was not continuously in its phosphorylated state) was sufficient for MCF-12A cells to re-enter the cell cycle is in

agreement with these reports (Meloche and Pouyssegur 2007; Kahan et al. 1992). Phosphorylation of Erk1/2 seemed repressed by the Src inhibitor PP2, but only at the latest time point assessed (7 hours), so that it is very likely that this observation instead mirrored the decreased phosphorylation of Erk1/2 at the time points 6 and 7 hours observed in Figure 41, where activity of Erk1/2 was assessed. However, phosphorylation of Erk1/2 during the 2nd pulse was clearly suppressed by an inhibitor specific for the PI3 kinase (LY294002). The inhibition was not total, since there were still bands detected for pErk1/2, whereas in the quiescent cells, no phosphorylation at all was seen. Taking these two observations into account, and considering at the same time that inhibition of Src decreased the percentage of S phase cells further than inhibition of MEK1 (PP2 resulted in S phase numbers equal to quiescent cells, whereas PD98059 resulted in cell cycle arrest of approximately half of the cells), the following conclusions can be drawn:

Firstly, that activation of the MAPK pathway was not decisive on its own for cell cycle re-entry, since S phase induction was disrupted even when MEK1 activity was seen, but contributed to it (since the MEK1 inhibitor PD98059 resulted in a decreased number of S phase cells). Secondly, that MEK1 activity was not triggered by the Src kinase. And finally, the disruption of Erk1/2 phosphorylation by the PI3K inhibitor points towards a crosstalk between the MAP and the PI3 kinases. The mechanisms that could be involved in such a crosstalk are discussed below.

It must be remembered that the PI3K may be activated in different ways. Firstly, the small, regulatory subunit p85 can bind to specific docking sites on the dimerized receptor, which then recruits the larger p110 subunit and completes the enzyme. Additionally, the p85 subunit may be bound indirectly to the receptor, through the Grb2 adaptor molecule which associated with its binder Gab-1. And lastly, an alternative binding through Grb2 is possible as well: Grb2 binds and activates Sos, which triggers Ras. The Ras kinase in turn activates the catalytic subunit (p110) of PI3K, and this independently of the p85 subunit. It is not clear yet if one of these possibilities predominates under specific physiological circumstances (Castellano and Downward 2011; Rodriguez-Viciana et al. 1994). Thus, activity of PI3K may be regulated by Ras, and it was shown that both enzymes together can form a positive feedback loop: initial Ras activation did not require PI3 kinase, but the level of Ras was reduced in the presence of the PI3K inhibitor LY294002, suggesting that Ras was, at least partly, activated by the PI3 kinase phosphate products (Sasaki et al. 2004). Ras in turn is a strong modulator of the MAP3K Raf-1, which activates the downstream effectors MEK1 and

MEK2 and thus the subsequent pathway (Kyriakis et al. 1992). The partial inhibition of the phosphorylation of Erk1/2 in the MCF-12A cells through LY294002, which disrupts the PI3K function, suggests that such a reversed signalling between Ras and PI3K might be in place here, so that the observation was not a direct effect of the kinase inhibition, but rather a result of a disrupted positive feedback loop. On the other hand, some studies have reported that induction of DNA synthesis caused by overexpression of activated MEK1 in quiescent fibroblasts, could be blocked by incubation with the PI3K inhibitor LY294002, used also in the present work, implying that activation of the Erk1/2 pathway induces the synthesis of autocrine growth factors (Meloche and Pouyssegur 2007; Treinies et al. 1999). Unfortunately, with the experimental set-up chosen here, it was not possible to distinguish further between these possibilities.

5.2.2 The phosphatidyl-inositol-3 kinase effector protein kinase B (Akt kinase)

Akt was phosphorylated readily upon addition of growth factors during the 2nd pulse. The phosphorylation of Akt was prevented almost completely with the PI3K inhibitor LY294002, which was to be expected because signalling from RTKs towards Akt is transmitted predominantly through PI3K. Inhibition with PP2 prevented Akt phosphorylation, but only after several hours of incubation during the second pulse. The observation that PI3K was triggered during the second pulse is in good agreement with the flow cytometric data presented in the previous chapter where PI3K inhibition was shown to hinder cell cycle re-entry (Chapter 6). Despite the fact that the inhibitor used acts rapidly to inhibit the targeted Src kinase (within 30min), inhibition of Akt phosphorylation was delayed (an effect comparable to the negative control was observed only at the 7h time point). This suggested that in the first 3 hours of the second pulse, other pathways were important for achieving PI3K and Akt activation, and that this activity was stronger than the suppression of Akt via PP2. Indeed, PI3K may also be activated independently of Src, as was discussed above. It is noteworthy, though, that strong phosphorylation of Akt was noticed occasionally in quiescent cells, pointing towards generally high levels of Akt activity.

Taken together, these observations indicate that the PI3K pathway is triggered following the second stimulation with growth factors, and that this activation was required to promote cell cycle progression, but this was not exclusively exerted via the Src kinase.

5.2.3 The Src kinase

Since the impact of disrupted Src activity on cell cycle progression was determined only during the second incubation in the discontinuous assay (established by flow cytometry, cf. Chapter 6), the effect of Src kinase inhibition with PP2 was assessed only during the second pulse for immunoblotting assays. The addition of EGF together with insulin led to an increase in Src phosphorylation, although not to the same extent as during the first pulse, and the phosphorylated state was maintained only for a couple of hours. The difference in the extent of phosphorylation between the first and the second pulse might be due to the cells being more responsive immediately after the starvation period, and less responsive for Src activation once they had been exposed to an initial stimulus. As expected, incubation with the Src inhibitor PP2 disrupted Src phosphorylation. At a first glance, the PI3K inhibitor seemed to have a similar effect on Src phosphorylation, but most likely the fainter bands were a result of the lower protein loadings, when compared to the loadings for the same time points with the Src inhibitor. This would also be in agreement with the hierarchy in the signalling cascade, where Src kinase is located upstream of PI3K. However, visual assessment of the bands was difficult by the strong background, and digital image analysis would be needed for quantification of the band intensities. It was suggested that for further work, the primary anti-phospho Src antibody should be diluted in TBST-T buffer only, without added proteins such as bovine serum albumin (BSA) or milk powder (cf. Chapter 2), in order to decrease the background on the immunoblots. The Src kinase most certainly holds an important position for S phase induction in the MCF-12A cells, since its inhibition resulted in a complete stop of cell cycle progression, and disrupted severely its downstream target c-Myc. In order to definitely establish the necessity of the Src kinase it must be triggered with a specific activator, that excludes the simultaneous activation of any other kinase, and cell cycle progression should be monitored subsequently.

5.2.4 The transcription factor c-Myc

Compared to the 2h time point, the level of c-Myc protein expression was decreased at 4.5 hours, but elevated again at 6 hours. The exact same pattern of c-Myc expression (band appears 2 hours after the start of growth factor stimulation) was observed during the first pulse. During the second pulse, the c-Myc protein levels faded slowly over several hours, and the protein was degraded entirely before the end of the assay, when mitogens were still present. This is evidence for a finely balanced signalling system where the transcription

factor is degraded after it has served its purpose, and is not synthesised constantly as a consequence of growth factor stimulation.

The inhibition pattern during the second phase was conclusive: at the 6h time point (where c-Myc started to appear when no inhibitor was present), it was detected also in the presence of either PP2 or LY294002 (Src or PI3 kinase inhibitor, respectively), meaning that these two inhibitors did not suppress the expression of the protein, or at least not immediately. However, one hour later the amount of c-Myc was markedly reduced with either inhibitor. Possibly, inhibition of Src or PI3K did not alter the induction of c-Myc synthesis, but it led to a faster degradation of the protein.

Degradation of c-Myc is triggered by its phosphorylation on the threonine residue (Thr58) through the enzyme GSK3β. GSK3β however is inhibited by Akt, once this kinase has been phosphorylated by PI3K. In NIH3T3 cells, the PI3 kinase was active in two phases, one immediately after growth factor addition, and one in late G1, just before onset of DNA synthesis, and the late PI3 kinase regulated c-Myc levels. Inhibition of PI3K at this time increased phosphorylation of c-Myc, resulting in reduced levels of stable c-Myc protein and hence impaired S phase onset (Kumar et al. 2006). In different fibroblasts (murine neuroblastoma cells), the PI3K inhibitor induced post-transcriptional suppression of c-Myc (Chesler et al. 2006). Hence, the delayed inhibition of c-Myc in the MCF-12A cells when the PI3 kinase pathway was disrupted is similar to the network found in fibroblasts, and confirmed the major effect of the inhibitor LY294002 on G1 progression assessed by cytometry. Since inhibition of the Src kinase by PP2 during the second pulse also contributed to a faster degradation of c-Myc, and impaired cell cycle progression, it may be assumed that the second wave of PI3K signalling was mediated partly through the Src kinase, and that this pathway is essential for stabilisation of the c-Myc protein. Our results suggest that c-Myc is decisive for cell cycle progression in the second pulse, but to reach firm conclusions, the impact of direct inhibition of c-Myc expression on S phase entry would need to be assessed.

5.3 mRNA regulation

5.3.1 Regulation of the c-MYC gene

In order to monitor at what time during mitogenic stimulation the mRNA levels of c-*MYC* started to be elevated, analysis of gene expression with RT-real time PCR was performed. Interestingly, induction of mRNA expression took place only once, promptly after addition of

EGF to the quiescent cells. The amount of c-*MYC* gene was increased approximately 5-fold after 30 minutes, declined rapidly to control levels and remained there throughout the remainder of the experiment. This was unexpected since expression of the protein was observed not only at 2 hours after the start of stimulation, but also a second time, after six hours (corresponding to 2h after the start of the second pulse). This result could mean that one or more transcription factors were involved in G1-S transition in these cells, such as activator protein (AP-1) or STATs, as was discussed in section 5.1.4 above. Another explanation could be that the early, but short increase in *c-MYC* was sufficient to induce Myc protein expression over an extended period of time, even beyond 8 hours after the mRNA levels had declined. Although the latter option may seem unlikely, given that the c-Myc protein has a short half-life, the possibility of an extended half-life cannot be ruled out entirely. Indeed, this idea is supported by the fact that for the protein stability to be sustained, signalling from the Ras/Raf-1/MAPK pathway is required (phosphorylation on Ser62 through MAPK stabilises c-Myc), as well as signalling through PI3K/Akt for delaying c-Myc degradation (by inhibiting phosphorylation on Thr58), and both cascades were present at these times in the MCF-12A cells, as shown in Figure 41 and Figure 45. For fibroblast cells it even has been reported that induction of c-*MYC*, together with signalling mediated by Erk1/2, at the very beginning of release from quiescence, was sufficient to drive the cells through the first portion of G1 phase (Jones and Kazlauskas 2001).

In addition to these arguments, the pattern of c-*MYC* mRNA expression was very similar in the populations that were serum stimulated to those that had discontinuous stimulation which confirmed once more that the MCF-12A cells did not require continuous presence of mitogens, but that the discontinuous exposure assay developed in this thesis was successful. Also the time elapsed between growth factor stimulation, increase in mRNA levels and subsequent protein expression was in agreement with published results (Wasylishen and Penn 2010; Chesler et al. 2006; Rosenwald et al. 1993; Wosikowski et al. 1992; Lin and Vilcek 1987; Kelly et al. 1983).

5.3.2 *Regulation of Cyclin D1*

The product of the c-*MYC* gene (c-Myc) is a transcription factor previously demonstrated to be required for cell cycle progression. One target gene for the c-Myc protein codes for cyclin D1 (CCND1). Hence it was interesting to follow the expression of *CCND1*, after the c-*MYC* levels had been monitored.

mRNA for *CCND1* started to be significantly amplified 4 hours after the start of the release from G0 block, meaning that this increase in transcription was a result of the first round of growth factor exposure only. The amount of transcript was augmented further gradually over time, however, the levels found in cells stimulated discontinuously did not match the corresponding induction in serum stimulated cells. There are several explanations for this: cyclin D1 usually is maximal in late G1, and this depends strongly on the activity of PI3 kinase (Gille and Downward 1999). The presence of the phosphorylated kinase in late G1 was confirmed by immunoblotting (Figure 45), therefore another factor must be missing for *CCND1* induction. It is unlikely that the reduced *CCND1* expression was a consequence of the lack of c-*MYC* gene amplification at the later times during G1 phase, because the pattern of c-*MYC* expression was similar in both experimental set-ups, discontinuous and continuous incubation (Figure 54). However, it is possible that one or more other transcription factors are activated in serum stimulated MCF-12A cells, and that these factors were missing in the discontinuous exposure, as was proposed before (cf. section 5.1.4). Candidates for such alternatives would be the activating protein (AP-1) or the signal transducer and activator of transcription (STAT) molecules. STATs are a family of proteins downstream of RTKs such as the EGFR whose up-regulation leads to cell cycle progression, aberrant proliferation and inhibition of apoptosis; notably STAT1 and STAT3 have been shown to be overexpressed in human cancers. STAT3 target genes include cyclin D1 and D3. In order to explore the role of the STATs in MCF-12A cells, analysis of their mRNA expression would be an interesting target, as well as inhibition of STATs (especially during the second pulse) followed by flow cytometric analysis for assessing cell cycle progression.

Clearly, the stimulation of the cells with EGF and insulin during the second pulse did not have the same effect on *CCND1* expression as did stimulation with complete culture medium. It might well be that this difference in *CCND1* transcription was a reason why not in all independent experiments a consistently high percentage of cells was detected in S phase in discontinuously stimulated cells, compared to continuously exposed samples (Chapter 4). Indeed, constitutive activation of D type cyclins had been shown to be sufficient to overcome mitogen requirement (Sherr and Roberts 1999).

5.4   A molecular basis for competence and progression in MCF-12A cells

The objective of this chapter was to examine more closely the events taking place in the MCF-12A cells when they were released from the quiescent state (induced by serum

depletion) into the cell cycle by pulsing them with defined sets of growth factors, as established before and termed *discontinuous exposure assay* throughout this thesis.

The pattern of activity of specific proteins, known to play crucial roles for cell cycle progression, during the discontinuous exposure assay was established by investigating the phosphorylation of Src, Erk1/2, and Akt (to monitor the activity of the PI3 kinase), and the c-Myc protein levels. Next, cells were subjected to inhibition of the kinases Src, MEK1, PI3K, and of PLC, and the same targets (Src, Erk1/2, Akt and c-Myc) were examined. From these results, the following signalling network, depicted in Figure 57 and Figure 58, emerged:

Binding of EGF to its receptor triggered phosphorylation of PI3K and Erk1/2, with and without mediation by Src, as well as PLC. PI3K/Akt, PLC and Erk1/2 signals induced c-Myc, but to achieve this, activation of Src kinase was not required (since inhibition of Src during the first pulse did not disrupt entirely c-Myc protein expression, and did not decrease at all the percentages of S phase cells). *c-MYC* mRNA was up-regulated immediately, and c-Myc protein was expressed swiftly. As a consequence, cyclin D1 mRNA was up-regulated.

At the beginning of the second pulse, Erk1/2 and Akt were phosphorylated strongly. No changes in *c-MYC* mRNA levels occurred, but protein expression increased again 2 hours later and expression levels were sustained, potentially because stabilisation of the c-Myc protein occurred through phosphorylation of Ser62 (mediated by the MAPK pathway, notably Erk1/2) and through inhibition of Thr58 phosphorylation (mediated by PI3K/Akt).

At the same time, Src was phosphorylated, but to a lesser extent than after the first pulse. Disruption of Src during the second pulse did not immediately inhibit phosphorylation of Akt, and expression of the c-Myc protein was not affected extensively. Nevertheless, Src signalling was crucial for subsequent cell cycle progression, as was PI3K activity. The finding that Src inhibition disrupts PI3K activity only partly, but suppresses S phase induction entirely, indicates that the Src kinase triggers other kinases as well that contributed to cell cycle re-entry. Additionally, it should be considered that two independent mechanisms of PI3K activation are in place, first through the direct binding of the p85 subunit to the RTK, and the indirect activation of PI3K through binding of the p85 subunit to Src. This consideration is further supported by the observation that PI3K was phosphorylated promptly, whereas the Src kinase itself was not activated immediately (strong phosphorylation was observed only two hours after the start of the second pulse). Hence disruption of Akt phosphorylation by the Src inhibitor could only be observed after the time points where Src

itself has been activated. However, the studies presented here did not allow it to determine which mechanism of PI3K activation was more prevalent in the MCF-12A cells.

One striking difference between the importance in the first and in the second pulse of the proteins monitored was that PLC activity during the first administration was crucial for cell cycle re-entry, but not during the second pulse, whereas Src activity was not required during the first pulse, but essential during the second pulse. Regarding PLC, it has been reported that its activity is induced within minutes following growth factor stimulation in quiescent NIH3T3 cells, and peaked after 2 hours of continuous stimulation, dropping markedly after 4 hours. Moreover, PLC activation as a contributor to cell proliferation was shown to be under the control of the (growth factor induced) MAPK pathway (Manzoli et al. 2005 and references herein; Ramoni et al. 2004; Manzoli et al. 1997). Considering that these observations were made in fibroblast cells, it is possible that PLC inhibition during the second pulse did not impact cell cycle progression in our epithelial cells, because this pathway was not active anymore, perhaps because the MAPK pathways had also become less important for S phase progression at this time. As for the Src kinase, a first approach would be to quantify the bands of total and phosphorylated Src kinase, comparing between the first and the second pulse, in order to investigate if the divergence in the importance of the kinase was due to less protein being phosphorylated as a result of the short first stimulation. It may also be considered that simultaneous exposure of the MCF-12A cells to insulin and EGF had a more important effect on Src activation than EGF alone, since one publication describes that upon stimulation of MCF-7 epithelial cells with insulin-like growth factor II, the Src kinase associated with the IGF-IR, followed by a cross-activation of the EGFR (Jones et al. 2006; Knowlden et al. 2005). In order to verify such a crosstalk in MCF-12A cells, stimulation with EGF only in both pulses needs to be performed (which also resulted in a high percentage of S phase cells, cf. Chapter 4), monitoring the activity level of Src kinase.

In summary, the observations made with the discontinuous exposure assay were consistent with other studies showing that even when cell cycle progression was achieved by continuous exposure to mitogens, the signalling events took place at two distinct times. This was reported mainly for PI3K which induces one early wave of signalling and a second wave in late G1 (Kumar et al. 2006; Balciunaite et al. 2000; Jones et al. 1999). Based upon this, Kazlauskas' group suggested a "two wave" hypothesis: a first, short (< 60 min) exposure to mitogens makes the cell *competent*, that is, it initiates the cell to leave the G0 state to progress into the early phase of G1. At this time, the cell needs a second mitogenic input that

results in elevation of cyclins and *progression* through late G1 into S phase (Jones and Kazlauskas 2001). The signals that drive cells through one or the other part of G1 are not necessarily mutually exclusive, as shown by Jones and Kazlauskas (2001). For example, MEK activity was required during both growth factor pulses for successful DNA synthesis, and c-Myc protein was expressed at two distinct time points in fibroblasts (Jones and Kazlauskas 2001). However, input from the signals must be temporally coordinated to provide the correct protein and lipid products at the right time. This explains why the intervening time between the two pulses of growth factor administration may not be extended infinitely. In fibroblast cells, the second growth factor was administered 8 hours after the first, but the longer the two pulses were apart, the fewer cells were able to progress into S phase. Indeed, the later wave of c-Myc protein expression was observed at 9h, shortly after the start of the 2nd pulse, whereas in continuously PDGF-stimulated cells, c-Myc was expressed after 6 hours already (Jones and Kazlauskas 2001). Taking together these observations, they suggest that c-Myc needed to be available at a certain time during the cell cycle for successful G1 progression, and that cells were unable to process the signals from the c-Myc protein if it was expressed too late. (To support this assumption one would need to monitor c-Myc expression in the fibroblasts under the conditions of a delayed second pulse). In the MCF-12A cells, it was shown that the resting time between the pulses may be up to six hours long for successful cell cycle re-entry, although higher S phase numbers were yielded with a shorter intervening time of four hours, which accordingly was chosen for the routine regimen (Chapter 4). The observations that the intervening time could not be extended to more than six hours and that c-Myc protein was strongly expressed at 6h (and could already be detected at 4.5h), was not only in excellent accordance with the results from fibroblasts; they also imply that similar to fibroblast cells, the mammary epithelial cells required c-Myc protein during a defined time frame to be able to progress through G1, whereas rapid degradation of the c-Myc (unstable protein due to PI3K inhibition), or lack of the late wave of protein expression altogether (due to the absence of a second pulse of growth factors), meant that the cells were not able to take the signals from the first pulse further. An appropriate experimental set-up to substantiate this would be to monitor c-Myc protein expression in MCF-12A cells that are continuously stimulated, as well in discontinuously exposed cells where the intervening time is prolonged. Despite the lack of such confirmation, it could be concluded that the results shown in this chapter, taken together with the observations presented in the previous chapters, make it plausible that a *competence / progression* system was in place also in the MCF-12A cells.
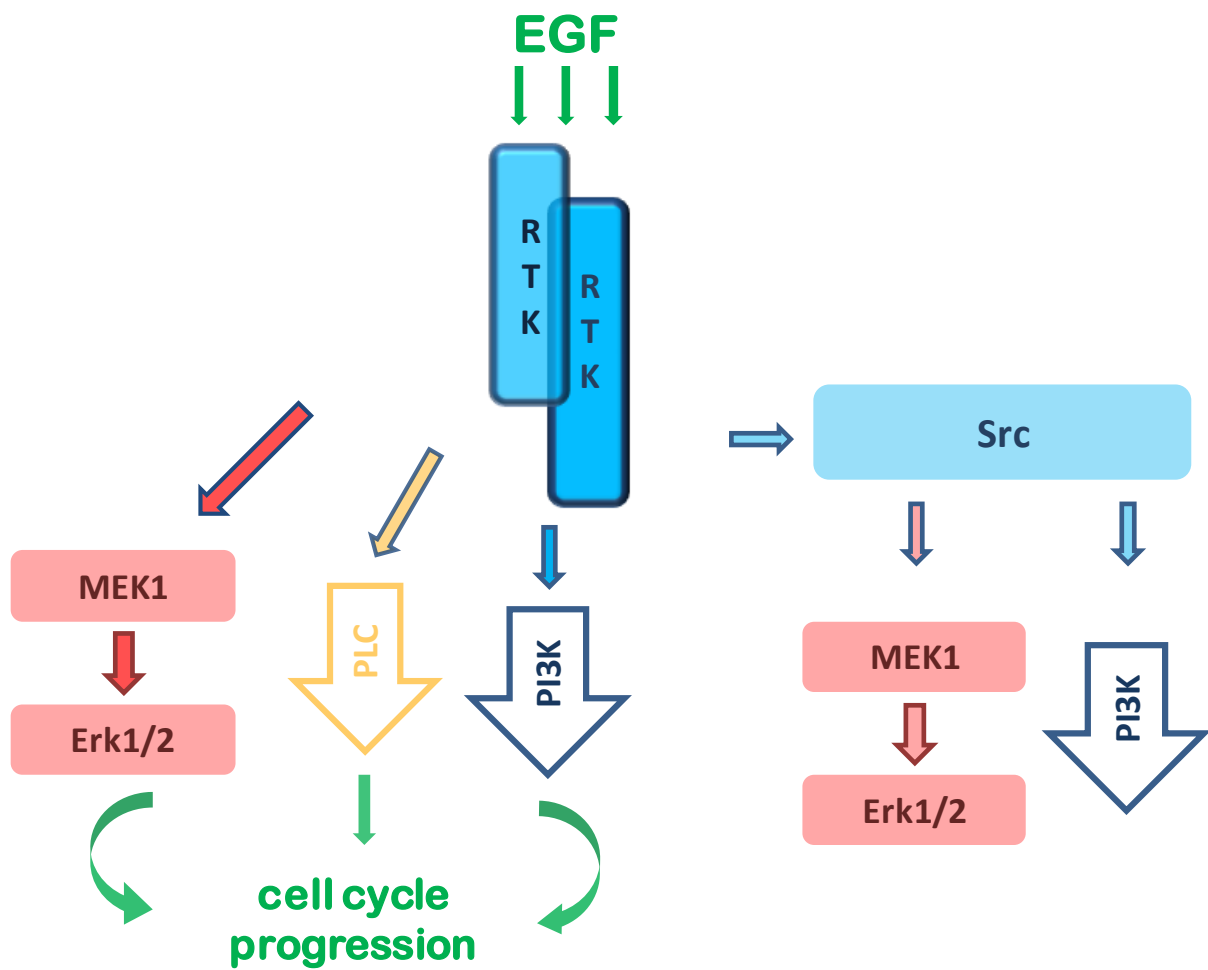
Figure 57 Schematic representation of signalling pathways activated in MCF-12A cells during the first pulse of growth factor administration

The kinases shown on the left side all contributed to cell cycle progression, although none of the three pathways examined (MAPK, PI3K and PLC) was decisive for cell cycle progression. The kinases shown on the right hand side of the diagram were also activated, as seen by immunoblotting; however, their disruption did not affect cell cycle progression.
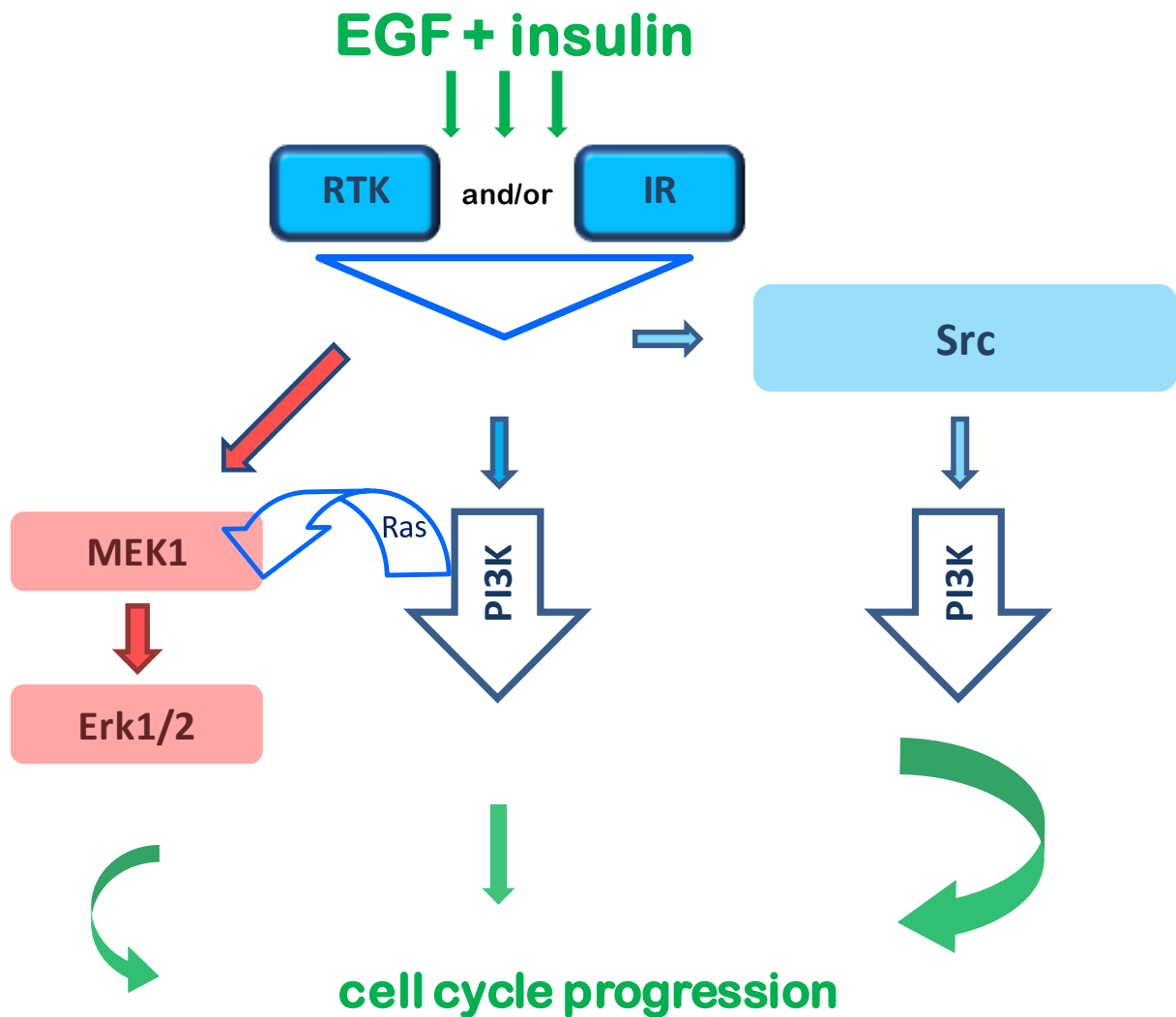
Figure 58 Schematic representation of signalling pathways activated in MCF-12A cells during the second pulse of growth factor administration

The EGRF and the IR, activated by EGF and insulin, respectively, triggered the MAPK and PI3K pathways, as well as the Src kinase, which activated PI3K additionally. All kinases added to cell cycle progression, but only the Src kinase was determined to be vital. It is suggested that the PI3 kinase contributed to MEK1 activity by a positive feedback loop via the Ras kinase.

6 CONCLUSIONS

A different set of proteins was activated with the first incubation with growth factors than after the second pulse. The first pulse resulted in strong phosphorylation of Erk1/2, Akt and Src, and c-Myc was expressed in a delayed fashion (2 hours later). The second pulse led again to an immediate phosphorylation of Erk1/2 and Akt, whereas Src was activated considerably later. Expression of c-Myc was delayed as well, as before. We could conclude that not all activated proteins were indeed required to induce the cell cycle, but selective activation, as well as protein quantification is needed to study the exact contribution of each kinase.

Chapter 8:
Summary

The objective of the work presented here was to investigate signals that are activated for cell cycle progression in normal mammary epithelial cells. This is of great importance, since it has been recognised that the vast majority of all breast cancers originate in the mammary epithelium. In the epithelium, the neoplastic cells initially are retained in the milk ducts by normal epithelial cells, and may even be reverted back to un-transformed states through signalling from the normal cells. The signalling in normal cells controls cell cycle progression, proliferation, and differentiation, and these features are of relevance for sustaining the protective barrier in the mammary epithelium. In order to better understand why this shield fails in tumorigenesis, it is necessary to better define the proliferative signals emitted by normal epithelial cells. The basic process for proliferation is cell cycle progression, which is regarded as successful when the R point is passed. The R point is defined as the hyperphosphorylation of the Rb protein, occurring up to several hours before entry into S phase. Previous research has shown that the passage of the R point does not require constant exposure to growth factors, but that proliferative signals are accumulated over time, resulting eventually in sufficient phosphorylation of the Rb protein. The accumulating signals are transmitted through cascades which form a complex network of kinase activities, triggered by a plethora of growth factors present in the culture medium. The networks in place for controlled proliferation need to be studied level by level and they can only be dissected if the effectors at the very top of the cascade are well defined as well.

As a model for the normal human mammary epithelium, we chose the MCF-12A cell line. This cell line is not used widely and comparatively little is known about its receptor phenotype and the signalling pathways initiated from there. Cell cycle re-entry was induced with defined growth factors, with the aim to elucidate these aspects: the role of three major pathways (MAPK, PI3K and PLC) for cell cycle progression was investigated closely by monitoring the kinases Akt, Erk1/2 and Src, as well as c-Myc and cyclin D1, and the impact of the endogenous hormone estradiol on estrogen-regulated targets was assessed.

1 MAIN CONTRIBUTIONS

In order to study in detail the cell cycle progression in MCF-12A cells, an assay was developed which first induced quiescence by serum depleting the cells for 24 hours, and then released the cells into S phase by exposing them to complete culture medium.

Entry into S phase was monitored with flow cytometry, and the acquired data was analysed using initially three different methods of cell cycle analysis (automated analysis based on the *Dean-Jett-Fox* algorithm, the *Watson* algorithm, or manual analysis), in order to determine the most suitable approach. A systematic comparison between these methods was then performed and showed that cell cycle specific software with an embedded algorithm based on the *Watson* model consistently gave higher percentages for the fraction of cells that make up the S and G2+M phase peaks than when the frequency histograms were analysed by the user (i.e. setting the gates between the cell cycle phases manually). However, the differences between these two approaches were statistically not significant. On the other hand, results obtained following analysis with an algorithm based on the model according to *Dean-Jett-Fox* were shown to be skewed. This led us to conclude that the *Dean-Jett-Fox* algorithm was not suitable for the work presented here.

Having established that the automated analysis using software with an embedded *Watson* algorithm was the most suitable method for our purpose, a discontinuous exposure regimen to induce cell cycle progression was put in place, which enabled us to determine a set of defined growth factors sufficient for cell cycle re-entry. In detail, the quiescent cells were stimulated with a first pulse of EGF, lasting for 30 minutes, after which the cells were left without any growth factors. The second pulse started 4 hours later and consisted of a combination of EGF with insulin, incubating for 10 hours. At the end of the second pulse, cells were left again without any growth factors for 4 hours, to give them time to progress into S phase. The total length of the assay therefore added up to 18 hours, which had been determined beforehand with continuous serum stimulation to be a reasonable time point to assess cell cycle re-entry. With this discontinuous assay we saw as many cells progress into S phase as after continuous exposure to complete growth medium. The precise timing of the discontinuous exposure assay, as well as the use of defined growth factors and the sequence in which they were administered, enabled us to study the important signals for progression out of quiescence and through G1 into S phase.

First of all, the significance of the two distinct pulses was assessed, and it was found that both pulses were required for full competence of the MCF-12A cells to progress into S phase, although the first pulse was considerably shorter than the second pulse. Omission of the first pulse resulted in a significant reduction of the number of cells able to leave the quiescent state, with around one third fewer cells found in S phase at the end of the assay time.

Next, we wanted to analyse whether the sequence of administration of different growth factors was important for S phase progression. Indeed, it was found that the combination of insulin in the first pulse and EGF in the second pulse resulted in a significant number of cells re-entering the cell cycle. The converse sequence, however (1st EGF, 2nd insulin), was not able to bring cells out of quiescence. One could argue that this result may be due to the second pulse being much longer than the first incubation, however, as was established above, both incubation periods were required by the cells. Moreover, when E2 was applied instead of a growth factor during the first pulse, and the cells were stimulated with EGF+insulin during the following longer administration, they were unable to exit the quiescent state. Hence, it seemed that the signals responsible for cell cycle progression needed not only to be switched on, but moreover to be triggered in a specific order.

An additional aim of the work with estradiol was to examine its effect on the regulation of proliferative genes. Estradiol is an endogenous hormone of the estrogen family which has an important function for the development of the mammary gland in general, but especially for the fate of epithelial cells. However, the role of estradiol in the MCF-12A cell line is not yet well characterised. PCR analysis of genes that, in human mammary cancer epithelial MCF-7 cells, are typically regulated by this steroid hormone showed that the proliferative genes *MYC* and *PRAD1* were not induced by estradiol, whereas EGF resulted in an increased expression. This was in line with the observations made on cell cycle progression. We also investigated genes that are under the control of the estrogen receptor ERα (*PGR*, *TFF1*, *BRCA1* and *ESR1*), but none of them was significantly altered after estradiol exposure. It has been suggested in the literature (Anderson 2002; Clarke et al. 1997) that estrogen-induced proliferation of breast epithelial cells is a sign of transformation, and our results support this hypothesis. It has become clear, that the molecular mechanisms involving the ERα are not the same in the MCF-12A cells than in other ERα$^+$ breast epithelial cells, such as the MCF-7 cells. Possibly, the relocation of the ligand-bound ER towards the ERE situated in the promoter region of target genes is disrupted, and the lack of effect of E2 on the regulation of

genes displaying an ERE may be explained by such a defective mechanism between the receptor and the responsive element.

Next, we sought to identify the signalling cascades that are triggered when the MCF-12A cells were stimulated to cell cycle re-entry. Cells were initially exposed to EGF for 30 minutes, after which the growth factors was washed out and cells were kept in basal medium until the beginning of the subsequent pulse. This ensured that during the first pulse, only EGFR was activated. Experiments with specific inhibitors for MEK1 (activator of the MAP kinases), PI3 kinase, Src kinase and PLC indicated that the signalling through EGFR in the first pulse was mediated through three pathways, the MAPK, the PI3K and the PLC pathways, and that all these pathways were employed to a similar extent. Surprisingly, the Src kinase did not seem to be involved in signal transduction from the EGFR to MEK1 or PI3K, suggesting that signalling from the dimerised EGFR to these two kinases was mediated entirely through the adaptor molecules Shc and Grb2.

During the second pulse, which lasted 10 hours, the cells were exposed to EGF and insulin. Tests with the same specific inhibitors as for the first pulse revealed that in this phase signalling through PI3K prevailed. The MAP kinase pathway was also triggered, albeit to a lesser extent than PI3K, whereas the PLC pathway had a minor role. Interestingly, inhibition of the Src kinase at this time resulted in an almost complete disruption of cell cycle progression. Several explanations for this difference to the function of Src during the first pulse can be considered: Firstly, it could be that the activation of the Src kinase was entirely triggered through the insulin receptor, which is ligand bound during the second, but obviously not during the first pulse. Interaction between insulin receptor substrates (IRS) and Src indeed has been shown in several cell lines, although not in epithelial cells. The second possibility would be that EGFR indeed triggered Src kinase, but only during the second pulse and not during the first. Even though such a selective (time dependent) association between these two kinases seems rather unlikely, it should not be ruled out entirely because the MCF-12A cells could be stimulated to cell cycle progression when exposed exclusively to EGF in the discontinuous assay (using a higher concentration of EGF during the second pulse when insulin was omitted).

Subsequently, activation of these kinases as a result of growth factor stimulation was confirmed with immunoblotting. In contrast to the flow cytometric analysis, where S phase entry was assessed only at the end of the assay, the phosphorylation status of the kinases was

monitored at several time points during the exposures. It was found that Erk1/2 as well as the Akt and Src kinases were phosphorylated readily upon addition of EGF during the first pulse, but the activated status was not sustained. Inhibition of Src reduced induction of these kinases, which suggested that upon Src inhibition, the cells were still able to trigger the MAPK and PI3K pathways to a sufficient extent, because Src disruption did not reduce the number of cells progressing into S phase. All kinases (Src, Erk1/2 and Akt) were again phosphorylated upon incubation with the second set of growth factors. This time the observations made with Src inhibition were in accordance with the flow cytometric results, as it resulted in disruption of Erk1/2 and Akt activation. Src itself was also phosphorylated as a result of stimulation with EGF and insulin.

Additionally, the protein and gene expression of the transcription factor c-Myc was examined. The protein was detected with a delay of approximately 2 hours after the start of each pulse, and was degraded during the incubation time of the second pulse, albeit the continued presence of growth factors. The expression levels of c-Myc mRNA were in good agreement with this observation, peaking 1.5 hours before the protein was first detected. However, the mRNA levels stayed low afterwards, albeit the renewed increase in protein levels during the second pulse. This was surprising, but the same observation was made in cells that were continuously exposed to complete growth medium (containing serum), suggesting that c-Myc protein indeed required only one initial stimulation to be fully expressed.

One more factor that was monitored on the gene expression level was cyclin D1, which must be elevated for successful transition from G1 into S phase. The mRNA levels of cyclin D1 lacked a sharp increase during the discontinuous exposure assay, but showed a significant raise in cells stimulated continuously. This result suggested that discontinuous exposure was not sufficient to induce this mitogenic gene to its full extent, but more importantly, that the cells were able to compensate to a large extent for this.

The initial idea to develop a discontinuous exposure assay for the MCF-12A stemmed from a publication by Jones and Kazlaukas (2001) who showed that fibroblast cells rendered quiescent were able to enter the cell cycle upon triggering of specific factors at distinct time points (Jones and Kazlauskas 2001). More precisely, they showed that the initial phase of signalling required activation of MEK and c-Myc, whereas the PI3K pathway dominated the second pulse. The authors hypothesised that any mitogen that triggers the named factors

would be able to drive quiescent cells into the cell cycle, and that there is a common signalling cascade by which growth factors elicit such a response.

As for the PI3K signalling during the second phase of stimulation, we were able to confirm the importance of this pathway for cell cycle progression of MCF-12A cells. The fact that it was activated by a different set of growth factors (EGF+insulin vs. PDGF used for the fibroblast cell line NIH3T3) supports further the aforementioned hypothesis. However, it is worth remembering that inhibition of MEK1 during the second pulse also markedly disrupted S phase entry of MCF-12A cells. Therefore, the signalling important at this time point for cell cycle progression, at least of MCF-12A cells, cannot be restricted to a single pathway.

Focusing on the factors activated during the first pulse, we found an up-regulation of *MYC*, followed by an increase in the protein expression of the transcription factor c-Myc, as a result of the exposure to EGF. Similar to in the NIH3T3 cells examined by Jones and Kazlauskas (2001), we showed that the activation of MEK1 in the initial wave was crucial for S phase entry of MCF-12A cells. In order to verify that triggering these two factors, MEK1 and c-Myc, was indeed sufficient to drive the cells through the first portion of G1 phase, it may be envisaged to assess other (growth) factors that are able to induce these two proteins in the MCF-12A cells. These (growth) factors should then be interchangeable with one another for the administration during the first pulse.

The order in which the proteins are required for cell cycle progression, could hence explain why a specific sequence of growth factors was unable to render cells competent for entry into S phase, such as the combination of EGF (1st pulse), followed by insulin (2nd pulse), as discussed above. This result suggests that insulin is not capable of activating fully the PI3 and the MAP kinases, but on the other hand it seems sufficient to induce MEK1 as well as expression of c-Myc. This hypothesis is further supported by the results obtained with E2 (administered during the first pulse), followed by an exposure to EGF+insulin, which did not induce cell cycle re-entry. Indeed, we saw that E2 had no effect on the *MYC* gene, of which an up-regulation would be needed to increase the expression of the transcription factor c-Myc.

One other aspect to consider when discussing the role of c-Myc is the degradation of this protein, which was completed before the end of the second pulse, when EGF and insulin were still available. This demonstrated that c-Myc is required at specific times only to support successful cell cycle progression, and does not need to be expressed constantly. We speculate

that this protein is one of the decisive factors why the intervening time between the two pulses cannot be stretched beyond 6 hours, in accordance with the competence/progression system described by Jones and Kazlauskas in 2001 (Jones and Kazlauskas 2001). This model proposes that the initial administration drives cells through the first portion of G1 phase, but most importantly renders them responsive to further stimulation. Then they require a second mitogenic input which enables them to actually progress into S phase. However, their responsiveness declines over time, and eventually the cells return to the quiescent state. Therefore, if the second stimulus is received too late, it will have no effect on the cell cycle. It may be that the MCF-12A cells require a certain amount of c-Myc protein to remain responsive, and if the expression falls below a certain threshold, e.g. by constant degradation after the first pulse, they are unable to compensate for this during the second administration.

1.1 Limitations

Conclusions drawn from the effect of specific kinase inhibitors, as well as from the immunoblotting assays for detection of kinase activities, were based on results obtained with the standard discontinuous exposure assay, developed for the work presented here. This assay used EGF and insulin as growth factors, but the importance of insulin to the overall outcome remained undetermined, since it was shown that EGF only in both pulses had a similarly strong mitogenic effect on the MCF-12A cells as the mixture of growth factors. Thus, if some key experiments were carried out with EGF as the sole growth factor, the role of insulin for mitogenic signalling in these cells may become clearer.

Although the use of specific inhibitors for MEK1, PI3K and Src contributed to the finding that activation of the Src/PI3K pathway during the second pulse was indispensable for cell cycle progression, the function of the Src kinase during the first pulse remained ambiguous, because it was shown to be phosphorylated after the first stimulation, but its inhibition did not hinder cell cycle re-entry. The use of a Src-specific activator could clarify these issues.

Similarly, the role of the PKC pathway could not be pinpointed, owing to the considerable inter-experimental differences in the cell cycle analysis seen with the PLC inhibitor during the second pulse. It should be considered to employ a different inhibitory compound, e.g. an inhibitor specific for PKC instead of PLC.

2 FUTURE WORK

The role of insulin in contributing to cell cycle progression did not become entirely clear. In order to reveal it further, it would be very informative to test whether all the protein phosphorylation events and gene expression patterns are the same when both pulses consist of EGF alone (at a higher dose). Especially the activity level of PI3K needs to be examined closely under these conditions, because the mechanism through which PI3K is activated upon EGF stimulation depends strongly on the composition of the EGF receptor: only a heterodimer consisting of EGFR, for which EGF is the ligand, and ErbB3, which contains a p85 recognition motif, is able to activate the PI3K. All other receptor dimer combinations recruit the p85 subunit in an indirect fashion, which involves several adaptor proteins. Mapping of the receptor population would help to understand which activation mechanism is predominant in these cells, and this could be achieved by immunocytochemistry, targeting the four ErbB subtypes. Additionally, such a staining could be performed also for the IR and its substrates IRS-1 and 2, to further elucidate the contribution of insulin in the original discontinuous exposure assay.

Analysis of the role of the Ras protein during the discontinuous exposure assay should be considered as well: since the specific PI3K inhibitor, when applied during the second pulse, had a suppressive effect on the phosphorylation of Erk1/2, it was assumed that a feedback loop was in place, which involved signalling through the Ras kinase. In order to test the probability of this suggestion, it would be interesting to assay for Ras activity. This should be done for several time points throughout the 18 hours duration of the discontinuous exposure assay. Additionally, the activity of Ras should be monitored in cells that are continuously stimulated, either with complete growth medium or only with EGF. This experiment would serve to elucidate whether the Ras kinase is activated in two waves in the MCF-12A cells. Such an alternating activity has been suggested to be a general feature of Ras action.

In order to utilise the ideas presented here for breast cancer treatment, a co-culture of MCF-12A together with the correspondent transformed line of MCF-7 cells should be set up. After inducing quiescence in both cell types, the growth factors and hormones examined in this thesis could be tested for their diverse effects on cell cycle progression in the cancer cell line, compared to the MCF-12A cells. To this end, flow cytometric analysis with previous sorting of cells according to the cell line would need to be performed. Mitogens may be found that induce S phase entry specifically in one cell line, but not the other. On the molecular level,

the pathways that are activated in each cell line for cell cycle progression should be compared. Again, if a kinase is found that is triggered in one cell line, but not the other, this protein may be specifically targeted to induce quiescence in the transformed cells. In summary, the findings from these examinations may have implications for cell cycle specific approaches to chemotherapy, targeting specifically the malignant cells in an environment in the mammary gland that consists of transformed as well as of normal tissue.

3 FINAL CONCLUSION

The MCF-12A cell line is derived from normal breast tissue and is therefore a good model for epithelium in the mammary gland. Evidence was presented that these cells do not necessitate continuous exposure to serum, but that timely targeted stimulation with defined growth factors is sufficient to trigger all signalling cascades required for cell cycle progression. An overall better understanding of the function of three major pathways and key proteins involved in cell cycle re-entry was achieved. Additionally, the effect of the endogenous hormone estradiol on important hormone-dependent genes and cell cycle progression was elucidated. These results may contribute to develop cell cycle phase specific cancer treatments, delivered into the tissue.

LIST OF REFERENCES

Albanese C, Johnson J, Watanabe G, Eklund N, Vu D, Arnold A, et al. 1995. Transforming p21ras mutants and c-Ets-2 activate the cyclin D1 promoter through distinguishable regions. J Biol Chem 270: 23589-23597.

Albrecht JH, Poon RY, Ahonen CL, Rieland BM, Deng C, Crary GS. 1998. Involvement of p21 and p27 in the regulation of CDK activity and cell cycle progression in the regenerating liver. Oncogene 16: 2141-2150.

Albrecht JH, Rieland BM, Nelsen CJ, Ahonen CL. 1999. Regulation of G(1) cyclin-dependent kinases in the liver: role of nuclear localization and p27 sequestration. Am J Physiol 277: G1207-G1216.

Alvarez E, Northwood IC, Gonzalez FA, Latour DA, Seth A, Abate C, et al. 1991. Pro-Leu-Ser/Thr-Pro is a consensus primary sequence for substrate protein phosphorylation. Characterization of the phosphorylation of c-myc and c-jun proteins by an epidermal growth factor receptor threonine 669 protein kinase. J Biol Chem 266: 15277-15285.

Amiry N, Kong X, Muniraj N, Kannan N, Grandison PM, Lin J, et al. 2009. Trefoil factor-1 (TFF1) enhances oncogenicity of mammary carcinoma cells. Endocrinology 150: 4473-4483.

Anderson E. 2002. The role of oestrogen and progesterone receptors in human mammary development and tumorigenesis. Breast Cancer Res 4: 197-201.

Arber N, Hibshoosh H, Moss SF, Sutter T, Zhang Y, Begg M, et al. 1996a. Increased expression of cyclin D1 is an early event in multistage colorectal carcinogenesis. Gastroenterology 110: 669-674.

Arber N, Lightdale C, Rotterdam H, Han KH, Sgambato A, Yap E, et al. 1996b. Increased expression of the cyclin D1 gene in Barrett's esophagus. Cancer Epidemiol Biomarkers Prev 5: 457-459.

Baisch H, Beck HP, Christensen IJ, Hartmann NR, Fried J, Dean PN, et al. 1982. A comparison of mathematical methods for the analysis of DNA histograms obtained by flow cytometry. Cell Tissue Kinet 15: 235-249.

Balciunaite E, Jones S, Toker A, Kazlauskas A. 2000. PDGF initiates two distinct phases of protein kinase C activity that make unequal contributions to the G0 to S transition. Curr Biol 10: 261-267.

Balciunaite E, Kazlauskas A. 2002. The timing and extent of activation of diacylglycerol-responsive protein kinase-cs determines their ability to inhibit or promote platelet-derived growth factor-dependent DNA synthesis. Exp Cell Res 281: 167-174.

Banting FG, Best CH. 1922. The internal secretion of the pancreas. Journal of Laboratory and Clinical Medicine 7: 251-266.

Barkhem T, Haldosen LA, Gustafsson JA, Nilsson S. 2002. pS2 Gene expression in HepG2 cells: complex regulation through crosstalk between the estrogen receptor alpha, an estrogen-responsive element, and the activator protein 1 response element. Mol Pharmacol 61: 1273-1283.

Barone MV, Courtneidge SA. 1995. Myc but not Fos rescue of PDGF signalling block caused by kinase-inactive Src. Nature 378: 509-512.

Bartek J, Lukas J. 2001. Mammalian G1- and S-phase checkpoints in response to DNA damage. Curr Opin Cell Biol 13: 738-747.

Batzer AG, Rotin D, Urena JM, Skolnik EY, Schlessinger J. 1994. Hierarchy of binding sites for Grb2 and Shc on the epidermal growth factor receptor. Mol Cell Biol 14: 5192-5201.

Bennett HL, Brummer T, Jeanes A, Yap AS, Daly RJ. 2008. Gab2 and Src co-operate in human mammary epithelial cells to promote growth factor independence and disruption of acinar morphogenesis. Oncogene 27: 2693-2704.

Berkenstam A, Glaumann H, Martin M, Gustafsson JA, Norstedt G. 1989. Hormonal regulation of estrogen receptor messenger ribonucleic acid in T47Dco and MCF-7 breast cancer cells. Mol Endocrinol 3: 22-28.

Bhatt RV. 2000. Environmental influence on reproductive health. Int J Gynaecol Obstet 70: 69-75.

Biscardi JS, Belsches AP, Parsons SJ. 1998. Characterization of human epidermal growth factor receptor and c-Src interactions in human breast tumor cells. Mol Carcinog 21: 261-272.

Biscardi JS, Ishizawar RC, Silva CM, Parsons SJ. 2000. Tyrosine kinase signalling in breast cancer: epidermal growth factor receptor and c-Src interactions in breast cancer. Breast Cancer Res 2: 203-210.

Biswas DK, Cruz AP, Gansberger E, Pardee AB. 2000. Epidermal growth factor-induced nuclear factor kappa B activation: A major pathway of cell-cycle progression in estrogen-receptor negative breast cancer cells. Proc Natl Acad Sci U S A 97: 8542-8547.

Bocchinfuso WP, Korach KS. 1997. Mammary gland development and tumorigenesis in estrogen receptor knockout mice. J Mammary Gland Biol Neoplasia 2: 323-334.

Bocchinfuso WP, Lindzey JK, Hewitt SC, Clark JA, Myers PH, Cooper R, et al. 2000. Induction of mammary gland development in estrogen receptor-alpha knockout mice. Endocrinology 141: 2982-2994.

Booth BW, Boulanger CA, Anderson LH, Smith GH. 2011. The normal mammary microenvironment suppresses the tumorigenic phenotype of mouse mammary tumor virus-neu-transformed mammary tumor cells. Oncogene 30: 679-689.

Bossenmeyer-Pourie C, Kannan R, Ribieras S, Wendling C, Stoll I, Thim L, et al. 2002. The trefoil factor 1 participates in gastrointestinal cell differentiation by delaying G1-S phase transition and reducing apoptosis. J Cell Biol 157: 761-770.

Bourdeau V, Deschenes J, Laperriere D, Aid M, White JH, Mader S. 2008. Mechanisms of primary and secondary estrogen target gene regulation in breast cancer cells. Nucleic Acids Res 36: 76-93.

Bourdeau V, Deschenes J, Metivier R, Nagai Y, Nguyen D, Bretschneider N, et al. 2004. Genome-wide identification of high-affinity estrogen response elements in human and mouse. Mol Endocrinol 18: 1411-1427.

Bracken AP, Ciro M, Cocito A, Helin K. 2004. E2F target genes: unraveling the biology. Trends Biochem Sci 29: 409-417.

Bravo R, Burckhardt J, Curran T, Muller R. 1985. Stimulation and inhibition of growth by EGF in different A431 cell clones is accompanied by the rapid induction of c-fos and c-myc proto-oncogenes. EMBO J 4: 1193-1197.

Bromann PA, Korkaya H, Courtneidge SA. 2004. The interplay between Src family kinases and receptor tyrosine kinases. Oncogene 23: 7957-7968.

Brown JR, Nigh E, Lee RJ, Ye H, Thompson MA, Saudou F, et al. 1998. Fos family members induce cell cycle entry by activating cyclin D1. Mol Cell Biol 18: 5609-5619.

Buday L, Downward J. 1993. Epidermal growth factor regulates p21ras through the formation of a complex of receptor, Grb2 adapter protein, and Sos nucleotide exchange factor. Cell 73: 611-620.

Bunone G, Briand PA, Miksicek RJ, Picard D. 1996. Activation of the unliganded estrogen receptor by EGF involves the MAP kinase pathway and direct phosphorylation. EMBO J 15: 2174-2183.

Burstein HJ, Polyak K, Wong JS, Lester SC, Kaelin CM. 2004. Ductal carcinoma in situ of the breast. N Engl J Med 350: 1430-1441.

Bussard KM, Smith GH. 2011. The mammary gland microenvironment directs progenitor cell fate in vivo. Int J Cell Biol 2011: 451676.

Castellano E, Downward J. 2011. RAS Interaction with PI3K: More Than Just Another Effector Pathway. Genes Cancer 2: 261-274.

Castro-Rivera E, Samudio I, Safe S. 2001. Estrogen regulation of cyclin D1 gene expression in ZR-75 breast cancer cells involves multiple enhancer elements. J Biol Chem 276: 30853-30861.

Chanprasert S, Geddis AE, Barroga C, Fox NE, Kaushansky K. 2006. Thrombopoietin (TPO) induces c-myc expression through a. Cell Signal 18: 1212-1218.

Chen C, Sytkowski AJ. 2001. Erythropoietin activates two distinct signaling pathways required for the initiation and the elongation of c-myc. J Biol Chem 276: 38518-38526.

Chen G, Li T, Zhang L, Yi M, Chen F, Wang Z, et al. 2011. Src-stimulated IRTKS phosphorylation enhances cell migration. FEBS Lett.

Chen Y, Farmer AA, Chen CF, Jones DC, Chen PL, Lee WH. 1996. BRCA1 is a 220-kDa nuclear phosphoprotein that is expressed and phosphorylated in a cell cycle-dependent manner. Cancer Res 56: 3168-3172.

Chesler L, Schlieve C, Goldenberg DD, Kenney A, Kim G, McMillan A, et al. 2006. Inhibition of phosphatidylinositol 3-kinase destabilizes Mycn protein and blocks malignant progression in neuroblastoma. Cancer Res 66: 8139-8146.

Cho HS, NG PA, Katzenellenbogen BS. 1991. Differential regulation of gene expression by estrogen in estrogen growth-independent and -dependent MCF-7 human breast cancer cell sublines. Mol Endocrinol 5: 1323-1330.

Choi JH, Hong WP, Yun S, Kim HS, Lee JR, Park JB, et al. 2005. Grb2 negatively regulates epidermal growth factor-induced phospholipase C-gamma1 activity through the direct interaction with tyrosine-phosphorylated phospholipase C-gamma1. Cell Signal 17: 1289-1299.

Chou JL, Fan Z, DeBlasio T, Koff A, Rosen N, Mendelsohn J. 1999. Constitutive overexpression of cyclin D1 in human breast epithelial cells does not prevent G1 arrest induced by deprivation of epidermal growth factor. Breast Cancer Res Treat 55: 267-283.

Ciocca DR, Fanelli MA. 1997. Estrogen receptors and cell proliferation in breast cancer. Trends Endocrinol Metab 8: 313-321.

Clarke RB, Howell A, Potten CS, Anderson E. 1997. Dissociation between steroid receptor expression and cell proliferation in the human breast. Cancer Res 57: 4987-4991.

Cohen S. 1962. Isolation of a mouse submaxillary gland protein accelerating incisor eruption and eyelid opening in the new-born animal. In: J. Biol. Chem. 237: 1555-1562.

Cohen S, Carpenter G, King L, Jr. 1980. Epidermal growth factor-receptor-protein kinase interactions. Co-purification of receptor and epidermal growth factor-enhanced phosphorylation activity. J Biol Chem 255: 4834-4842.

Colditz GA. 1998. Relationship between estrogen levels, use of hormone replacement therapy, and breast cancer. J Natl Cancer Inst 90: 814-823.

Cormier EM, Wolf MF, Jordan VC. 1989. Decrease in estradiol-stimulated progesterone receptor production in MCF-7 cells by epidermal growth factor and possible clinical implication for paracrine-regulated breast cancer growth. Cancer Res 49: 576-580.

Courtneidge SA, Fumagalli S, Koegl M, Superti-Furga G, Twamley-Stein GM. 1993. The Src family of protein tyrosine kinases: regulation and functions. Dev Suppl: 57-64.

Couse JF, Lindzey J, Grandien K, Gustafsson JA, Korach KS. 1997. Tissue distribution and quantitative analysis of estrogen receptor-alpha (ERalpha) and estrogen receptor-beta (ERbeta) messenger ribonucleic acid in the wild-type and ERalpha-knockout mouse. Endocrinology 138: 4613-4621.

Cowley S, Paterson H, Kemp P, Marshall CJ. 1994. Activation of MAP kinase kinase is necessary and sufficient for PC12 differentiation and for transformation of NIH 3T3 cells. Cell 77: 841-852.

Curran T, Bravo R, Muller R. 1985. Transient induction of c-fos and c-myc in an immediate consequence of growth factor stimulation. Cancer Surv 4: 655-681.

Darbre P, Yates J, Curtis S, King RJ. 1983. Effect of estradiol on human breast cancer cells in culture. Cancer Res 43: 349-354.

De MP. 2004. Insulin and its receptor: structure, function and evolution. Bioessays 26: 1351-1362.

Dean M, Levine RA, Ran W, Kindy MS, Sonenshein GE, Campisi J. 1986. Regulation of c-myc transcription and mRNA abundance by serum growth factors and cell contact. J Biol Chem 261: 9161-9166.

Dean PN, Jett JH. 1974. Mathematical analysis of DNA distributions derived from flow microfluorometry. J Cell Biol 60: 523-527.

DeCosse JJ, Gossens C, Kuzma JF, Unsworth BR. 1975. Embryonic inductive tissues that cause histologic differentiation of murine mammary carcinoma in vitro. J Natl Cancer Inst 54: 913-922.

DeCosse JJ, Gossens CL, Kuzma JF, Unsworth BR. 1973. Breast cancer: induction of differentiation by embryonic tissue. Science 181: 1057-1058.

Deng CX. 2006. BRCA1: cell cycle checkpoint, genetic instability, DNA damage response and cancer evolution. Nucleic Acids Res 34: 1416-1426.

DeSantis C, Siegel R, Bandi P, Jemal A. 2011. Breast cancer statistics, 2011. CA Cancer J Clin 61: 409-418.

Dubik D, Dembinski TC, Shiu RP. 1987. Stimulation of c-myc oncogene expression associated with estrogen-induced proliferation of human breast cancer cells. Cancer Res 47: 6517-6521.

Dubik D, Shiu RP. 1988. Transcriptional regulation of c-myc oncogene expression by estrogen in hormone-responsive human breast cancer cells. J Biol Chem 263: 12705-12708.

-----. 1992. Mechanism of estrogen activation of c-myc oncogene expression. Oncogene 7: 1587-1594.

Dufourny B, Alblas J, van Teeffelen HA, van Schaik FM, van der Burg B, Steenbergh PH, et al. 1997. Mitogenic signaling of insulin-like growth factor I in MCF-7 human breast cancer cells requires phosphatidylinositol 3-kinase and is independent of mitogen-activated protein kinase. J Biol Chem 272: 31163-31171.

Dufourny B, van Teeffelen HA, Hamelers IH, Sussenbach JS, Steenbergh PH. 2000. Stabilization of cyclin D1 mRNA via the phosphatidylinositol 3-kinase pathway in MCF-7 human breast cancer cells. J Endocrinol 166: 329-338.

Eagle H. 1955. Nutrition needs of mammalian cells in tissue culture. In: Science (122): 501-514.

Eastment CT, Sirbasku DA. 1978. Platelet derived growth factor(s) for a hormone-responsive rat mammary tumor cell line. J Cell Physiol 97: 17-27.

Ekholm SV, Reed SI. 2000. Regulation of G(1) cyclin-dependent kinases in the mammalian cell cycle. Curr Opin Cell Biol 12: 676-684.

El AS, Gautier N, Baron V. 2001. Focal adhesion kinase and Src mediate integrin regulation of insulin receptor phosphorylation. FEBS Lett 507: 247-252.

El-Tanani MK, Green CD. 1997. Interaction between estradiol and growth factors in the regulation of specific gene expression in MCF-7 human breast cancer cells. J Steroid Biochem Mol Biol 60: 269-276.

Emami S, Rodrigues S, Rodrigue CM, Le FN, Rivat C, Attoub S, et al. 2004. Trefoil factor family (TFF) peptides and cancer progression. Peptides 25: 885-898.

English JM, Pearson G, Baer R, Cobb MH. 1998. Identification of substrates and regulators of the mitogen-activated protein kinase ERK5 using chimeric protein kinases. J Biol Chem 273: 3854-3860.

Espino PS, Li L, He S, Yu J, Davie JR. 2006. Chromatin modification of the trefoil factor 1 gene in human breast cancer cells by the Ras/mitogen-activated protein kinase pathway. Cancer Res 66: 4610-4616.

Ewen ME, Sluss HK, Sherr CJ, Matsushime H, Kato J, Livingston DM. 1993. Functional interactions of the retinoblastoma protein with mammalian D-type cyclins. Cell 73: 487-497.

Facchini LM, Penn LZ. 1998. The molecular role of Myc in growth and transformation: recent discoveries lead to new insights. FASEB J 12: 633-651.

Fan WH, Lu YL, Deng F, Ge XM, Liu S, Tang PH. 1998. EGFR antisense RNA blocks expression of the epidermal growth factor receptor and partially reverse the malignant phenotype of human breast cancer MDA-MB-231 cells. Cell Res 8: 63-71.

Feng Y, Manka D, Wagner KU, Khan SA. 2007. Estrogen receptor-alpha expression in the mammary epithelium is required for ductal and alveolar morphogenesis in mice. Proc Natl Acad Sci U S A 104: 14718-14723.

Filmus J, Robles AI, Shi W, Wong MJ, Colombo LL, Conti CJ. 1994. Induction of cyclin D1 overexpression by activated ras. Oncogene 9: 3627-3633.

Ford D, Easton DF, Bishop DT, Narod SA, Goldgar DE. 1994. Risks of cancer in BRCA1-mutation carriers. Breast Cancer Linkage Consortium. Lancet 343: 692-695.

Foster FM, Traer CJ, Abraham SM, Fry MJ. 2003. The phosphoinositide (PI) 3-kinase family. J Cell Sci 116: 3037-3040.

Foster JS, Wimalasena J. 1996. Estrogen regulates activity of cyclin-dependent kinases and retinoblastoma protein phosphorylation in breast cancer cells. Mol Endocrinol 10: 488-498.

Fox MH. 1980. A model for the computer analysis of synchronous DNA distributions obtained by flow cytometry. Cytometry 1: 71-77.

Fry MJ. 1994. Structure, regulation and function of phosphoinositide 3-kinases. Biochim Biophys Acta 1226: 237-268.

-----. 2001. Phosphoinositide 3-kinase signalling in breast cancer: how big a role might it play? Breast Cancer Res 3: 304-312.

Gill GN, Bertics PJ, Santon JB. 1987. Epidermal growth factor and its receptor. Mol Cell Endocrinol 51: 169-186.

Gille H, Downward J. 1999. Multiple ras effector pathways contribute to G(1) cell cycle progression. J Biol Chem 274: 22033-22040.

Gilmore AP, Valentijn AJ, Wang P, Ranger AM, Bundred N, O'Hare MJ, et al. 2002. Activation of BAD by therapeutic inhibition of epidermal growth factor receptor and transactivation by insulin-like growth factor receptor. J Biol Chem 277: 27643-27650.

Gjorevski N, Nelson CM. 2011. Integrated morphodynamic signalling of the mammary gland. Nat Rev Mol Cell Biol 12: 581-593.

Graham JD, Clarke CL. 1997. Physiological action of progesterone in target tissues. Endocr Rev 18: 502-519.

Gregory H. 1975. Isolation and structure of urogastrone and its relationship to epidermal growth factor. Nature 257: 325-327.

Gregory H, Willshire IR. 1975. The isolation of the urogastrones - inhibitors of gastric acid secretion - from human urine. Hoppe Seylers Z Physiol Chem 356: 1765-1774.

Gu H, Maeda H, Moon JJ, Lord JD, Yoakim M, Nelson BH, et al. 2000. New role for Shc in activation of the phosphatidylinositol 3-kinase/Akt pathway. Mol Cell Biol 20: 7109-7120.

Gu H, Neel BG. 2003. The "Gab" in signal transduction. Trends Cell Biol 13: 122-130.

Gudas JM, Li T, Nguyen H, Jensen D, Rauscher FJ, III, Cowan KH. 1996. Cell cycle regulation of BRCA1 messenger RNA in human breast epithelial cells. Cell Growth Differ 7: 717-723.

Gudas JM, Nguyen H, Li T, Cowan KH. 1995. Hormone-dependent regulation of BRCA1 in human breast cancer cells. Cancer Res 55: 4561-4565.

Hagemann C, Blank JL. 2001. The ups and downs of MEK kinase interactions. Cell Signal 13: 863-875.

Hallak H, Moehren G, Tang J, Kaou M, Addas M, Hoek JB, et al. 2002. Epidermal growth factor-induced activation of the insulin-like growth factor I receptor in rat hepatocytes. Hepatology 36: 1509-1518.

Hamelers IH, Steenbergh PH. 2003. Interactions between estrogen and insulin-like growth factor signaling pathways in human breast tumor cells. Endocr Relat Cancer 10: 331-345.

Hamelers IH, van Schaik RF, Sussenbach JS, Steenbergh PH. 2003. 17beta-Estradiol responsiveness of MCF-7 laboratory strains is dependent on an autocrine signal activating the IGF type I receptor. Cancer Cell Int 3: 10.

Handler JA, Danilowicz RM, Eling TE. 1990. Mitogenic signaling by epidermal growth factor (EGF), but not platelet-derived growth factor, requires arachidonic acid metabolism in BALB/c 3T3 cells. Modulation of EGF-dependent c-myc expression by prostaglandins. J Biol Chem 265: 3669-3673.

Hanke JH, Gardner JP, Dow RL, Changelian PS, Brissette WH, Weringer EJ, et al. 1996. Discovery of a novel, potent, and Src family-selective tyrosine kinase inhibitor. Study of Lck- and FynT-dependent T cell activation. J Biol Chem 271: 695-701.

Hanson KD, Shichiri M, Follansbee MR, Sedivy JM. 1994. Effects of c-myc expression on cell cycle progression. Mol Cell Biol 14: 5748-5755.

Harbour JW, Dean DC. 2000. The Rb/E2F pathway: expanding roles and emerging paradigms. Genes Dev 14: 2393-2409.

Harrington MA, Wharton W, Pledger WJ. 1987. Platelet-derived growth factor stimulation of [3H]-glucosamine incorporation in density-arrested BALB/c-3T3 cells. J Cell Physiol 130: 93-102.

Heldin CH, Westermark B. 1999. Mechanism of action and in vivo role of platelet-derived growth factor. Physiol Rev 79: 1283-1316.

Hengst L, Reed SI. 1996. Translational control of p27Kip1 accumulation during the cell cycle. Science 271: 1861-1864.

Henry JA, Nicholson S, Hennessy C, Lennard TW, May FE, Westley BR. 1990. Expression of the oestrogen regulated pNR-2 mRNA in human breast cancer: relation to oestrogen receptor mRNA levels and response to tamoxifen therapy. Br J Cancer 61: 32-38.

Hermeking H, Funk JO, Reichert M, Ellwart JW, Eick D. 1995. Abrogation of p53-induced cell cycle arrest by c-Myc: evidence for an inhibitor of p21WAF1/CIP1/SDI1. Oncogene 11: 1409-1415.

Holgado-Madruga M, Emlet DR, Moscatello DK, Godwin AK, Wong AJ. 1996. A Grb2-associated docking protein in EGF- and insulin-receptor signalling. Nature 379: 560-564.

Holley RW. 1975. Control of growth of mammalian cells in cell culture. Nature 258: 487-490.

Howard A, Pelc SR. 1953. Synthesis of deoxyribonucleic acid in normal and irradiated cells and its relation to chromosome breakage. In: Heredity (Suppl) 6: 261-271.

Hu M, Peluffo G, Chen H, Gelman R, Schnitt S, Polyak K. 2009. Role of COX-2 in epithelial-stromal cell interactions and progression of ductal carcinoma in situ of the breast. Proc Natl Acad Sci U S A 106: 3372-3377.

Hu M, Yao J, Carroll DK, Weremowicz S, Chen H, Carrasco D, et al. 2008a. Regulation of in situ to invasive breast carcinoma transition. Cancer Cell 13: 394-406.

Hu YP, Patil SB, Panasiewicz M, Li W, Hauser J, Humphrey LE, et al. 2008b. Heterogeneity of receptor function in colon carcinoma cells determined by cross-talk between type I insulin-like growth factor receptor and epidermal growth factor receptor. Cancer Res 68: 8004-8013.

Hubbard SR. 2006. EGF receptor activation: push comes to shove. Cell 125: 1029-1031.

Hulka BS, Moorman PG. 2001. Breast cancer: hormones and other risk factors. Maturitas 38: 103-113.

Hutchings SE, Sato GH. 1978. Growth and maintenance of HeLa cells in serum-free medium supplemented with hormones. Proc Natl Acad Sci U S A 75: 901-904.

Hutchinson J, Jin J, Cardiff RD, Woodgett JR, Muller WJ. 2001. Activation of Akt (protein kinase B) in mammary epithelium provides a critical cell survival signal required for tumor progression. Mol Cell Biol 21: 2203-2212.

Hvid H, Klopfleisch R, Vienberg S, Hansen BF, Thorup I, Jensen HE, et al. 2011. Unique expression pattern of the three insulin receptor family members in the rat mammary gland: dominance of IGF-1R and IRR over the IR, and cyclical IGF-1R expression. J Appl Toxicol 31: 312-328.

Ing NH. 2005. Steroid hormones regulate gene expression posttranscriptionally by altering the stabilities of messenger RNAs. Biol Reprod 72: 1290-1296.

Jayme DW, Watanabe T, Shimada T. 1997. Basal medium development for serum-free culture: a historical perspective. In: Cytotechnology (23): 95-101.

Jeffy BD, Hockings JK, Kemp MQ, Morgan SS, Hager JA, Beliakoff J, et al. 2005. An estrogen receptor-alpha/p300 complex activates the BRCA-1 promoter at an AP-1 site that binds Jun/Fos transcription factors: repressive effects of p53 on BRCA-1 transcription. Neoplasia 7: 873-882.

Jemal A, Bray F, Center MM, Ferlay J, Ward E, Forman D. 2011. Global cancer statistics. CA Cancer J Clin 61: 69-90.

Jiang SY, Jordan VC. 1992. Growth regulation of estrogen receptor-negative breast cancer cells transfected with complementary DNAs for estrogen receptor. J Natl Cancer Inst 84: 580-591.

Jin Q, Esteva FJ. 2008. Cross-talk between the ErbB/HER family and the type I insulin-like growth factor receptor signaling pathway in breast cancer. J Mammary Gland Biol Neoplasia 13: 485-498.

Jones HE, Gee JM, Hutcheson IR, Knowlden JM, Barrow D, Nicholson RI. 2006. Growth factor receptor interplay and resistance in cancer. Endocr Relat Cancer 13 Suppl 1: S45-S51.

Jones SM, Kazlauskas A. 2000. Connecting signaling and cell cycle progression in growth factor-stimulated cells. Oncogene 19: 5558-5567.

-----. 2001. Growth-factor-dependent mitogenesis requires two distinct phases of signalling. Nat Cell Biol 3: 165-172.

Jones SM, Klinghoffer R, Prestwich GD, Toker A, Kazlauskas A. 1999. PDGF induces an early and a late wave of PI 3-kinase activity, and only the late wave is required for progression through G1. Curr Biol 9: 512-521.

Jorissen RN, Walker F, Pouliot N, Garrett TP, Ward CW, Burgess AW. 2003. Epidermal growth factor receptor: mechanisms of activation and signalling. Exp Cell Res 284: 31-53.

Jura N, Endres NF, Engel K, Deindl S, Das R, Lamers MH, et al. 2009. Mechanism for activation of the EGF receptor catalytic domain by the juxtamembrane segment. Cell 137: 1293-1307.

Kahan C, Seuwen K, Meloche S, Pouyssegur J. 1992. Coordinate, biphasic activation of p44 mitogen-activated protein kinase and S6 kinase by growth factors in hamster fibroblasts. Evidence for thrombin-induced signals different from phosphoinositide turnover and adenylylcyclase inhibition. J Biol Chem 267: 13369-13375.

Kaproth-Joslin KA, Li X, Reks SE, Kelley GG. 2008. Phospholipase C delta 1 regulates cell proliferation and cell-cycle progression from G1- to S-phase by control of cyclin E-CDK2 activity. Biochem J 415: 439-448.

Karey KP, Marquardt H, Sirbasku DA. 1989. Human platelet-derived mitogens. I. Identification of insulinlike growth factors I and II by purification and N alpha amino acid sequence analysis. Blood 74: 1084-1092.

Karey KP, Sirbasku DA. 1988. Differential responsiveness of human breast cancer cell lines MCF-7 and T47D to growth factors and 17 beta-estradiol. Cancer Res 48: 4083-4092.

Kastner P, Krust A, Turcotte B, Stropp U, Tora L, Gronemeyer H, et al. 1990. Two distinct estrogen-regulated promoters generate transcripts encoding the two functionally different human progesterone receptor forms A and B. EMBO J 9: 1603-1614.

Katzenellenbogen BS. 1996. Estrogen receptors: bioactivities and interactions with cell signaling pathways. Biol Reprod 54: 287-293.

Katzenellenbogen BS, Kendra KL, Norman MJ, Berthois Y. 1987. Proliferation, hormonal responsiveness, and estrogen receptor content of MCF-7 human breast cancer cells grown in the short-term and long-term absence of estrogens. Cancer Res 47: 4355-4360.

Kazlauskas A. 1994. Receptor tyrosine kinases and their targets. Curr Opin Genet Dev 4: 5-14.

Kelly K, Cochran BH, Stiles CD, Leder P. 1983. Cell-specific regulation of the c-myc gene by lymphocyte mitogens and platelet-derived growth factor. Cell 35: 603-610.

Kelsey JL, Gammon MD, John EM. 1993. Reproductive factors and breast cancer. Epidemiol Rev 15: 36-47.

Kim J, Jonasch E, Alexander A, Short JD, Cai S, Wen S, et al. 2009. Cytoplasmic sequestration of p27 via AKT phosphorylation in renal cell carcinoma. Clin Cancer Res 15: 81-90.

Kim YK, Seo DW, Kang DW, Lee HY, Han JW, Kim SN. 2006. Involvement of HDAC1 and the PI3K/PKC signaling pathways in NF-kappaB activation by the HDAC inhibitor apicidin. Biochem Biophys Res Commun 347: 1088-1093.

King SE, Schottenfeld D. 1996. The "epidemic" of breast cancer in the U.S.--determining the factors. Oncology (Williston Park) 10: 453-462.

Klein EA, Assoian RK. 2008. Transcriptional regulation of the cyclin D1 gene at a glance. J Cell Sci 121: 3853-3857.

Knowlden JM, Hutcheson IR, Barrow D, Gee JM, Nicholson RI. 2005. Insulin-like growth factor-I receptor signaling in tamoxifen-resistant breast cancer: a supporting role to the epidermal growth factor receptor. Endocrinology 146: 4609-4618.

Knowlden JM, Hutcheson IR, Jones HE, Madden T, Gee JM, Harper ME, et al. 2003. Elevated levels of epidermal growth factor receptor/c-erbB2 heterodimers mediate an autocrine growth regulatory pathway in tamoxifen-resistant MCF-7 cells. Endocrinology 144: 1032-1044.

Koivunen J, Aaltonen V, Peltonen J. 2006. Protein kinase C (PKC) family in cancer progression. Cancer Lett 235: 1-10.

Kortenkamp A, Faust M, Scholze M, Backhaus T. 2007. Low-level exposure to multiple chemicals: reason for human health concerns? Environ Health Perspect 115 Suppl 1: 106-114.

Kortylewski M, Heinrich PC, Kauffmann ME, Bohm M, MacKiewicz A, Behrmann I. 2001. Mitogen-activated protein kinases control p27/Kip1 expression and growth of human melanoma cells. Biochem J 357: 297-303.

Kotelevets L, van HJ, Bruyneel E, Mareel M, van RF, Chastre E. 2001. The lipid phosphatase activity of PTEN is critical for stabilizing intercellular junctions and reverting invasiveness. J Cell Biol 155: 1129-1135.

Kraus WL, Katzenellenbogen BS. 1993. Regulation of progesterone receptor gene expression and growth in the rat uterus: modulation of estrogen actions by progesterone and sex steroid hormone antagonists. Endocrinology 132: 2371-2379.

Kumar A, Marques M, Carrera AC. 2006. Phosphoinositide 3-kinase activation in late G1 is required for c-Myc stabilization and S phase entry. Mol Cell Biol 26: 9116-9125.

Kurita T, Lee KJ, Cooke PS, Taylor JA, Lubahn DB, Cunha GR. 2000. Paracrine regulation of epithelial progesterone receptor by estradiol in the mouse female reproductive tract. Biol Reprod 62: 821-830.

Kushi LH, Byers T, Doyle C, Bandera EV, McCullough M, McTiernan A, et al. 2006. American Cancer Society Guidelines on Nutrition and Physical Activity for cancer prevention: reducing the risk of cancer with healthy food choices and physical activity. CA Cancer J Clin 56: 254-281.

Kypta RM, Goldberg Y, Ulug ET, Courtneidge SA. 1990. Association between the PDGF receptor and members of the src family of tyrosine kinases. Cell 62: 481-492.

Kyriakis JM, App H, Zhang XF, Banerjee P, Brautigan DL, Rapp UR, et al. 1992. Raf-1 activates MAP kinase-kinase. Nature 358: 417-421.

Lange CA. 2008. Integration of progesterone receptor action with rapid signaling events in breast cancer models. J Steroid Biochem Mol Biol 108: 203-212.

Lavoie JN, Rivard N, L'Allemain G, Pouyssegur J. 1996. A temporal and biochemical link between growth factor-activated MAP kinases, cyclin D1 induction and cell cycle entry. Prog Cell Cycle Res 2: 49-58.

Lee J, Pilch PF. 1994. The insulin receptor: structure, function, and signaling. Am J Physiol 266: C319-C334.

Lee KY, Ladha MH, McMahon C, Ewen ME. 1999. The retinoblastoma protein is linked to the activation of Ras. Mol Cell Biol 19: 7724-7732.

Lehr S, Kotzka J, Herkner A, Sikmann A, Meyer HE, Krone W, et al. 2000. Identification of major tyrosine phosphorylation sites in the human insulin receptor substrate Gab-1 by insulin receptor kinase in vitro. Biochemistry 39: 10898-10907.

Lenferink AE, Busse D, Flanagan WM, Yakes FM, Arteaga CL. 2001. ErbB2/neu kinase modulates cellular p27(Kip1) and cyclin D1 through multiple signaling pathways. Cancer Res 61: 6583-6591.

Leone G, DeGregori J, Sears R, Jakoi L, Nevins JR. 1997. Myc and Ras collaborate in inducing accumulation of active cyclin E/Cdk2 and E2F. Nature 387: 422-426.

Li Y, Guessous F, Johnson EB, Eberhart CG, Li XN, Shu Q, et al. 2008. Functional and molecular interactions between the HGF/c-Met pathway and c-Myc in large-cell medulloblastoma. Lab Invest 88: 98-111.

Liang J, Slingerland JM. 2003. Multiple roles of the PI3K/PKB (Akt) pathway in cell cycle progression. Cell Cycle 2: 339-345.

Lichtenstein P, Holm NV, Verkasalo PK, Iliadou A, Kaprio J, Koskenvuo M, et al. 2000. Environmental and heritable factors in the causation of cancer--analyses of cohorts of twins from Sweden, Denmark, and Finland. N Engl J Med 343: 78-85.

Lin JX, Vilcek J. 1987. Tumor necrosis factor and interleukin-1 cause a rapid and transient stimulation of c-fos and c-myc mRNA levels in human fibroblasts. J Biol Chem 262: 11908-11911.

Linebaugh BE, Rillema JA. 1977. Hydrocortisone enhancement of insulin's action on macromolecular synthesis in MCF-7 cells. Mol Cell Endocrinol 7: 335-343.

Liu JJ, Chao JR, Jiang MC, Ng SY, Yen JJ, Yang-Yen HF. 1995. Ras transformation results in an elevated level of cyclin D1 and acceleration of G1 progression in NIH 3T3 cells. Mol Cell Biol 15: 3654-3663.

Longnecker MP, Newcomb PA, Mittendorf R, Greenberg ER, Clapp RW, Bogdan GF, et al. 1995. Risk of breast cancer in relation to lifetime alcohol consumption. J Natl Cancer Inst 87: 923-929.

Luttrell DK, Lee A, Lansing TJ, Crosby RM, Jung KD, Willard D, et al. 1994. Involvement of pp60c-src with two major signaling pathways in human breast cancer. Proc Natl Acad Sci U S A 91: 83-87.

Luttrell DK, Luttrell LM, Parsons SJ. 1988. Augmented mitogenic responsiveness to epidermal growth factor in murine fibroblasts that overexpress pp60c-src. Mol Cell Biol 8: 497-501.

Ma L, Gauville C, Berthois Y, Degeorges A, Millot G, Martin PM, et al. 1998. Role of epidermal-growth-factor receptor in tumor progression in transformed human mammary epithelial cells. Int J Cancer 78: 112-119.

Madigan MP, Ziegler RG, Benichou J, Byrne C, Hoover RN. 1995. Proportion of breast cancer cases in the United States explained by well-established risk factors. J Natl Cancer Inst 87: 1681-1685.

Magne N, Melis A, Chargari C, Castadot P, Guichard JB, Barani D, et al. 2011. Recommendations for a lifestyle which could prevent breast cancer and its relapse: Physical activity and dietetic aspects. Crit Rev Oncol Hematol 80: 450-459.

Manzoli L, Billi AM, Rubbini S, Bavelloni A, Faenza I, Gilmour RS, et al. 1997. Essential role for nuclear phospholipase C beta1 in insulin-like growth factor I-induced mitogenesis. Cancer Res 57: 2137-2139.

Manzoli L, Martelli AM, Billi AM, Faenza I, Fiume R, Cocco L. 2005. Nuclear phospholipase C: involvement in signal transduction. Prog Lipid Res 44: 185-206.

Marcotte R, Smith HW, Sanguin-Gendreau V, McDonough RV, Muller WJ. 2011. Mammary epithelial-specific disruption of c-Src impairs cell cycle progression and tumorigenesis. Proc Natl Acad Sci U S A.

Marks JR, Huper G, Vaughn JP, Davis PL, Norris J, McDonnell DP, et al. 1997. BRCA1 expression is not directly responsive to estrogen. Oncogene 14: 115-121.

Mawson A, Lai A, Carroll JS, Sergio CM, Mitchell CJ, Sarcevic B. 2005. Estrogen and insulin/IGF-1 cooperatively stimulate cell cycle progression in MCF-7 breast cancer cells through differential regulation of c-Myc and cyclin D1. Mol Cell Endocrinol 229: 161-173.

May FE, Johnson MD, Wiseman LR, Wakeling AE, Kastner P, Westley BR. 1989. Regulation of progesterone receptor mRNA by oestradiol and antioestrogens in breast cancer cell lines. J Steroid Biochem 33: 1035-1041.

McClelland RA, Barrow D, Madden TA, Dutkowski CM, Pamment J, Knowlden JM, et al. 2001. Enhanced epidermal growth factor receptor signaling in MCF7 breast cancer cells after long-term culture in the presence of the pure antiestrogen ICI 182,780 (Faslodex). Endocrinology 142: 2776-2788.

Means AR, O'Malley BW. 1972. Mechanism of estrogen action: early transcriptional and translational events. Metabolism 21: 357-370.

Meloche S. 1995. Cell cycle reentry of mammalian fibroblasts is accompanied by the sustained activation of p44mapk and p42mapk isoforms in the G1 phase and their inactivation at the G1/S transition. J Cell Physiol 163: 577-588.

Meloche S, Pouyssegur J. 2007. The ERK1/2 mitogen-activated protein kinase pathway as a master regulator of the G1- to S-phase transition. Oncogene 26: 3227-3239.

Miki Y, Swensen J, Shattuck-Eidens D, Futreal PA, Harshman K, Tavtigian S, et al. 1994. A strong candidate for the breast and ovarian cancer susceptibility gene BRCA1. Science 266: 66-71.

Millikan R, DeVoto E, Newman B, Savitz D. 1995. Studying environmental influences and breast cancer risk: suggestions for an integrated population-based approach. Breast Cancer Res Treat 35: 79-89.

Mittnacht S, Paterson H, Olson MF, Marshall CJ. 1997. Ras signalling is required for inactivation of the tumour suppressor pRb cell-cycle control protein. Curr Biol 7: 219-221.

Mori S, Ronnstrand L, Yokote K, Engstrom A, Courtneidge SA, Claesson-Welsh L, et al. 1993. Identification of two juxtamembrane autophosphorylation sites in the PDGF beta-receptor; involvement in the interaction with Src family tyrosine kinases. EMBO J 12: 2257-2264.

Moriarty K, Kim KH, Bender JR. 2006. Minireview: estrogen receptor-mediated rapid signaling. Endocrinology 147: 5557-5563.

Motti ML, De MC, Califano D, Fusco A, Viglietto G. 2004. Akt-dependent T198 phosphorylation of cyclin-dependent kinase inhibitor p27kip1 in breast cancer. Cell Cycle 3: 1074-1080.

Muir KR. 2005. Endocrine-disrupting pesticides and selected hormonally dependent cancers. Scand J Work Environ Health 31 Suppl 1: 55-61.

Muise-Helmericks RC, Grimes HL, Bellacosa A, Malstrom SE, Tsichlis PN, Rosen N. 1998. Cyclin D expression is controlled post-transcriptionally via a phosphatidylinositol 3-kinase/Akt-dependent pathway. J Biol Chem 273: 29864-29872.

Mulcahy LS, Smith MR, Stacey DW. 1985. Requirement for ras proto-oncogene function during serum-stimulated growth of NIH 3T3 cells. Nature 313: 241-243.

Murray A. 1994. Cell cycle checkpoints. Curr Opin Cell Biol 6: 872-876.

Muthuswamy SK, Siegel PM, Dankort DL, Webster MA, Muller WJ. 1994. Mammary tumors expressing the neu proto-oncogene possess elevated c-Src tyrosine kinase activity. Mol Cell Biol 14: 735-743.

Najid A, Nicolas A, Tixier M, Habrioux G. 1989. Mitogenic effect of estradiol on MCF-7 human breast cancer cells can be modulated by serum. Exp Cell Biol 57: 139-145.

Nardulli AM, Greene GL, O'Malley BW, Katzenellenbogen BS. 1988. Regulation of progesterone receptor messenger ribonucleic acid and protein levels in MCF-7 cells by estradiol: analysis of estrogen's effect on progesterone receptor synthesis and degradation. Endocrinology 122: 935-944.

Neel BG, Gu H, Pao L. 2003. The 'Shp'ing news: SH2 domain-containing tyrosine phosphatases in cell signaling. Trends Biochem Sci 28: 284-293.

Nef S, Verma-Kurvari S, Merenmies J, Vassalli JD, Efstratiadis A, Accili D, et al. 2003. Testis determination requires insulin receptor family function in mice. Nature 426: 291-295.

Nenci I, Marchetti E, Querzoli P. 1988. Commentary on human mammary preneoplasia. The estrogen receptor-promotion hypothesis. J Steroid Biochem 30: 105-106.

Newby JC, Johnston SR, Smith IE, Dowsett M. 1997. Expression of epidermal growth factor receptor and c-erbB2 during the development of tamoxifen resistance in human breast cancer. Clin Cancer Res 3: 1643-1651.

Newman B, Moorman PG, Millikan R, Qaqish BF, Geradts J, Aldrich TE, et al. 1995. The Carolina Breast Cancer Study: integrating population-based epidemiology and molecular biology. Breast Cancer Res Treat 35: 51-60.

Nishizuka Y. 1995. Protein kinase C and lipid signaling for sustained cellular responses. FASEB J 9: 484-496.

O'Lone R, Frith MC, Karlsson EK, Hansen U. 2004. Genomic targets of nuclear estrogen receptors. Mol Endocrinol 18: 1859-1875.

O'Malley BW, McGuire WL, Middleton PA. 1968. Altered gene expression during differentiation: population changes in hybridizable RNA after stimulation of the chick oviduct with oestrogen. Nature 218: 1249-1251.

Oleksiewicz MB, Bonnesen C, Hegelund AC, Lundby A, Holm GM, Jensen MB, et al. 2011. Comparison of intracellular signalling by insulin and the hypermitogenic AspB10 analogue in MCF-7 breast adenocarcinoma cells. J Appl Toxicol 31: 329-341.

Paine TM, Soule HD, Pauley RJ, Dawson PJ. 1992. Characterization of epithelial phenotypes in mortal and immortal human breast cells. Int J Cancer 50: 463-473.

Papendorp JT, Schatz RW, Soto AM, Sonnenschein C. 1985. On the role of 17 alpha-estradiol and 17 beta-estradiol in the proliferation of MCF7 and T47D-A11 human breast tumor cells. J Cell Physiol 125: 591-595.

Pardee AB. 1974. A restriction point for control of normal animal cell proliferation. Proc Natl Acad Sci U S A 71: 1286-1290.

-----. 1989. G1 events and regulation of cell proliferation. Science 246: 603-608.

Paul D, Lipton A, Klinger I. 1971. Serum factor requirements of normal and simian virus 40-transformed 3T3 mouse fibroplasts. Proc Natl Acad Sci U S A 68: 645-652.

Pearson G, Robinson F, Beers GT, Xu BE, Karandikar M, Berman K, et al. 2001. Mitogen-activated protein (MAP) kinase pathways: regulation and physiological functions. Endocr Rev 22: 153-183.

Peeper DS, Upton TM, Ladha MH, Neuman E, Zalvide J, Bernards R, et al. 1997. Ras signalling linked to the cell-cycle machinery by the retinoblastoma protein. Nature 386: 177-181.

Pelicci G, Lanfrancone L, Grignani F, McGlade J, Cavallo F, Forni G, et al. 1992. A novel transforming protein (SHC) with an SH2 domain is implicated in mitogenic signal transduction. Cell 70: 93-104.

Perez-Roger I, Kim SH, Griffiths B, Sewing A, Land H. 1999. Cyclins D1 and D2 mediate myc-induced proliferation via sequestration of p27(Kip1) and p21(Cip1). EMBO J 18: 5310-5320.

Perry JK, Kannan N, Grandison PM, Mitchell MD, Lobie PE. 2008. Are trefoil factors oncogenic? Trends Endocrinol Metab 19: 74-81.

Pervez S, Shaikh H, Aijaz F, Aziz SA, Naqvi M, Hasan SH. 1994. Immunohistochemical estrogen receptor determination in human breast carcinoma: correlation with histologic differentiation and age of the patients. J Pak Med Assoc 44: 133-136.

Pfaffl MW. 2001. A new mathematical model for relative quantification in real-time RT-PCR. Nucleic Acids Res 29: e45.

Philipp-Staheli J, Payne SR, Kemp CJ. 2001. p27(Kip1): regulation and function of a haploinsufficient tumor suppressor and its misregulation in cancer. Exp Cell Res 264: 148-168.

Pierce JH, Arnstein P, DiMarco E, Artrip J, Kraus MH, Lonardo F, et al. 1991. Oncogenic potential of erbB-2 in human mammary epithelial cells. Oncogene 6: 1189-1194.

Pietras RJ, Arboleda J, Reese DM, Wongvipat N, Pegram MD, Ramos L, et al. 1995. HER-2 tyrosine kinase pathway targets estrogen receptor and promotes hormone-independent growth in human breast cancer cells. Oncogene 10: 2435-2446.

Planas-Silva MD, Donaher JL, Weinberg RA. 1999. Functional activity of ectopically expressed estrogen receptor is not sufficient for estrogen-mediated cyclin D1 expression. Cancer Res 59: 4788-4792.

Planas-Silva MD, Weinberg RA. 1997a. Estrogen-dependent cyclin E-cdk2 activation through p21 redistribution. Mol Cell Biol 17: 4059-4069.

-----. 1997b. The restriction point and control of cell proliferation. Curr Opin Cell Biol 9: 768-772.

Pledger WJ, Stiles CD, Antoniades HN, Scher CD. 1977. Induction of DNA synthesis in BALB/c 3T3 cells by serum components: reevaluation of the commitment process. Proc Natl Acad Sci U S A 74: 4481-4485.

Polyak K, Kalluri R. 2010. The role of the microenvironment in mammary gland development and cancer. Cold Spring Harb Perspect Biol 2: a003244.

Poulsom R, Hanby AM, Lalani EN, Hauser F, Hoffmann W, Stamp GW. 1997. Intestinal trefoil factor (TFF 3) and pS2 (TFF 1), but not spasmolytic polypeptide (TFF 2) mRNAs are co-expressed in normal, hyperplastic, and neoplastic human breast epithelium. J Pathol 183: 30-38.

Prall OW, Sarcevic B, Musgrove EA, Watts CK, Sutherland RL. 1997. Estrogen-induced activation of Cdk4 and Cdk2 during G1-S phase progression is accompanied by increased cyclin D1 expression and decreased cyclin-dependent kinase inhibitor association with cyclin E-Cdk2. J Biol Chem 272: 10882-10894.

Prest SJ, May FE, Westley BR. 2002. The estrogen-regulated protein, TFF1, stimulates migration of human breast cancer cells. FASEB J 16: 592-594.

Puck TT. 1964. STUDIES OF THE LIFE CYCLE OF MAMMALIAN CELLS. Cold Spring Harb Symp Quant Biol 29: 167-176.

Putti TC, El-Rehim DM, Rakha EA, Paish CE, Lee AH, Pinder SE, et al. 2005. Estrogen receptor-negative breast carcinomas: a review of morphology and immunophenotypical analysis. Mod Pathol 18: 26-35.

Pysz MA, Leontieva OV, Bateman NW, Uronis JM, Curry KJ, Threadgill DW, et al. 2009. PKCalpha tumor suppression in the intestine is associated with transcriptional and translational inhibition of cyclin D1. Exp Cell Res 315: 1415-1428.

Quastler H. 1960. Cell population kinetics. In: Ann.N.Y.Acad.Sci. 90: 580-591.

Quelle DE, Ashmun RA, Shurtleff SA, Kato JY, Bar-Sagi D, Roussel MF, et al. 1993. Overexpression of mouse D-type cyclins accelerates G1 phase in rodent fibroblasts. Genes Dev 7: 1559-1571.

Quesnelle KM, Boehm AL, Grandis JR. 2007. STAT-mediated EGFR signaling in cancer. J Cell Biochem 102: 311-319.

Rabbitts PH, Watson JV, Lamond A, Forster A, Stinson MA, Evan G, et al. 1985. Metabolism of c-myc gene products: c-myc mRNA and protein expression in the cell cycle. EMBO J 4: 2009-2015.

Rabinovitch PS. 1994. DNA content histogram and cell-cycle analysis. Methods Cell Biol 41: 263-296.

Radford DM, Phillips NJ, Fair KL, Ritter JH, Holt M, Donis-Keller H. 1995. Allelic loss and the progression of breast cancer. Cancer Res 55: 5180-5183.

Radiloff DR, Wakeman TP, Feng J, Schilling S, Seto E, Wang XF. 2011. Trefoil factor 1 acts to suppress senescence induced by oncogene activation during the cellular transformation process. Proc Natl Acad Sci U S A 108: 6591-6596.

Ramoni C, Spadaro F, Barletta B, Dupuis ML, Podo F. 2004. Phosphatidylcholine-specific phospholipase C in mitogen-stimulated fibroblasts. Exp Cell Res 299: 370-382.

Ramos JW. 2008. The regulation of extracellular signal-regulated kinase (ERK) in mammalian cells. Int J Biochem Cell Biol 40: 2707-2719.

Ran W, Dean M, Levine RA, Henkle C, Campisi J. 1986. Induction of c-fos and c-myc mRNA by epidermal growth factor or calcium ionophore is cAMP dependent. Proc Natl Acad Sci U S A 83: 8216-8220.

Ravichandran KS. 2001. Signaling via Shc family adapter proteins. Oncogene 20: 6322-6330.

Rieber M, Rieber MS. 2006. Cyclin D1 overexpression induces epidermal growth factor-independent resistance to apoptosis linked to BCL-2 in human A431 carcinoma. Apoptosis 11: 121-129.

Rillema JA, Linebaugh BE. 1977. Characteristics of the insulin stimulation of DNA, RNA and protein metabolism in cultured human mammary carcinoma cells. Biochim Biophys Acta 475: 74-80.

Roche S, Koegl M, Barone MV, Roussel MF, Courtneidge SA. 1995. DNA synthesis induced by some but not all growth factors requires Src family protein tyrosine kinases. Mol Cell Biol 15: 1102-1109.

Rockhill B, Spiegelman D, Byrne C, Hunter DJ, Colditz GA. 2001. Validation of the Gail et al. model of breast cancer risk prediction and implications for chemoprevention. J Natl Cancer Inst 93: 358-366.

Rodrigues S, Attoub S, Nguyen QD, Bruyneel E, Rodrigue CM, Westley BR, et al. 2003. Selective abrogation of the proinvasive activity of the trefoil peptides pS2 and spasmolytic polypeptide by disruption of the EGF receptor signaling pathways in kidney and colonic cancer cells. Oncogene 22: 4488-4497.

Rodriguez-Viciana P, Warne PH, Dhand R, Vanhaesebroeck B, Gout I, Fry MJ, et al. 1994. Phosphatidylinositol-3-OH kinase as a direct target of Ras. Nature 370: 527-532.

Rosenwald IB, Rhoads DB, Callanan LD, Isselbacher KJ, Schmidt EV. 1993. Increased expression of eukaryotic translation initiation factors eIF-4E and eIF-2 alpha in response to growth induction by c-myc. Proc Natl Acad Sci U S A 90: 6175-6178.

Rosenzweig T, Aga-Mizrachi S, Bak A, Sampson SR. 2004. Src tyrosine kinase regulates insulin-induced activation of protein kinase C (PKC) delta in skeletal muscle. Cell Signal 16: 1299-1308.

Ross R, Raines EW, Bowen-Pope DF. 1986. The biology of platelet-derived growth factor. Cell 46: 155-169.

Rozakis-Adcock M, Fernley R, Wade J, Pawson T, Bowtell D. 1993. The SH2 and SH3 domains of mammalian Grb2 couple the EGF receptor to the Ras activator mSos1. Nature 363: 83-85.

Rozengurt E, Pardee AB. 1972. Opposite effects of dibutyryl adenosine 3':5' cyclic monophosphate and serum on growth of Chinese hamster cells. J Cell Physiol 80: 273-279.

Ruedl C, Cappelletti V, Coradini D, Granata G, Di FG. 1990. Influence of culture conditions on the estrogenic cell growth stimulation of human breast cancer cells. J Steroid Biochem Mol Biol 37: 195-200.

Sabbah M, Courilleau D, Mester J, Redeuilh G. 1999. Estrogen induction of the cyclin D1 promoter: involvement of a cAMP response-like element. Proc Natl Acad Sci U S A 96: 11217-11222.

Sakakibara K, Kubota K, Worku B, Ryer EJ, Miller JP, Koff A, et al. 2005. PDGF-BB regulates p27 expression through ERK-dependent RNA turn-over in vascular smooth muscle cells. J Biol Chem 280: 25470-25477.

Sasaki AT, Chun C, Takeda K, Firtel RA. 2004. Localized Ras signaling at the leading edge regulates PI3K, cell polarity, and directional cell movement. J Cell Biol 167: 505-518.

Sasaoka T, Kobayashi M. 2000. The functional significance of Shc in insulin signaling as a substrate of the insulin receptor. Endocr J 47: 373-381.

Sasco AJ. 2003. Breast cancer and the environment. Horm Res 60 Suppl 3: 50.

Scarpin KM, Graham JD, Mote PA, Clarke CL. 2009. Progesterone action in human tissues: regulation by progesterone receptor (PR) isoform expression, nuclear positioning and coregulator expression. Nucl Recept Signal 7: e009.

Schild C, Wirth M, Reichert M, Schmid RM, Saur D, Schneider G. 2009. PI3K signaling maintains c-myc expression to regulate transcription of E2F1 in pancreatic cancer cells. Mol Carcinog 48: 1149-1158.

Schonfeld SJ, Pfeiffer RM, Lacey JV, Jr., Berrington de GA, Doody MM, Greenlee RT, et al. 2011. Hormone-related risk factors and postmenopausal breast cancer among nulliparous versus parous women: An aggregated study. Am J Epidemiol 173: 509-517.

Scully R, Chen J, Ochs RL, Keegan K, Hoekstra M, Feunteun J, et al. 1997. Dynamic changes of BRCA1 subnuclear location and phosphorylation state are initiated by DNA damage. Cell 90: 425-435.

Sears R, Leone G, DeGregori J, Nevins JR. 1999. Ras enhances Myc protein stability. Mol Cell 3: 169-179.

Sears R, Nuckolls F, Haura E, Taya Y, Tamai K, Nevins JR. 2000. Multiple Ras-dependent phosphorylation pathways regulate Myc protein stability. Genes Dev 14: 2501-2514.

Sheng H, Shao J, DuBois RN. 2001. Akt/PKB activity is required for Ha-Ras-mediated transformation of intestinal epithelial cells. J Biol Chem 276: 14498-14504.

Sherr CJ, Roberts JM. 1999. CDK inhibitors: positive and negative regulators of G1-phase progression. Genes Dev 13: 1501-1512.

Silva E, Kabil A, Kortenkamp A. 2010. Cross-talk between non-genomic and genomic signalling pathways--distinct effect profiles of environmental estrogens. Toxicol Appl Pharmacol 245: 160-170.

Simm A, Hoppe V, Karbach D, Leicht M, Fenn A, Hoppe J. 1998. Late signals from the PDGF receptors leading to the activation of the p70S6-kinase are necessary for the transition from G1 to S phase in AKR-2B cells. Exp Cell Res 244: 379-393.

Sisken JE, Morasca L. 1965. Intrapopulation kinetics of the mitotic cycle. In: J. Cell Biol. (25): 179-189.

Skolnik EY, Batzer A, Li N, Lee CH, Lowenstein E, Mohammadi M, et al. 1993. The function of GRB2 in linking the insulin receptor to Ras signaling pathways. Science 260: 1953-1955.

Slamon DJ, Clark GM, Wong SG, Levin WJ, Ullrich A, McGuire WL. 1987. Human breast cancer: correlation of relapse and survival with amplification of the HER-2/neu oncogene. Science 235: 177-182.

Soltoff SP, Carraway KL, III, Prigent SA, Gullick WG, Cantley LC. 1994. ErbB3 is involved in activation of phosphatidylinositol 3-kinase by epidermal growth factor. Mol Cell Biol 14: 3550-3558.

Soto AM, Sonnenschein C. 1985. The role of estrogens on the proliferation of human breast tumor cells (MCF-7). J Steroid Biochem 23: 87-94.

Spillman MA, Bowcock AM. 1996. BRCA1 and BRCA2 mRNA levels are coordinately elevated in human breast cancer cells in response to estrogen. Oncogene 13: 1639-1645.

Stacey D, Kazlauskas A. 2002. Regulation of Ras signaling by the cell cycle. Curr Opin Genet Dev 12: 44-46.

Stern DF. 2003. ErbBs in mammary development. Exp Cell Res 284: 89-98.

Stoica A, Saceda M, Doraiswamy VL, Coleman C, Martin MB. 2000. Regulation of estrogen receptor-alpha gene expression by epidermal growth factor. J Endocrinol 165: 371-378.

Straus DS. 1984. Growth-stimulatory actions of insulin in vitro and in vivo. Endocr Rev 5: 356-369.

Sun XJ, Pons S, Asano T, Myers MG, Jr., Glasheen E, White MF. 1996. The Fyn tyrosine kinase binds Irs-1 and forms a distinct signaling complex during insulin stimulation. J Biol Chem 271: 10583-10587.

Surmacz E, Burgaud JL. 1995. Overexpression of insulin receptor substrate 1 (IRS-1) in the human breast cancer cell line MCF-7 induces loss of estrogen requirements for growth and transformation. Clin Cancer Res 1: 1429-1436.

Sutherland RL, Watts CK, Musgrove EA. 1993. Cyclin gene expression and growth control in normal and neoplastic human breast epithelium. J Steroid Biochem Mol Biol 47: 99-106.

Takuwa N, Takuwa Y. 1997. Ras activity late in G1 phase required for p27kip1 downregulation, passage through the restriction point, and entry into S phase in growth factor-stimulated NIH 3T3 fibroblasts. Mol Cell Biol 17: 5348-5358.

Tamm I, Kikuchi T. 1990. Insulin-like growth factor-1 (IGF-1), insulin, and epidermal growth factor (EGF) are survival factors for density-inhibited, quiescent Balb/c-3T3 murine fibroblasts. J Cell Physiol 143: 494-500.

Tan M, Yao J, Yu D. 1997. Overexpression of the c-erbB-2 gene enhanced intrinsic metastasis potential in human breast cancer cells without increasing their transformation abilities. Cancer Res 57: 1199-1205.

Temin HM. 1971. Stimulation by serum of multiplication of stationary chicken cells. J Cell Physiol 78: 161-170.

Terasima T, Tolmach LJ. 1963. Growth and nucleic acid synthesis in synchronously dividing populations of HeLa cells. In: Exp. Cell Res. 30: 344-362.

Thomas SM, Brugge JS. 1997. Cellular functions regulated by Src family kinases. Annu Rev Cell Dev Biol 13: 513-609.

Thompson CB, Challoner PB, Neiman PE, Groudine M. 1985. Levels of c-myc oncogene mRNA are invariant throughout the cell cycle. Nature 314: 363-366.

Thompson ME, Jensen RA, Obermiller PS, Page DL, Holt JT. 1995. Decreased expression of BRCA1 accelerates growth and is often present during sporadic breast cancer progression. Nat Genet 9: 444-450.

Tice DA, Biscardi JS, Nickles AL, Parsons SJ. 1999. Mechanism of biological synergy between cellular Src and epidermal growth factor receptor. Proc Natl Acad Sci U S A 96: 1415-1420.

Timms JF, White SL, O'Hare MJ, Waterfield MD. 2002. Effects of ErbB-2 overexpression on mitogenic signalling and cell cycle progression in human breast luminal epithelial cells. Oncogene 21: 6573-6586.

Tobey RA, Petersen DF, Anderson EC, Puck TT. 1966. Life cycle analysis of mammalian cells. 3. The inhibition of division in Chinese hamster cells by puromycin and actinomycin. Biophys J 6: 567-581.

Treinies I, Paterson HF, Hooper S, Wilson R, Marshall CJ. 1999. Activated MEK stimulates expression of AP-1 components independently of phosphatidylinositol 3-kinase (PI3-kinase) but requires a PI3-kinase signal To stimulate DNA synthesis. Mol Cell Biol 19: 321-329.

van der Burg B, Rutteman GR, Blankenstein MA, de Laat SW, van Zoelen EJ. 1988. Mitogenic stimulation of human breast cancer cells in a growth factor-defined medium: synergistic action of insulin and estrogen. J Cell Physiol 134: 101-108.

van Weeren PC, de Bruyn KM, de Vries-Smits AM, van LJ, Burgering BM. 1998. Essential role for protein kinase B (PKB) in insulin-induced glycogen synthase kinase 3 inactivation. Characterization of dominant-negative mutant of PKB. J Biol Chem 273: 13150-13156.

Vaughn JP, Davis PL, Jarboe MD, Huper G, Evans AC, Wiseman RW, et al. 1996. BRCA1 expression is induced before DNA synthesis in both normal and tumor-derived breast cells. Cell Growth Differ 7: 711-715.

Vlahos CJ, Matter WF, Hui KY, Brown RF. 1994. A specific inhibitor of phosphatidylinositol 3-kinase, 2-(4-morpholinyl)-8-phenyl-4H-1-benzopyran-4-one (LY294002). J Biol Chem 269: 5241-5248.

Vojtek AB, Hollenberg SM, Cooper JA. 1993. Mammalian Ras interacts directly with the serine/threonine kinase Raf. Cell 74: 205-214.

Walker F, Orchard SG, Jorissen RN, Hall NE, Zhang HH, Hoyne PA, et al. 2004. CR1/CR2 interactions modulate the functions of the cell surface epidermal growth factor receptor. J Biol Chem 279: 22387-22398.

Ward CW, Lawrence MC, Streltsov VA, Adams TE, McKern NM. 2007. The insulin and EGF receptor structures: new insights into ligand-induced receptor activation. Trends Biochem Sci 32: 129-137.

Wasylishen AR, Penn LZ. 2010. Myc: the beauty and the beast. Genes Cancer 1: 532-541.

Waters CM, Littlewood TD, Hancock DC, Moore JP, Evan GI. 1991. c-myc protein expression in untransformed fibroblasts. Oncogene 6: 797-805.

Watson JV. 1992. Flow Cytometry Data Analysis - Basic Concepts and Statistics. In.

Watson JV, Chambers SH, Smith PJ. 1987. A pragmatic approach to the analysis of DNA histograms with a definable G1 peak. Cytometry 8: 1-8.

Weber JD, Raben DM, Phillips PJ, Baldassare JJ. 1997. Sustained activation of extracellular-signal-regulated kinase 1 (ERK1) is required for the continued expression of cyclin D1 in G1 phase. Biochem J 326 (Pt 1): 61-68.

Weinberg RA. 1995. The retinoblastoma protein and cell cycle control. Cell 81: 323-330.

Weinstat-Saslow D, Merino MJ, Manrow RE, Lawrence JA, Bluth RF, Wittenbel KD, et al. 1995. Overexpression of cyclin D mRNA distinguishes invasive and in situ breast carcinomas from non-malignant lesions. Nat Med 1: 1257-1260.

Wells A. 1999. EGF receptor. Int J Biochem Cell Biol 31: 637-643.

Welshons WV, Jordan VC. 1987. Adaptation of estrogen-dependent MCF-7 cells to low estrogen (phenol red-free) culture. Eur J Cancer Clin Oncol 23: 1935-1939.

Westermark B, Wasteson A. 1976. A platelet factor stimulating human normal glial cells. Exp Cell Res 98: 170-174.

Wilcken NR, Prall OW, Musgrove EA, Sutherland RL. 1997. Inducible overexpression of cyclin D1 in breast cancer cells reverses the growth-inhibitory effects of antiestrogens. Clin Cancer Res 3: 849-854.

Wilson CA, Cajulis EE, Green JL, Olsen TM, Chung YA, Damore MA, et al. 2005. HER-2 overexpression differentially alters transforming growth factor-beta responses in luminal versus mesenchymal human breast cancer cells. Breast Cancer Res 7: R1058-R1079.

Wilson CA, Ramos L, Villasenor MR, Anders KH, Press MF, Clarke K, et al. 1999. Localization of human BRCA1 and its loss in high-grade, non-inherited breast carcinomas. Nat Genet 21: 236-240.

Winston JT, Coats SR, Wang YZ, Pledger WJ. 1996. Regulation of the cell cycle machinery by oncogenic ras. Oncogene 12: 127-134.

Wisdom R, Johnson RS, Moore C. 1999. c-Jun regulates cell cycle progression and apoptosis by distinct mechanisms. EMBO J 18: 188-197.

Wohrle FU, Daly RJ, Brummer T. 2009a. Function, regulation and pathological roles of the Gab/DOS docking proteins. Cell Commun Signal 7: 22.

-----. 2009b. How to Grb2 a Gab. Structure 17: 779-781.

Wosikowski K, Eppenberger U, Kung W, Nagamine Y, Mueller H. 1992. c-fos, c-jun and c-myc expressions are not growth rate limiting for the human MCF-7 breast cancer cells. Biochem Biophys Res Commun 188: 1067-1076.

Xu CF, Chambers JA, Solomon E. 1997. Complex regulation of the BRCA1 gene. J Biol Chem 272: 20994-20997.

Yamamoto T, Ebisuya M, Ashida F, Okamoto K, Yonehara S, Nishida E. 2006. Continuous ERK activation downregulates antiproliferative genes throughout G1 phase to allow cell-cycle progression. Curr Biol 16: 1171-1182.

Yarden Y, Sliwkowski MX. 2001. Untangling the ErbB signalling network. Nat Rev Mol Cell Biol 2: 127-137.

Yoon S, Lee JY, Yoon BK, Bae DS, Choi DS. 2004. Effects of HMGB-1 overexpression on cell-cycle progression in MCF-7 cells. J Korean Med Sci 19: 321-326.

Zajchowski DA, Sager R, Webster L. 1993. Estrogen inhibits the growth of estrogen receptor-negative, but not estrogen receptor-positive, human mammary epithelial cells expressing a recombinant estrogen receptor. Cancer Res 53: 5004-5011.
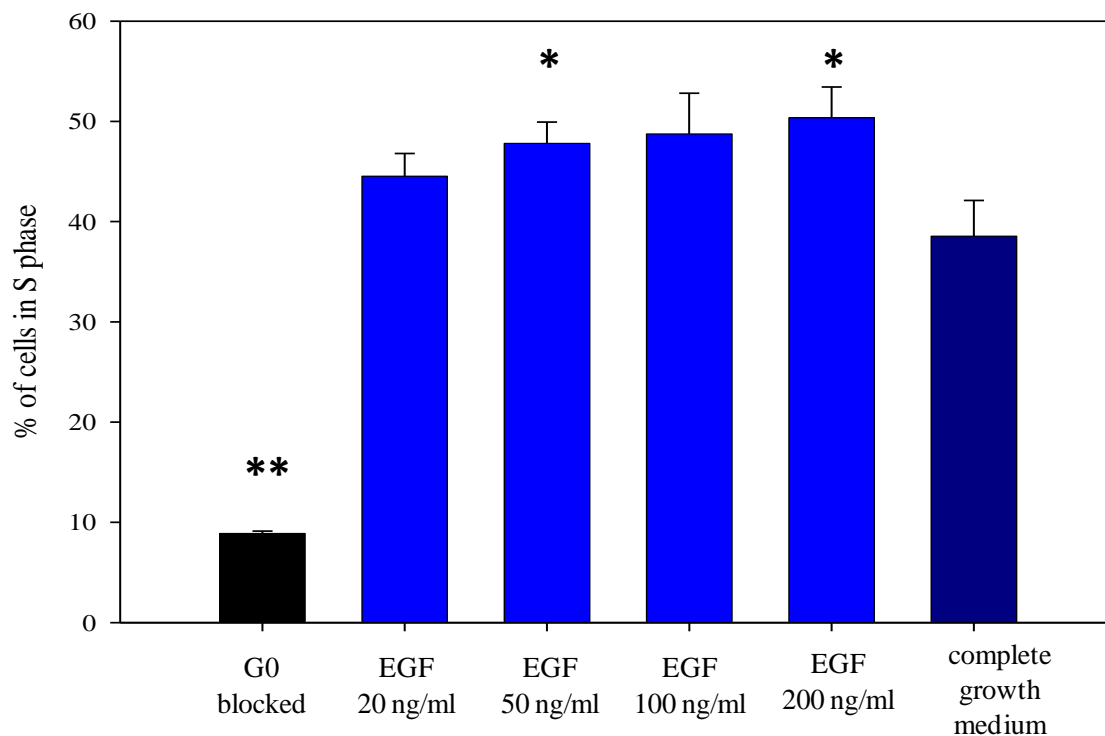
Appendix Figure i Percentage of MCF-12A cells in S phase after release with different concentrations of EGF

G0 accumulation was induced with serum-depletion for 24 hours (0.5% CD-HS), after which the starvation medium was removed and different concentrations of EGF in starvation medium were added for 20 hours. Cell cycle analysis was performed by flow cytometry carried out after staining of DNA with PI. Values show the mean of 3 independent experiments, error bars show SEM. Student's *t*-test was performed for significance testing. Samples marked with * (P=0.1) and ** (P=0.05) are significantly different from the positive control released with complete growth medium.

regulation of mRNA expression in MCF-7 cells
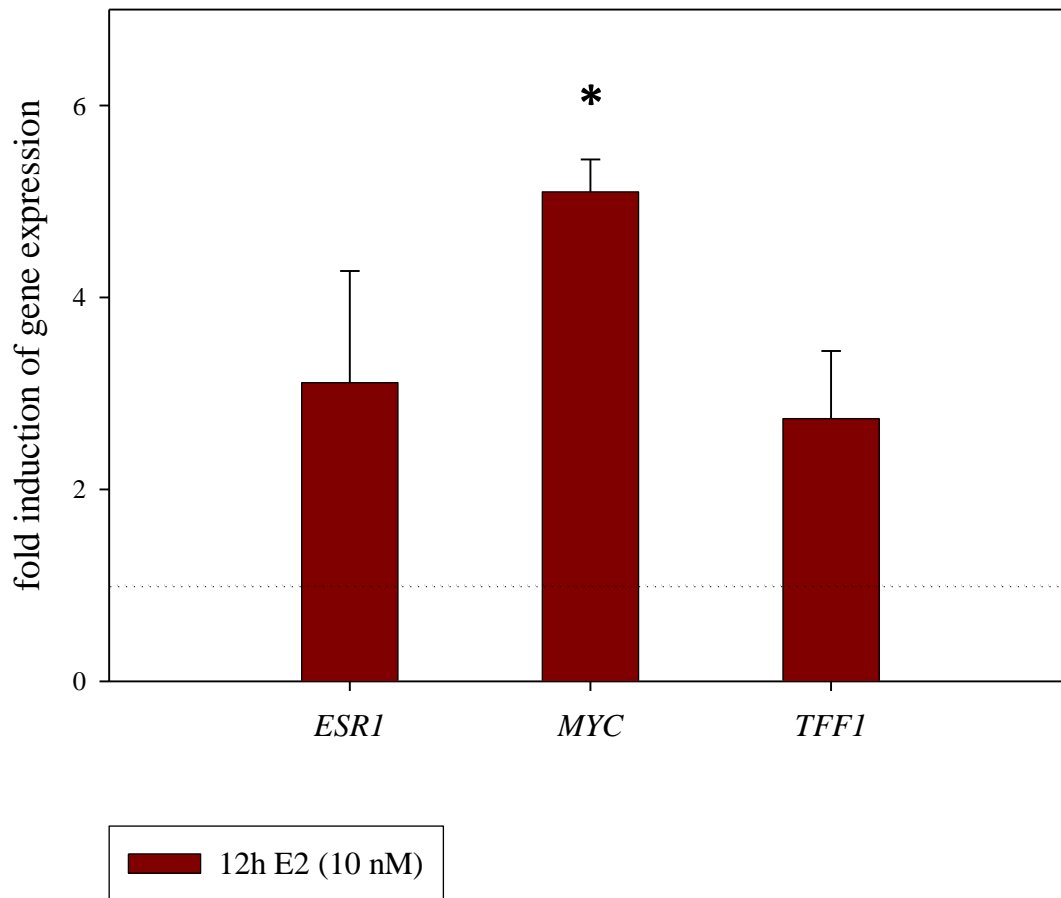
Appendix Figure ii Regulation of mRNA in MCF-7 cells following 12h incubation with 10nM estradiol (E2)

MCF-7 cells were seeded in 6-well plates with complete growth medium (MEMα with 5% fetal bovine serum (FBS)) and incubated 24h at 37°C. Subsequently, cells were incubated 24h (37°C) in assay medium (phenol red-free MEMα with 2% CD-treated FBS) before treatment with estradiol (10 nM in assay medium, 12h at 37°C) was performed. RNA-extraction and rt-PCR analysis was performed as described for MCF-12A cells in Chapter 2 above. Values show the mean of 3 independent experiments, error bars show SEM. Student's *t*-test was performed for significance testing. Sample marked with * are significantly different (P=0.1) from the negative (vehicle) control which was set to 1 (dotted line) and to which all other samples were normalised. After 12h with estradiol, MCF-7 cells showed detectable up-regulation of ESR1, MYC and TFF1 genes, coding for the estrogen receptor α (ERα), c-Myc transcription factor and trefoil peptide 1, respectively. Following from these results, incubation of MCF-12A cells with E2 and EGF was decided to be performed for 12h.

regulation of mRNA expression in MCF-12A cells
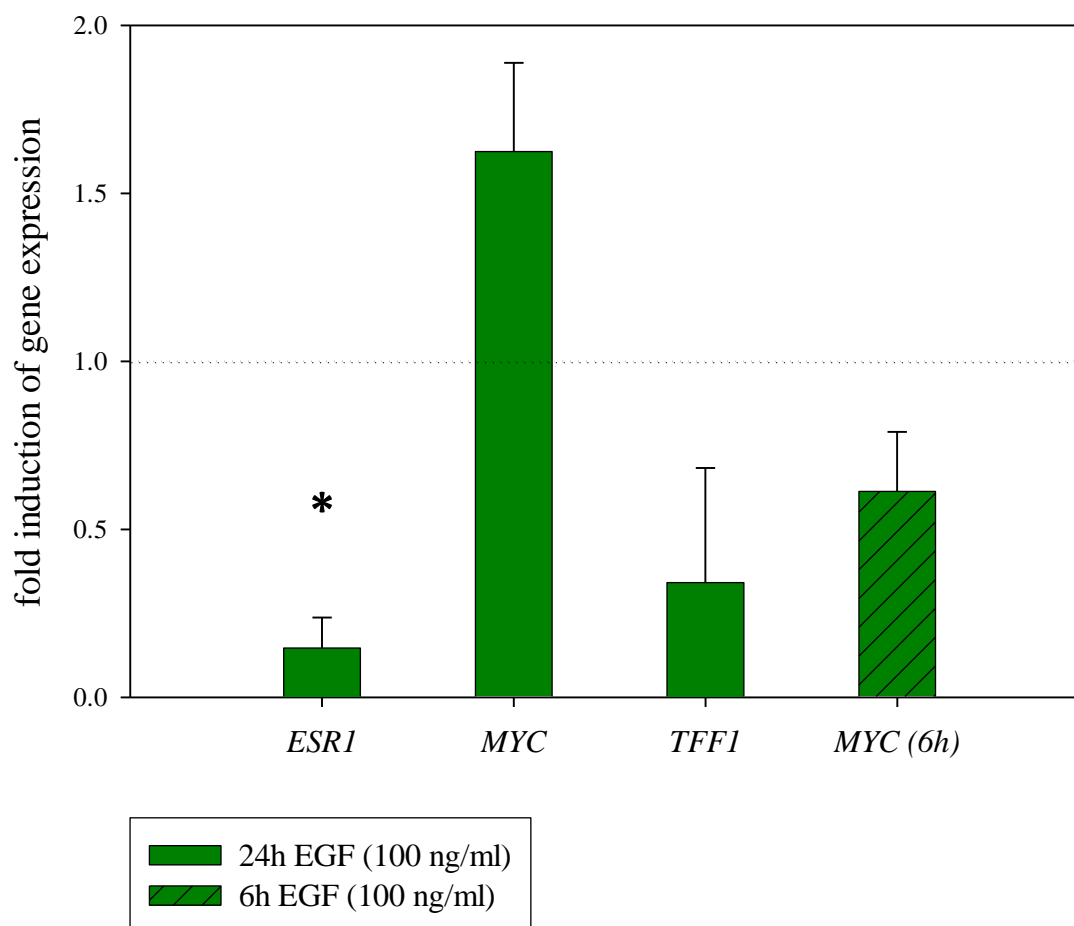
Appendix Figure iii Regulation of mRNA in MCF-12A cells following 24h and 6h incubation with 10nM EGF

MCF-12A cells were seeded and samples were prepared for mRNA expression analysis as described above in Chapter 2. Before mRNA extraction, samples were incubated for 24h with EGF (100 ng/ml). Values show the mean of 3 independent experiments, error bars show SEM. Student's *t*-test was performed for significance testing. Sample marked with * are significantly different (P=0.1) from the negative (vehicle) control which was set to 1 (dotted line) and to which all other samples were normalised. Significant regulation was observed on ESR1 mRNA only (coding for ERα). However, since no significant induction was seen for the proliferative genes MYC and TFF1, MYC was analysed additionally after 6h, but no up-regulation was observed. In the light of the findings for the same genes in MCF-7 cells (cf. Appendix Figure ii), it was decided to analyse mRNA regulation in MCF-12A cells exclusively after 12h of incubation with EGF (100 ng/ml) or E2 (10 nM).

Appendix Table i Overview of G0/G1 percentages found for negative control samples with flow cytometry

The table shows for each figure presented the lowest and the highest percentage found for the negative control sample (G0 blocked sample), as well as the number of different batches used for independent experiments presented in each table.

Figure	G0 block range [%]	G0 block range [%]	number of batches
Figure 10	58.01	92.9	2
Figure 15	50	81.3	4
Figure 17	60.5		1
Figure 18	60.5		1
Figure 19	77.2		1
Figure 20	83.38		1
Figure 21	83.9	86	1
Figure 22	64.2	86	1
Figure 23	71.8	89	3
Figure 25	60.5	70.8	2
Figure 26	82.9	92.9	3
Figure 27	62.7	87.5	3
Figure 28	74	87.5	3
Figure 29	79.2	89.83	2
Figure 30	70.91	72.8	2
Figure 36	74	89.83	3
Figure 37	74	89.83	3
Figure 38	83.95	88.42	1